PB87-103594

Scale-Up of Rapid Small-Scale Adsorption Tests to Field-Scale Adsorbers Theoretical and Experimental Basis

Michigan Technological Univ., Houghton

Prepared for

Environmental Protection Agency, Cincinnati, OH

Sep 86

U.S. Department of Commerce
National Technical Information Service
NTIS

PB87-103594

EPA/600/2-86/086
September 1986

SCALE-UP OF RAPID SMALL-SCALE ADSORPTION TESTS TO FIELD-SCALE ADSORBERS: THEORETICAL AND EXPERIMENTAL BASIS

by

John K. Berrigan, Jr.
Michigan Technological University
Houghton, Michigan 49931

Cooperative Agreement CR 811150

Project Officer

Benjamin Lykins
Drinking Water Research Division
Water Engineering Research Laboratory
Cincinnati, Ohio 45268

WATER ENGINEERING RESEARCH LABORATORY
OFFICE OF RESEARCH AND DEVELOPMENT
U.S. ENVIRONMENTAL PROTECTION AGENCY
CINCINNATI, OHIO 45268

REPRODUCED BY
U.S. DEPARTMENT OF COMMERCE
NATIONAL TECHNICAL
INFORMATION SERVICE
SPRINGFIELD, VA. 22161

TECHNICAL REPORT DATA

(Please read Instructions on the reverse before completing)

1. REPORT NO.
EPA/600/2-86/086

2.

3. RECIP
PB87 103594/AS

4. TITLE AND SUBTITLE
SCALE-UP OF RAPID SMALL-SCALE ADSORPTION TESTS TO FIELD-SCALE ADSORBERS: THEORETICAL AND EXPERIMENTAL BASIS

5. REPORT DATE
September 1986

6. PERFORMING ORGANIZATION CODE

7. AUTHOR(S)
J.K. Berrigan, Jr.

8. PERFORMING ORGANIZATION REPORT NO.

9. PERFORMING ORGANIZATION NAME AND ADDRESS
Michigan Technological University
Houghton, Michigan 49931

10. PROGRAM ELEMENT NO.

11. CONTRACT/GRANT NO.
CR 811150-byproduct

12. SPONSORING AGENCY NAME AND ADDRESS
Water Engineering Research Laboratory- Cincinnati, OH
Office of Research and Development
U.S. Environmental Protection Agency
Cincinnati, OH 45268

13. TYPE OF REPORT AND PERIOD COVERED
Published Paper

14. SPONSORING AGENCY CODE
EPA/600/14

15. SUPPLEMENTARY NOTES
Project Officer, B.W. Lykins, (513-569-7460)
Master of Science in Chemical Engineering Thesis

16. ABSTRACT

Design of full-scale adsorption systems typically includes expensive and time-consuming pilot studies to simulate full-scale adsorber performance. Accordingly, the rapid small-scale column test (RSSCT) was developed and evaluated experimentally. The RSSCT can simulate months of full-scale adsorber operation in several days without extensive isotherm and kinetic data.

The disperse-flow, pore- surface- diffusion model (DFPSDM) was used to determine the scaling factors because the DFPSDM includes most of the important phenomena that occur in fixed-bed adsorbers. Examination of dimensionless groups appearing in the DFPSDM shows that the ratio of the adsorbent particle size of the RSSCT to that of the full-scale adsorber determines the proper ratios of hydraulic loadings and empty-bed contact times. Using these scaling relationships, similar breakthrough profiles for the RSSCT and full-scale adsorber are expected when they are compared in terms of the number of bed volumes that were fed.

Experimental RSSCT breakthrough profiles for a six solute mixture at influent concentrations between 3000-6000 ug/L were found to be identical to those of a pilot-scale column test. At concentrations of 0 to 120 ug/L, a RSSCT simulated pilot-scale data successfully in the field.

micro gram/l

17. KEY WORDS AND DOCUMENT ANALYSIS

a. DESCRIPTORS	b. IDENTIFIERS/OPEN ENDED TERMS	c. COSATI Field/Group

18. DISTRIBUTION STATEMENT
RELEASE TO PUBLIC

19. SECURITY CLASS *(This Report)*
UNCLASSIFIED

20. SECURITY CLASS *(This page)*
UNCLASSIFIED

21. NO. OF PAGES
221

22. PRICE

EPA Form 2220-1 (Rev. 4-77) PREVIOUS EDITION IS OBSOLETE

DISCLAIMER

This research is based upon work supported by the National Science Foundation under grant CEE-8300213 from the Environmental and Water Quality Engineering Program, by the Environmental Protection Agency (No. CR811150-01-0), and by the Water and Waste Management Programs at Michigan Technological University. Any opinions, findings, and conclusions or recommendations expressed in this publication are those of the author and do not necessarily reflect the views of the National Science Foundation, Environmental Protection Agency, or the Water and Waste Management Programs. and the Water and Waste Management Programs at Michigan Technological University.

FOREWORD

The U.S. Environmental Protection Agency is charged by Congress with protecting the Nation's land, air, and water systems. Under a mandate of national environmental laws, the agency strives to formulate and implement actions leading to a compatible balance between human activities and the ability of natural systems to support and nurture life. The Clean Water Act, the Safe Drinking Water Act, and the Toxics Substances Control Act are three of the major congressional laws that provide the framework for restoring and maintaining the integrity of our Nation's water, for preserving and enhancing the water we drink, and for protecting the environment from toxic substances. These laws direct the EPA to perform research to define our environmental problems, measure the impacts, and search for solutions.

The Water Engineering Research Laboratory is that component of EPA's Research and Development program concerned with preventing, treating, and managing municipal and industrial wastewater discharges; establishing practices to control and remove contaminants from drinking water and to prevent its deterioration during storage and distribution; and assessing the nature and controllability of releases of toxic substances to the air, water, and land from manufacturing processes and subsequent product uses. This publication is one of the products of that research and provides a vital communication link between the researcher and the user community.

The effect of low-level contaminants on public health has encouraged the research needed to identify, monitor, and remove toxic agents from drinking water, wastewater, and groundwater. A rapid method to design large-scale fixed-bed adsorbers from small column studies has been developed and evaluated. In this study, a dimensional analysis on the dispersed-flow pore-surface- diffusion model (DFPSDM) was used to determine the scaling factors because the DFPSDM includes most of the known transport of kinetic phenomena that occur in fixed-bed adsorbers.

Francis T. Mayo, Director
Water Engineering Research Laboratory

ABSTRACT

Design of full-scale adsorption systems typically includes expensive and time-consuming pilot studies to simulate full-scale adsorber performance. Accordingly, the rapid small-scale column test (RSSCT) was developed and evaluated experimentally. The RSSCT can simulate months of full-scale adsorber operation in several days without extensive isotherm and kinetic data.

The dispersed-flow, pore- surface- diffusion model (DFPSDM) was used to determine the scaling factors because the DFPSDM includes most of the important phenomena that occur in fixed-bed adsorbers. Examination of dimensionless groups appearing in the DFPSDM shows that the ratio of the adsorbent particle size of the RSSCT to that of the full-scale adsorber determines the proper ratios of hydraulic loadings and empty-bed contact times. Using these scaling relationships, similar breakthrough profiles for the RSSCT and full-scale adsorber are expected when they are compared in terms of the number of bed volumes that were fed.

Experimental RSSCT breakthrough profiles for a six solute mixture at influent concentrations between 3000-6000 μg/L were found to be identical to those of a pilot-scale column test. At concentrations of 0 to 120 μg/L, a RSSCT simulated pilot-scale data successfully in the field.

TABLE OF CONTENTS

Page

FOREWORD iii

ABSTRACT iv

TABLE OF CONTENTS v

LIST OF TABLES viii

LIST OF FIGURES x

I. INTRODUCTION 1

II. APPROACH 3

  A. Previous Work 5

  B. The Dispersed-Flow Pore and Surface Diffusion Model (DFPSDM) 5

  C. Dimensionless Groups Characterizing the DFPSDM 10

    1. Surface Solute Distribution Parameter 12

    2. Pore Solute Distribution Parameter 12

    3. Combined and Total Solute Distribution Patameters Mass throughput 12

    4. Stanton Number 13

    5. Surface Diffusion Modulus 14

    6. Pore Diffusion Modulus 14

    7. Peclet Number 14

  D. Development of Scaling Equations 15

    1. Perfect Similarity Assuming Constant Surface Diffusivity 16

    2. Similarity for Diffusion Controlled Processes Assuming Surface Diffusivity Proportional to Particle Radius 18

    3. Similarity where Surface Diffusion Coefficient Measurements are Available for a Solute 25

III. EXPERIMENTAL MATERIALS AND METHODS 26

  A. Materials of Construction 26

  B. Experimental Procedures 31

page

1. Laboratory Study Procedure 31

2. Field Study Procedure 32

C. Chemicals 32

D. Chemical Analysis 32

1. Laboratory Study Chemical Analysis 33

2. Field Study Chemical Analysis 33

E. Carbon Preparation 34

F. Flow Measurement and Determination of Bed Volumes Fed 34

VI. THEORETICAL VERIFICATION OF SCALING EQUATIONS 37

A. Chemical and Physical Property Estimation 37

1. Freundlich Isotherm Parameters 39

2. Intraparticle Mass Transfer Parameters 39

3. Liquid Phase Mass Transfer Coefficients 41

4. Estimated Pressure Drop across Fixed-Beds 41

B. Single and Multicomponent Results for Perfect Similarity 42

C. Estimation of the EBCT of the Mass Transfer Zone for Single Components 45

D. Scaling of Surface Diffusion Controlled Processes 48

V. RSSCT PARAMETER SENSITIVITY 54

A. Mass Transfer parameters 57

B. Physical/Chemical Properties 62

C. Selected Operating Conditions 70

VI. EXPERIMENTAL VERIFICATION OF SCALING EQUATIONS 76

A. Effects of Size Reduction upon Physical/Chemical Properties of Granular Activated Carbon 76

B. Laboratory Study Results and Discussion 80

C. Field-Study Pilot and Small-Column Tests 82

page

1. RSSCT Results for Simulation of 1.0 Minute EBCT Adsorbers Assuming Constant Surface Diffusivity........93

2. RSSCT Results for Simulation of 3.2 Minute EBCT Adsorber Assuming Constant Surface Diffusivity........116

3. RSSCT Results for Simulation of 5.4 Minute EBCT Adsorber Assuming Constant Surface Diffusivity........126

4. RSSCT Dissimilarity in the Field Study....................136

5. RSSCT Results for Simulation of 5.4 Minute EBCT Adsorber Assuming D_s Linearly Proportional to R...138

6. Methods for RSSCT Interpretation where Influent Concentrations Change..............................139

VII. CONCLUSIONS 158

VIII. RECOMENDATIONS FOR FUTURE WORK 161

Appendix I. References 162

Appendix II. Nomenclature 166

Appendix III. Development of Scaling Equations from the DFPSDM 170

Appendix IV. Trichloroethene Isotherm Data for 60x80 Mesh Size Granular Activated Carbon 182

Appendix V. Laboratory Study Pilot Scale Data 183

Appendix VI. Laboratory Study Small Column Data 186

Appendix VII. Field Study Pilot Scale Data 190

Appendix VIII. Field Study Small Column Data 198

LIST OF TABLES

Table Title page

Table 1. Comparison of column parameters for scale-down of a large scale column to a small-column test: design and operational parameters for a full-scale adsorber, a rapid small-scale column test (RSSCT) which is designed to simulate full scale performance, and a RSSCT which is just long enough to measure the length of the mass transfer zone (MTZ) of TCE as a single solute....38

Table 2. Comparison of DFHSDM column parameters for scale-down of a large scale column to a small-column test: chemical and dimensionless parameters for a full-scale adsorber, a rapid small-scale column test (RSSCT) which is designed to simulate full scale performance, and a RSSCT which is just long enough to measure the length of the mass transfer zone (MTZ) of TCE as a single solute....43

Table 3. Chemical and dimensionless parameters for large-scale and small-scale columns for cis-dichloroethylene, trichloroethylene, tetrachloroethylene, toluene, and xylene....46

Table 4. Comparison of column parameters for scale-down of a large scale column to a small-column test: design and operational parameters for a full-scale adsorber, a rapid small-scale column test (RSSCT) for the sensitivity analysis which is designed assuming constant diffusivity to simulate full scale performance, a RSSCT which is designed to maintain similar Ed_s where the surface diffusivity is linearly dependent on the particle radius, and a RSSCT designed to maintain similar Ed_s and reduce the loading rate yet maintaining similar dispersive mechanisms....55

Table 5. Comparison of DFPSDM column parameters for scale-down of a large scale column to a small-column test: chemical and dimensionless parameters for a full-scale adsorber, a rapid small-scale column test (RSSCT) for the sensitivity analysis which is designed assuming constant diffusivity to simulate full scale performance, a RSSCT which is designed to maintain similar Ed_s where the surface diffusivity is linearly dependent on the particle radius, and a RSSCT designed to maintain similar Ed_s and reduce the loading rate yet maintaining similar dispersive mechanisms....56

Table 6. Pilot-scale and small-scale design parameters for the laboratory study....81

Table 7. Pilot-scale design and operational parameters for the field pilot studies: F-400 carbon and EBCTs of 1, 3, and 5 minutes, WV-G carbon and EBCT of 1 minute....89

Table 8. RSSCT design and operational Parameters for the field studies: simulation of pilot adsorbers, Table 7 (a-d)........91

LIST OF FIGURES

Figure	Title	page
Figure 1.	Axial mass transfer mechanisms incorporated into the dispersed flow pore and surface diffusion model...........	6
Figure 2.	Intraparticle mechanisms and assumptions incorporated into the pore and surface diffusion model.................	7
Figure 3.	p-Nitrophenol surface diffusivity of Hydraffin 71 and Filtrasorb 300 particle sizes with least-squares fits and 95% confidence intervals shown. (After Schneider, Frick, and Sontheimer, Univ. of Karlsruhe, 1982).........	20
Figure 4.	The various regimes of dispersion: (a) pure molecular dispersion, (b) predominant molecular diffusion, (c) predominant mechanical dispersion, (d) pure mechanical dispersion. After Fried (1975)...........................	24
Figure 5.	Experimental fixed-bed adsorption column diagram for (a) laboratory pilot-scale column and (b) RSSCT adsorbers...	28
Figure 6.	Laboratory study adsorber equipment diagram..............	29
Figure 7.	Field-study RSSCT equipment diagram......................	30
Figure 8.	Comparison of the DFHSDM model prediction of the trichloroethene breakthrough profile for a full-scale adsorber to the DFPSDM prediction for a small-column test.	44
Figure 9.	Comparison of DFHSDM model predictions of full-scale adsorber breakthrough profiles for dichloroethene, trichloroethene, tetrachloroethene, toluene, and xylenes to the DFHSDM predictions for a small-column test assuming constant surface diffusivity...............	47
Figure 10.	Comparison of the DFHSDM model small-column test predictions for trichloroethene. (a) perfect similarity - constant diffusivity, (b) surface diffusivity linearly dependent on particle size, (c) surface diffusivity determined experimentally....................	49
Figure 11.	Comparison of DFHSDM model predictions of full-scale adsorber breakthrough profiles for dichloroethene, trichloroethene, tetrachloroethene, toluene, and xylenes to the PSDM predictions for a small-column test where the surface diffusivity is a linear function of the adsorbent particle size. Scaling equations assume constant diffusivity..............................	51

Figure No. Title page

Figure 12. Comparison of the DFPSDM model small-column test predictions for trichloroethene: (a) full-scale adsorber (b) RSSCT scaled to maintain constant Ed_s - surface diffusivity linearly dependent on particle size............52

Figure 13. DFPSDM prediction of the RSSCT sensitivity to 10% and 50% changes in the dispersion coefficient.......................58

Figure 14. DFPSDM prediction of the RSSCT sensitivity to 10% and 50% changes in the film transfer coefficient....................59

Figure 15. DFPSDM prediction of the RSSCT sensitivity to 10% and 50% changes in the pore diffisivity..............................60

Figure 16. DFPSDM prediction of the RSSCT sensitivity to 10% and 50% changes in the surface diffusivity..........................61

Figure 17. DFPSDM prediction of the RSSCT sensitivity to 10% and 50% changes in the adsorbent particle radius....................63

Figure 18. DFPSDM prediction of the RSSCT sensitivity to 10% and 50% changes in the adsorbent void fraction......................64

Figure 19. DFPSDM prediction of the RSSCT sensitivity to 10% changes in the adsorbent particle density..........................65

Figure 20. DFPSDM prediction of the RSSCT sensitivity to 10% changes in the bed void fraction....................................66

Figure 21. DFPSDM prediction of the RSSCT sensitivity to 10% and 50% changes in the Freundlich isotherm capacity................67

Figure 22. DFPSDM prediction of the RSSCT sensitivity to 10% and 50% changes in the Freundlich isotherm intensity constant, 1/n...68

Figure 23. DFPSDM prediction of the RSSCT sensitivity to 10% and 50% changes in the dimensionless influent concentration.........71

Figure 24. DFPSDM prediction of the RSSCT sensitivity to 10% and 50% changes in the influent concentration in µg/L...............72

Figure 25. DFPSDM prediction of the RSSCT sensitivity to 10% and 50% changes in the hydraulic loading rate.......................73

Figure 26. DFPSDM prediction of the RSSCT sensitivity to 10% and 50% changes in the flowrate....................................74

Figure 27. Trichloroethene isotherm data and fitted Freundlich isotherm parameters with 95% confidence intervals shown.....78

Figure No. Title page

Figure 28. Comparison of the chloroform breakthrough profile for the small-column test to the pilot-scale column in the laboratory study. Influent data are shown. 83

Figure 29. Comparison of the trichloroethene breakthrough profile for the small-column test to the pilot-scale column in the laboratory study. Influent data are shown. Operating parameters are presented in Table 6..........................84

Figure 30. Comparison of the chlorodibromomethane breakthrough profile for the small-column test to the pilot-scale column in the laboratory study. Influent data are shown. Operating parameters are presented in Table 6...............85

Figure 31. Comparison of the 1,2 dibromoethane breakthrough profile for the small-column test to the pilot-scale column in the laboratory study. Influent data are shown. Operating parameters are presented in Table 6..........................86

Figure 32. Comparison of the bromoform breakthrough profile for the small-column test to the pilot-scale column in the laboratory study. Influent data are shown. Operating parameters are presented in Table 6..........................87

Figure 33. Comparison of the tetrachloroethene breakthrough profile for the small-column test to the pilot-scale column in the laboratory study. Influent data are shown. Operating parameters are presented in Table 6..........................88

Figure 34. Comparison of the dichloroethene breakthrough profile for the small-column test to the pilot-scale column in the field study. Influent data are shown. Operating parameters are presented in Tables 7 and 8 (a)..............94

Figure 35. Comparison of the trichloroethene breakthrough profile for the small-column test to the pilot-scale column in the field study. Influent data are shown. Operating parameters are presented in Tables 7 and 8 (a)..............95

Figure 36. Comparison of the tetrachloroethene breakthrough profile for the small-column test to the pilot-scale column in the field study. Influent data are shown. Operating parameters are presented in Tables 7 and 8 (a)..............96

Figure 36a. The first portion of the comparison of the tetrachloroethene breakthrough profile for the small-column test to the pilot-scale column in the field study expanded along the bed volumes axis. Influent data are shown. Operating parameters are presented in Tables 7 and 8 (a)..97

Figure No. Title page

Figure 37. Comparison of the vinyl chloride breakthrough profile for the small-column test to the pilot-scale column in the field study. Influent data are shown. Operating parameters are presented in Tables 7 and 8 (a)..............98

Figure 37a. The first portion of the comparison of the vinyl chloride breakthrough profile for the small-column test to the pilot-scale column in the field study expanded along the bed volumes axis. Influent data are shown. Operating parameters are presented in Tables 7 and 8 (a)..............99

Figure 38. Comparison of the 1,1,1 trichloroethane breakthrough profile for the small-column test to the pilot-scale column in the field study. Influent data are shown. Operating parameters are presented in Tables 7 and 8 (a)...100

Figure 39. Comparison of the toluene breakthrough profile for the small-column test to the pilot-scale column in the field study. Influent data are shown. Operating parameters are presented in Tables 7 and 8 (a)............................101

Figure 40. Comparison of the ethyl benzene breakthrough profile for the small-column test to the pilot-scale column in the field study. Influent data are shown. Operating parameters are presented in Tables 7 and 8 (a).............102

Figure 41. Comparison of the m-xylene breakthrough profile for the small-column test to the pilot-scale column in the field study. Influent data are shown. Operating parameters are presented in Tables 7 and 8 (a)............................103

Figure 42. Comparison of the c,p-xylene breakthrough profile for the small-column test to the pilot-scale column in the field study. Influent data are shown. Operating parameters are presented in Tables 7 and 8 (a)............................104

Figure 43. Comparison of the dichloroethene breakthrough profile for the small-column test to the pilot-scale column in the field study. Influent data are shown. Operating parameters are presented in Tables 7 and 8 (d).............106

Figure 44. Comparison of the trichloroethene breakthrough profile for the small-column test to the pilot-scale column in the field study. Influent data are shown. Operating parameters are presented in Tables 7 and 8 (d).............107

Figure 45. Comparison of the tetrachloroethene breakthrough profile for the small-column test to the pilot-scale column in the field study. Influent data are shown. Operating parameters are presented in Tables 7 and 8 (d).............108

Figure No. Title page

Figure 46. Comparison of the vinyl chloride breakthrough profile for the small-column test to the pilot-scale column in the field study. Influent data are shown. Operating parameters are presented in Tables 7 and 8 (d)............109

Figure 47. Comparison of the toluene breakthrough profile for the small-column test to the pilot-scale column in the field study. Influent data are shown. Operating parameters are presented in Tables 7 and 8 (d)..........................110

Figure 48. Comparison of the ethyl benzene breakthrough profile for the small-column test to the pilot-scale column in the field study. Influent data are shown. Operating parameters are presented in Tables 7 and 8 (d)............111

Figure 49. Comparison of the m-xylene breakthrough profile for the small-column test to the pilot-scale column in the field study. Influent data are shown. Operating parameters are presented in Tables 7 and 8 (d)..........................112

Figure 50. Comparison of the o,p-xylene breakthrough profile for the small-column test to the pilot-scale column in the field study. Influent data are shown. Operating parameters are presented in Tables 7 and 8 (d)..........................113

Figure 51. Comparison of the dichloroethene breakthrough profile for the small-column test to the pilot-scale column in the field study. Influent data are shown. Operating parameters are presented in Tables 7 and 8 (b)............117

Figure 52. Comparison of the trichloroethene breakthrough profile for the small-column test to the pilot-scale column in the field study. Influent data are shown. Operating parameters are presented in Tables 7 and 8 (b)............118

Figure 53. Comparison of the tetrachloroethene breakthrough profile for the small-column test to the pilot-scale column in the field study. Influent data are shown. Operating parameters are presented in Tables 7 and 8 (b)............119

Figure 54. Comparison of the vinyl chloride breakthrough profile for the small-column test to the pilot-scale column in the field study. Influent data are shown. Operating parameters are presented in Tables 7 and 8 (b)............120

Figure 55. Comparison of the 1,1,1 trichloroethane breakthrough profile for the small-column test to the pilot-scale column in the field study. Influent data are shown. Operating parameters are presented in Tables 7 and 8 (b)...121

Figure No. Title page

Figure 56. Comparison of the toluene breakthrough profile for the small-column test to the pilot-scale column in the field study. Influent data are shown. Operating parameters are presented in Tables 7 and 8 (b)..........................122

Figure 57. Comparison of the ethyl benzene breakthrough profile for the small-column test to the pilot-scale column in the field study. Influent data are shown. Operating parameters are presented in Tables 7 and 8 (b)............123

Figure 58. Comparison of the m-xylene breakthrough profile for the small-column test to the pilot-scale column in the field study. Influent data are shown. Operating parameters are presented in Tables 7 and 8 (b)..........................124

Figure 59. Comparison of the o,p-xylene breakthrough profile for the small-column test to the pilot-scale column in the field study. Influent data are shown. Operating parameters are presented in Tables 7 and 8 (b)..........................125

Figure 60. Comparison of the dichloroethene breakthrough profile for the small-column test to the pilot-scale column in the field study. Influent data are shown. Operating parameters are presented in Tables 7 and 8 (c)............127

Figure 61. Comparison of the trichloroethene breakthrough profile for the small-column test to the pilot-scale column in the field study. Influent data are shown. Operating parameters are presented in Tables 7 and 8 (c)............128

Figure 62. Comparison of the tetrachloroethene breakthrough profile for the small-column test to the pilot-scale column in the field study. Influent data are shown. Operating parameters are presented in Tables 7 and 8 (c)............129

Figure 63. Comparison of the vinyl chloride breakthrough profile for the small-column test to the pilot-scale column in the field study. Influent data are shown. Operating parameters are presented in Tables 7 and 8 (c)............130

Figure 64. Comparison of the 1,1,1 trichloroethane breakthrough profile for the small-column test to the pilot-scale column in the field study. Influent data are shown. Operating parameters are presented in Tables 7 and 8 (c)...131

Figure 65. Comparison of the toluene breakthrough profile for the small-column test to the pilot-scale column in the field study. Influent data are shown. Operating parameters are presented in Tables 7 and 8 (c)..........................132

Figure No. Title page

Figure 66. Comparison of the ethyl benzene breakthrough profile for the small-column test to the pilot-scale column in the field study. Influent data are shown. Operating parameters are presented in Tables 7 and 8 (c)............133

Figure 67. Comparison of the m-xylene breakthrough profile for the small-column test to the pilot-scale column in the field study. Influent data are shown. Operating parameters are presented in Tables 7 and 8 (c)..........................134

Figure 68. Comparison of the o,p-xylene breakthrough profile for the small-column test to the pilot-scale column in the field study. Influent data are shown. Operating parameters are presented in Tables 7 and 8 (c)..........................135

Figure 69. Comparison of the dichloroethene breakthrough profile for the small-column test to the pilot-scale column in the field study. Influent data are shown. Operating parameters are presented in Tables 7 (a) and 8 (c).........140

Figure 70. Comparison of the trichloroethene breakthrough profile for the small-column test to the pilot-scale column in the field study. Influent data are shown. Operating parameters are presented in Tables 7 (a) and 8 (c).........141

Figure 71. Comparison of the toluene breakthrough profile for the small-column test to the pilot-scale column in the field study. Influent data are shown. Operating parameters are presented in Tables 0 7 (a) and 8(c).......................142

Figure 72. Comparison of the o- and p-xylene breakthrough profile for the small-column test to the pilot-scale column in the field study. Influent data are shown. Operating parameters are presented in Tables 7 (a) and 8 (c).........143

Figure 73. Comparison of the dichloroethene breakthrough profile for the small-column test to the pilot-scale column in the field study. Concentrations are normalized by the average influent concentration. Influent data are shown. Operating parameters are presented in Tables 7 (a) and 8 (c)..145

Figure 74. Comparison of the trichloroethene breakthrough profile for the small-column test to the pilot-scale column in the field study. Concentrations are normalized by the average influent concentration. Influent data are shown. Operating parameters are presented in Tables 7 (a) and 8 (c)..146

Figure No. Title page

Figure 75. Comparison of the toluene breakthrough profile for the small-column test to the pilot-scale column in the field study. Concentrations are normalized by the average influent concentration. Influent data are shown. Operating parameters are presented in Tables 7 (a) and 8 (c)....147

Figure 76. Comparison of the o- and p-xylenes breakthrough profile for the small-column test to the pilot-scale column in the field study. Concentrations are normalized by the average influent concentration. Influent data are shown. Operating parameters are presented in Tables 7 (a) and 8 (c)....148

Figure 77. Comparison of the dichloroethene breakthrough profile for the small-column test to the pilot-scale column in the field study expressed as the grams of solute fed through the adsorber per kilogram carbon in the bed versus reduced concentration to normalize the effects of differing influent concentrations. Influent data are shown. Operating parameters are presented in Tables 7 (a) and 8 (c)....149

Figure 78. Comparison of the trichloroethene breakthrough profile for the small-column test to the pilot-scale column in the field study expressed as the grams of solute fed through the adsorber per kilogram carbon in the bed versus reduced concentration to normalize the effects of differing influent concentrations. Influent data are shown. Operating parameters are presented in Tables 7 (a) and 8 (c)....150

Figure 79. Comparison of the tetrachloroethene breakthrough profile for the small-column test to the pilot-scale column in the field study expressed as the grams of solute fed through the adsorber per kilogram carbon in the bed versus reduced concentration to normalize the effects of differing influent concentrations. Influent data are shown. Operating parameters are presented in Tables 7 (a) and 8 (c)....151

Figure 80. Comparison of the toluene breakthrough profile for the small-column test to the pilot-scale column in the field study expressed as the grams of solute fed through the adsorber per kilogram carbon in the bed versus reduced concentration to normalize the effects of differing influent concentrations. Influent data are shown. Operating parameters are presented in Tables 7 (a) and 8 (c)....152

Figure No. Title page

Figure 81. Comparison of the dichloroethene breakthrough profile for the small-column test to the pilot-scale column in the field study expressed as the grams of solute fed through the adsorber per kilogram carbon in the bed versus reduced concentration to normalize the effects of differing influent concentrations. Influent data are shown. Operating parameters are presented in Tables 7 (c) and 8 (c) 154

Figure 82. Comparison of the trichloroethene breakthrough profile for the small-column test to the pilot-scale column in the field study expressed as the grams of solute fed through the adsorber per kilogram carbon in the bed versus reduced concentration to normalize the effects of differing influent concentrations. Influent data are shown. Operating parameters are presented in Tables 7 (c) and 8 (c) 155

Figure 83. Comparison of the tetrachloroethene breakthrough profile for the small-column test to the pilot-scale column in the field study expressed as the grams of solute fed through the adsorber per kilogram carbon in the bed versus reduced concentration to normalize the effects of differing influent concentrations. Influent data are shown. Operating parameters are presented in Tables 7 (c) and 8 (c) 156

Figure 84. Comparison of the toluene breakthrough profile for the small-column test to the pilot-scale column in the field study expressed as the grams of solute fed through the adsorber per kilogram carbon in the bed versus reduced concentration to normalize the effects of differing influent concentrations. Influent data are shown. Operating parameters are presented in Tables 7 (c) and 8 (c) 157

I. INTRODUCTION

Recent attention about the impact of low-level contaminants on the public health has encouraged a major research effort to develop effective means to identify, monitor, and remove toxic agents from drinking water, wastewater, and groundwater. Granular activated carbon (GAC) is an effective treatment technique for the removal of some toxic organics from drinking water or wastewater; however, it can be a relatively expensive process, especially if it is designed improperly. The proper design of full-scale adsorbers typically includes time-consuming and expensive pilot-scale studies.

Accordingly, a rapid method for the design of large-scale fixed-bed adsorbers from small column studies, known as the rapid small-scale column test (RSSCT), has been developed and evaluated. The two primary advantages in using the small column studies for design are that a small-column technique may be conducted in a fraction of the time that is required to conduct pilot studies, and that unlike predictive methods that utilize mathematical models, no isotherm or kinetic studies are required to perform the small column tests. Replacing a pilot study with a small experimental test significantly reduces the cost of full-scale design. The benefits of a rapid performance prediction and the cost savings which is associated with proper design make such a test very attractive.

In the RSSCT method, mathematical models are utilized to scale-down the full-scale adsorber to a small-scale adsorber and maintain perfect similarity between the performance of the adsorbers. If perfect similarity is maintained, the small scale column which utilizes a smaller adsorbent particle size than the full scale adsorber will have identical breakthrough profiles as the full-scale process. Accordingly, a number of small scale column tests could be used to evaluate the importance of design variables such as empty bed contact time (EBCT) or bed operations such as beds in series or in parallel.

In this study, a dimensional analysis on the dispersed-flow, pore-surface- diffusion model (DFPSDM) was used to determine the scaling factors because the DFPSDM includes most of the known transport and kinetic phenomena which occur in fixed-bed adsorbers. By examining the dimensionless groups that appeared in the DFPSDM, it was found that the adsorbent particle sizes of the small- and large- scale columns determined the scaling relationships between hydraulic loadings and EBCTs of the small-scale and full-scale columns.

The scaling procedure was evaluated by both model calculations and experimental data. Example calculations for RSSCT and full-scale adsorber with the DFPSDM and the homogeneous solid diffusion model (HSDM) were compared for single and multicomponent breakthrough profiles for which the RSSCT was designed to simulate adsorber performance in 1.05% of the time of a full-scale study. A RSSCT was conducted to simulate a pilot-scale column adsorber study with a six solute influent at individual concentrations of 3000-6000 µg/L. This demonstrated experimentally that at high concentrations, the RSSCT can be run in 4% of the time required for a pilot study. Four RSSCT's were conducted using a naturally occurring groundwater as influent and the resulting breakthrough profiles compared to the breakthrough profiles of corresponding pilot-scale adsorbers treating the same groundwater. Three of the field-study comparisons were performed using Calgon F-400 carbon, and one study was performed using Westvaco WV-G carbon. The RSSCT's were run in substantially less than the time required for a pilot study. The amount time saved using an RSSCT is dependent upon the magnitude of the carbon particle reduction and the possible change in the surface diffusivities as a result of the size reduction. In addition, physical/chemical properties of the GAC used in RSSCT's and pilot-scale adsorbers were measured and compared to verify the assumptions of the design method and to account for deviations from expected results.

II. APPROACH

The use of mathematical models and governing equations to define scaling relationships of the design and operational parameters between the small and full scale processes has been demonstrated by Langhaar (1951), Gukhman (1965), and Taylor (1974). Beckner (1976) discusses many other contributions to the subject. In summary, the following three conditions are applied to the governing equations of a system in order for the design and operation of a small-scale process to give similar operating data to that of the full scale process. First, the boundary conditions for the large and small scale processes must occur at the same dimensionless coordinate values in the dimensionless differential equations. Second, the dimensionless parameters that appear in the dimensionless differential equations for the full-scale process must equal those for the small-scale process. Finally, no change in mechanism can occur with the change in process size.

Three phenomena that could change with the process size are the effects of backwashing, equilibrium capacity, and adsorption kinetics, thereby, resulting in a poor representation of a full scale adsorber performance by the RSSCT. The impact of backwashing was not considered in developing the scaling equations and is not discussed in this work. However, it may be possible to simulate backwashing in the RSSCT, if the adsorbent particles were distributed in a similar fashion during and after backwashing in the small and full scale processes. This would probably imply that the smaller size GAC which is used in the RSSCT would have to have a particle size distribution, roughness and density which is identical to the full-scale adsorber. In addition, the small-scale column would have to have a large enough diameter to prevent wall effects that would impact the distribution of particles during and after backwashing.

The scale-up of the RSSCT was based on the DFPSDM because it contains most of the phenomena which are known to occur in fixed-bed adsorbers (Friedman 1984). In the section on the development of scaling equations, it will be shown that if exact similarity can be guaranteed for the DFPSDM, then similarity will exist for simpler models, for example, the plug-flow, pore- surface- diffusion model (PFPSDM), the dispersed-flow homogeneous solid-diffusion model (DFHSDM), or the plug flow homogeneous solid diffusion model (PFHSDM).

In the past, the PFHSDM has been shown to predict adsorption, desorption, and multicomponent competition in fixed-beds (Crittenden et al., 1978 a,b,c, Thacker et al., 1983, Thacker et al., 1984, Luft, 1984). Crittenden et al. (1980) and Thacker et al. (1983, 1984) discussed recent work in which the PFHSDM has been used to predict fixed-bed performance.

Using the DFPSDM, it is a simple matter to apply the three conditions of similarity to the model equations in dimensionless form to design a small-scale adsorber to yield similar operating data to that of the full-scale process. In Section II.B., the model equations are presented in dimensionless form such that the boundary conditions for the large and small scale processes occur at the same dimensionless coordinate values in the DFPSDM. In Section II.D., the dimensionless parameters from the model equations for the full-scale process are equated to those for the small-scale process to develop scaling equations that may be used to design and operate a RSSCT. Accordingly, if the dimensionless groups from the full-scale process are set equal to the small-scale process then exact similarity will be guaranteed. Sections IV.D., V., and VI.A. discuss process size change considerations and the impact of size reduction on kinetic, isotherm, and physical parameters of granular activated carbon.

A. Previous Work

A small column technique has been used successfully by Beaudet et al (1980), Billelo et al (1983), and Rosene et al (1983) to determine carbon usage rates. These methods employ a fixed-bed column of fine mesh carbon and high pressure liquid chromatography (HPLC) methods. In addition, with a multicomponent influent the resulting elution profiles provided qualitative information on the order of breakthrough.

Frick (1982) proposed a method of interpreting small-scale adsorber information with scaling equations based upon Stanton number and the solid diffusion modulus, Ed. The resulting scaling equations account for mass-transport mechanisms of solid diffusion, liquid film transfer, and advection. A small-scale experimental test could be designed from these equations to simulate full-scale adsorber performance.

B. Dispersed-Flow Pore- Surface- Diffusion Model

As shown in Figures 1 and 2, the DFPSDM incorporates the following mechanisms: (a) advective flow, (b) axial dispersion and diffusion (This may be important when mass transfer rates are high or when low flow rates occur in the small scale columns.), (c) liquid-phase mass transfer resistance, (d) local adsorption equilibrium at the exterior surface of the adsorbent, (e) surface diffusion, (g) pore diffusion flux, and (h) competitive equilibrium of solutes upon the carbon surface (Competitive effects are assumed to be fully accounted for by multi-solute equilibrium expressions and there are no diffusion interactions.)

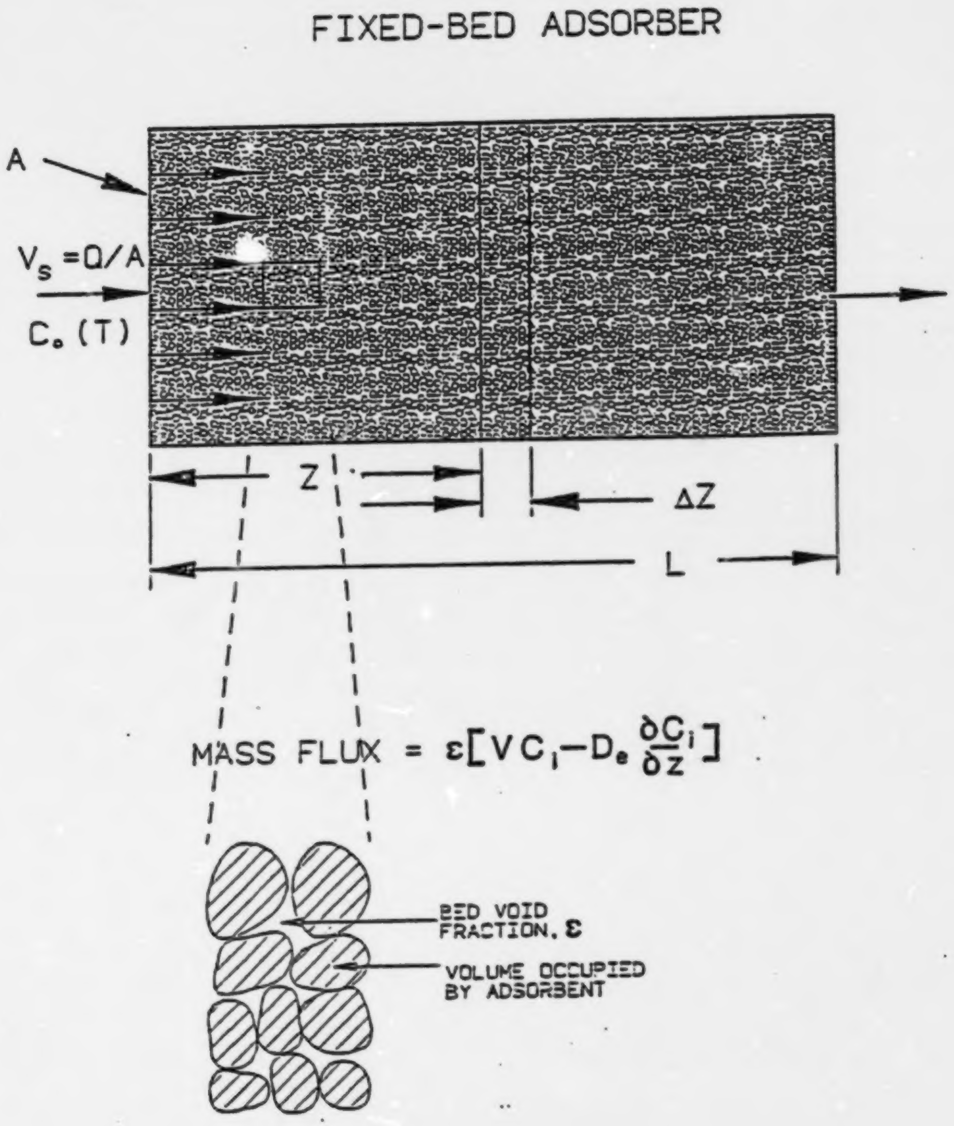
FIXED-BED ADSORBER
A
$V_s = Q/A$
C_o (T)
Z
ΔZ
L
MASS FLUX = $\varepsilon[VC_i - D_e \frac{\partial C_i}{\partial z}]$
BED VOID FRACTION, ε
VOLUME OCCUPIED BY ADSORBENT

Figure 1. Axial mass transfer mechanisms incorporated into the dispersed flow pore and surface diffusion model.

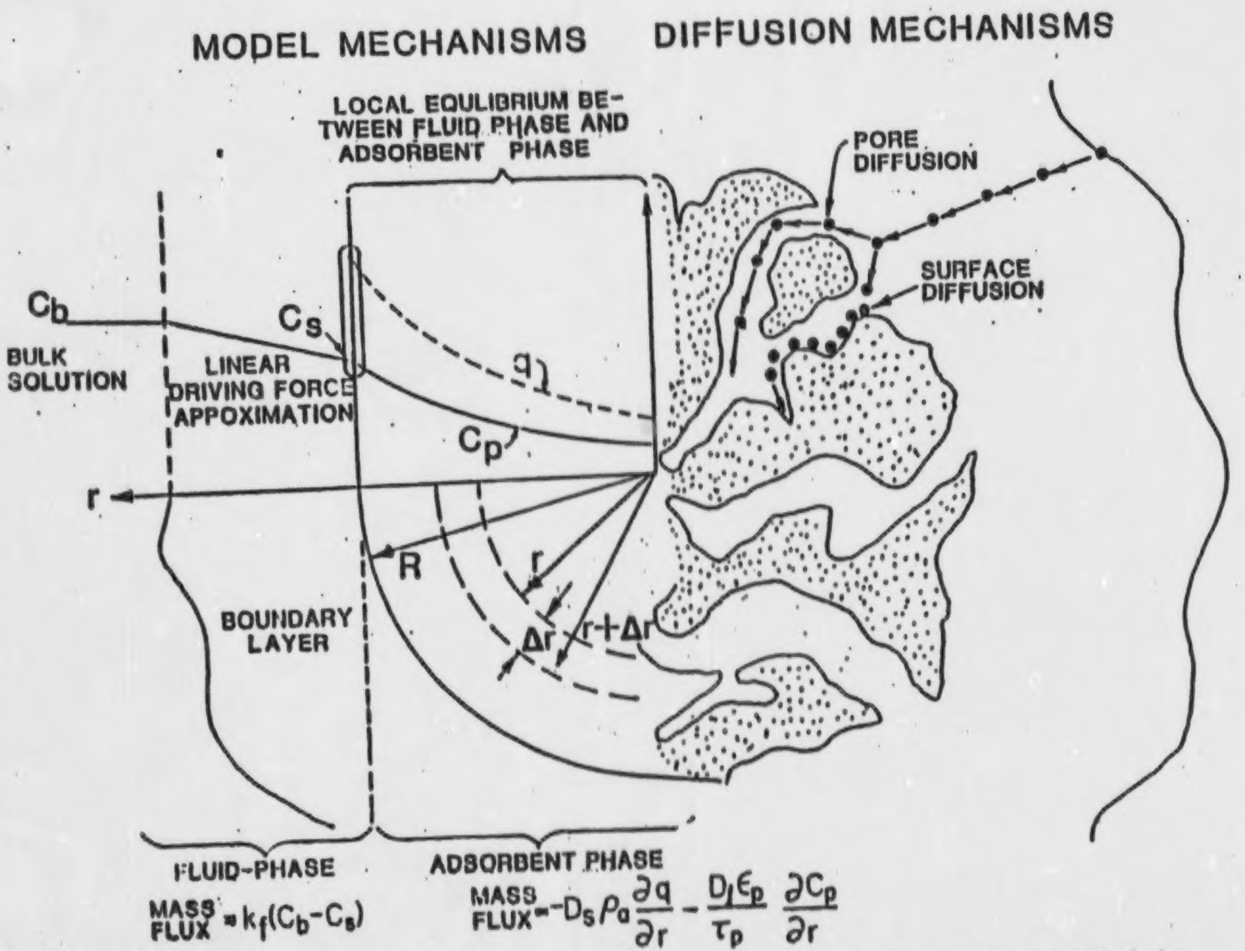
MODEL MECHANISMS
DIFFUSION MECHANISMS
LOCAL EQULIBRIUM BE- TWEEN FLUID PHASE AND ADSORBENT PHASE
PORE DIFFUSION
SURFACE DIFFUSION
C_b
C_s
BULK SOLUTION
LINEAR DRIVING FORCE APPOXIMATION
q
C_p
r
R
r
Δr
$r+\Delta r$
BOUNDARY LAYER
FLUID-PHASE
ADSORBENT PHASE
MASS FLUX $= k_f(C_b - C_s)$
MASS FLUX $= -D_s \rho_a \frac{\partial q}{\partial r} - \frac{D_l \epsilon_p}{\tau_p} \frac{\partial C_p}{\partial r}$

Figure 2. Intraparticle mechanisms and assumptions incorporated into the pore and surface diffusion model.

For DFPSDM calculations, equilibrium isotherms equations are needed to describe multicomponent interactions. To estimate the competitive effects of solutes upon the adsorbent surface in DFPSDM calculations, ideal adsorbed solution theory (IAST - Radke and Prausnitz, 1972, Luft, 1984, Crittenden _et al_. 1985 a) was used to describe multi-solute competition. Crittenden _et al_. (1985) confirmed that IAST could be used to predict competitive interactions between volatile organic chemicals (VOCs) which were used in the model calculation portion of this work. For the experimental work, demonstration of equal isotherm capacities of small- and full-scale carbons will confirm assumptions regarding solute distribution.

If the Freundlich isotherm equation is used to describe single solute behavior, IAST yields the following equation for each adsorbate:

$$\overline{C}_{p,i}(\overline{r},\overline{z},T) = \frac{\overline{Y}_i(\overline{r},\overline{z},T)Y_{e,i} - \frac{\varepsilon_p}{\rho_a}\overline{C}_{p,i}(\overline{r},\overline{z},T)C_{o,i}}{C_{o,i}\sum_{j=1}^{m}\left[\overline{Y}_j(\overline{r},\overline{z},T)Y_{e,j} - \frac{\varepsilon_p}{\rho_a}\overline{C}_{p,j}(\overline{r},\overline{z},T)C_{o,j}\right]}$$

$$\cdot \left[\frac{\sum_{k=1}^{m}\left[n_k[\overline{Y}_k(\overline{r},\overline{z},T)Y_{e,k} - \frac{\varepsilon_p}{\rho_a}\overline{C}_{p,j}(\overline{r},\overline{z},T)C_{o,i}]\right]}{n_i K_i}\right]^{n_i} \tag{1}$$

See Appendix II for the nomenclature which is used in all equations. As shown in Figure 2, Equation 1 was used to couple the liquid and solid phase concentrations at both the internal and external adsorbent surfaces.

The DFPSDM, Equations 2-9, describe the fate of an adsorbate, i, within a fixed-bed adsorber (Friedman, 1984). The liquid-phase mass balance for each adsorbate in dimensionless form is:

$$-\frac{\partial \bar{C}_i(\bar{z},T)}{\partial \bar{z}} + \frac{1}{Pe_i}\frac{\partial^2 \bar{C}_i(\bar{z},T)}{\partial \bar{z}^2} = \frac{1}{(Dg_t + 1)}\frac{\partial \bar{C}_i(\bar{z},T)}{\partial T} + 3\,St_i\left[\bar{C}_i(\bar{z},T) - \bar{C}_{p,i}(\bar{r}=1,\bar{z},T)\right] \tag{2}$$

The terms which appear in Eq. 2 account for advective flow, axial dispersion and diffusion, accumulation in the liquid-phase, and transport from the liquid- to solid-phase by liquid-phase mass transfer. The initial condition for Eq. 2 is:

$$\bar{C}_i\,(0 \le \bar{z} \le 1\;,\; T = 0) = 0 \tag{3}$$

The boundary conditions for the liquid-phase mass balance are those proposed by Danckwerts (1953):

$$1 - \bar{C}_i(\bar{z}=1,T) = \frac{1}{(Dg_t + 1)}\frac{\partial}{\partial T}\left[\int_0^1 \left[\bar{C}_i(\bar{z},T) + 3\,Dg_i \int_0^1 \bar{Y}_i(\bar{r},\bar{z},T)\,\bar{r}^2 d\bar{r}\right] \partial\bar{z}\right] \tag{4}$$

$$\frac{\partial^2 \bar{C}_i(\bar{z}=1,T)}{\partial \bar{z}\,\partial T} = 0 \quad \text{and} \quad \frac{\partial \bar{C}_i(\bar{z},T=0)}{\partial \bar{z}} = 0 \tag{5}$$

Equations 4 and 5 are derived from equating the mass flux entering and leaving the bed, assuming that transport of the adsorbate into or out of the fixed-bed by axial dispersion and diffusion is negligible when compared to advection. (This is usually referred to as a closed vessel.)

The intraparticle mass balance is expressed by:

$$\frac{1}{\bar{r}^2}\frac{\partial}{\partial \bar{r}}\left[\bar{r}^2\left[(Ed_{s,i} + D_i\, Ed_{p,i})\frac{\partial \bar{Y}_i(\bar{r},\bar{z},T)}{\partial \bar{r}} + (Ed_{p,i} - D_i\, Ed_{p,i})\frac{\partial \bar{C}_{p,i}(\bar{r},\bar{z},T)}{\partial \bar{r}}\right]\right] = \frac{Dg_{,i}}{Dg_t + 1}\frac{\partial \bar{Y}_i(\bar{r},\bar{z},T)}{\partial T} \tag{6}$$

The terms which appears in Eq. 6 account for surface and pore diffusion, and accumulation in the intraparticle-phase, respectively. The initial condition for Eq. 6 is:

$$\bar{Y}_i(0 \le \bar{r} \le 1\,, 0 \le \bar{z} \le 1\,, T = 0) = 0 \tag{7}$$

The boundary conditions for Eq. 6 are:

$$\frac{\partial}{\partial \bar{r}}\bar{Y}_i(\bar{r} = 0, 0 \le \bar{z} \le 1\,, T \ge 0) = 0 \tag{8}$$

$$\frac{Dg_i}{Dg_t + 1}\frac{\partial}{\partial t}\int_0^1 \bar{Y}_i(\bar{r},\bar{z},T)\,\bar{r}^2 d\bar{r} = St_i\left[\bar{C}_i(\bar{z},T) - \bar{C}_{p,i}(\bar{r}=1,\bar{z},T)\right] \tag{9}$$

Equation 8 results from symmetry. In Eq. 9, the liquid-phase mass flux is equated to the intraparticle-phase mass flux.

C. Dimensionless Groups which Characterize the DFPSDM

Friedman (1984) described the nature of dimensionless groups appearing in the DFPSDM equations. These groups express the relative importance of competing kinetic mechanisms, or the relative partitioning between phases or thermodynamic states. Specifying values of these dimensionless coefficients determines a solution to DFPSDM. By holding the values of these groups constant as the process is scaled up or down, the DFPSDM yields the same solution. In this manner, a properly designed RSSCT may simulate the performance of a full-scale adsorber. If all these dimensionless coefficients cannot be held constant as the process is scaled, it may be possible to ignore some of the less important effects and determine scaling factors from the more important dimensionless groups.

The following dimensionless groups appear in Eqs. 1-9:

$$Dg_{s,i} = \frac{\rho_a q_{e,i}(1-\varepsilon)}{\varepsilon C_{o,i}} \tag{10}$$

$$Dg_{p,i} = \frac{\varepsilon_p(1-\varepsilon)}{\varepsilon} \tag{11}$$

$$Dg_i = Dg_{s,i} + Dg_{p,i} \tag{12}$$

$$Dg_t = \sum_i (Dg_{s,i} + Dg_{p,i}) \qquad (i = 1, \text{no. components}) \tag{13}$$

$$St_i = \frac{k_{f,i}L(1-\varepsilon)}{vR\varepsilon} = \frac{k_{f,i}\tau(1-\varepsilon)}{R\varepsilon} \tag{14}$$

$$Ed_{s,i} = \frac{LD_{s,i}Dg_{s,i}}{vR^2} = \frac{\tau D_{s,i}Dg_{s,i}}{R^2} \tag{15}$$

$$Ed_{p,i} = \frac{LD_{p,i}Dg_{p,i}}{vR^2} = \frac{\tau D_{p,i}Dg_{p,i}}{R^2} \tag{16}$$

$$Pe_i = \frac{Lv}{D_{e,i}} \tag{17}$$

$$D_i = \frac{D_{s,i}}{D_{p,i}} \tag{18}$$

Oravitz (1984) compared the effects of Ed_s, Ed_p, St, and Pe, along with Dg, for single solute systems and provided a relationship between the four for which the same rate of transport would be seen. Crittenden *et al.* (1985 b) related the effect of individual mechanisms upon the spreading of the mass transfer zone. By assuming that an individual mechanism is dominant, that the Freundlich 1/n value is less than 1.0, and that the adsorption column is sufficiently long, the dimensionless groups may be related such that equivalent amounts of spreading will occur due to the various mechanisms. The following equation is valid for 1/n values near 1.0 and Dg values greater than 1000:

$$Pe = 3St = 15Ed_s = 15Ed_p \qquad (19)$$

These ratios will decrease with decreasing 1/n. Equation 19 can be used to estimate which mechanism is likely to control chemical transport within a fixed-bed adsorber for a given set of conditions. For instance, if the value of Ed_s is estimated to be 1.0 then a Stanton number of 5.0 will produce an equivalent amount of spreading, as will a Peclet number of 15.0. Then, if surface diffusion controls the Stanton number must be much greater than 5.0, the Peclet number much greater than 15.0.

1. Surface Solute Distribution Parameter ($Dg_{s,i}$)

The surface solute distribution parameter is a partitioning coefficient between the mass of adsorbate i on the adsorbent phase and the mass of i in the liquid phase under equilibrium conditions. It is based on the single solute capacity. As the adsorbate's affinity for the adsorbent phase increases, $Dg_{s,i}$ increases. $Dg_{s,i}$ is important in describing GAC adsorption as it is a measure of the relative adsorptive strength of a compound.

2. Pore Solute Distribution Parameter ($Dg_{p,i}$)

The pore solute distribution parameter is a partitioning coefficient between the mass of adsorbate i in the adsorbent pores and the mass of adsorbate i in the liquid phase. Because $Dg_{p,i}$ is a function of only adsorbent properties, bed void fraction and the adsorbent void fraction, it is a constant for all solutes in a given system.

3. Combined Solute Distribution Parameter (Dg_i).

Total Solute Distribution Parameter (Dg_t), and Mass Throughput (T)

Dg_i is the sum of $Dg_{s,i}$ and $Dg_{p,i}$ making Dg_i the total mass partitioning coefficient of adsorbate i in the adsorbent phase and the mass of adsorbate i in the liquid phase at equilibrium. Since $Dg_{s,i}$ is based on single solute capacities, Dg_i will also be a single solute group. The total solute distribution parameter, Dg_t, is the total equilibrium mass partitioning coefficient for all solutes present.

Throughput, T, is the dimensionless time scale used in the fixed-bed model. It may be expressed as ratio of the mass of solute fed to the mass of solute adsorbed as a single component in equilibrium with the influent bulk phase concentration. T is defined as:

$$T_i = \frac{t}{\tau(Dg_i + 1)} \qquad (20)$$

4. Stanton Number (St_i)

The Stanton number is a ratio of the rate of solute transport by film transfer to the rate by advection. As St_i increases, the rate of advective transport becomes the limiting transport mechanism. The role of the Stanton number in fixed bed adsorption may be estimated by ignoring other mass transfer mechanisms in the liquid-phase mass balance and solving for the concentration profile assuming steady-state operation (Hand, 1984). Kirwan (*loc. cit.* Fleck *et al*. 1973) developed an analytical solution for the case in which liquid phase mass transfer controls, constant pattern conditions exist, and 1/n is less than 1.0:

$$T_i = \frac{Dg_i}{3St_i(Dg_i + 1)} \left[1 + \ln(C_i/C_{o,i}) - (n-1)\ln[(1-C_i/C_{o,i})^{(1/(n-1)}] + \frac{1/n}{1/n - 1} \sum_{k=1} \frac{1/n}{k[k(1-1/n) + 1/n]} \right] + 1 \qquad (21)$$

Where n is the reciprocal of 1/n.

Under normal operating conditions, this function decays rapidly. The portion of the mass transfer zone can be attributed to film transfer effects can be estimated using the Kirwan solution and mass transfer correlations.

5. Surface Diffusion Modulus ($Ed_{s,i}$)

The surface diffusion modulus is the ratio of the rate of solute transport by intraparticle surface diffusion to that of advection. As $Ed_{s,i}$ increases, the rate of advective transport becomes dominant over intraparticle diffusion. As Ed_s becomes much greater than 1/5 St_i, film transfer controls and as $Ed_{s,i}$ decreases well below 1/5 St, surface diffusion controls. In most fixed-bed adsorption processes, the rate of film transfer is rarely the limiting mass transfer mechanism and the Stanton number is usually large enough to be considered unimportant. The surface diffusion modulus is often an important consideration as the mass transport in fixed-bed adsorption is often surface diffusion controlled.

6. Pore Diffusion Modulus ($Ed_{p,i}$)

The pore diffusion modulus compares the transport rate by pore diffusion to the advective rate. Like $Ed_{s,i}$, as $Ed_{p,i}$ increases, advective transport becomes controlling. Usually pore diffusion is not an important adsorption mechanism, especially in long beds where the mass transfer zones of influent components separate.

7. Peclet Number (Pe_i)

The Peclet number based on column length and interstitial velocity is the ratio of the rate of advection to the rate of dispersion. As the rate of transport due to dispersion increases, the Peclet number decreases. Dispersion is due to a number of phenomena, including molecular diffusion, eddy diffusion, and hydrodynamic dispersion. These mechanisms are discussed by Ogata (1970), Fried (1975), and Greenkorn (1983). The Peclet number based on particle diameter, $Pe_{D,i} = 2Rv/D_{e,i}$, is an alternative form of the expression.

D. Development of Scaling Equations

Six independent dimensionless quantities, $Dg_{s,i}$, $Dg_{p,i}$, $Ed_{s,i}$, $Ed_{p,i}$, Pe_i, and St_i appear in Eqs. 1 - 9. The mechanisms by which solute is transported in a fixed-bed are described by the Stanton number, surface diffusion modulus, pore diffusion modulus, and Peclet number. Each mechanism will affect the rate at which solute travels through the bed. For perfect simulation of a full-scale adsorber each of the six independent dimensionless groups appearing in Eqs. 2 - 10 must remain constant as a full-scale adsorber is scaled down to the size of a small-column test. By setting the dimensionless groups of a small-scale adsorber (SC) equal to those of a large-scale column (LC), relationships between key design variables were found (Frick, 1982).

In this study, the important design and operation parameters were related to the adsorbent radii in the small- and large- scale adsorbers. Because the development of proper scaling equations required some assumption of the relationship between adsorbent particle radius and the surface diffusion coefficient, D_s, two approaches were used. Preliminary work by Dobrzelewski (1985) indicated that, at concentrations of 10.0 µmol/L, the value of D_s for trichloroethene was not significantly dependent on the particle radius. The development of scaling equations in Section II.D.1., assume that the surface diffusion coefficients are constant with particle size based upon laboratory measurements of D_s (Dobrzelewski, 1985). Consequently, perfect similarity may be achieved. Another study for p-nitrophenol at 64.4 μmol/L found possible dependencies of the surface diffusion coefficient on particle size. The second approach assumes some change of the surface diffusion coefficients with adsorbent particle radius. Perfect similarity is not attainable in the second approach. Consequently, the scaling equations are developed to maintain similar surface diffusion effects because film transfer effects may be calculated using the Kirwan solution (Eq. 21) and mass transfer correlations discussed in Section IV.A.3. In Section II.D.2., another set of scaling equations is developed where the particle radius is assumed proportional to the surface diffusivity based on other experimental evidence (Schneider, 1982). Section II.D.3 presents a general method for determining the proper scaling equations by measurement of surface diffusivities of small- and full-sized carbons for one solute of the influent matrix.

1. Perfect Similarity Assuming Constant Surface Diffusivity

By equating the surface diffusivity modulus, $Ed_{s,i}$, and the pore diffusivity modulus, $Ed_{p,i}$ of a small column to that of a full-scale adsorber, the proper relationship between the small column and large column empty bed contact times (EBCTs) may be found.

$$\frac{EBCT_{LC}}{EBCT_{SC}} = \left[\frac{R_{LC}}{R_{SC}}\right]^2 = \frac{t_{LC}}{t_{SC}} \qquad (22)$$

See Appendix III for the details of scaling equation development. The relationship which is defined in Eq. 22 is valid for various combinations of mass transfer resistance controlling the intraparticle resistance: (a) pore diffusion, (b) surface diffusion or (c) both pore and surface diffusion control. Accordingly, Eq. 22 would be valid for pore, surface, or both pore and diffusion controlled processes.

To obtain Eq. 22, the solute distribution parameters, Dg_i, were assumed to be the same for carbons in the small and full scale processes which is valid if theses properties are all identical: (a) the equilibrium capacity (b) the bed void fractions, (c) particle densities are the same and (d) the influent concentrations must be the same. In addition, the pore diffusivities and the surface diffusivities must be identical. In addition, the packed-bed residence time, τ, is substituted with the equivalent expression, εEBCT, to use the more conventional term, empty-bed contact time. The time frame acceleration of the RSSCT is also given by Eq. 22 by multiplying the EBCT of both adsorbers by the treatment objective expressed in total bed volumes fed. The ratio t_{LC}/t_{SC} is a measure of the time savings given by the RSSCT and is determined by the magnitude of the size reduction of the original GAC in the full-scale system for the RSSCT.

Similarly, in order to have identical Stanton Numbers, St_i, the liquid-phase mass transfer coefficients may be related by the following equation:

$$\frac{k_{f,SC}}{k_{f,LC}} = \frac{R_{LC}}{R_{SC}} \tag{23}$$

In order to satisfy the constraints set forth in Eq. 23, the Sherwood numbers of the small and large columns must be equal for all the adsorbates. Most liquid-phase mass transfer correlations (Treybal, 1980) have the following general form:

$$Sh_i = F(Re_i, Sc_i) \tag{24}$$

The correlations of Wilson and Geankopolis (1966) and Williamson and Geankopolis (1963), have been shown to accurately determine film transfer coefficients in fixed-beds adsorbers (Thacker _et al._, 1983, 1984, Crittenden _et al._, 1978a,b, 1980.). Both correlations have the form of Eq. 24. Consequently, the hydraulic loading of the small and large scale columns are related to the particle size by this expression:

$$\frac{V_{SC}}{V_{LC}} = \frac{R_{LC}}{R_{SC}} \tag{25}$$

Equation 25 ensures that the Reynolds number of the small-scale process is the same as the large-scale process. Since the Reynolds and Schmidt numbers are identical for the large and small scale columns, Fried (1975), Ebach and White (1958), and Miyuachi and Kikuchi (1975) have shown that Peclet numbers which are based on particle size, Pe_d, will be identical. Furthermore, the column length to particle size ratios, L/R, for the small- and large-scale columns are equal. This implies that the small- and large-scale column have equal Peclet numbers which are based on column length (Pe_L). Consequently, Eq. 25 guarantees exact similarity whether plug flow or dispersed flow conditions exist.

2. Similarity for Surface Diffusion Controlled Processes Assuming Surface Diffusivity Proportional to Adsorbent Particle Radius

Equation 19 can be used to determine which mechanism is likely to control chemical transport within a fixed-bed adsorber for a given set of conditions. From Eq. 19, surface diffusion may be assumed to be the controlling process where Ed_s is much less than St/5, and Pe/15 and much larger than Ed_p. The following scaling procedure is applicable where surface diffusion is the controlling process and the effects of other mechanisms are relatively unimportant.

The RSSCT procedure described in the previous section assumes that the diffusion coefficients of the smaller carbon would be equal to the diffusion coefficients of the full-sized GAC. Schneider (1982) measured the solid diffusion coefficient for sieved fractions of two types of GAC. A least-squares analysis on this data yields a slope of one on the log-log plot. This implies that the surface diffusivity, D_s, is a linear function of the adsorbent particle size. Figure 3 shows the relationship between R and D_s of the carbon types F-300 and Hydraffin 71 for p-nitrophenol at initial concentrations of approximately 73 µmol/L. The impact of the diffusivity dependence on the particle size was examined by assuming the following relationship between D_s and the particle radius which would be well within the observed confidence limits for the data of Schneider (1982):

$$\frac{D_{s,LC}}{D_{s,SC}} = \frac{R_{LC}}{R_{SC}} \tag{26}$$

By equating the surface diffusivity modulus, $Ed_{s,i}$ of a small column to that of a full-scale adsorber, and substituting Equation 26 for $D_{s,i}$, an alternate scaling relationship between the small column and large column empty bed contact times (EBCTs) may be found.

$$\frac{EBCT_{LC}}{EBCT_{SC}} = \frac{R_{LC}}{R_{SC}} = \frac{t_{LC}}{t_{SC}} \tag{27}$$

The time savings of the RSSCT that is designed from Eq. 27 is not as great as is the operating rate of an RSSCT that is designed from Eq. 22.

Using Equation 27 and equating the Stanton Numbers, St_i, the liquid-phase mass transfer coefficients may be related by the following equation:

$$k_{f,LC} = k_{f,SC} \tag{28}$$

Similarly, through the Wilson or Williamson correlations, the hydraulic loading of the small and large scale columns are related to the particle size by this expression:

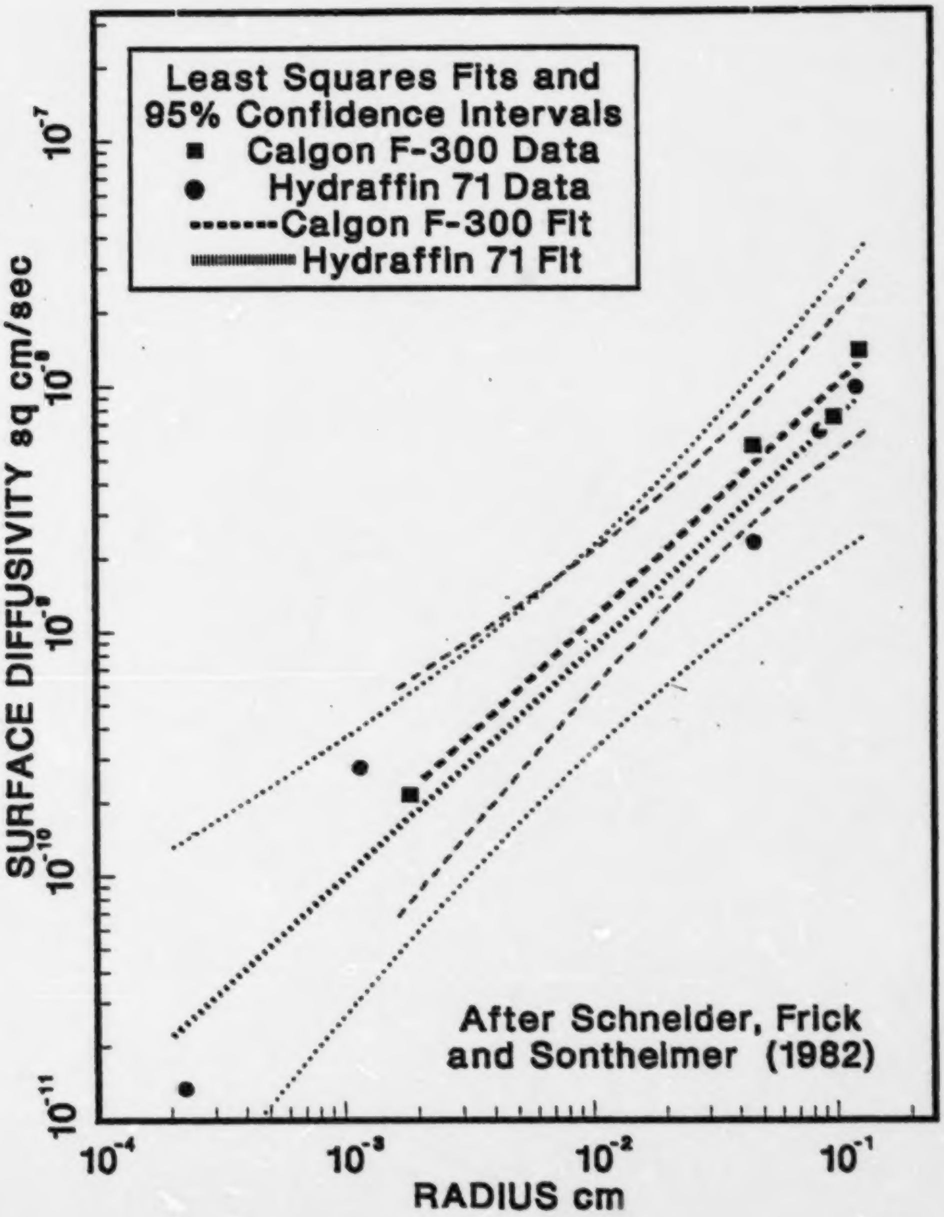

Figure 3. p-Nitrophenol surface diffusivity of Hydraffin 71 and Filtrasorb 300 particle sizes with least-squares fits and 95% confidence intervals shown. (After Schneider, Frick, and Sontheimer, Univ. of Karlsruhe, 1982).

$$\frac{V_{SC}}{VLC} = \left[\frac{R_{SC}}{RLC} \right]^2 \qquad (29)$$

Unfortunately, the use of Eqs. 27 and 29 will result in an RSSCT design that is neither practical nor possible to conduct because the Reynolds numbers will be very low. As a result, the Peclet number based on column length (Pe_L) for the small-column would be reduced to where axial diffusion effects become the controlling mechanism. Therefore, for the purposes of RSSCT design, Eq. 29 should not be used.

To ensure that the effects of dispersion remain remain negligible, Eq. 25 could be used. As discussed above, Eq. 25 ensures that the Reynolds number of the small-scale process is the same as the large-scale process. Since the Reynolds and Schmidt numbers are identical for the large and small scale columns, Fried (1975), Ebach and White (1958), Miyuachi and Kikuchi (1975) have shown that Peclet numbers which are based on particle size, Pe_d, will be identical. Equations 25 and 27 do not ensure equal column length to particle size ratios, L/R, for the small- and large-scale columns which is necessary to have equal Peclet numbers based on column length. Although the small- and large- scale column will not have equal Pe_L, the effects of dispersion, for most fixed-bed adsorbers, is negligible. To verify this, the small-column study may be conducted to evaluate the length of the mass transfer zones. The experimentally determined mass-transfer zone (MTZ) length can be used to estimate the Peclet number of the MTZ and the effect of axial dispersion can be shown to be negligible.

Therefore, Eqs. 25 and 27 could be used where the surface diffusivity is known to vary linearly with particle size. However, if Eqs. 25 and 27 are used, then the Stanton numbers of the RSSCT will be larger than those of the full-scale adsorbers using Eqs. 25 and 27. Consequently, the mass-transfer zones in the RSSCT will be smaller than in the full-scale system. Where film transfer is the dominant mass transport mechanism, the chemical breakthrough profiles in the RSSCT will be much sharper and shorter than would be found in the full-scale adsorber. Where the mass transport is intraparticle diffusion controlled, little difference would be expected in the chemical breakthrough profiles between RSSCT and full-scale adsorber. The difference in the mass-transfer zone lengths due to film transfer can be calculated using the Kirwan solution (*loc. cit.* Fleck *et al.*, 1973, Hand *et. al.*, 1984) and film transfer correlations (Williamson, 1963, Wilson, 1966). In addition, it is less important to simulate the mass-transfer zone of a film transfer controlled process because the MTZ's are very short. It is appropriate, then, to define scaling relationships to simulate the effects of intraparticle mechanisms. The use of Eq. 27 will ensure that the proper EBCT will be selected for the surface diffusion moduli of the RSSCT to equal the surface diffusion moduli of the full-scale adsorber where the surface diffusivity is proportional to the particle radius. Equation 25 will ensure that the effects of film transfer are reduced further for the small-column test.

Equation 25 may be used to determine a reasonable hydraulic loading rate for a RSSCT. However, the resulting design requires the length of the RSSCT to be equal to the length of the full-scale process. The headloss and total volume requirements for such a test may be quite undesirable, especially if the test were to be conducted in the laboratory. It may be possible to reduce the loading rate in the RSSCT and maintain the EBCT defined by Eq. 27. This would reduce the total influent volume that is required for the RSSCT. The headloss would be reduced due to the shorter length required and the and the lower loading rate. To determine an appropriate loading rate that will yet limit the effects of dispersion, a minimum Reynolds number for the RSSCT must be chosen.

Fried (1975) described the magnitude of dispersive effects (Peclet number) in terms of the product of the Reynolds and Schmidt numbers. Figure 4 displays the relationship between Peclet number and Reynolds-Schmidt numbers product. The region (d) of purely mechanical dispersion is the normal operating region of most fixed-bed adsorbers. The minimum Reynolds number may be chosen as the Reynolds number at the lower limit of the of this region. The minimum value of the Re·Sc product that may be used is near 200 from Fig. 4 or a more conservative minimum Re·Sc product of 1000 may be chosen to ensure an RSSCT design operates in the mechanical dispersion region (d) of Fig. 4. This will ensure that the dispersive effects in the RSSCT are caused by the same mechanical dispersion mechanism as in the full-scale system. Because the Schmidt number is a constant in this calculation, the Re·Sc product may be used in determining the appropriate Reynolds number reduction ratio. To obtain the value of the Reynolds number at this limit, the Schmidt number may be estimated using the known liquid diffusivity of a influent component, it may be estimated using parameter correlations that are described in section IV.A., or it may be roughly estimated using typical liquid diffusivities from typical values. The ratio of the minimum desirable Reynolds number of the RSSCT, $Re_{SC,min}$, and the Reynolds number of the prototype full-scale adsorber may be used to calculate the minimum hydraulic loading rate of the RSSCT by the following equation:

$$\frac{V_{SC}}{V_{LC}} = \frac{R_{LC}}{R_{SC}} \cdot \frac{Re_{SC,min}}{Re_{LC}} \qquad (30)$$

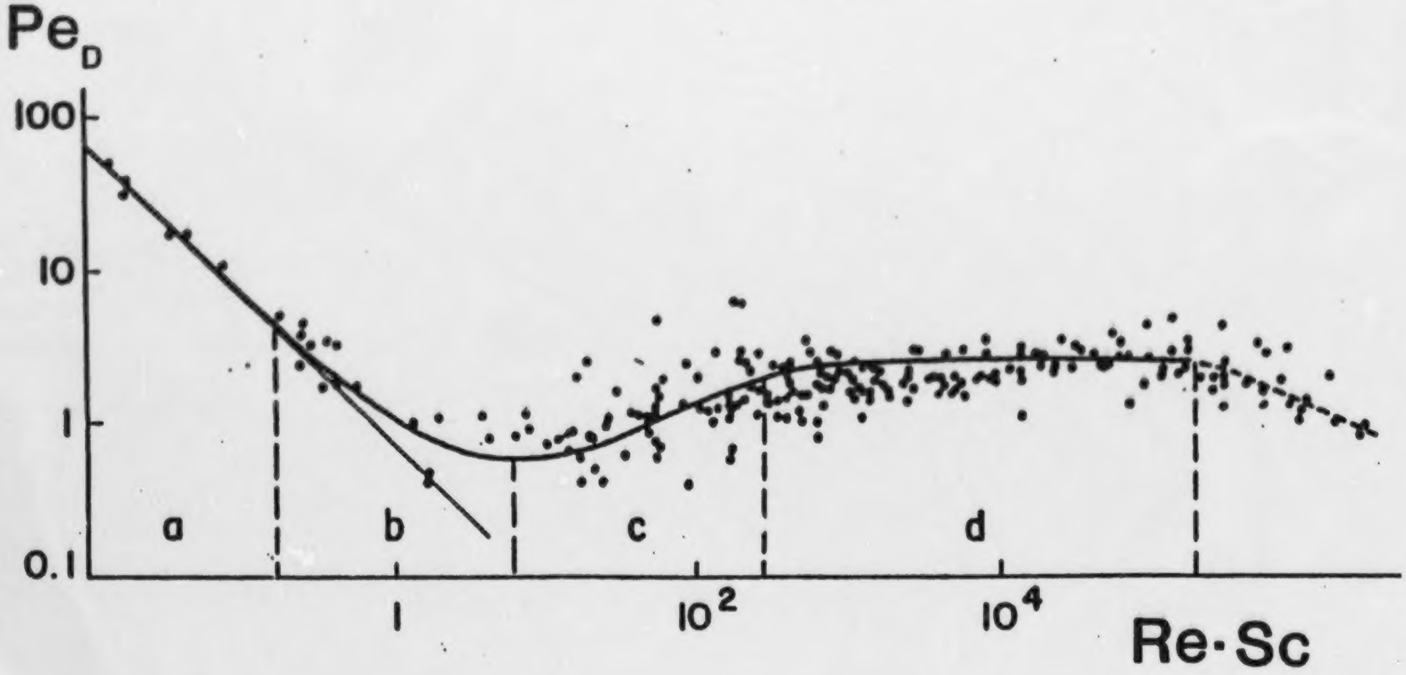

Figure 4. The various regimes of dispersion: (a) pure molecular dispersion, (b) predominant molecular diffusion, (c) predominant mechanical dispersion, (d) pure mechanical dispersion. After Fried (1975).

3. Similarity where Measured Surface Diffusion Coefficients are Available for a Solute

Discussion in the preceding sections has been limited to cases where the surface diffusion coefficient is either assumed constant or assumed to be linearly proportional to the adsorbent particle size. Because there is some experimental evidence for both cases, it is recommended that D_s values of a compound for the desired application be measured for GAC samples in both full- and test- scale adsorber. The ratio $D_{s,i,LC}/D_{s,i,SC}$ may be incorporated into the contact time scaling equation to yield more generally applicable scaling criterion:

$$\frac{EBCT_{LC}}{EBCT_{SC}} = \left[\frac{R_{LC}}{R_{SC}} \right]^2 \cdot \frac{D_{s,SC}}{D_{s,LC}} = \frac{t_{LC}}{t_{SC}} \qquad (31)$$

Only Eqs. 30 and 31 are needed to specify the operating characteristics of a small-column test to simulate a large-scale adsorber. Although, it is important to recognize that the small-column test must operate at the same influent conditions of temperature and solute concentrations as the full scale adsorber.

III. EXPERIMENTAL MATERIALS AND METHODS

To experimentally evaluate the accuracy of this procedure in predicting the breakthrough profiles of a large adsorber, a RSSCT was designed to simulate the performance of a pilot-scale adsorber. The particle size for the RSSCT was selected to be as small as possible, thus shortening the duration of the experiment and yet be large enough to maintain a practicable sampling schedule and avoid excessive headloss. In order to conduct a pilot-scale adsorber study in a reasonable period of time, the EBCT and the influent characteristics were carefully chosen. The method was tested further by using RSSCT's to simulate the performance of pilot-scale adsorbers treating raw well water contaminated with chlorinated and aromatic organic compounds.

A. Apparatus and Materials

All laboratory column experiments were conducted at 10°C, a typical groundwater temperature for the northern United States. These experiments were performed in a temperature-controlled room where temperatures of 10-12°C were maintained. Field RSSCT studies were conducted at the operating temperatures of the pilot-scale adsorbers, 13-16°C. All experimental equipment was constructed of glass, teflon, or stainless steel to minimize adsorption of organics.

Glass columns (Ace Glass, Inc.) of 5.0 cm and 1.1 cm diameter were used for pilot-scale and RSSCT studies, respectively. The effects of channeling and wall effects were avoided by exceeding the ratio of the particle diameter to column diameter above 50. To minimize the bed volume, the particle to column diameter ratio was kept near 50. This minimized the required influent volume while keeping the wall channeling effects negligible. Teflon endcaps were seated with Teflon or Teflon-wrapped rubber o-rings on each end of the column to ensure a proper seal. Spherical borosilicate glass beads (3 or 5 mm diameter) were used to support the fixed-bed and to minimize dispersive effects. Porous glass plates or glass wool plugs provided level and fixed boundaries for the carbon bed. A thin layer of Teflon was used around glass plates to seal the edges against the glass column walls eliminating flow around the edges of the plates. Figure 5 shows the column apparatus.

Feed solutions for the laboratory studies were prepared by mixing a concentrated aqueous solution of the volatile organic chemicals with laboratory reagent water in a tightly-closed, headspace-free, mixing vessel prior to being fed into the column. The concentrated solution was applied to the mixing vessel with a positive displacement metering pump (ISCO, Inc.). The reagent water was introduced to the mixing vessel using positive displacement pumps (Fluid Metering, Inc.).

The concentrated solution of volatile organic chemicals was contained in a headspace-free, fifty-liter, teflon, gas-sampling bag. The gas sampling bag was supported by a water bath to minimize the strain on the seams of the bag. The feed was introduced to the columns through a two-way stainless-steel sampling valve (Whitney Co.) to the bottom endcap. Column effluent was collected from a two-way sampling valve (Hamilton Co.) at the top of the column in a stoppered 12 gal carboy. Figure 6 displays the diagram of the experimental apparatus.

Feed for the field studies was obtained directly from the influent line of the pilot-scale study. The raw water was introduced to the field RSSCT's using positive displacement pumps (Fluid Metering, Inc.). Figure 7 displays the diagram of the field RSSCT apparatus.

The volume between the carbon bed and the effluent sampling valve was estimated to consider possible end effects. The hydraulic retention time in

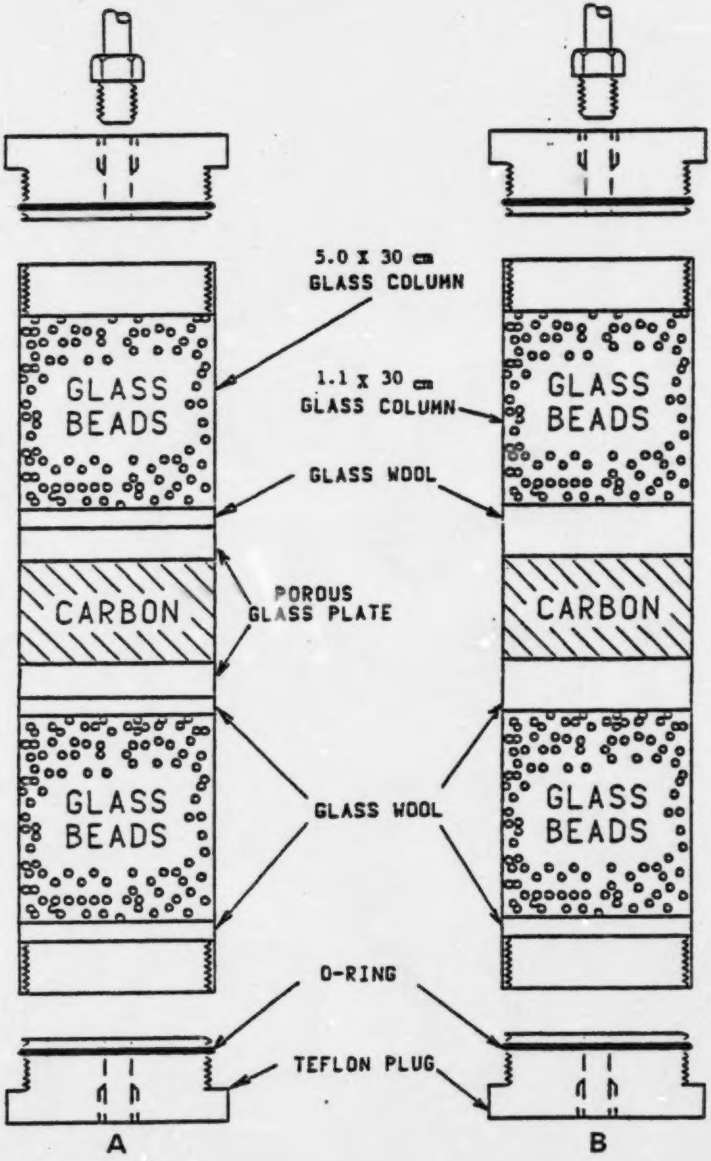
5.0 X 30 cm
GLASS COLUMN
1.1 x 30 cm
GLASS COLUMN
GLASS BEADS
GLASS BEADS
GLASS WOOL
CARBON
CARBON
POROUS
GLASS PLATE
GLASS BEADS
GLASS BEADS
GLASS WOOL
O-RING
TEFLON PLUG
A
B

Figure 5. Experimental fixed-bed adsorption column diagram for (a) laboratory pilot-scale column and (b) RSSCT adsorbers.

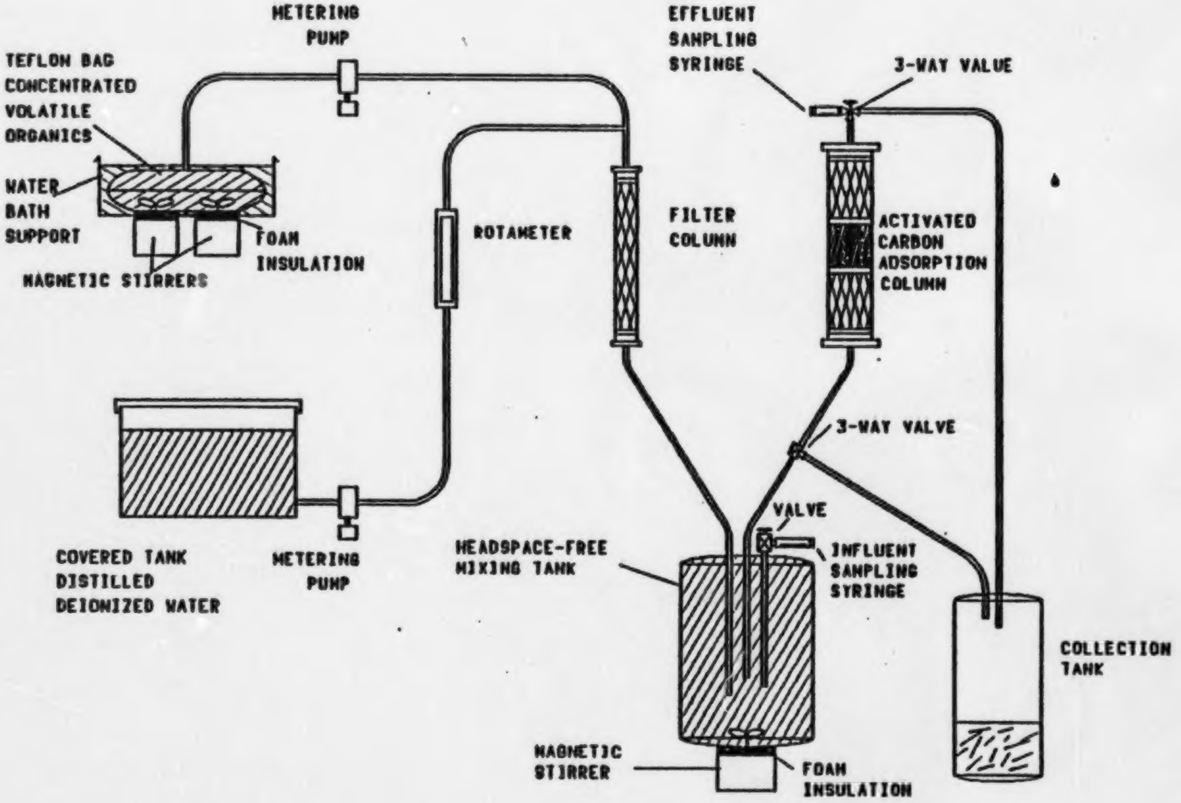
METERING PUMP
TEFLON BAG CONCENTRATED VOLATILE ORGANICS
WATER BATH SUPPORT
FOAM INSULATION
MAGNETIC STIRRERS
ROTAMETER
FILTER COLUMN
EFFLUENT SAMPLING SYRINGE
3-WAY VALUE
ACTIVATED CARBON ADSORPTION COLUMN
3-WAY VALVE
VALVE
INFLUENT SAMPLING SYRINGE
HEADSPACE-FREE MIXING TANK
COVERED TANK DISTILLED DEIONIZED WATER
METERING PUMP
MAGNETIC STIRRER
FOAM INSULATION
COLLECTION TANK

Figure 6. Laboratory study adsorber equipment diagram.

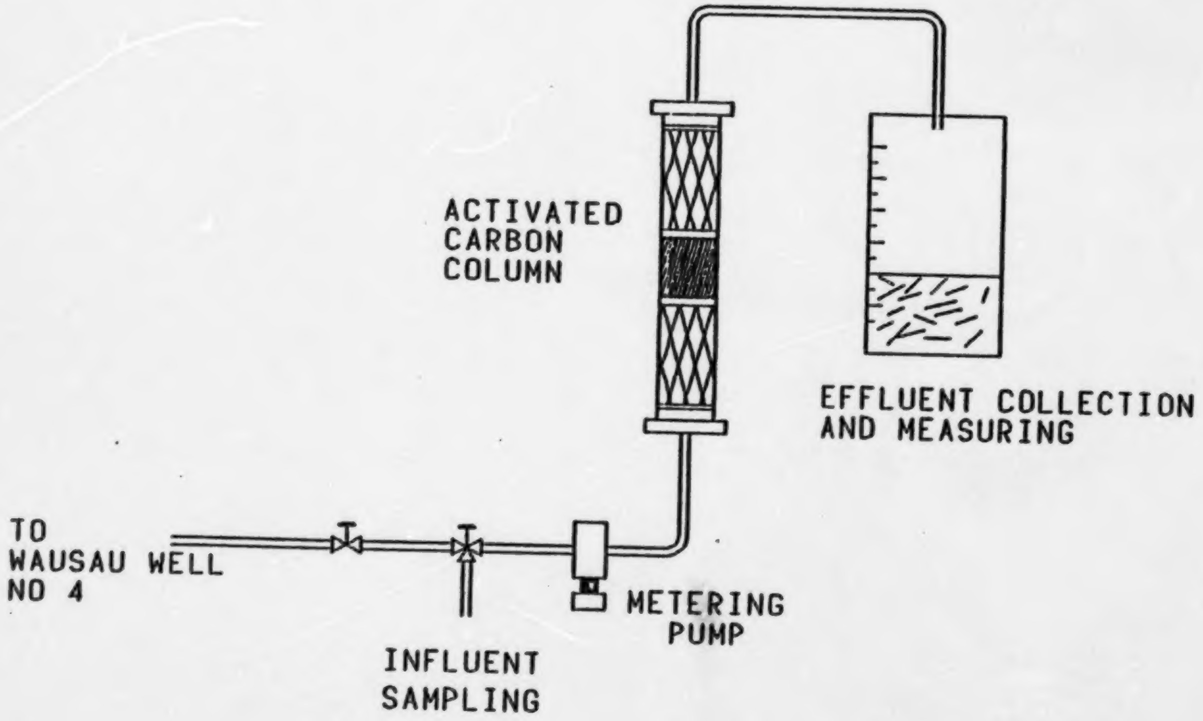
ACTIVATED
CARBON
COLUMN
EFFLUENT COLLECTION
AND MEASURING
TO
WAUSAU WELL
NO 4
METERING
PUMP
INFLUENT
SAMPLING

Figure 7. Field-study RSSCT equipment diagram.

the column was negligible when compared to the time corresponding to the spreading of the chemical fronts. Dispersion at the column inlet and outlet, therefore, should not affect experimental results.

B. Experimental Procedures

All glassware and equipment were washed with Micro laboratory detergent and then rinsed with tap water, distilled-deionized water, and methanol. Glassware was baked in a 230°C oven to remove any remaining organics and then wrapped in aluminum foil to store. Teflon and stainless steel parts were baked in a 150°C oven to remove any remaining organics and then wrapped in aluminum foil to store.

1. Laboratory Study Procedure

The feed concentrate was prepared by injecting a stock methanol solution of the VOCs into the Teflon bag containing distilled, deionized and filtered water purified by a Milli-Q reagent water system. The contents of the Teflon bag were allowed to mix using magnetic stirrers for twenty-four hours. Flow from the Teflon bag was set prior to introduction of flow to the columns and measured by weight. Flow of the dilution reagent water was set and measured by volume and by a calibrated flowmeter. The total flow was monitored continually during the experiments at the effluent collection point.

All influent lines were flushed with feed solution prior to start-up, and influent samples were analyzed to insure complete mixing and flushing before starting the experiment. Influent samples were also collected periodically throughout the experiment from a sampling valve in the mixing vessel without interrupting flow to the column. Turbulent mixing was observed in the mixing vessel.

The pH of the influent and effluent was monitored occasionally throughout the laboratory experiments using an Orion model 501 digital pH/mV meter. The electrode was calibrated repeatedly during the experiments to monitor any response drift.

2. Field Study Procedure

Flow to the RSSCT was set prior to introduction of flow to the columns and measured by volume. The total flow was monitored continually during the experiments at the effluent collection point. Due to the high iron content of the water, 5 mg/L, special care was taken to remove trapped air from the RSSCT to prevent iron hydroxide precipitation, which could fill the column voids or block the carbon pores.

All influent lines were flushed with raw water prior to start-up. Influent samples were also collected periodically throughout the experiment from an influent sampling valve.

The pH of the influent was assumed to be the the same as the pilot-scale influent pH.

C. Chemicals and Milli-Q Water System

All chemicals that were used in the laboratory study were reagent grade or better. 1,2-dibromoethane, bromoform, and chlorodibromomethane were obtained from Aldrich Chemical Co., Milwaukee, Wisconsin. Methanol, 2,2,4-trimethylpentane, chloroform and trichloroethene were obtained from Burdick and Jackson Co., Muskegon, Michigan. Tetrachloroethene and 1,1,1-trichloroethane were obtained from J.T. Baker Chemical Co., Phillipsburg, New Jersey. Two activated carbons were used in the laboratory and field studies; Calgon's (Pittsburgh, PA) Filtrasorb-400 and Westvaco's (Charleston, SC) WV-G. Water for influent and other solution preparation was distilled, deionized, and filtered by a Milli-Q purification system.

D. Chemical Analysis

The volatile organic compounds (VOCs) were analyzed using gas chromatographs (GC), and liquid-liquid extraction (LLE) and purge and trap methods (EPA 1979). Laboratory samples were prepared for GC analysis using LLE. The samples for LLE method were extracted using 5-30 ml of solution with 5-10 ml 2,2,4-trimethylpentane following the procedure which was described by Mieure (1977). 1,1,1-trichloroethane was used as the internal standard for the LLE method. Electron capture and photo-ionization detectors were used for identification. Chemical analyses of samples from both pilot-scale adsorbers and RSSCT's were performed by Zimpro, Inc. (Rothschild, WI) using purge and trap methods.

1. Laboratory Study Analysis

Effluent samples were collected from a two-way sampling valve at the column outlet at designated times by directing flow to fill a glass sampling syringe. These samples containing organic solutes were injected under the surface of a preweighed amount of iso-octane. The extraction ratios used were measured by weight. Sample vials were shaken vigorously for at least 30 seconds to extract, and 2 ml of the organic phase was drawn off for analysis and stored if necessary at 4°C in inverted, headspace-free sample vials with teflon lined caps.

When possible, the samples were injected immediately into a Hewlett-Packard model 5840 or 5880 gas chromatograph. Concentration was determined from calibration curves obtained by injecting standard solutions between samples. Water phase concentration was then back-calculated using extraction ratios. A FORTRAN routine was used to convert times, chromatographic results, calibration parameters, and extraction weights to adjusted times and water phase concentrations.

2. Field RSSCT Chemical Analysis

Influent and effluent samples were collected from two-way sampling valves at designated times by directing flow to fill duplicate 45 ml glass sample vials. These samples containing organic solutes were preserved from biodegradation by adding two drops of saturated aqueous mercuric chloride solution. Sample vials were tightly capped, head-space free then shaken vigorously to distribute the mercuric chloride. The samples were refrigerated until analyzed.

E. Carbon Preparation

Representative samples of the GAC were obtained by mixing and splitting the GAC. The GAC from these samples (12x40 mesh) was used directly in the pilot-scale work. A smaller activated carbon, 60x80 mesh, was used in RSSCT studies. The smaller carbon for the RSSCT experiments was obtained by crushing 10 gram samples of the original carbon to a smaller size. The crushed carbon was sieved, retaining the desired size fraction, and recrushed. The crushing and sieving was continued until all the carbon had passed through the 60 mesh sieve tray. The GAC which was retained on a 80 mesh sieve was then washed with Milli-Q water and dried overnight at 105°C.

F. Flow Measurement and Determination of Bed Volumes Fed

Total volume of flow for the field pilot-scale studies was determined by a direct reading of a flow measurement device. Total flow in the other studies, the laboratory and field RSSCT studies and the laboratory pilot-scale study was determined by the measurement of the flowrate before and after each sampling and pump adjustment. The total flow between sampling times was calculated from the elapsed time between flow measurements and the average flowrate for that interval. The total flow for studies other than the field pilot-scale studies was determined at any sampling time by the sum of the total flow between intervals. The total flow was measured directly as a check and compared favorably to this method. An alternate method measured total flow directly measuring elapsed time between sampling intervals and the total effluent volume for that interval.

The volume of the bed was measured before and after operation, some settling of the longer pilot-scale columns occurred in the field studies. For the calculation of the number of bed volumes fed (BVF), the initial bed volume was used.

THIS PAGE INTENTIONALLY LEFT BLANK.

IV. THEORETICAL VERIFICATION OF SCALING EQUATIONS

The dispersed flow homogeneous solid diffusion model (DFHSDM) and the DFPSDM were used to predict both full scale and RSSCT performance as a check on the scaling procedure. The computer algorithms are described by Friedman (1984). Model predictions were obtained for a full-scale adsorber with typical operating characteristics as shown in Table 1. Also displayed in Table 1 are the operational and design parameters for a RSSCT which is designed to simulate full scale performance and a RSSCT which is just long enough to measure the length of the mass transfer zone (MTZ).

Equations 22 and 25 were used to determine the RSSCT parameters which is designed to simulate full scale performance. In order to simulate 72,800 bed volumes of treatment for the full-scale adsorber, it would take only 2.65 days using the RSSCT. This represents about 1.05 percent of the 252 days that would be required for a pilot study with an EBCT of 5 minutes. In general, the time to run the RSSCT, t_{SC}, may be related to the time to run the large-scale adsorber, t_{LC}, from this equation:

$$t_{SC} = t_{LC} \left[\frac{R_{LC}}{R_{SC}} \right]^2 \tag{32}$$

As shown in Table 1, another advantage of the RSSCT is that only 67.2 liters of water are required for the RSSCT which could be transported to a central laboratory to conduct the test.

A. Chemical and Physical Property Estimation

To obtain solutions for these models, it is necessary to measure or estimate various equilibrium and kinetic parameters. The correlations which were used in this work are the identical to those used by Friedman (1984); the correlations are presented here for completeness.

The parameters for the chlorinated aliphatics were measured in our laboratory and those for the other adsorbates were estimated from

Table 1. Comparison of Column Parameters for Scale-Down of a Large Scale Column to a Small-Column Test: Design and Operational Parameters for a Full-Scale Adsorber, a rapid small-scale column test (RSSCT) (a) which is designed to simulate full scale performance, and a RSSCT (b) which is just long enough to measure the length of the mass transfer zone (MTZ) of TCE as a single solute.

		Full Scale Adsorber	RSSCT (a)	RSSCT (b)
GAC Packing Characteristics				
ρ_a	g/cm^3	0.8034	0.8034	0.8034
ε		0.40	0.40	0.40
R	cm	0.0513	0.00525	0.00525
Column and Flow Specifications				
Column Diameter	cm	244.	0.525	0.525
Column Length	cm	41.7	4.26	1.86
EBCT	s	300	3.14	1.37
CSA	cm^2	46,700	0.216	0.216
V_s	m/hr	5.00	48.9	48.9
Bed Volume	cm^3	1,946,000	0.923	0.403
Flow rate	cm^3/min	389,000	17.6	17.6
BVF_{max}		72,800	72,800	72,800
Required Volume	liters	141,720,000	67.2	29.3
Run time	days	252.	2.65	1.15
Head loss	N/m^2	591	56,400	24,600
	PSI	0.10	8.18	3.57

correlations and rate and isotherm studies that were reported in the literature (Dobbs and Cohen, 1980, Crittenden and Hand, 1983).

1. Freundlich Isotherm Parameters

The Freundlich isotherm parameters, K and 1/n, were determined experimentally by Luft (1984) for most of the compounds presented herein. Luft provided various K and 1/n values which were experimentally determined at 10°C (naturally-occurring groundwater temperature) and 20°C. Dobbs and Cohen (1980) also presented isotherm values for a wide range of compounds. However, Luft (1984) showed that Dobbs and Cohen failed to run their isotherms for a long enough period of time to ensure equilibrium. The Freundlich capacity constants determined by Dobbs and Cohen were two to three times lower than what Luft reported. Therefore, all necessary isotherm parameters were either measured by Luft or were determined from Dobbs and Cohen. Tables 2 and 3 contain the isotherm parameters used for model calculations. Isotherm parameters that were determined from Dobbs and Cohen (1980) are marked with an asterisk (*).

2. Intraparticle Mass Transfer Coefficients

The pore diffusivity, D_p, was calculated from the liquid diffusivity by the following equation:

$$D_p = \frac{D_L}{\tau_p} \qquad (32)$$

in which, D_L is the liquid diffusivity; and τ_p is the tortuosity of the adsorbent. The liquid diffusivity was determined from a correlation given by Hayduk and Laudie (1974):

$$D_L = \frac{13.26 \times 10^{-5}}{\mu^{1.14}\, V_b^{.589}} \qquad (33)$$

in which, μ is the viscosity of water; and V_b is the molal volume at the normal boiling point estimated from atomic volumes of Le Bas (loc cit, Sherwood, Pigford, and Wilke, 1975).

The tortuosity, τ_p, is a measure of the actual length an adsorbing molecule must travel as compared to the radial distance traveled and ranges from 2 to 6. Since limited research has been conducted on the tortuosity, a value of 1 was assumed for τ_p in all calculations and the actual value of the tortuosity is absorbed into a correction factor, the pore to surface diffusion flux ratio (PSDFR), which is explained below.

The surface diffusivity, D_s, for most compounds, was determined experimentally by Dobrzelewski (1984). Surface diffusivities of other compounds were estimated by equating the surface diffusion flux to the pore diffusion flux (Crittenden, 1976). Dobrzelewski (1984) observed that the surface flux was approximately a constant factor times the pore flux for a number of VOCs. Accordingly, the surface diffusivity was calculated by multiplying the pore flux by the PSDFR:

$$D_s = \frac{D_L \, \varepsilon_p \, C_o}{\tau_p \, \rho_a \, K \, C_o^{1/n}} \times (\text{PSDFR}) \qquad (34)$$

in which, ε_p is the adsorbent void fraction; and ρ_a is the apparent density of the adsorbent. The best fit PSDFR was determined to have value of 6.58, with most values ranging from 4 to 12. The PSDFR which was used in this study was 8.0. However, this over-estimated the value of surface diffusion coefficients. Dobrzelewski (1984) measured a trichloroethene surface diffusivity of 3.75×10^{-10} as compared to the calculated value of 6.19×10^{-10}, which was used in the sensitivity analysis. This will tend to make intraparticle diffusion less important in the parameter sensitivity analysis, Section V.

3. Liquid Phase Mass Transfer Coefficients

The liquid film transfer coefficient, k_f was calculated using the Williamson correlation (Williamson, 1963):

$$k_f = \frac{2.4\ v_s}{Re^{.66}\ Sc^{.58}} \tag{35}$$

in which, v_s is the superficial velocity; ε is the bed void fraction; and ρ_L is the density of water. Reynolds and Schmidt numbers were calculated by:

$$Re = \frac{2\rho_L\ R\ v_s}{\mu\varepsilon} \tag{36}$$

$$Sc = \frac{\mu}{\rho_L\ D_L} \tag{37}$$

in which, R is the adsorbent radius; D_L was calculated from Eq. 33; and μ is the liquid viscosity.

The axial dispersivity, D_e, was estimated from the correlation proposed by Fried (1975):

$$D_e = D_L\ [\ 0.67 + 1.15(v_s R/\varepsilon D_L)^{1.2}\ ] \tag{38}$$

in which D_L is again calculated from Eq. 33.

4. Estimated Pressure Drop Across Fixed-Bed

Headloss calculations are for the initial loss estimated by the Ergun equation (1952) assuming the adsorbent particles are nearly spherical:

$$\frac{\Delta P}{\rho_L v_s w}\ \frac{2R}{L}\ \frac{\varepsilon^3}{1 - \varepsilon} = \frac{150(1 - \varepsilon)}{2Rv_s\rho_L/\mu} + 1.75 \tag{39}$$

Experience with these calculations indicates the headloss will increase significantly above the estimates from Eq. 39 during operation.

B. Single and Multicomponent Results for Perfect Similarity

The assumptions associated with Eqs. 22 and 25 make the scale-up procedure equally valid for the HSDM. Therefore the dispersed flow homogeneous solid diffusion model was used to calculate the single and multicomponent predictions which were reported herein. To test the validity of the RSSCT design equations, the DFHSDM was used to predict performance of adsorbers using typical mass transfer, isotherm, design, and operational parameters for a influent containing TCE at concentrations similar to those of the field studies. Table 2 displays the kinetic and isotherm information that were used in the single solute calculations for trichloroethene (TCE). The surface diffusivity reported in Table 2 is a measured value. As shown by the dimensionless groups in Table 2, perfect similarity may be achieved with RSSCT. (Although the effects of dispersion were included in the scaling procedure, it is negligible for the single solute TCE calculation because the Peclet number is sufficiently large.) Figure 8 displays the DFHSDM predictions for small-scale, RSSCT, and large-scale adsorbers. Accordingly, the RSSCT should, in theory, yield identical results as large-scale adsorber.

To further illustrate the applicability of the scaling procedure, the DFHSDM was used to predict the multicomponent effluent concentration history profiles of the large-scale adsorber and the small-scale adsorber which is designed to simulate full-scale performance. The design and operational parameters are identical to the TCE single solute calculation and are given in Table 1. The influent contained cis-dichloroethylene (DCE), trichloroethene (TCE), tetrachloroethene (PCE), toluene, and xylene at concentrations near those measured in the field study. The chemical, mass

Table 2. Comparison of DFHSDM Column Parameters for Scale-Down of a Large Scale Column to a Small-Column Test: Chemical and Dimensionless Parameters for a Full-Scale Adsorber, a rapid small-scale column test (RSSCT) (a) which is designed to simulate full scale performance, and a RSSCT (b) which is just long enough to measure the length of the mass transfer zone (MTZ) of TCE as a single solute.

Chemical and Mass Transfer Parameters		Full Scale Adsorber	RSSCT (a)	RSSCT (b)
D_e	cm^2/s	9.93E-2	9.93E-2	9.93E-2
D_s	cm^2/s	3.75E-10	3.75E-10	3.75E-10
k_f	cm/s	2.15E-3	2.10E-2	2.10E-2
1/n		0.4163	0.4163	0.4163
K	μmol/g (L/μmol)$^{1/n}$	196.6	196.6	196.6
C_o	μmol/L	1.52	1.52	1.52
q_e	μmol/g	234.	234.	234.

Dimensionless Parameters

	Full Scale Adsorber	RSSCT (a)	RSSCT (b)
Pe_D	0.355	0.355	0.355
Pe_L	144.06	144.06	62.8
Pe_{MTZ}	47.5	47.5	47.5
Dg	182,000	182,000	182,000
St	7.50	7.50	3.30
Bi	2.38	2.38	2.38
Ed	3.14	3.14	1.38

Parameters which Were Used in MTZ Calculations

		Full Scale Adsorber	RSSCT (a)
St_{min}		3.30	3.30
$EBCT_{min}$	sec	131	1.373
$EBCT_{MTZ}$	sec	97.8	1.02
L_{min}	cm	18.2	1.86
L_{MTZ}	cm	13.6	1.39

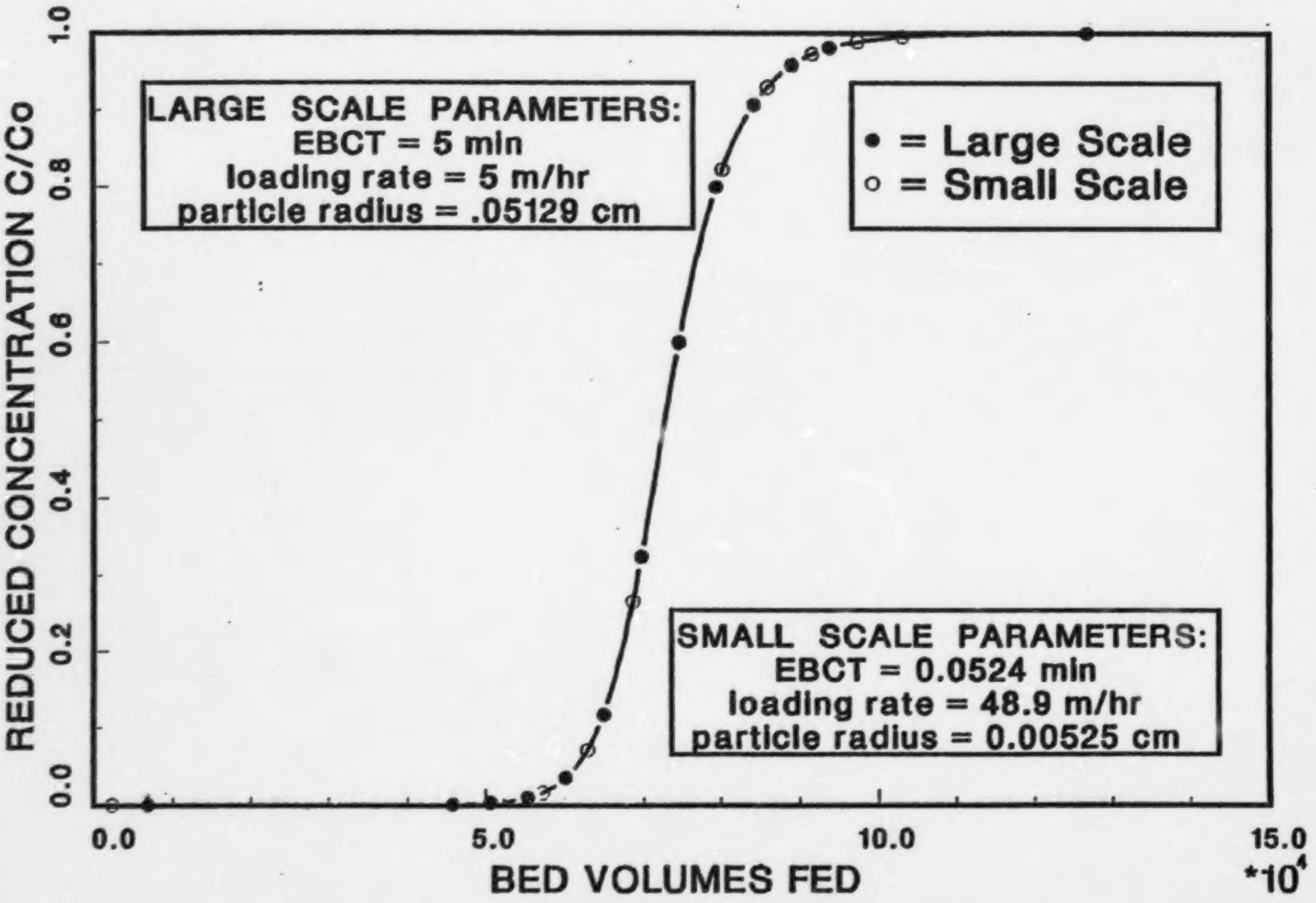

Figure 8. Comparison of the DFHSDM model prediction of the trichloroethene breakthrough profile for a full-scale adsorber to the DFPSDM prediction for a small-column test.

transfer and dimensionless parameters for these adsorbates are shown in Table 3. The surface diffusivities for components other than TCE are calculated values and are over-estimated. The RSSCT and large-scale dimensionless parameters are identical; consequently, only one set is given for each adsorbate. As shown in Figure 9, the breakthrough profiles for the RSSCT and large scale breakthrough profiles of the RSSCT and large scale adsorber are identical for each component. Therefore, in theory, the RSSCT can be conducted in 1.05% of the time required for a pilot-scale adsorber, regardless of the adsorbate mixture, if the GAC particle radius is reduced from 0.0513 cm to 0.00525 cm and the surface diffusivity is identical for the small and large GAC particle sizes.

C. Estimation of the EBCT of the Mass Transfer Zone for Single Components

Following the procedure which is discussed by Hand et al. (1984) and Crittenden and Hand (1983), one could use the breakthrough profiles of the RSSCT to estimate the EBCT of the MTZ of the large adsorber for a single component, if a constant pattern exists. To determine whether constant pattern has been achieved, breakthrough profiles from several RSCCTs with different EBCTs should be plotted as a function of time to examine whether they are parallel. [See Hand et al. (1984) for more discussion of this procedure.] As the EBCT increases the breakthrough profiles will become parallel and constant pattern will be achieved. (The minimum EBCT which is required for constant pattern exists is defined as $\mathrm{EBCT}_{\mathrm{min}}$.) Once constant pattern has been achieved, the $\mathrm{EBCT}_{\mathrm{MTZ}}$ of the RSSCT may be estimated directly from the breakthrough curves. [Alternatively, the mass transfer parameters may estimated from the $\mathrm{EBCT}_{\mathrm{MTZ}}$ using procedure which is proposed by Hand et al (1984).] The expected $\mathrm{EBCT}_{\mathrm{MTZ}}$ of the full scale column would be related to the RSSCT as shown in Eq. 22. See Hand et al. (1984) and

Table 3. Chemical and Dimensionless Parameters for Large-scale and Small-scale Columns for (a) Cis-dichloroethylene, (b) Trichloroethylene, (c) Tetrachloroethylene, (d) Toluene, and (e) Xylene.

	(a)	(b)	(c)	(d)	(e)
K	39.0*	196.6	650.0*	300.0*	1500.0*
1/n	0.7045	0.4163	0.4579	0.4400	0.3500
D_s	7.17E-10	3.75E-10	7.41E-11	2.36E-10	6.28E-11
D_e	0.0981	0.0993	0.1028	0.1033	0.1052
k_f large-scale	2.19E-3	2.03E-3	1.91E-3	1.89E-3	1.79E-3
k_f small-scale	2.14E-2	1.98E-2	1.87E-2	1.85E-2	1.74E-2
Pe	147.0	145.2	140.3	139.7	137.2
St	7.69	7.12	6.71	6.64	6.28
Bi	8.46	2.50	2.67	1.94	0.831
Ed	0.908	2.85	2.51	3.42	7.56

Column parameters may be found in Table 1 under the headings of full scale adsorber and RSSCT which is designed to simulate full scale performance, RSSCT (a).

* Determined from Dobbs and Cohen (1980).

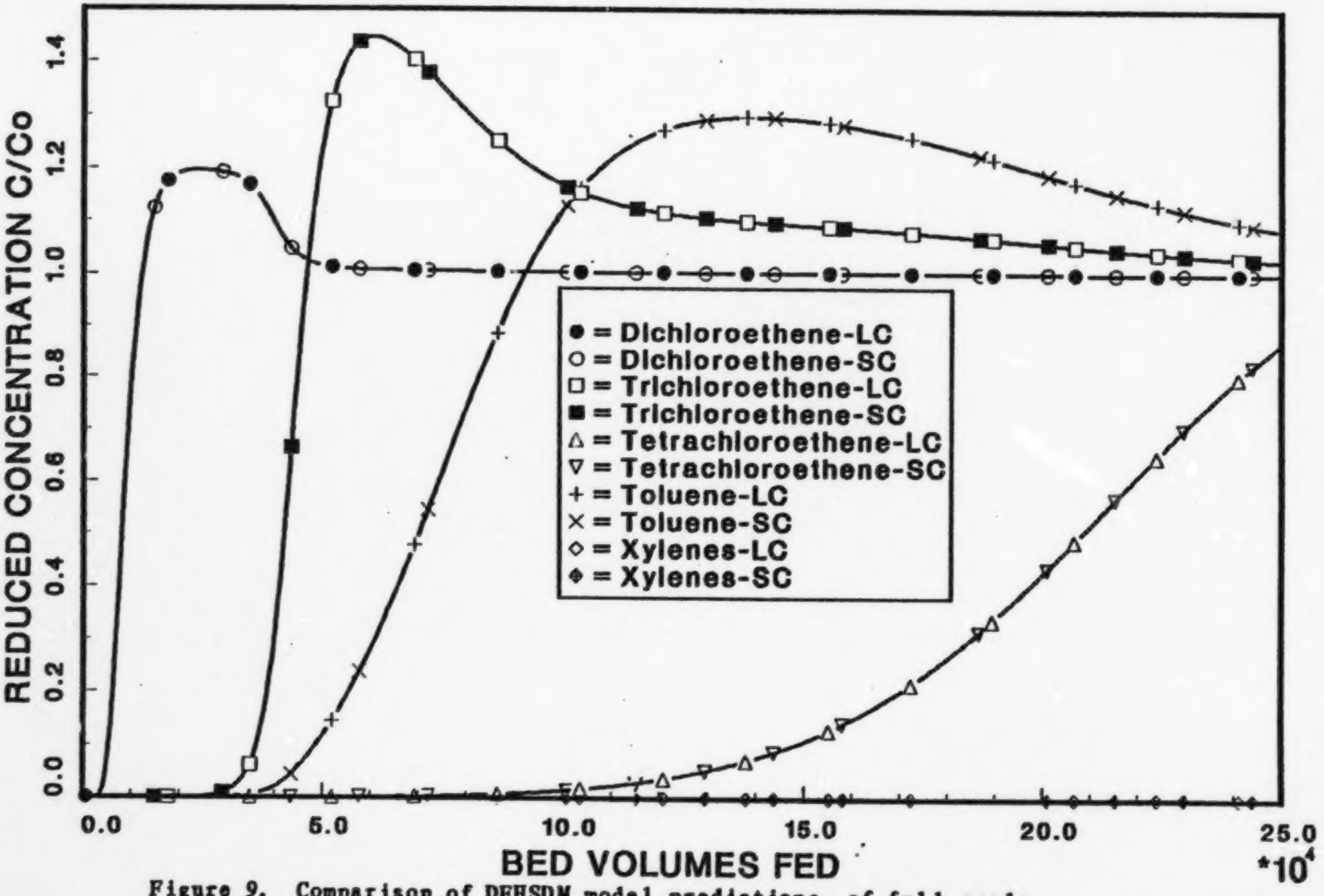

Figure 9. Comparison of DFHSDM model predictions of full-scale adsorber breakthrough profiles for dichloroethene, trichloroethene, tetrachloroethene, toluene, and xylenes to the DFHSDM predictions for a small-column test assuming constant surface diffusivity.

Crittenden and Hand (1983) for the proper design of an adsorber system for which the $EBCT_{MTZ}$ is known.

Tables 1 and 2 contain the mass transfer, and design and operational parameters for a RSSCT for which constant pattern would exist; i. e., EBCT is equal to $EBCT_{min}$. In this case, the effects of dispersion are negligible; accordingly, the procedure which is presented by Hand et al (1984) was used to estimate the $EBCT_{min}$ or L_{min}. Although the calculations which were used to estimate the $EBCT_{MTZ}$ and $EBCT_{min}$ in Tables 1 and 2 assume that the mass transfer parameters are known, it is interesting to note that if the $EBCT_{min}$ is used in the design of the RSSCT, the time required to conduct the RSSCT may be reduced to 1.15 days and the required volume to 29.3 liters as shown in Table 1.

D. Scaling of Surface Diffusion Controlled Processes

If Eqs. 22 and 25 are used for a surface diffusion controlled process where the surface diffusivity is linearly dependent upon the adsorbent particle radius then the RSSCT will not perfectly simulate the performance of the prototype full-scale system. To illustrate the magnitude of the deviation from perfect similarity, Figure 10 displays the DFHSDM predictions of the RSSCT given in Table 1 which is designed to simulate the full-scale adsorber for these three values of D_s: (a) D_s equal to 3.75×10^{-10} cm^2/sec which was measured by Dobrzelewski (1984) at an initial concentration of 1322.7 μg/L which assumes no change in D_s with particle size at the lower concentrations of the field study; (b) D_s equal to 7.68×10^{-11} which assumes that Ds decreases linearly with particle size; and, (c) D_s equal to 5.20×10^{-10} measured by Dobrzelewski (1984) at an initial concentration of 1329.8 μg/L which was the actual measured D_s for the smaller particle size.

According to Fig. 10, the RSSCT which assumes no change in D_s with

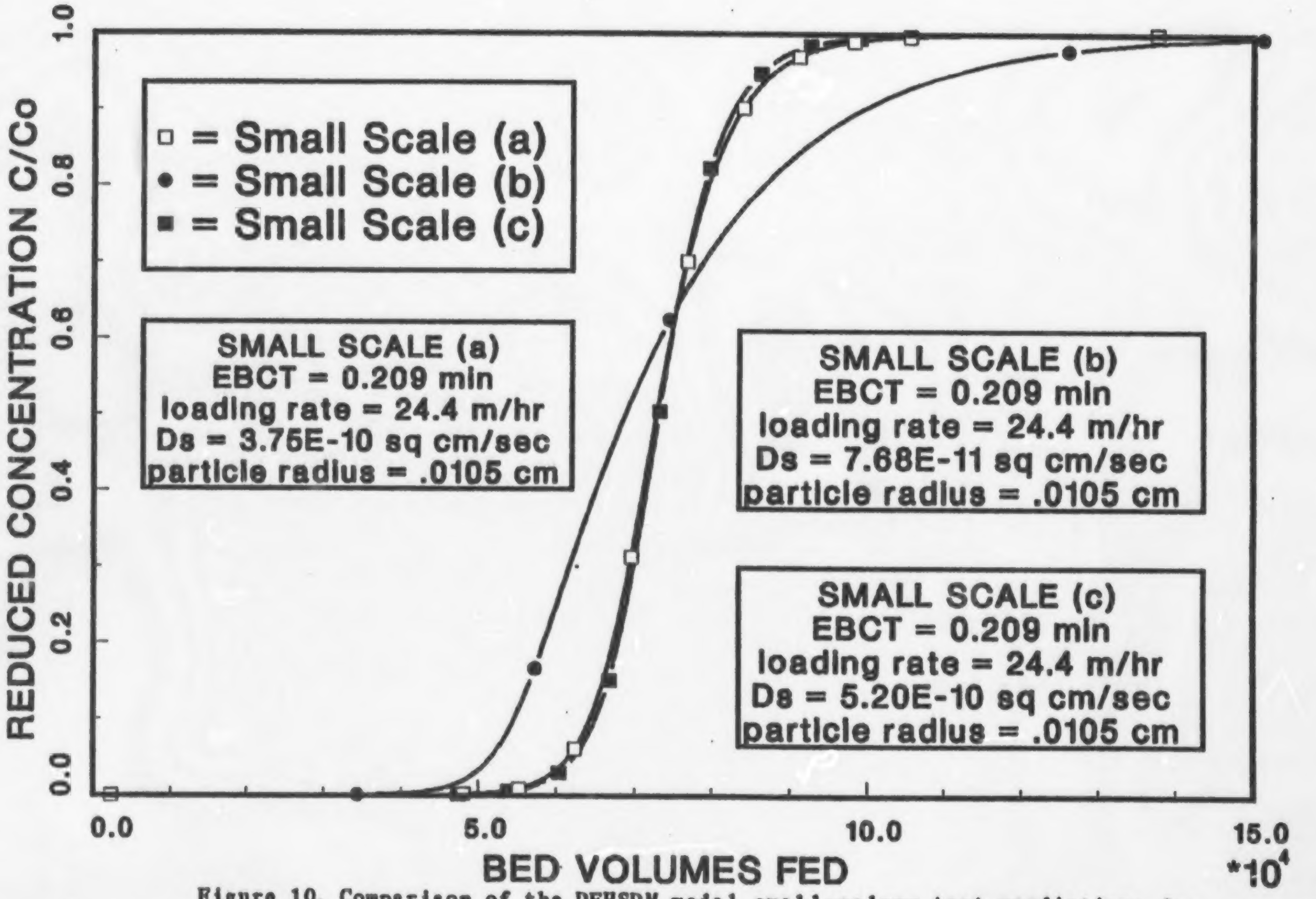

Figure 10. Comparison of the DFHSDM model small-column test predictions for trichloroethene. (a) perfect similarity - constant diffusivity, (b) surface diffusivity linearly dependent on particle size, (c) surface diffusivity determined experimentally.

particle size is nearly identical the expected breakthrough profile with the measured D_s value. Furthermore, if a linear decrease in D_s with particle size is observed and is ignored in the design of the small-adsorber test, an increase in the length of the MTZ can be expected which makes the RSSCT a conservative estimate of full-scale adsorber performance because earlier breakthrough of the adsorbates would be observed. The effect of the linearly dependent $D_{s,i}$ on the performance of a RSSCT treating the multisolute influent is displayed in Figure 11. The kinetic and isotherm data is taken from Table 3 but $D_{s,i}$ for the RSSCT is reduced by R_{SC}/R_{LC}. An RSSCT used in this manner would be greatly over-estimate the carbon use rate.

The scaling methods presented so far are compared in Tables 4 and 5. Under the conditions where $D_{s,i}$ changes linearly with R, Eq. 27 was used to maintain similar $Ed_{s,i}$. Equation 25 maintains similar $Pe_{D,i}$ in the RSSCT and full-scale columns. To evaluate the usefulness of these scaling equations RSSCT's were designed from the full scale design in Table 1. Tables 4 and 5 display the chemical and operating parameters of these adsorbers: (1) a full-scale adsorber (from Table 1), (2) a RSSCT (Tables 4a and 5a) designed for perfect similarity assuming constant D_s and using a particle of radius 0.0105 cm, (3) a RSSCT (Tables 4b and 5b) designed from Eqs. 25 and 27 for similar Ed_s assuming surface diffusivities proportional to R and a particle radius of 0.0105, and (4) a RSSCT (Tables 4c and 5c) designed to maintain similar Ed_s assuming D_s proportional to R (Eq. 27) and using Eq. 30 to reduce the required hydraulic loading and yet maintain similar dispersive mechanisms.

Figure 12 compares the DFPSDM breakthrough profile predictions of trichloroethene for the full-scale adsorber and the RSSCT (b) from Tables 4 and 5. As seen in Fig. 12 the RSSCT shows a much sharper breakthrough

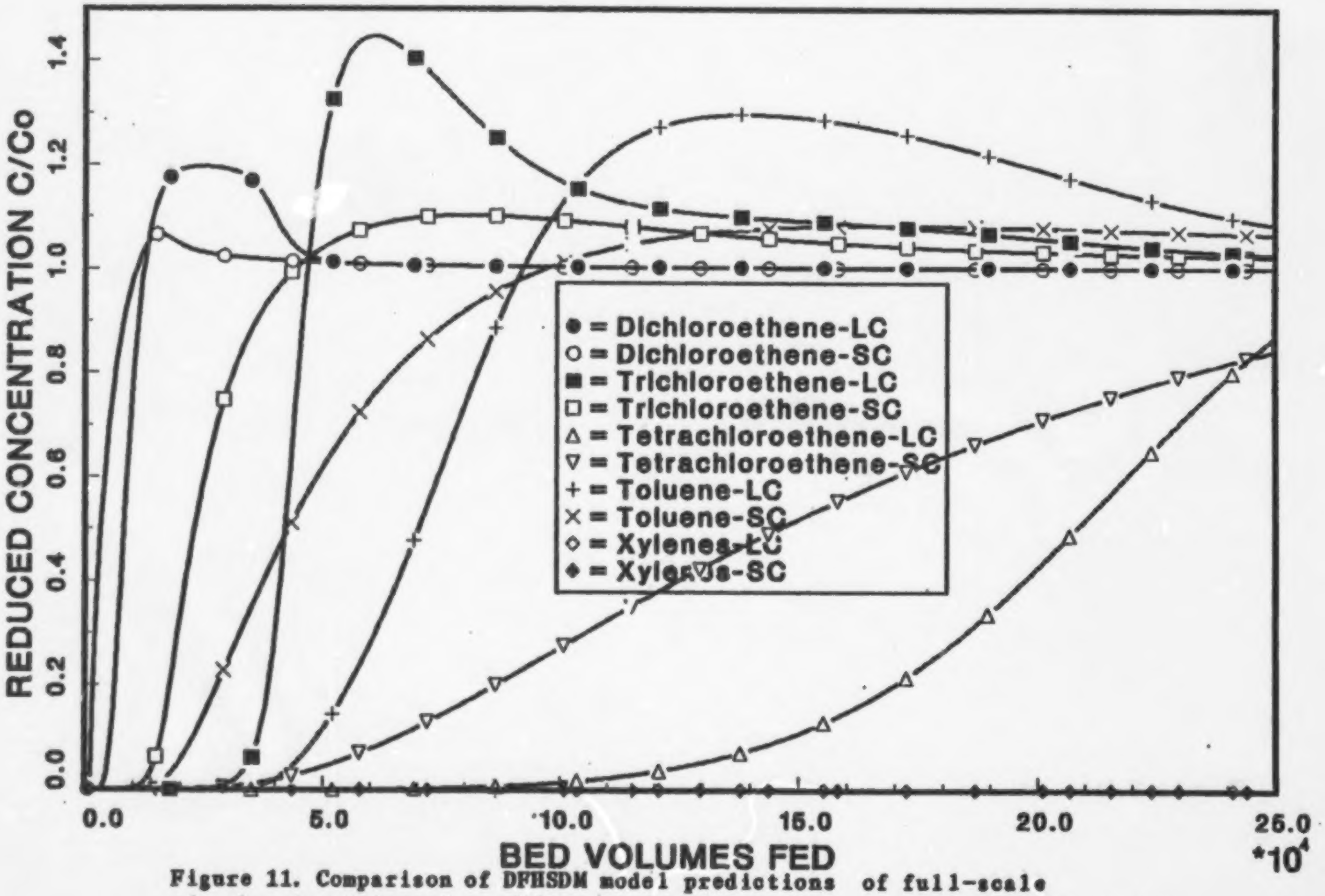

Figure 11. Comparison of DFHSDM model predictions of full-scale adsorber breakthrough profiles for dichloroethene, trichloroethene, tetrachloroethene, toluene, and xylenes to the PSDM predictions for a small-column test where the surface diffusivity is a linear function of the adsorbent particle size. Scaling equations assume constant diffusivity.

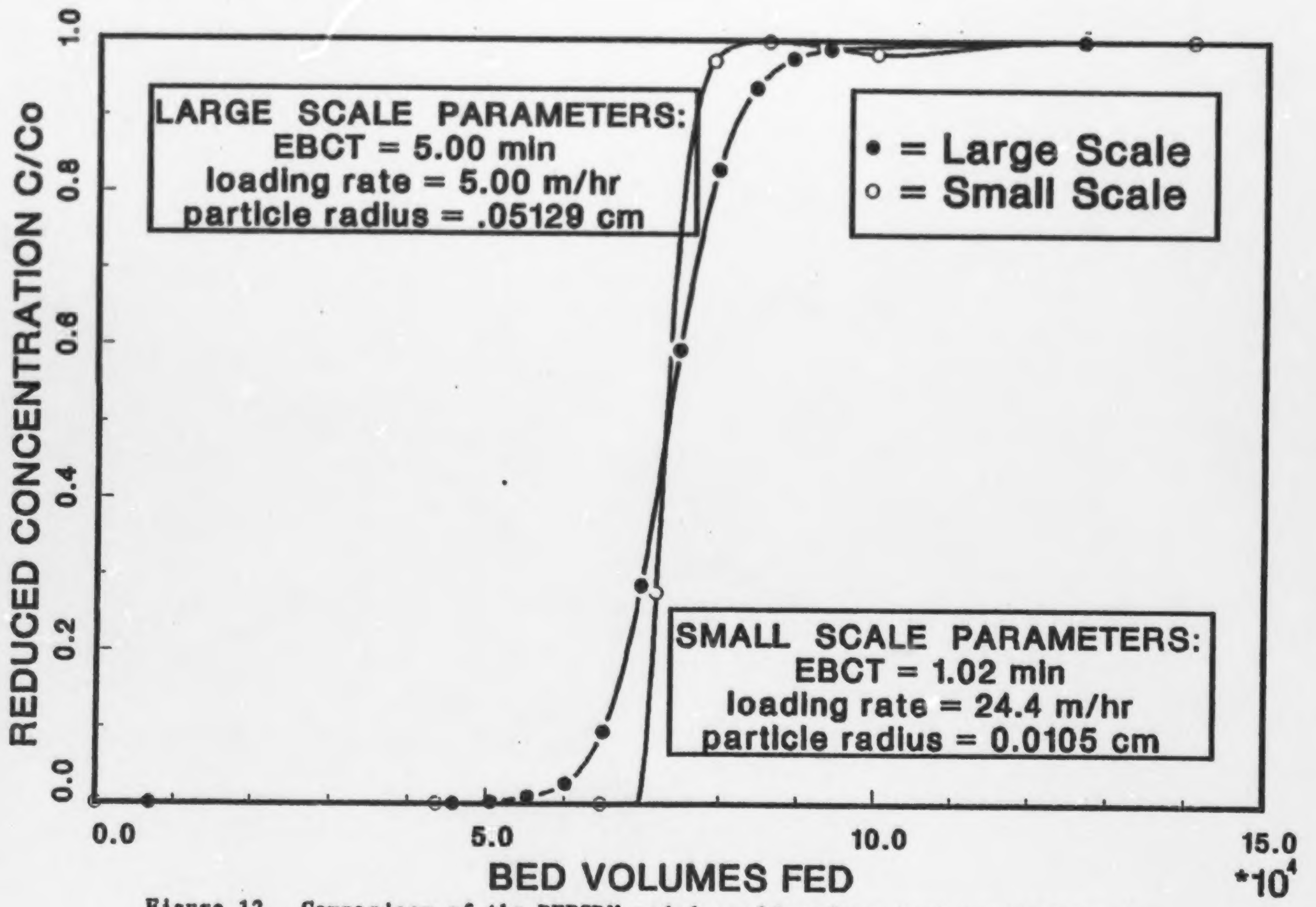

Figure 12. Comparison of the DFPSDM model small-column test predictions for trichloroethene: (a) full-scale adsorber (b) RSSCT scaled to maintain constant Ed_s - surface diffusivity linearly dependent on particle size.

profile than the full-scale column. But this example exaggerates the effects of film transfer because the calculated diffusivity was much nearly twice the measured value and in most cases, greater intraparticle control is observed. The agreement between the breakthrough profile comparisons shows that where D_s is proportional to R, a RSSCT scaled for similar Ed_s can simulate full-scale adsorber performance well. The dissimilarity will be less noticeable in experimental data where intraparticle transport controls the length of the mass transfer zone.

The RSSCT described in Tables 4c and 5c illustrate the use of Eq. 30 to reduce the flowrate and yet maintain similar Ed_s. The estimated Schmidt number of 2108 and Re$\cdot$Sc product, 5668 allow a reduction of the hydraulic loading rate of 1000/5668 assuming a minimum Re$\cdot$Sc product of 1000. The required RSSCT loading rate from Table 4c becomes 3.96 m/hr, a substantial reduction from 24.4 m/hr required for the RSSCT in Table 4b. This would reduce the required volume from 2882 liters to 473 liters and reduce the pressure drop across the bed from 10 psi to 0.26 psi.

Because the relationship between D_s and R is uncertain, Eqs 30 and 31 are recommended to design a proper RSSCT. Surface diffusivities of a test compound must be measured to determine the proper ratio of surface diffusivities between the two sized carbons. Equation 30 can aid in determining the lowest required loading rate to minimize the required volume needed to conduct the test and to minimize the headloss and is recommended for RSSCT design.

V. RSSCT PARAMETER SENSITIVITY

The ability of an RSSCT to simulate full scale adsorber performance is dependent upon the accuracy of the design of the RSSCT, the operation of the RSSCT, and the known or assumed properties of the GAC used in full-scale adsorbers and RSSCT. For the purposes of determining the sensitivity of the RSSCT to chemical and physical parameters, the DFPSDM was used to predict the effects of changes of mass transfer, isotherm, design, and operational parameters for a influent containing TCE at concentrations similar to those of the field studies. The RSSCT operational mass transfer parameters for the the sensitivity analysis may be found in Tables 4(a) and 5(a). In this example, the surface diffusivities were overestimated and are not good representative values. As a result, the surface diffusion mechanism is not the dominant mechanism in these calculations. Consequently, the mass transfer zones in these calculations are shorter than would be expected in actual circumstances, indicating also that the surface diffusion effects are underestimated and that film transfer effects are overstated in this parameter sensitivity analysis.

Film transfer is of less concern because the film transfer effects may be directly estimated using the Kirwan solution, Eq. 21 (loc. cit. Fleck et al. 1973; Hand et al., 1984). For the example case that is used for the sensitivity analysis, the effects of film transfer are more important. The analysis will display an artificially heightened sensitivity to parameters affecting the Stanton number and film transfer coefficients. The RSSCT simulated here will display a greater deviation from similarity than will occur in actual situations. Therefore, this particular sensitivity analysis is conservative because the RSSCT design is based upon similarity for intraparticle mechanisms where film transfer is important. Where the Stanton number is altered by a parameter variation, the effect upon the

Table 4. Comparison of Column Parameters for Scale-Down of a Large Scale Column to a Small-Column Test: Design and Operational Parameters for a Full-Scale Adsorber, a rapid small-scale column test (RSSCT) (a) for the sensitivity analysis which is designed assuming constant diffusivity to simulate full scale performance, a RSSCT (b) which is designed to maintain similar Ed_s where the surface diffusivity is linearly dependent on the particle radius, and a RSSCT (c) which is designed to maintain similar Ed_s where D_s is proportional to the particle radius and the loading rate is reduced as much as possible and yet remain in the region of mechanical dispersion (See Fig. 4).

		Full Scale Adsorber	RSSCT (a)	RSSCT (b)	RSSCT (c)
GAC Packing Characteristics					
ρ_a	g/cm^3	0.8034	0.8034	0.8034	0.8034
ε		0.40	0.40	0.40	0.40
ε_p		0.643	0.643	0.643	0.643
R	cm	0.0513	0.0105	0.0105	0.0105
Column and Flow Specifications					
Column Diameter	cm	244.	1.10	1.10	1.10
Column Length	cm	41.7	8.53	41.7	6.75
EBCT	s	300	12.6	61.4	61.4
CSA	cm^2	46,700	0.950	0.950	0.950
V_s	m/hr	5.00	24.4	24.4	3.96
Bed Volume	cm^3	1,946,000	8.10	39.6	6.42
Flow rate	cm^3/min	389,000	38.7	38.7	6.27
BVF_{max}		72,800	72,800	72,800	72,800
Required Volume	liters	141,720,000	590.0	2882	473
Run time	days	252.	10.6	51.7	51.7
Head loss	N/m^2	591	14100	68900	1780
	PSI	0.10	2.05	10.0	0.26

Table 5. Comparison of DFPSDM Column Parameters for Scale-Down of a Large Scale Column to a Small-Column Test: Chemical and Dimensionless Parameters for a Full-Scale Adsorber, a rapid small-scale column test (RSSCT) (a) for the sensitivity analysis which is designed assuming constant diffusivity to simulate full scale performance, and a RSSCT (b) which is designed to maintain similar Ed_s where the surface diffusivity is linearly dependent on the particle radius.

Chemical and Mass Transfer Parameters		Full Scale Adsorber	RSSCT (a)	RSSCT (b)	RSSCT (c)
D_e	cm^2/s	9.93E-2	9.93E-2	9.93E-2	1.12E-1
D_s	cm^2/s	6.19E-10	6.19E-10	1.27E-10	1.27E-10
D_p	cm^2/s	6.21E-6	6.21E-6	6.21E-6	6.21E-6
k_f	cm/s	2.15E-3	1.05E-2	1.05E-2	5.73E-3
1/n		0.4163	0.4163	0.4163	0.4163
K	µmol/g (L/µmol)$^{1/n}$	196.6	196.6	196.6	196.6
C_o	µmol/L	1.52	1.52	1.52	1.52
q_e	µmol/g	234.	234.	234.	234.

Dimensionless Parameters

Dimensionless Parameters	Full Scale Adsorber	RSSCT (a)	RSSCT (b)	RSSCT (c)
Pe_D	0.355	0.355	0.355	0.510
Pe_L	144.1	144.1	703.7	164.1
Dg_s	182,000	182,000	182,000	182,000
Dg_p	0.943	0.943	0.943	0.943
St	7.50	7.50	36.6	20.0
Ed_s	5.20	5.20	5.20	5.20
Ed_p	0.270	0.270	1.32	1.32
Bi_s	1.44	1.44	7.04	3.84
Bi_p	27.7	27.7	27.7	15.1

breakthrough profile may be considered an exaggerated case.

Most parameters were varied plus and minus ten and fifty percent with the exception of bed void fraction and particle density which were varied over a range of possible values, plus and minus ten percent. As a single process or chemical parameter was changed, all other parameters were held constant. This is important to consider as many parameters are interrelated and will not vary independently. It should be noted that some of the parameters discussed here, such as the surface diffusivity, may tend to vary over several orders of magnitude while others may tend to vary a few percent. This section indicates which parameters are the most critical to determine, control, or account for in the design of a proper RSSCT at the approximate conditions of the field studies.

A. Mass Transfer Parameters

Figures 13-16 display the sensitivity of the RSSCT to variations in the dispersion coefficient, De, the film transfer coefficient, k_f, the pore diffusivity, D_p, and the surface diffusivity, D_s respectively. As seen from Figs. 13 and 15, a difference of fifty percent in D_e and D_p produces no significant change in the expected TCE breakthrough profile. As shown in Fig. 16, an increase or decrease in the surface diffusivity will result in a slight sharpening or broadening of the breakthrough profile respectively through a corresponding change in Ed_s. Because values of the surface diffusivity may vary over orders of magnitude, differences in the values of D_s between carbons can have a significant impact upon the accuracy of the RSSCT. Surface diffusivities of the two carbons that will be used in the RSSCT and full-scale system should be accurately measured for a solute in the class of compounds that are targeted for removal.

Figure 14 displays the effect of a difference of the value of the film

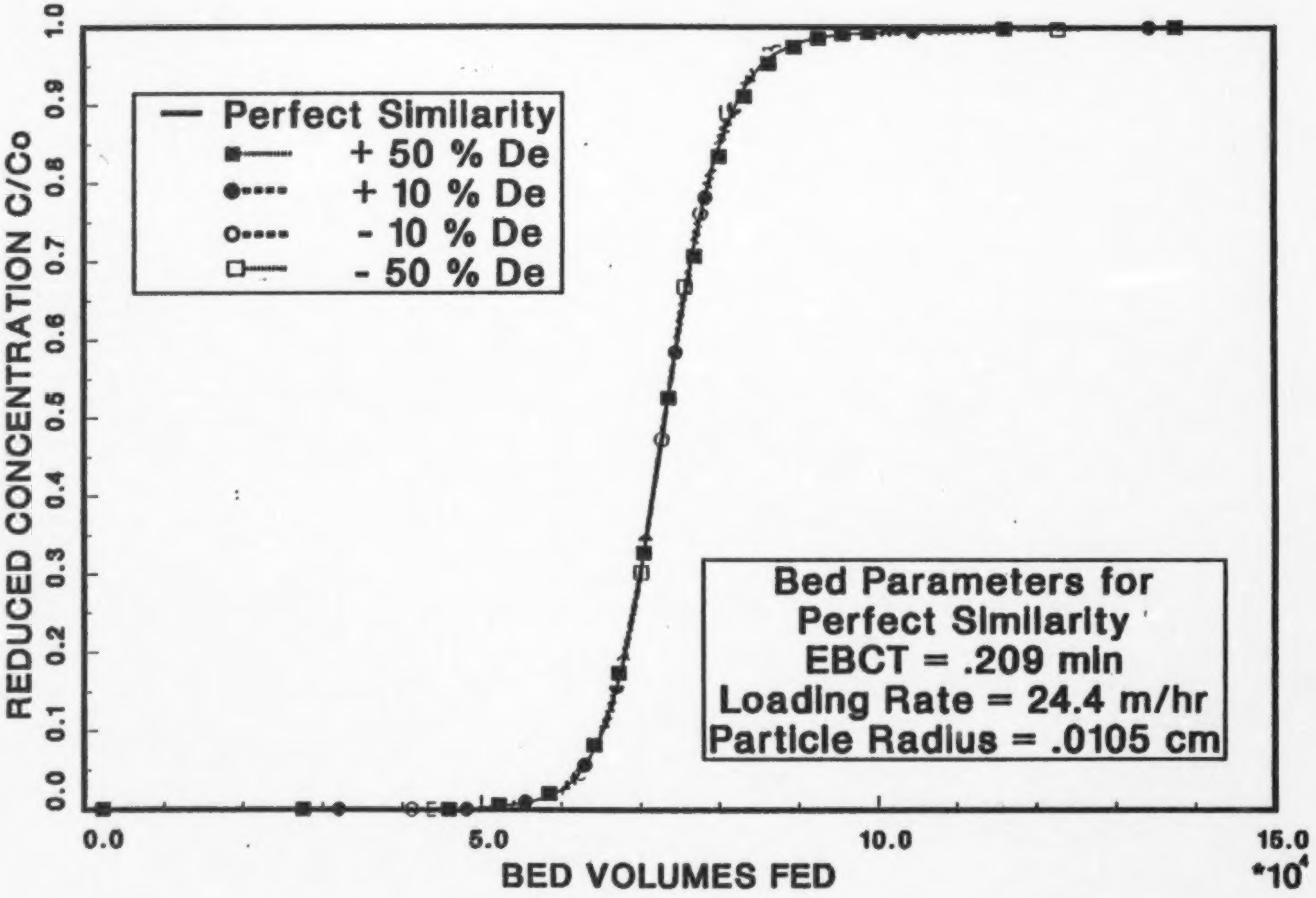

Figure 13. DFPSDM prediction of the RSSCT sensitivity to 10% and 50% changes in the dispersion coefficient.

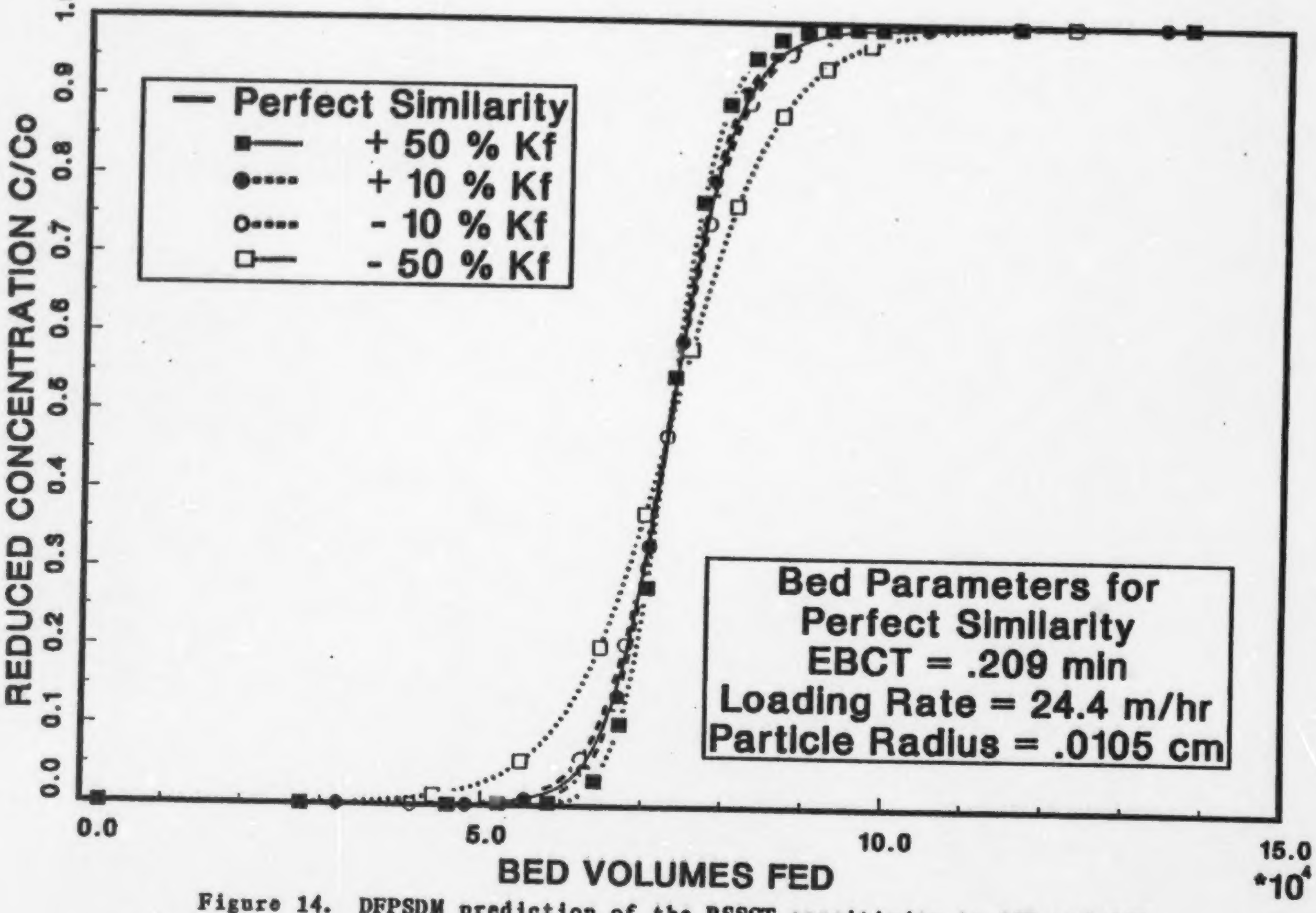

Figure 14. DFPSDM prediction of the RSSCT sensitivity to 10% and 50% changes in the film transfer coefficient.

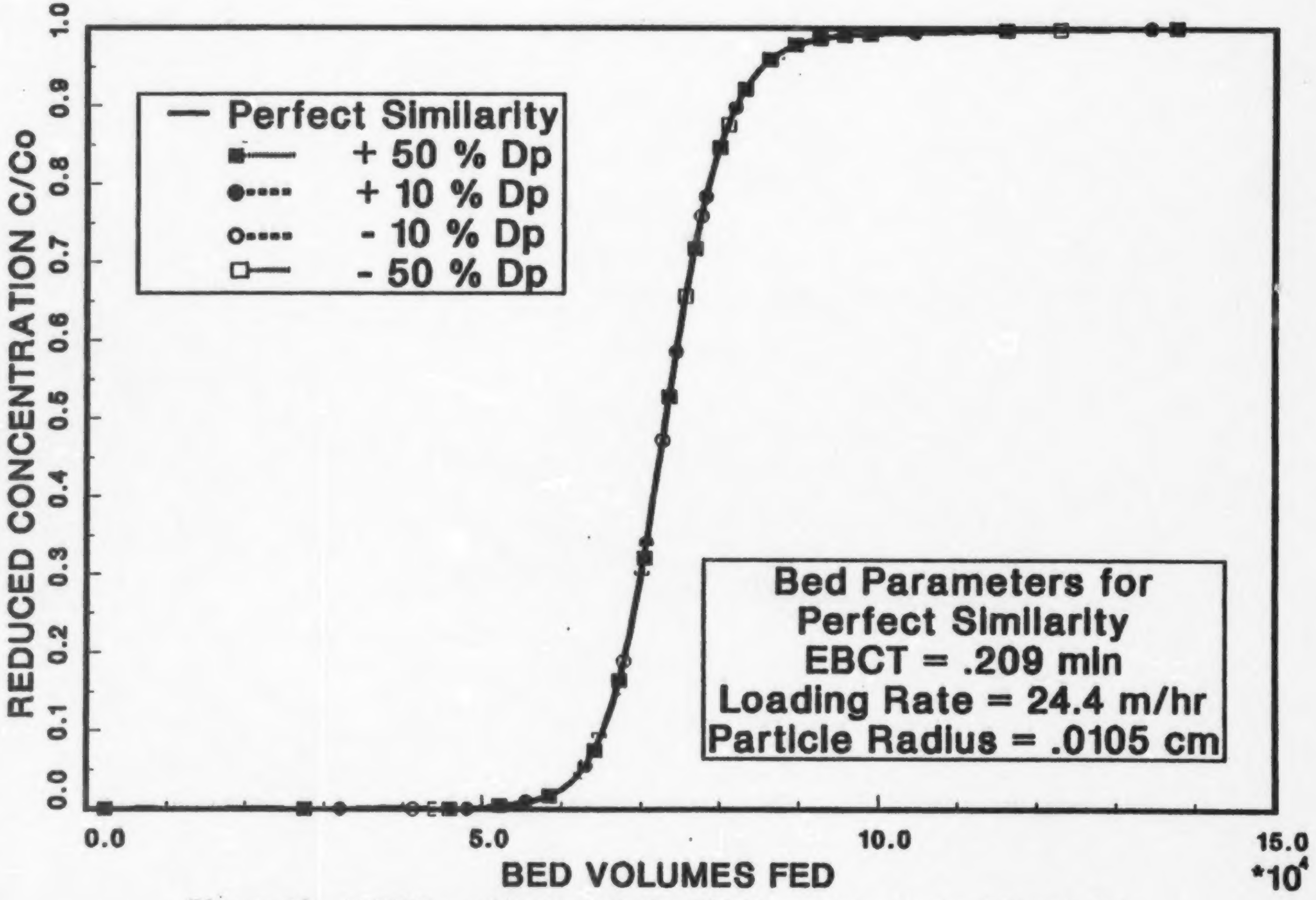

Figure 15. DFPSDM prediction of the RSSCT sensitivity to 10% and 50% changes in the pore diffisivity.

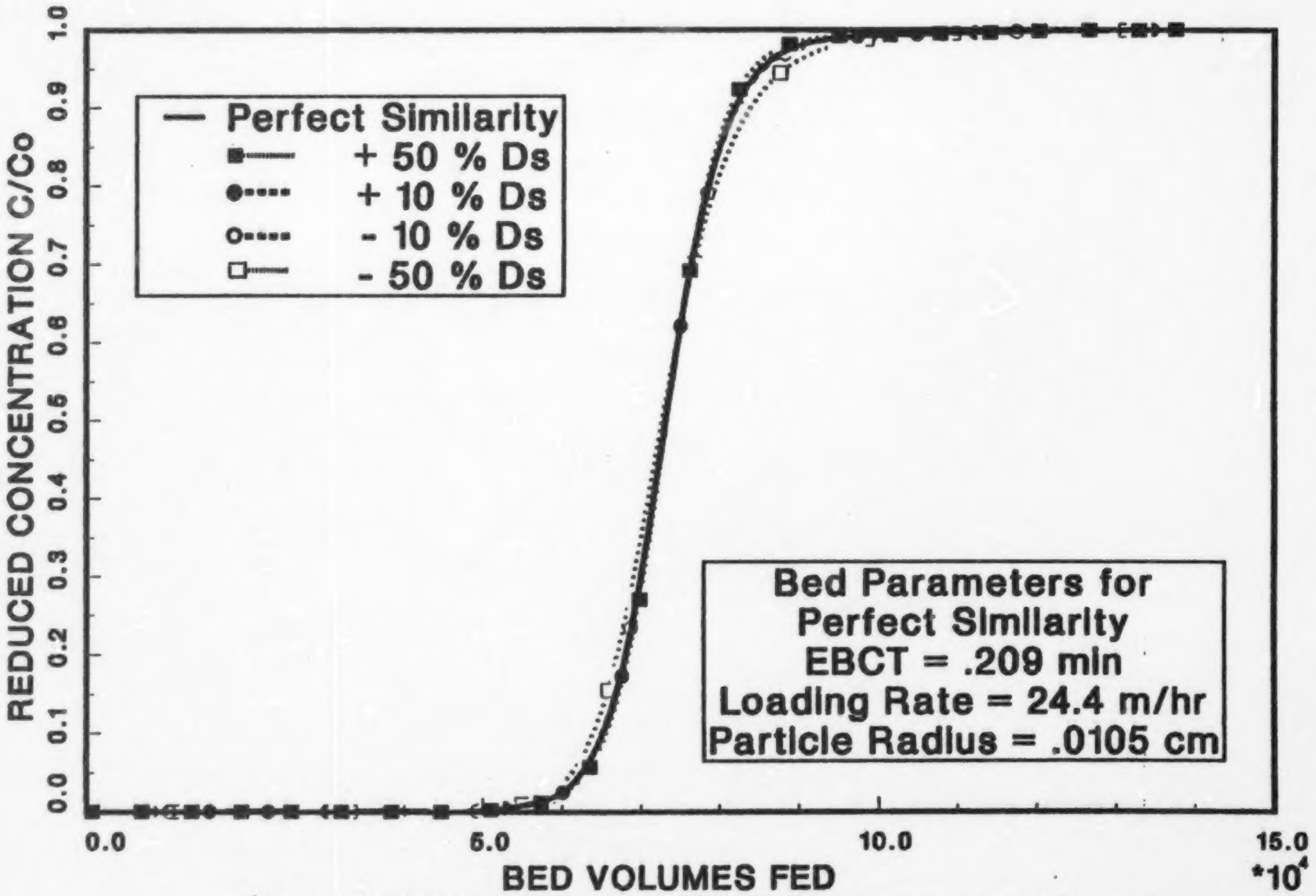

Figure 16. DFPSDM prediction of the RSSCT sensitivity to 10% and 50% changes in the surface diffusivity.

transfer coefficient. Here, an increase or decrease in the film transfer coefficient will result in a sharpening or broadening of the breakthrough profile and a corresponding change in the Stanton number. The effect of a change in k_f is greater than a that of an equal change in D_s. A ten percent change in k_f corresponds to a fifty percent change in the surface diffusivity. In other words, a ten percent change in St yields approximately the same change in the breakthrough profile as a fifty percent change in Ed_s. This is consistant with the results of Oravitz (1984) and Crittenden _et al_. (1985) which is expressed by Eq. 19.

B. Sensitivity to Physical/Chemical Properties

Figures 17-22 display the sensitivity of the RSSCT to variations in the adsorbent particle size, R, the adsorbent void fraction, ε_p, the adsorbent particle density, ρ_a, the bed void fraction, ε, the Freundlich isotherm capacity, K, and the Freundlich isotherm intensity constant, 1/n, respectively. As seen from Figure 18, a fifty percent change in the adsorbent void fraction does not alter the breakthrough profile appreciably. Figure 19 shows that a ten percent deviation of ρ_a will not change the breakthrough profile of TCE significantly. The adsorbent void fraction and the particle density affect the pore diffusion modulus and in this example and in most situations these parameters will not need to be known as accurately as some of the other parameters.

As seen in Figure 17, an adsorbent particle radius that is larger than expected will increase the length of the mass-transfer zone. Because R appears in the denominator of the mathematical expression for the Stanton number, Eq. 14, and is squared in the denominator of the surface and pore diffusion moduli, Eqs. 15 and 16 respectively, an increase of the adsorbent particle size will decrease St, $Ed_{p,i}$, and $Ed_{s,i}$. A difference of 50% between the actual and the expected particle radius will cause the RSSCT to

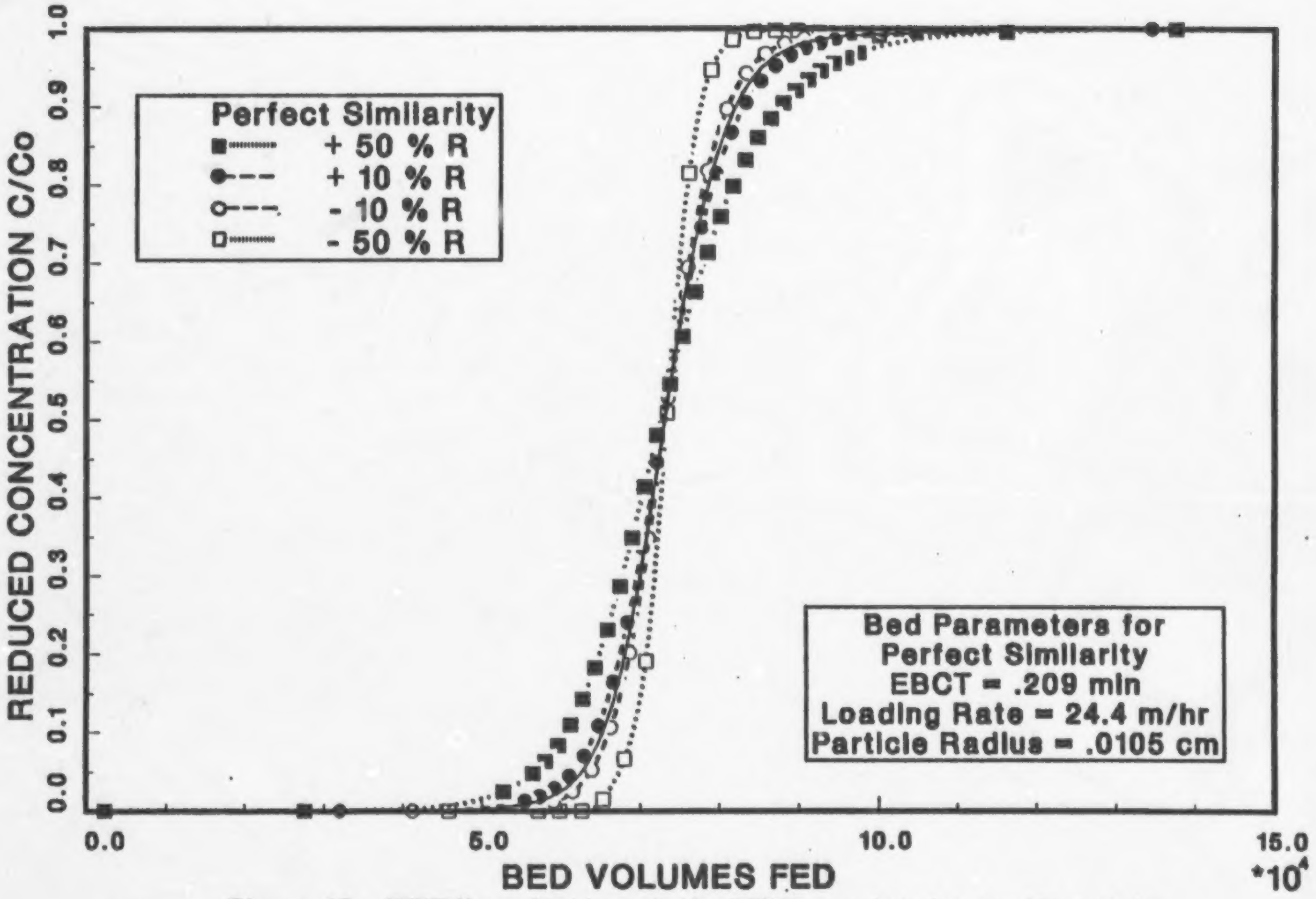

Figure 17. DFPSDM prediction of the RSSCT sensitivity to 10% and 50% changes in the adsorbent particle radius.

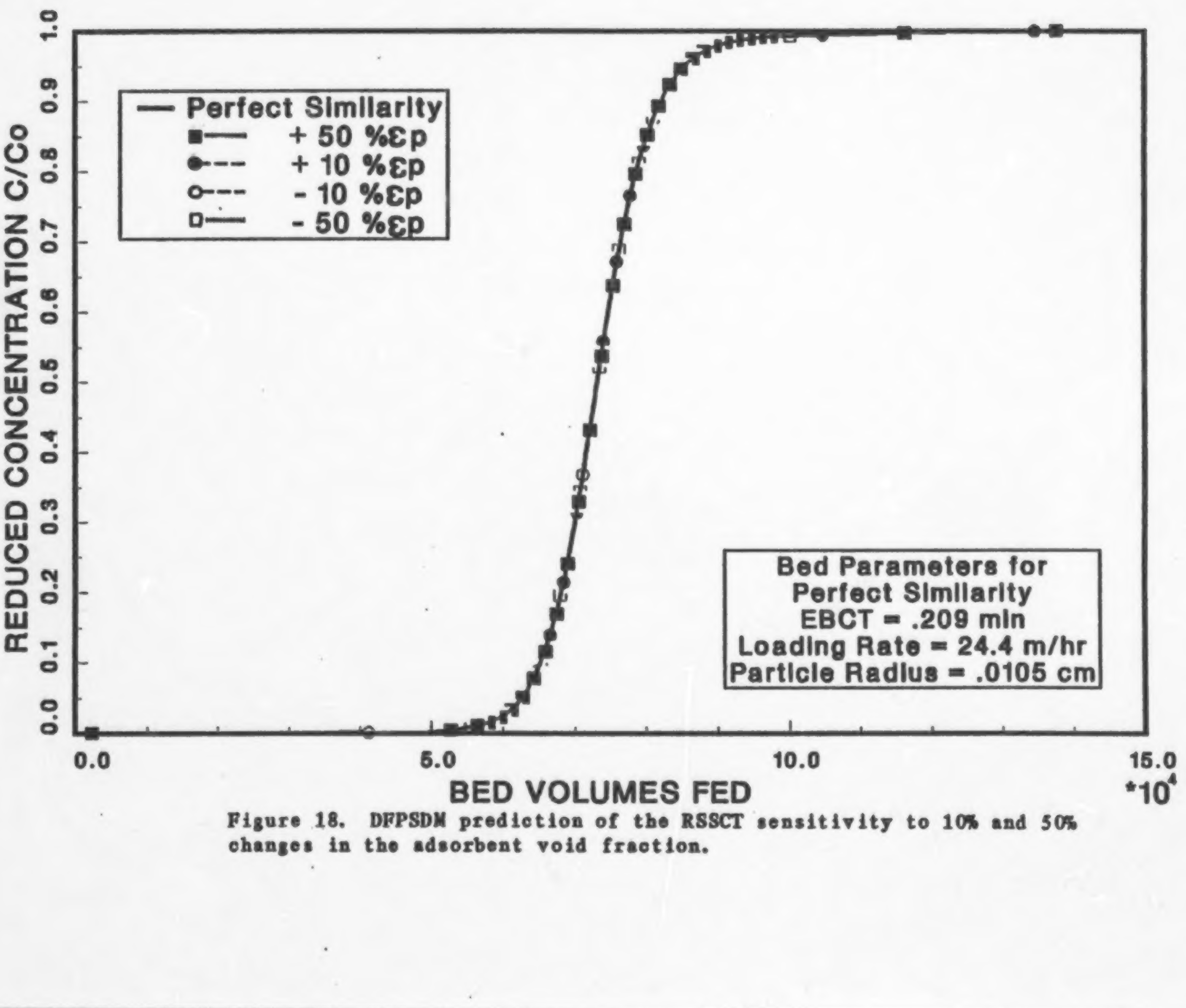

Figure 18. DFPSDM prediction of the RSSCT sensitivity to 10% and 50% changes in the adsorbent void fraction.

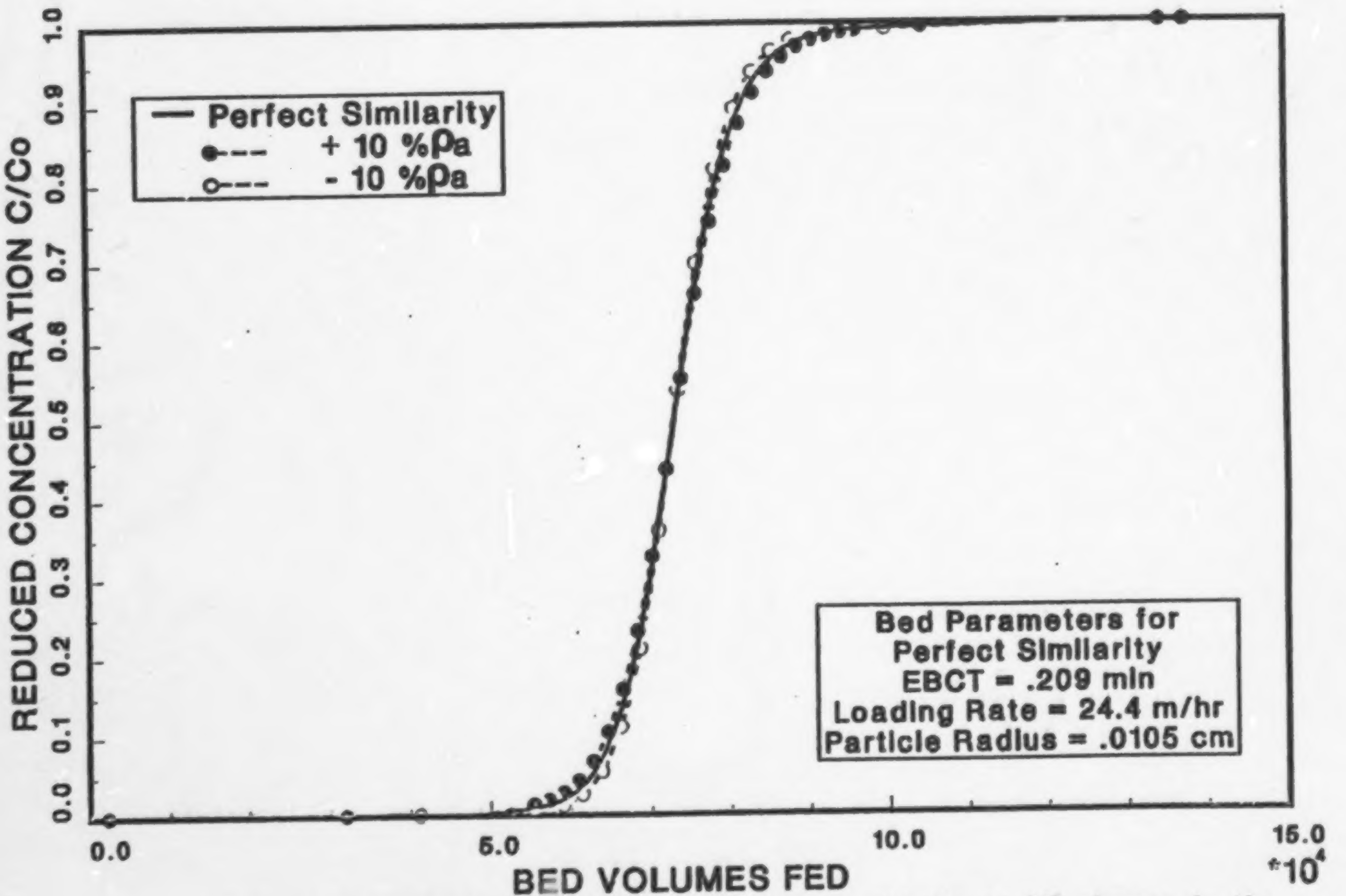

Figure 19. DFPSDM prediction of the RSSCT sensitivity to 10% changes in the adsorbent particle density.

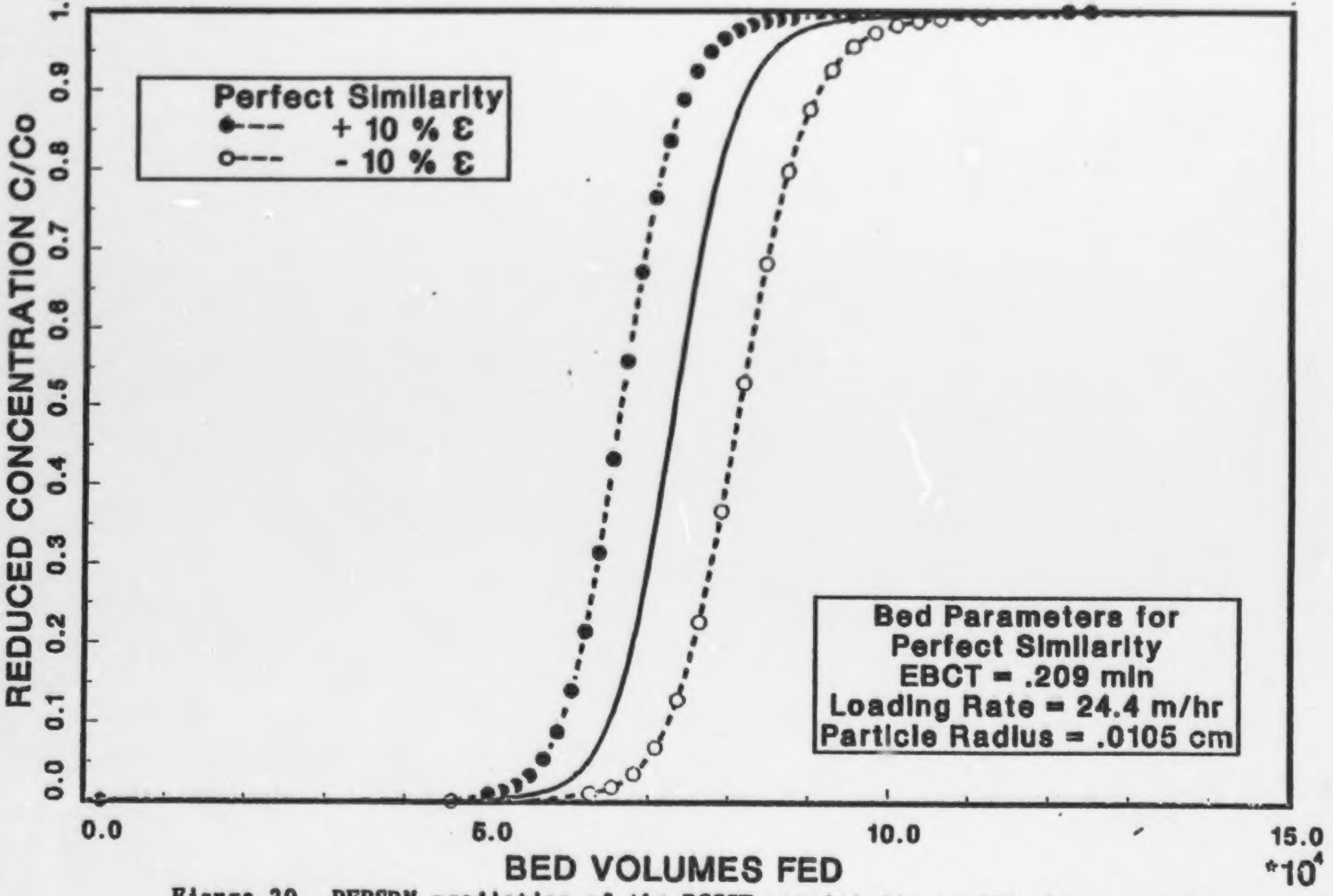

Figure 20. DFPSDM prediction of the RSSCT sensitivity to 10% changes in the bed void fraction.

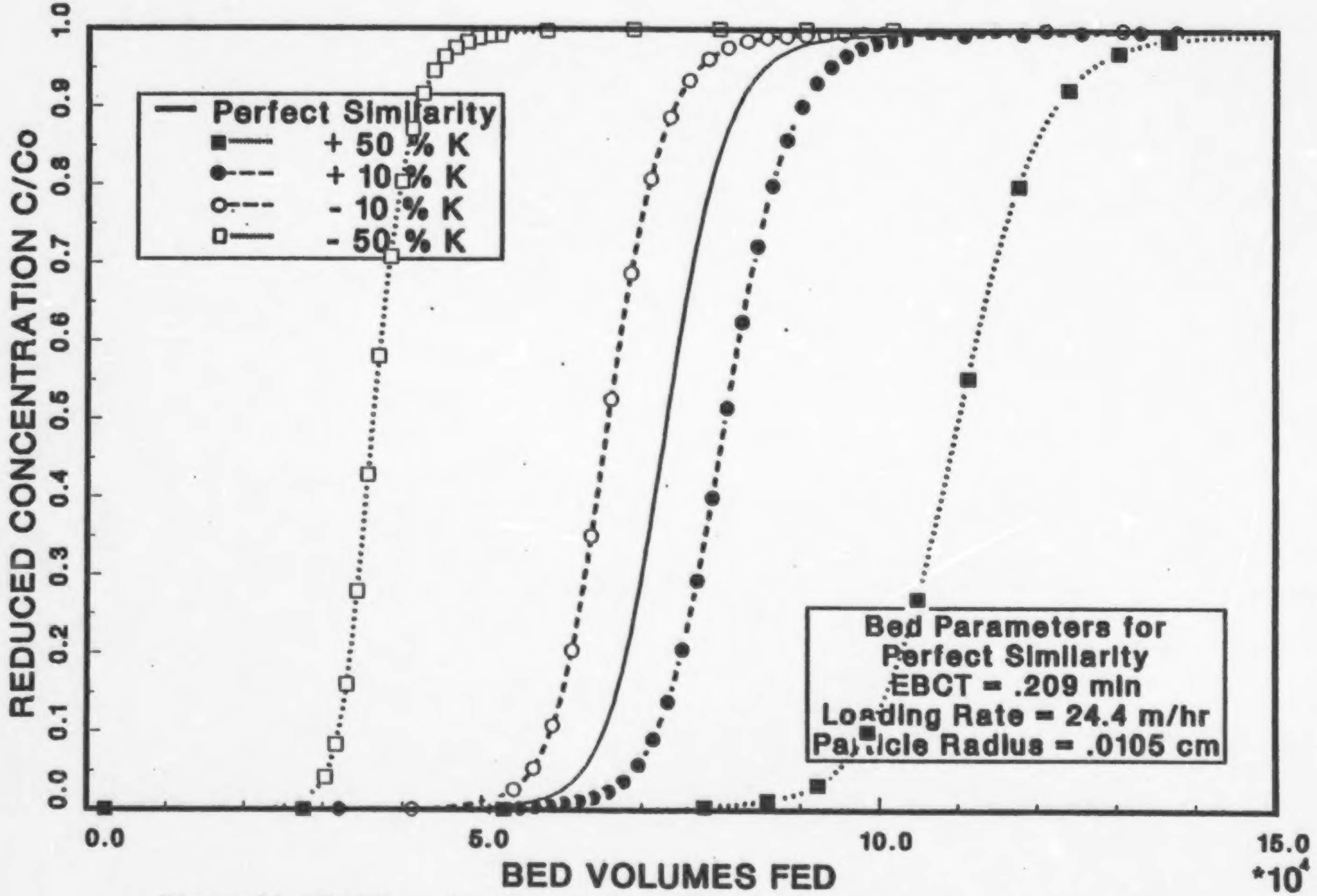

Figure 21. DFPSDM prediction of the RSSCT sensitivity to 10% and 50% changes in the Freundlich isotherm capacity.

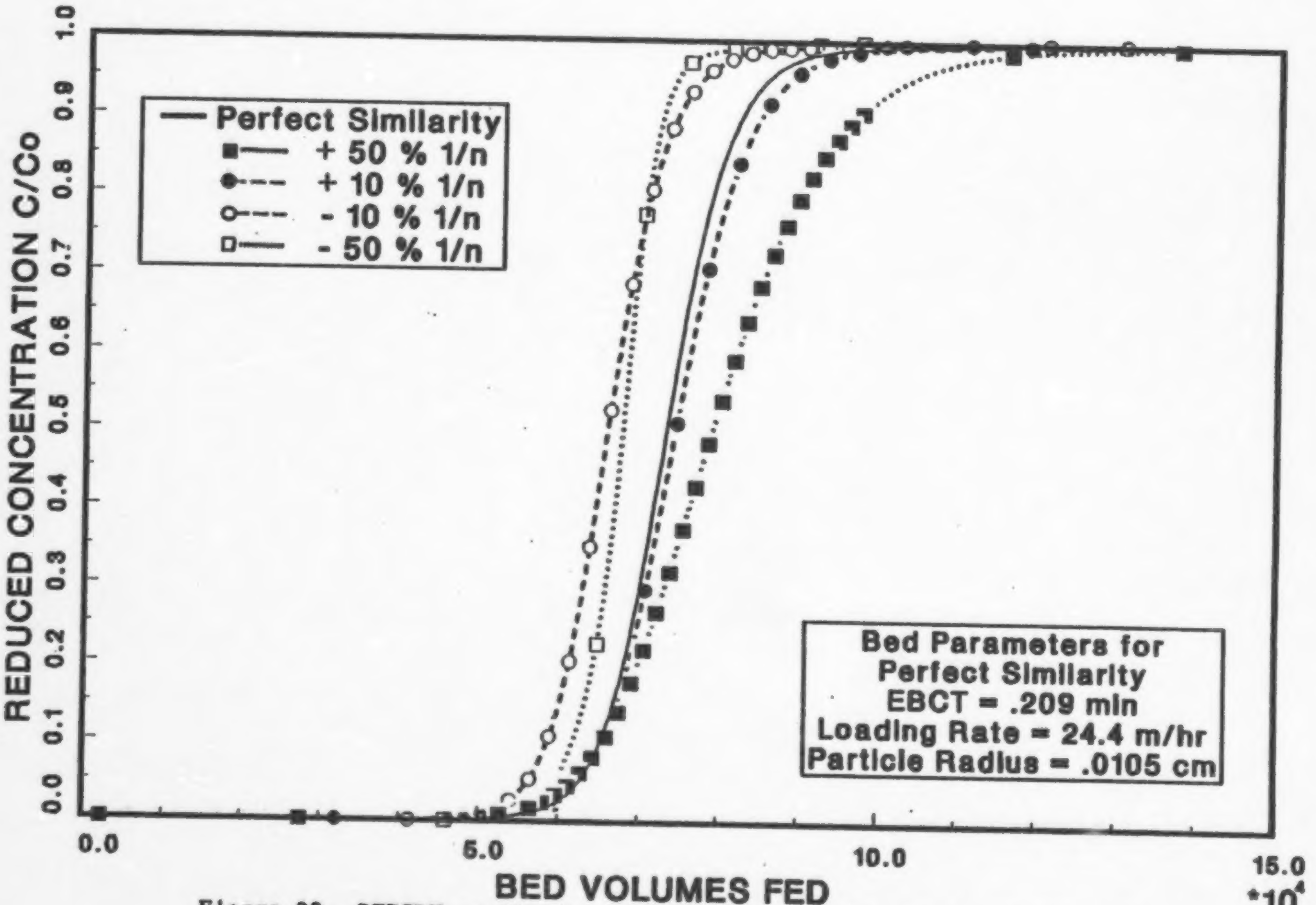

Figure 22. DFPSDM prediction of the RSSCT sensitivity to 10% and 50% changes in the Freundlich isotherm intensity constant, 1/n.

have a significantly different from the full-scale performance. To minimize the uncertainty of the GAC particle sizes, the full-size particle radius was determined by sieve analysis (Dobrzelewski 1984) and the smaller 60x80 mesh-size GAC for the RSCT's was examined under magnification for size and shape uniformity.

Figure 20 shows the influence that uncertainty in determining the bed void fraction, ε, has on the solute distribution parameters and the Stanton number. If the void fraction is larger than the assumed value for the RSSCT, then the RSSCT bed volume will be larger than calculated for perfect similarity. As a result of using the smaller calculated bed volume for plotting the data, an earlier breakthrough profile will be seen because the information is plotted in terms of a smaller-than-actual bed volume. In terms of the DFPSDM dimensionless groups, this is the result of using decreased solute distribution parameters and Stanton numbers.

The uncertainty of isotherm parameters, K and 1/n, can have a significant impact on the As seen in Figure 21, an opposite effect is observed with an increase in the Freundlich K. A difference between the actual and expected value in K results in a corresponding difference in the surface solute distribution parameter and the surface diffusion modulus. The result is shown in Fig. 21 as a displacement of the breakthrough profile forward or backward on the bed volumes axis. As seen in Figure 22, a larger 1/n value than expected can significantly increase the length of the mass transfer zone. Because a different equilibrium capacity in the RSSCT than that of the full-scale adsorber greatly affects the accuracy of the RSSCT, the equilibrium capacities of the GAC for the RSSCT must be measured and compared and found equal to that of the full-scale adsorber to ensure the accuracy of the test.

C. RSSCT Sensitivity to Changes in Selected Operating Conditions

Figures 23-26 display the sensitivity of the RSSCT to differences in the influent concentration, C_0, hydraulic loading rate, v_s, and the flowrate, respectively. The influent concentration is perhaps the least controllable of operating conditions. Changing influent concentrations make RSSCT's and pilot studies more difficult to interpret. On the other hand, flowrates and hydraulic loading rates are perhaps the most controllable process parameter. These parameters should be controlled as well as possible because they affect the surface diffusion modulus, the Stanton number, and the Peclet number.

Figure 23 shows the displacement of the expected breakthrough profile due to the change in influent concentration. Figure 24 shows the same information displayed in terms of actual concentrations. Changes in the influent concentration affect the surface solute distribution parameter and the surface diffusion modulus. A difference in the influent concentration may not change the length of the mass-transfer zone significantly, but will yield a significant displacement of the breakthrough profile. This may complicate interpretation of the RSSCT in determining the proper full-scale design and carbon use rates. However, differences may be accounted for by plotting the same effluent profile in terms of mass of solute fed per mass of adsorbent instead of the bed volumes fed.

For Fig. 25, the loading rate was changed by varying the diameter of the RSSCT while maintaining a constant bulk density and a constant bed volume, without recalculating other parameters that are dependent upon v_s, including k_f and D_e in Tables 4(a) and 5(a). The length was adjusted to retain the same EBCT. A change in the loading rate, v_s, as seen in Fig. 25, yields a corresponding change in the Stanton number. Because an increase in the hydraulic loading rate would also increase the values of k_f

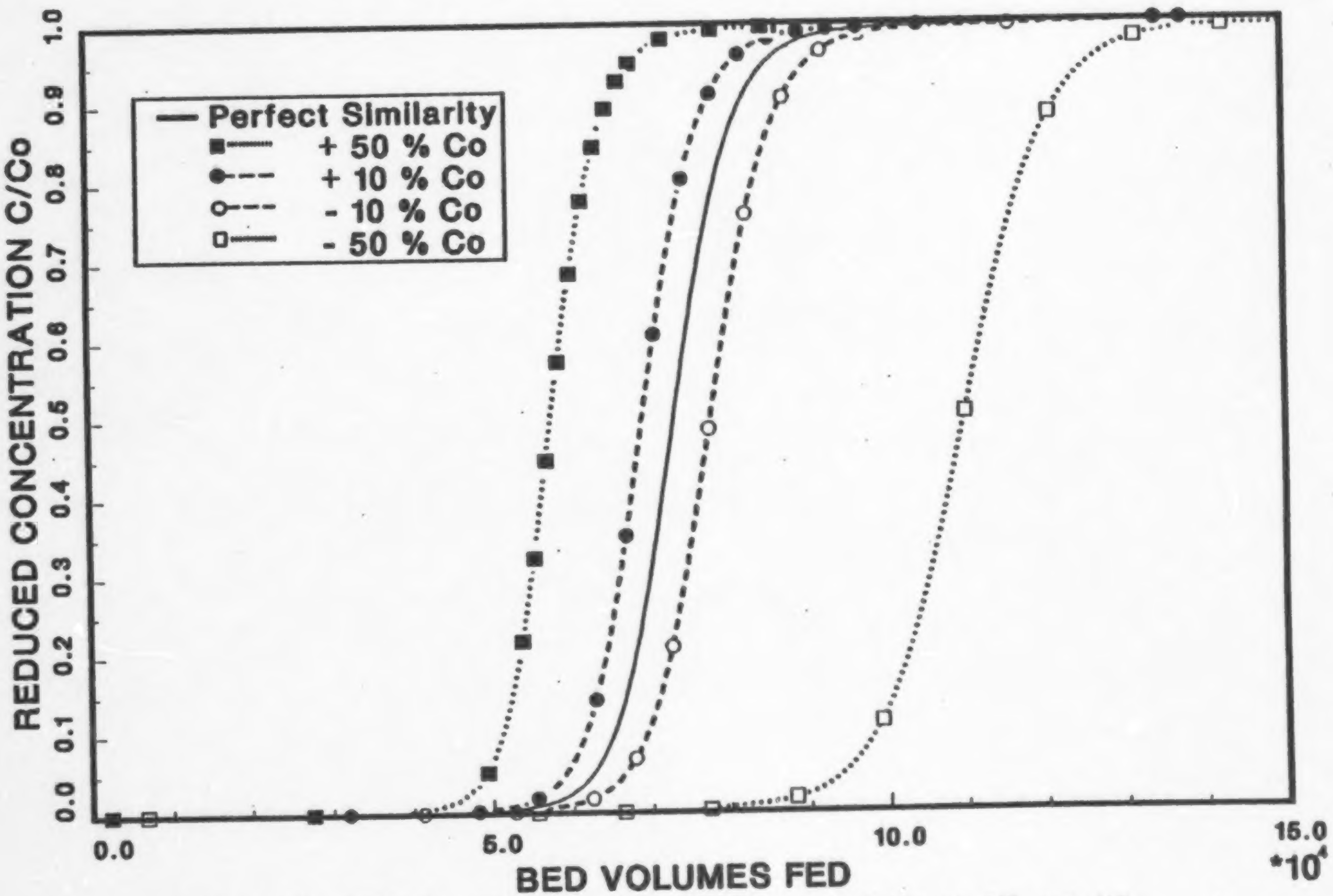

Figure 23. DFPSDM prediction of the RSSCT sensitivity to 10% and 50% changes in the dimensionless influent concentration.

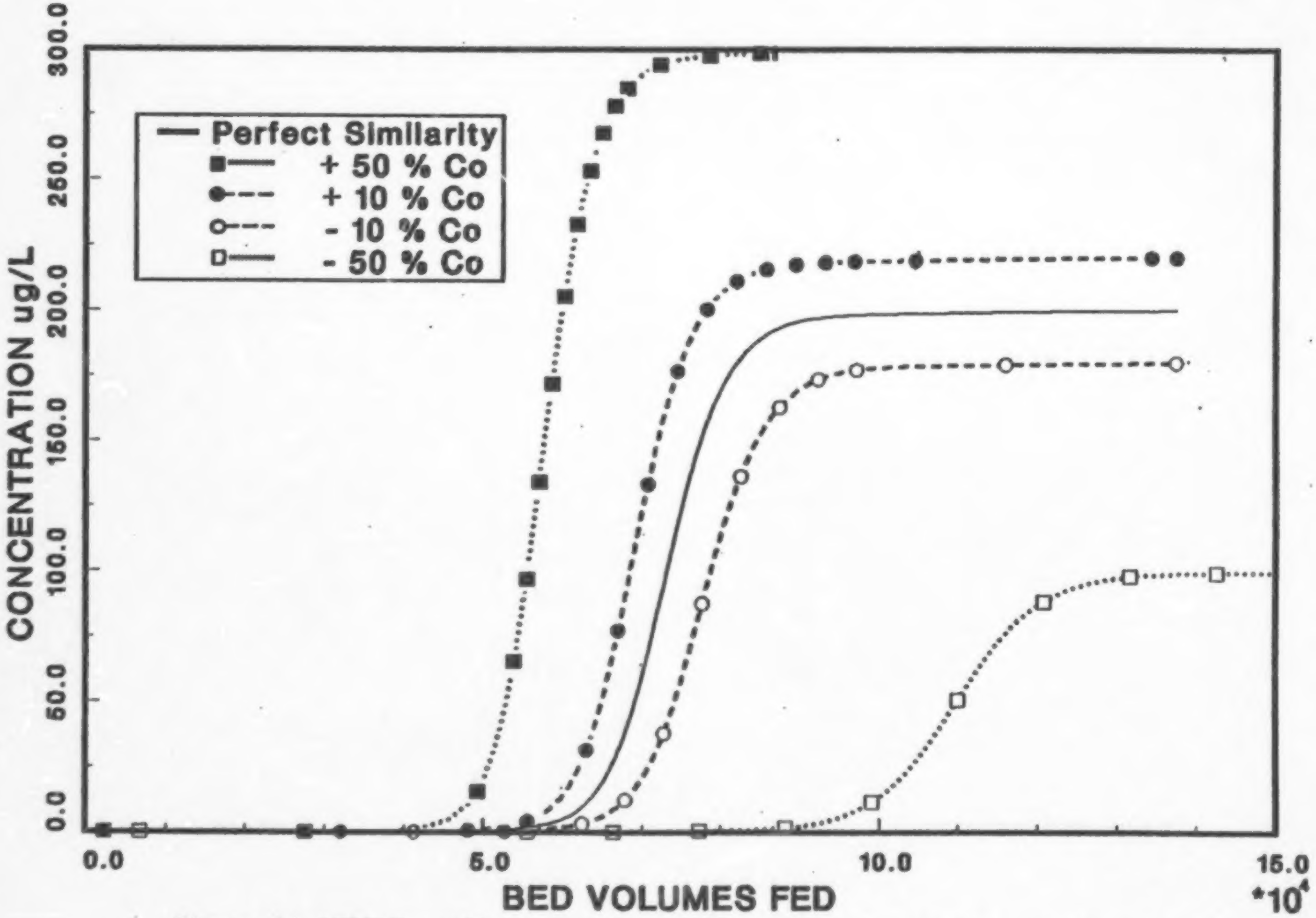

Figure 24. DFPSDM prediction of the RSSCT sensitivity to 10% and 50% changes in the influent concentration in μg/L.

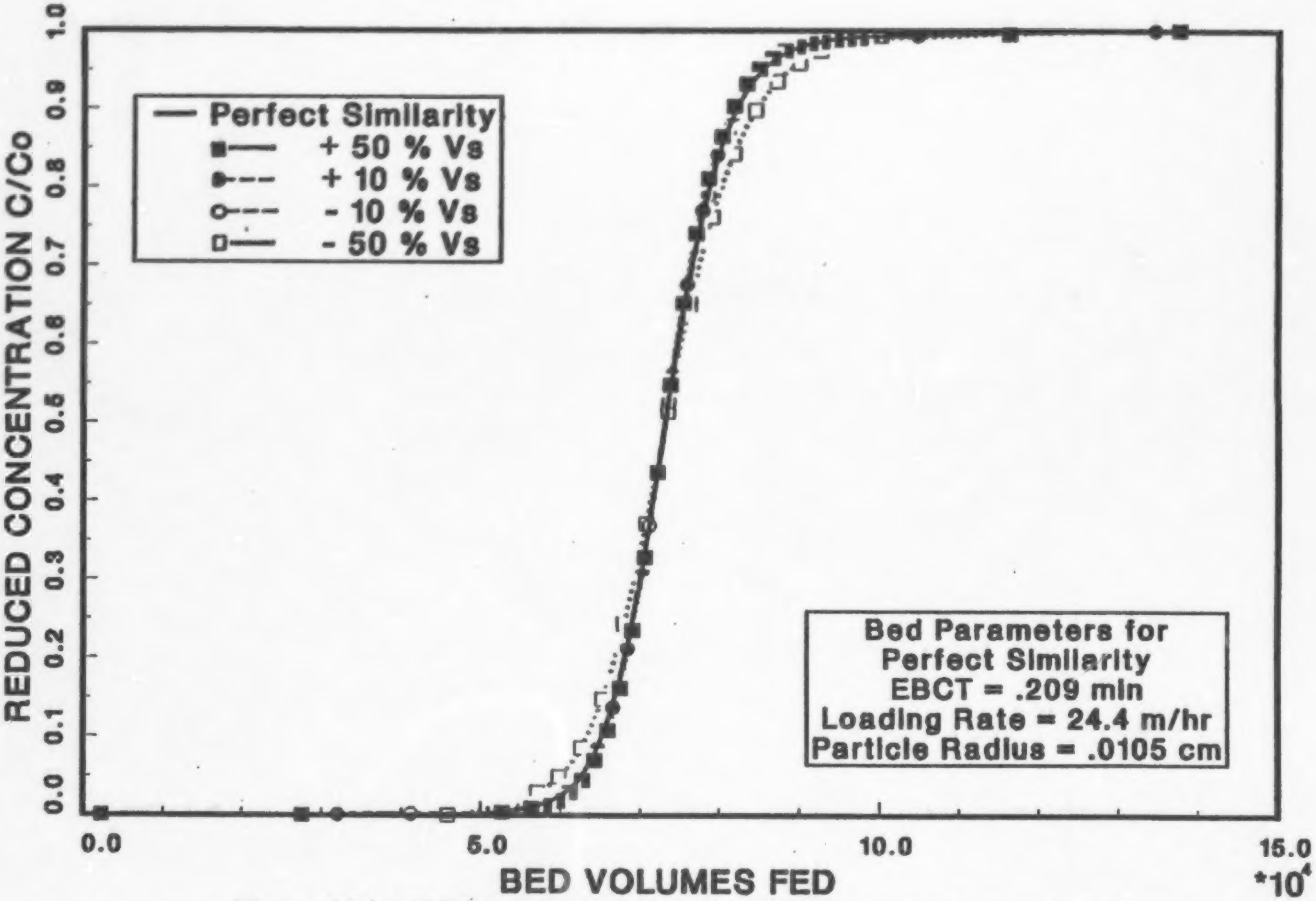

Figure 25. DFPSDM prediction of the RSSCT sensitivity to 10% and 50% changes in the hydraulic loading rate.

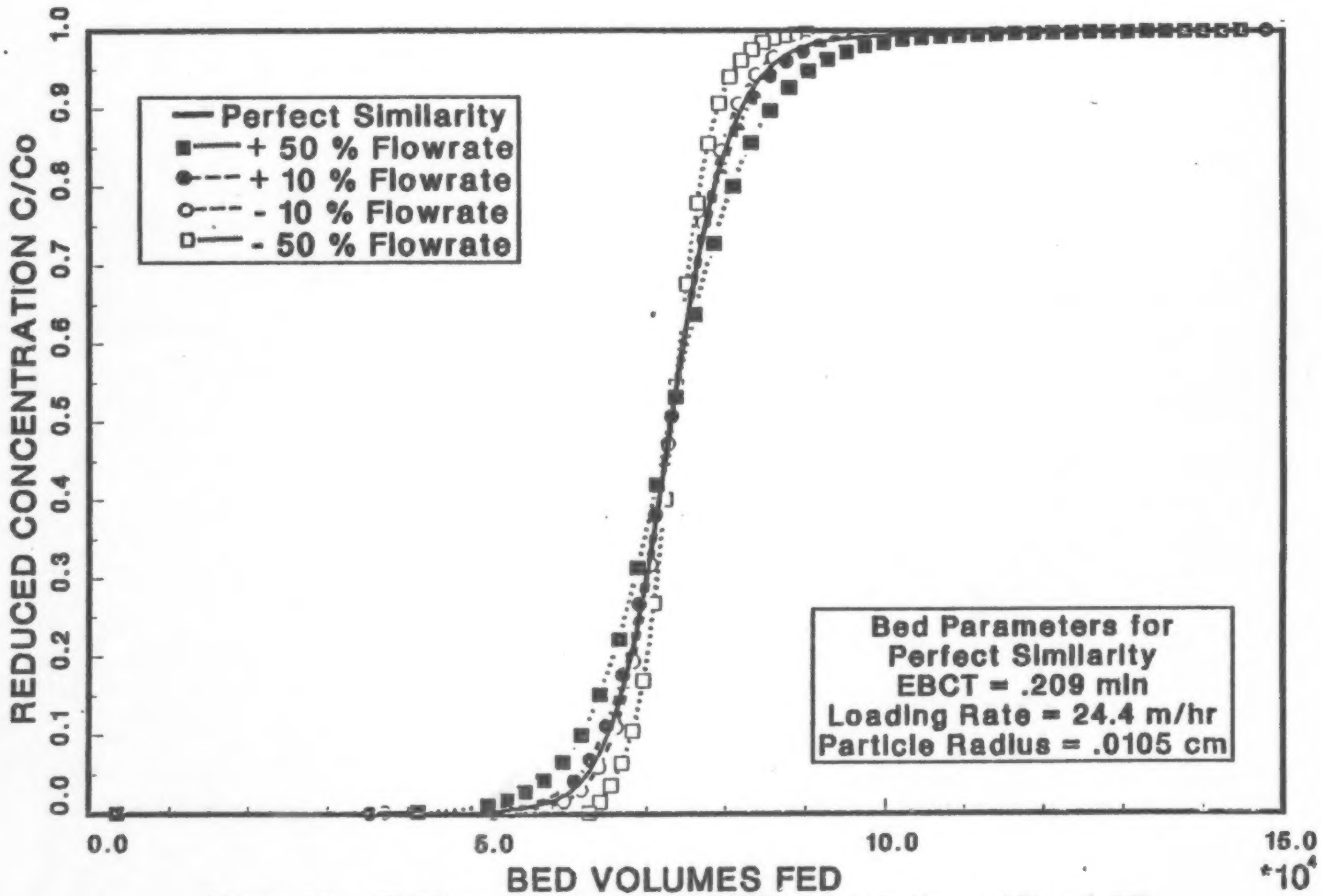

Figure 26. DFPSDM prediction of the RSSCT sensitivity to 10% and 50% changes in the flowrate.

and D_e, a change in the hydraulic loading rate would, in practice, produce a greater change in the breakthrough profile for this example due to the additional effects of the change in k_f and D_e. Figure 26 displays the slightly greater sensitivity is observed for changes in the flowrate in Table 4(a). Where the flowrate was increased, the hydraulic loading rate increases and the EBCT decreases. An increase in flowrate would also increase k_f and D_e. However, the effects of a difference in D_e and k_f have been shown previously in Figs. 13 and 14, respectively. For Fig. 26, only the loading rate and the EBCT were changed. The net effect for an increase in the flowrate is one of spreading of the mass transfer zone.

VI. EXPERIMENTAL VERIFICATION OF SCALING EQUATIONS

The scaling procedure was evaluated by a laboratory test at influent concentrations of 2000-5500 μg/L and by field tests and influent concentrations of less than 120 μg/L where RSSCT's were designed to simulate the performance of pilot-scale adsorbers. The proper scaling equations for the laboratory test were chosen by measurement of the effective diffusion coefficients of the full-size GAC and the smaller GAC that was used in the RSSCT. At the higher concentrations of the laboratory study, the diffusion coefficients of trichloroethene were found to be about the same for different particle sizes and the scaling equations that assume constant surface diffusivity (Eqs. 22 and 25) were applied for the design of the laboratory RSSCT. The laboratory RSSCT successfully simulated the breakthrough profiles of the laboratory pilot-scale adsorber.

Based upon the success of the work done in the laboratory at higher concentrations, the same scaling approach was applied to design RSSCT's to simulate the performance of pilot-scale adsorbers that were treating contaminated groundwater in Wausau, Wisconsin. The surface diffusivities of solutes in the Wausau groundwater were assumed to be equal for the GAC's that were used in the RSSCT's and pilot-scale studies. However, the field study results show that the RSSCT's which were designed under this assumption did not simulate the performance of pilot-scale adsorbers. The apparent surface diffusivity was much smaller for the smaller RSSCT carbon. An alternative approach to RSSCT design that is based upon the work of Schneider (1982) assumes a surface diffusivity linearly proportional to the particle radius. This scaling method was evaluated in the field study as an alternative and was found to be successful.

A. Effects of Size Reduction upon Selected Physical/Chemical Properties of Granular Activated Carbon

Previous discussion has shown that the void fraction, the equilibrium capacity, and the surface diffusivity have a significant impact upon the accuracy of the RSSCT. The method for scale-up of RSSCT's to field-scale adsorbers that is presented in this work assumes that the void fraction and the equilibrium capacities of the full-sized carbon are the same as those of the reduced size GAC in the RSSCT.

Trichloroethene isotherm parameters of the 60x80 mesh-size carbon were measured and were found to be the same as those of the 12x40 GAC that was used in the pilot studies. The bed void fractions measured for the RSSCT and pilot-scale carbon beds in the laboratory study were found to be equal between RSSCT and pilot-scale adsorber. However, in longer full- and pilot-scale adsorbers, the carbon begins to compact under its own weight and in this manner decreases the value of the void fraction. Surface diffusivities of carbons used in RSSCT and pilot-scale adsorber were measured for trichloroethene near the conditions of the laboratory study. Because the surface diffusivities were nearly the same, the scaling method used for most of the laboratory and field studies assumed a constant surface diffusivity.

The Freundlich isotherm parameters were determined from a bottle point isotherm conducted for TCE at 13°C using the 60x80 mesh size F-400 carbon. The 60x80 mesh size carbon was reduced to 200x400 mesh size to hasten the time to equilibrium. This size reduction has been shown not to affect isotherm capacities (Hand et al. 1984). Figure 27 displays the best fit of the Freundlich K and 1/n though the experimental data. The K and 1/n values of 187.0 $\mu mol/g(L/\mu mol)^{1/n}$ and 0.4179 respectively are very close to the Freundlich isotherm parameters of 196.6 (K) and 0.4163 (1/n) measured by Luft (1984), and those measured by Kato (1985) of 193.1 (K) and 0.4299 (1/n), for F-400 carbon. Therefore, the capacity of the smaller carbon for the RSSCT's is the same as the capacity of the full-size carbon for the

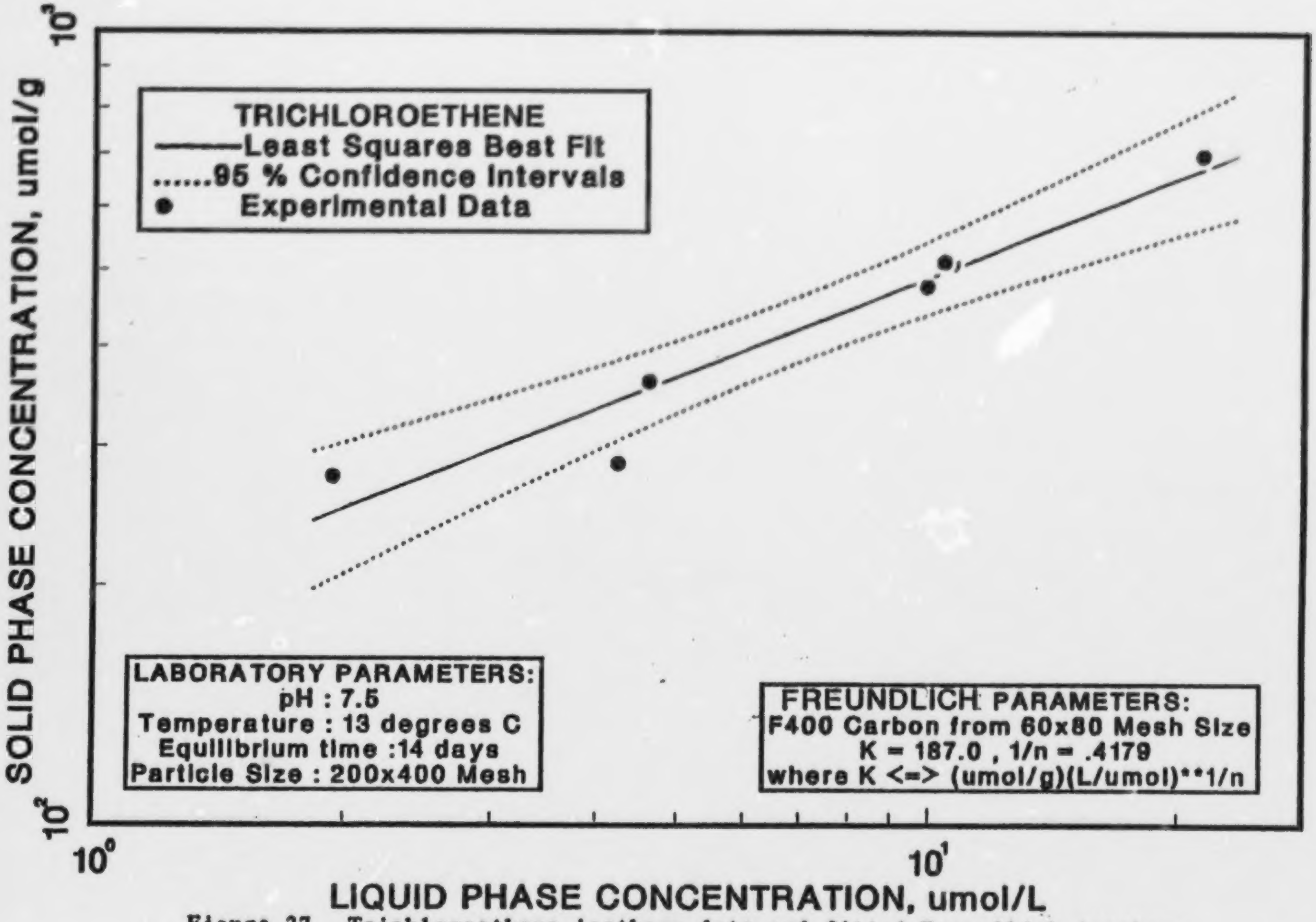

Figure 27. Trichloroethene isotherm data and fitted Freundlich isotherm parameters with 95% confidence intervals shown.

pilot-scale studies.

The void fraction of the smaller 60x80 mesh size carbon was determined assuming a 60x80 particle density of 0.8034 which is the value for the 12x40 F-400 carbon. A bulk density of 478 kg/m^3 was measured for the 60x80 carbon by determining the volume of a preweighed sample of carbon in a cylinder of known diameter. This value is the same as the manufacturer's reported value of 478 kg/m^3 for 12x40 F-400 carbon. The cylinder was tapped to settle the carbon to a constant height. The bed was wetted to replace the air in the voids with water and to account for any swelling effects. The void fraction of the 60x80 mesh size carbon bed was determined from the equation $\varepsilon = 1 - \rho_b/\rho_a$, where ρ_b is the weight of carbon divided by the volume of the carbon bed. A void fraction of 0.405 was calculated for the 60x80 carbon, which is nearly the same for the 12x40 mesh size carbon. Therefore, the RSSCT may be expected to have the same void fraction as the pilot-scale adsorbers, although in longer beds the carbon in pilot-and full-scale adsorbers may crush under its own weight, resulting in lower void fractions for pilot- and full-scale adsorbers.

As a further check for the void fraction, the shape of the 60x80 mesh size F-400 carbon that is used in the RSSCT's was observed under low magnification to determine the shape of the carbon particles. The smaller carbon particle shape was determined to be only slightly more angular than the 12x40 mesh size F-400 carbon. The smaller carbon was slightly more uniform in size and shape than the full-size carbon. This similar particle shape implies that packing of the bed would yield similar bed void fractions. From these observations, the value of the smaller carbon bed void fraction can be near the value for the full-size carbon.

Trichloroethene surface diffusivities of were measured by Dobrzelewski

(1984) at 11°C for 12x40 and 60x80 mesh size F-400 carbons. The values of 3.75×10^{-10} cm²/s for 12x40 mesh and 5.20×10^{-10} cm²/s for 60x80 mesh carbon at initial concentrations of 1322.7 µg/L and 1329 µg/L respectively. The 95% confidence intervals were calculated for both measurements and were found to overlap. Because the confidence intervals for these measurements overlap, it may be assumed that the trichloroethene surface diffusivities of both carbons are the same or nearly so.

The results of the trichloroethene diffusivity measurement indicate that it could be possible to design an RSSCT for perfect similarity and assume a constant surface diffusivity using Eqs. 22 and 25. The results of Schneider (1982)for p-nitrophenol, which are discussed in Section II.D.2, indicate that the assumption of a constant surface diffusivity may not always be valid.

The results of this study confirm two important assumptions of this scaling method: (1) that the bed void fraction of the reduced size carbon in the RSSCT can be the same as that of the full-size carbon, and (2) that the equilibrium capacity of the reduced size carbon is the same as that of the full-size carbon.

B. Laboratory Study Results and Discussion

The scaling procedure was tested in the laboratory by comparing effluent concentration profiles of a pilot- scale adsorber to those of a RSSCT with 60 X 80 mesh size GAC. The influent mixture contained the following adsorbates: chloroform, chlorodibromomethane, 1,2-dibromoethane, bromoform, trichloroethene, and tetrachloroethene. Equations 22 and were used 25 to design the RSSCT from the pilot-scale column specifications. The design and operational parameters of the pilot-scale column and the RSSCT are listed in Table 6.

The influent and effluent concentrations of the six components for the

Table 6. Pilot-Scale and Small-Scale Design Parameters for the Laboratory Study.

GAC Packing Characteristics		Large Column	Small Column
ρ_b	g/cm^3	0.478	0.482
ρ_a	g/cm^3	0.8034	0.8034
e		0.40	0.40
R	cm	0.0513	0.0105
Flow Specifications			
Column Diameter	cm	5.0	1.10
Column Length	cm	8.33	1.71
EBCT	s	60	2.51
CSA	cm^2	19.63	0.950
V_s	m/hr	5.00	24.4
Bed Volume	cm^3	163.6	1.621
Flow rate	cm^3/min	163.6	38.7
BVF_{max}		16000	16000
Required Volume	liters	2618	25.9
Run time	days	11.1	0.466
Head loss	N/m^2	118	3220
	PSI	0.02	0.47
Average Influent Concentrations μg/L			
Chloroform		2609	2670
Trichloroethene		3397	3763
Chlorodibromomethane		5367	5293
1,2 Dibromoethane		5730	5845
Bromoform		4366	4731
Tetrachloroethane		2281	3018
Influent Temperature	°C	11±1	11±1

pilot-scale adsorber and the RSSCT are plotted in Figures 28-33. The pilot-scale adsorber study which required 818 liters of water was only conducted for 5000 bed volumes of treatment because mechanical failure forced the end of operation. However, in twenty-four hours, the small-scale adsorber had treated 33,000 bed volumes using only 60 liters of water. The slight discrepancies that appear between breakthrough profiles for the pilot-scale adsorber and the RSSCT appear to correspond with differences in the influent concentrations which are plotted in Figs. 28-33 and summarized in Table 6. Consequently, the agreement between the pilot-scale adsorbers and the RSSCT was good and the RSSCT which is conducted with 60X80 mesh GAC can be conducted in 4.2% of the time that the pilot-scale column can be conducted.

The verification of the RSSCT which is shown in Figures 28-33 was a general test of the scaling equation because Friedman (1984) demonstrated that both the effects of pore and surface diffusion were present in this study. Moreover, Friedman (1984) demonstrated that both pore and surface diffusion are more likely to be significant when the MTZs of the adsorbates overlap as was observed in this study.

C. Field Study Results and Discussion

A pilot study conducted in Wausau, Wisconsin, was used to evaluate the accuracy of the RSSCT in predicting pilot-scale performance in the field. This pilot study used Calgon's F-400 and Westvaco's WV-G activated carbons in a beds-in series operation to evaluate several EBCT's. This pilot study provided the operating parameters and the performance data to compare to RSSCT data. Table 7 contains the operating parameters of pilot-scale adsorbers of (a) 1 minute EBCT using F-400 carbon, (b) 3.2 minute EBCT using F-400, (c) 5.4 minute EBCT using F-400 carbon, and (d) 1 minute EBCT using WV-G carbon. Table 7 also contains the average influent concentrations of

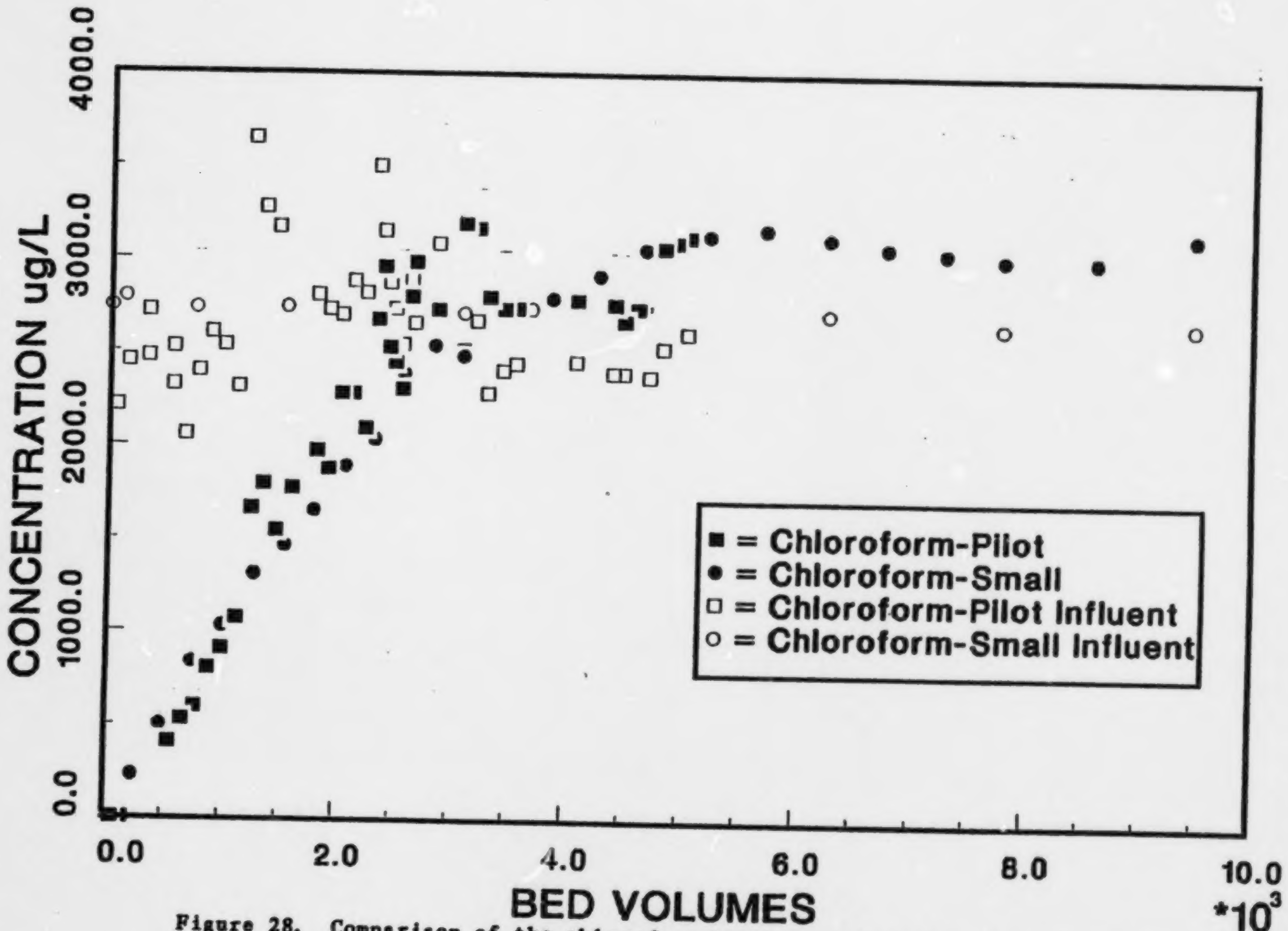

Figure 28. Comparison of the chloroform breakthrough profile for the small-column test to the pilot-scale column in the laboratory study. Influent data are shown. Operating parameters are presented in Table 6.

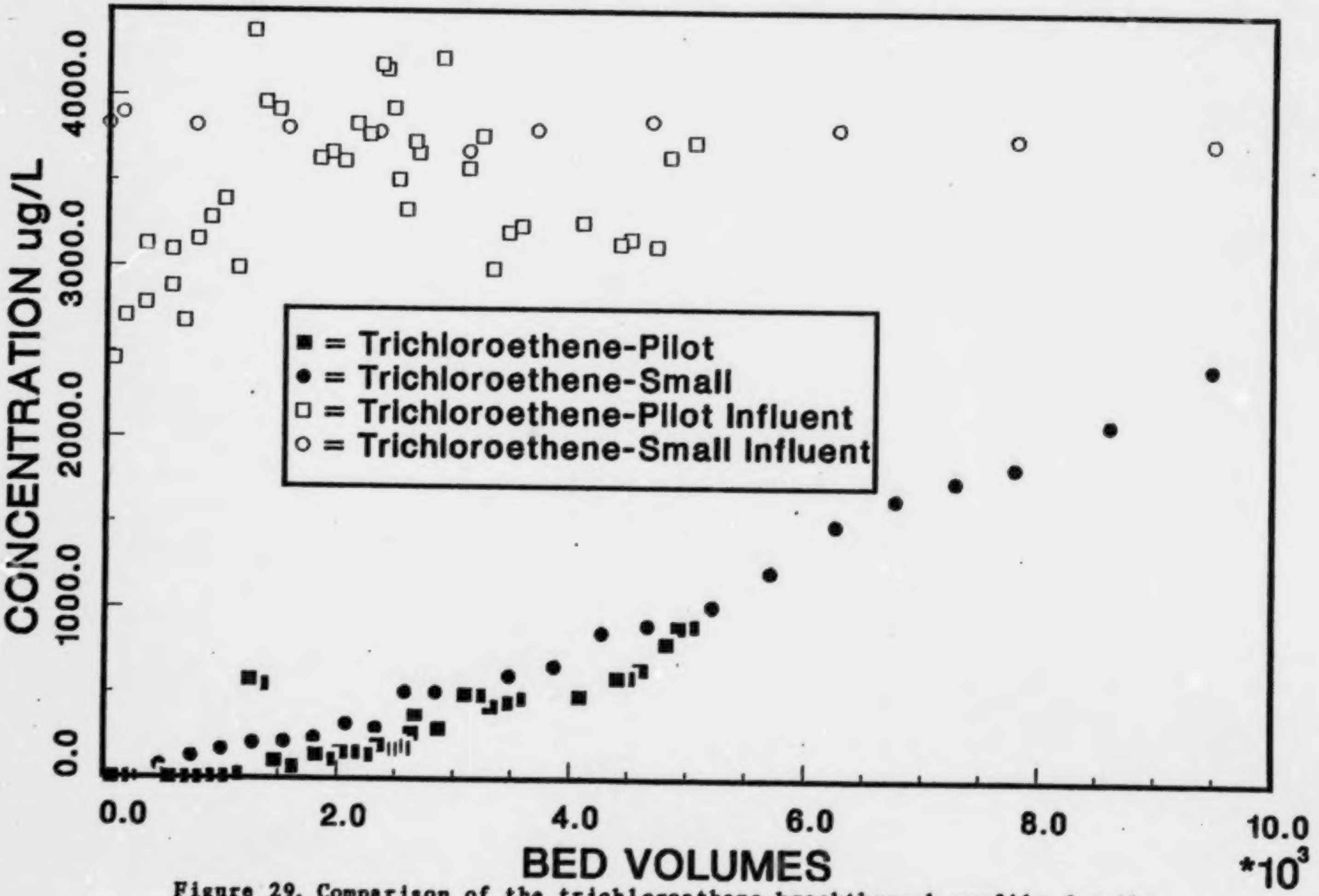

Figure 29. Comparison of the trichloroethene breakthrough profile for the small-column test to the pilot-scale column in the laboratory study. Influent data are shown. Operating parameters are presented in Table 6.

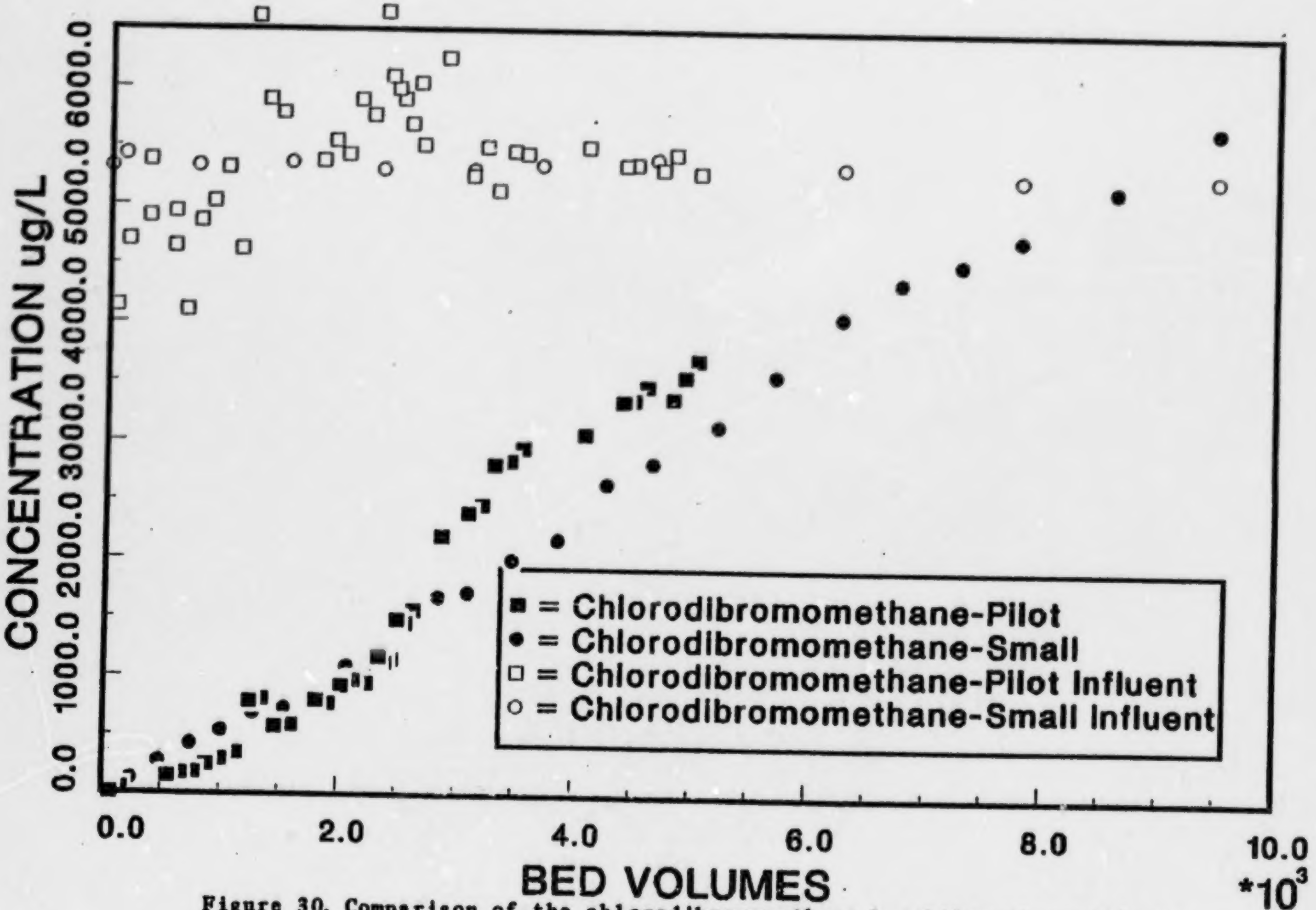

Figure 30. Comparison of the chlorodibromomethane breakthrough profile for the small-column test to the pilot-scale column in the laboratory study. Influent data are shown. Operating parameters are presented in Table 6.

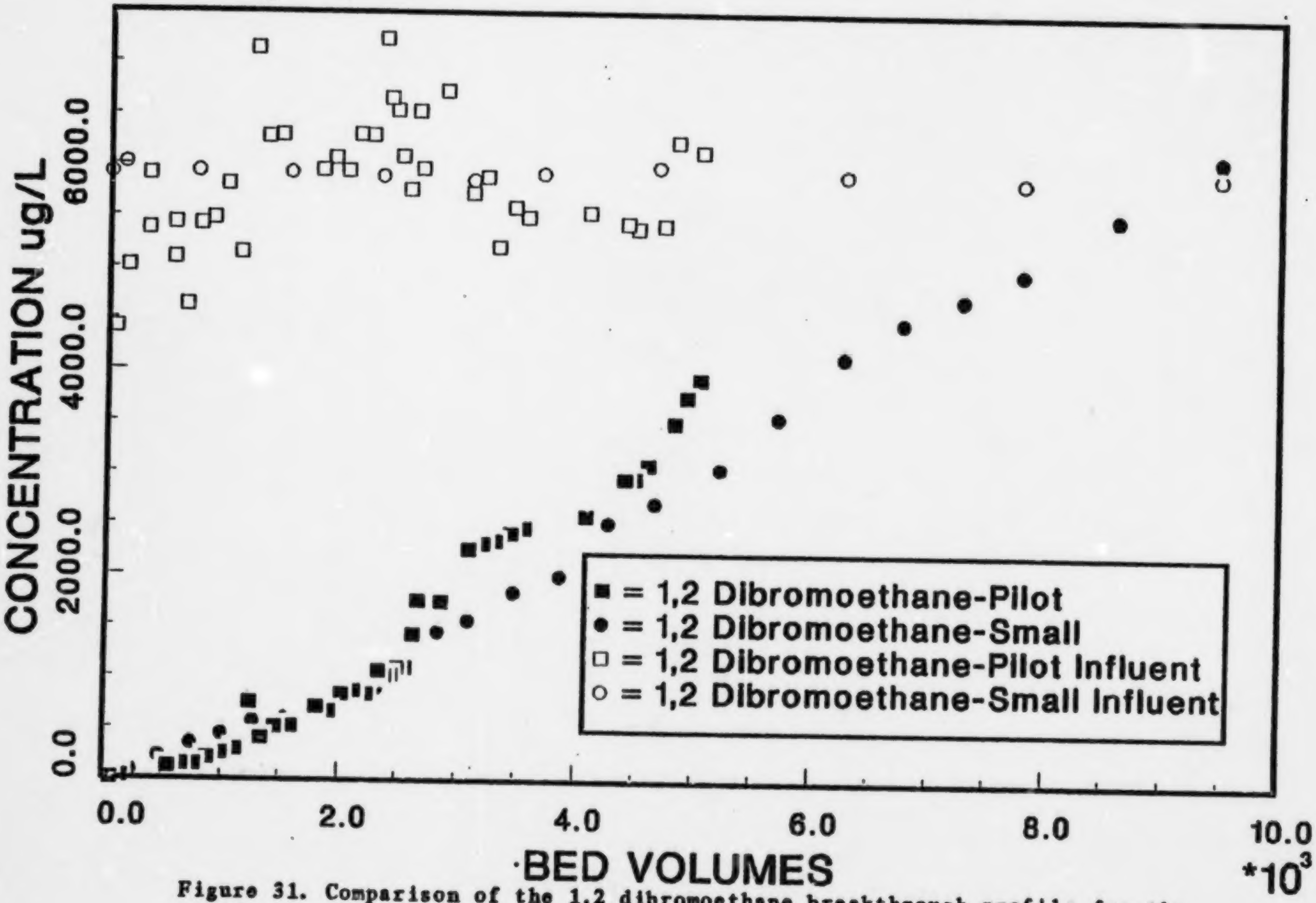

Figure 31. Comparison of the 1,2 dibromoethane breakthrough profile for the small-column test to the pilot-scale column in the laboratory study. Influent data are shown. Operating parameters are presented in Table 6.

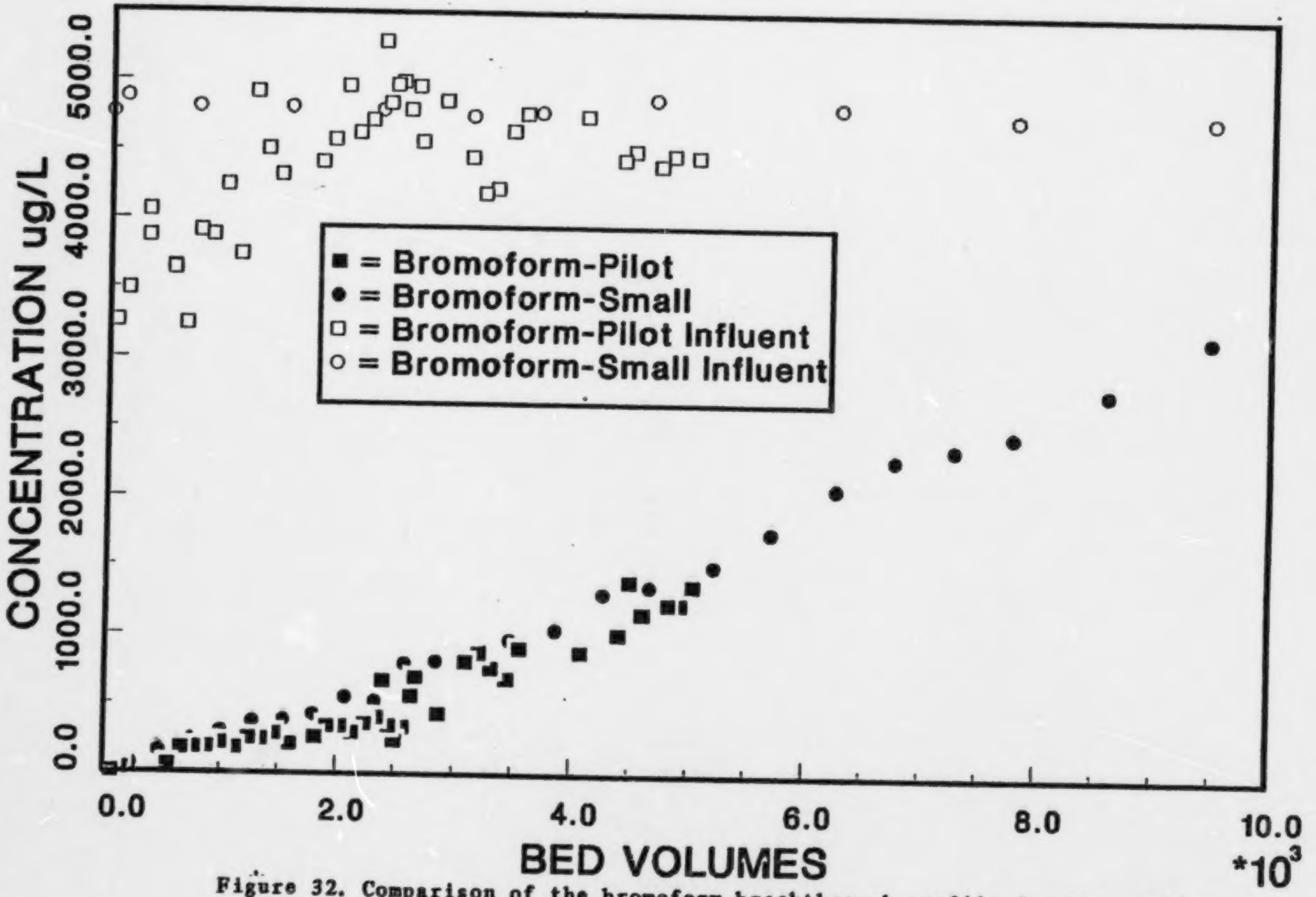

Figure 32. Comparison of the bromoform breakthrough profile for the small-column test to the pilot-scale column in the laboratory study. Influent data are shown. Operating parameters are presented in Table 6.

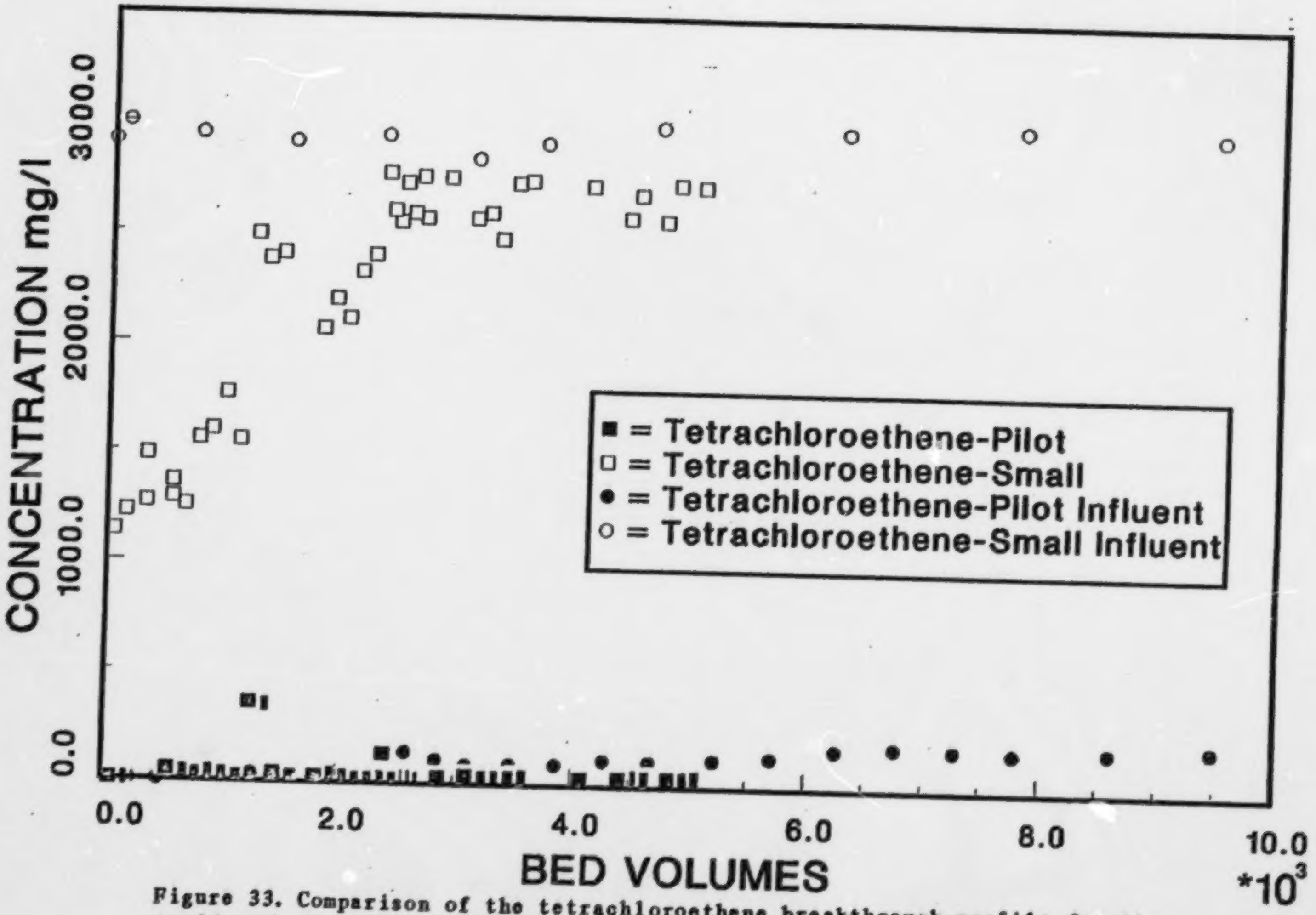

Figure 33. Comparison of the tetrachloroethene breakthrough profile for the small-column test to the pilot-scale column in the laboratory study. Influent data are shown. Operating parameters are presented in Table 6.

Table 7. Pilot-Scale Design and Operational Parameters for the Field Pilot Studies: (a) EBCT - 1 minute (b) EBCT - 3 minutes (c) EBCT 5 minutes (d) EBCT 1 minute. Data calculated from operation August 26, 1984 to January 24, 1985.

		F-400 (a)	F-400 (b)	F-400 (c)	WV-G (d)
GAC Packing Characteristics					
ρ_b	g/cm^3	480	520	520	429
ρ_a	g/cm^3	0.8034	0.8034	0.8034	0.7530
ε		0.40	0.35	0.35	0.43
R	cm	0.05129	0.05129	0.05129	0.05370
Flow Specifications					
Column Diameter	cm	5.03	5.03	5.03	5.03
Column Length	cm	7.65	24.48	41.31	7.33
EBCT	s	60	192	324	60
CSA	cm^2	19.9	19.9	19.9	19.9
V_s	m/hr	4.59	4.59	4.59	4.40
Bed Volume	cm^3	152.2	487.2	822.1	145.9
Flow rate	cm^3/min	152.2	152.2	152.2	145.9
Average Influent Concentration: µg/L					
Dichloroethene		80.9	80.9	80.9	81.9
Trichloroethene		66.6	66.6	66.6	69.7
Tetrachloroethene		45.2	45.2	45.2	36.7
Vinyl Chloride		7.5	7.5	7.5	7.7
1,1,1 Trichloroethane		1.3	1.3	1.3	1.4
Toluene		22.0	22.0	22.0	20.4
Ethyl Benzene		4.1	4.1	4.1	3.7
m-Xylene		4.7	4.7	4.7	4.0
o,p-Xylenes		8.4	8.4	8.4	8.0
Influent Temperature	°C	12±2	12±2	12±2	12±2

the monitored contaminants. The data for the pilot study was collected over a period from August 26, 1984 to January 24, 1985.

Four RSSCT's were designed to evaluate the scaling methods described previously. The influent mixture for this study was a raw groundwater containing cis-dichloroethene, trichloroethene, tetrachloroethene, vinyl chloride, 1,1,1 trichloroethane, toluene, ethyl benzene, m-xylene, o-xylene, and p-xylenes. The o- and p- xylene concentrations are reported as a sum. In addition to the numerous volatile organic chemicals, iron and manganese were present in approximate concentrations of 5 mg/L and 1 mg/L respectively.

Equations 22 and 25 were used to design the four RSSCT's from the pilot-scale adsorber operating parameters corresponding to 1 minute, 3.2 minutes, and 5.4 minutes of empty-bed contact time using F-400 carbon, and pilot-scale adsorber parameters of 1 minute EBCT using WV-G carbon. RSSCT's were designed for perfect similarity using Eqs. 22 and 25 because the laboratory RSSCT successfully simulated the laboratory pilot-scale adsorber at higher concentrations using Eqs. 22 and 25 for the RSSCT design.

Table 8 contains the operating parameters of RSSCT's to simulate (a) 1 minute EBCT using F-400 carbon, (b) 3.2 minute EBCT using F-400, (c) 5.4 minute EBCT using F-400 carbon, and (d) 1 minute EBCT using WV-G carbon. To also evaluate RSSCT design where surface diffusivities change linearly with adsorbent particle size, the RSSCT in Table 8(c) may be used to simulate the pilot-scale adsorber in Table 7(a) using Eqs. 25 and 27 which assume surface diffusion control. RSSCT's described in Tables 8(a) and 8(d) were conducted during August 26-31, 1984. The RSSCT described in Table 8(b) was conducted during the period January 9-18, 1985 and the RSSCT in Table 8(c) was conducted during March 1-6, 1985.

Table 8. RSSCT Design and Operational Parameters for the Field Studies: (a) simulation of pilot adsorber 'a'in Table 7. (b) simulation of pilot adsorber 'b'in Table 7. (c) simulation of pilot adsorber 'c' in Table 7 assuming constant diffusivity and 'a' in Table 7 assuming linearly dependent diffusivity. (d) simulation of pilot adsorber 'd'in Table 7

		F-400 (a)	F-400 (b)	F-400 (c)	WV-G (d)
GAC Packing Characteristics					
ρ_b	g/cm^3	478	478	481	433
ρ_a	g/cm^3	0.8034	0.8034	0.8034	0.7530
ε		0.39	0.41	0.40	0.44
R	cm	0.0105	0.0105	0.0105	0.0105
Flow Specifications					
Column Diameter	cm	1.1	1.1	1.1	1.03
Column Length	cm	1.70	5.12	7.70	1.67
EBCT (actual)	s	2.51	9.54	12.21	2.57
EBCT (calculated)*	s	2.51	8.05	13.57	2.29
EBCT (calculated for D_s R)**				12.28	
CSA	cm^2	0.95	0.95	0.83	0.95
V_s	m/hr	24.5	19.1	22.7	23.4
V_s (calculated)	m/hr	22.4	22.4	22.4	22.5
Bed Volume	cm^3	1.58	4.86	6.42	1.66
Flow rate	cm^3/min	38.0	30.4	31.5	38.6
Average Influent Concentration: µg/L					
Dichloroethene		109	69.8	68.5	109
Trichloroethene		76.1	45.1	33.4	76.1
Tetrachloroethene		56.4	33.3	25.9	56.4
Vinyl Chloride		7.5	6.8	6.7	7.5
1,1,1 Trichloroethane		1.3	0.96	0.76	1.3
Toluene		25.3	11.7	16.0	25.3
Ethyl Benzene		3.1	2.4	3.7	3.1
m-Xylene		6.0	3.6	4.3	6.0
o,p-Xylenes		9.3	6.8	6.5	9.3
Influent Temperature		13±2	14±2	14±2	13±2
Dates of operation		8/26/84 to 8/31/84	1/9/85 to 1/18/85	3/1/85 to 3/6/85	8/26/84 to 8/31/84

* Calculated from parameters in Table 7 using Eq. 22 for perfect similarity.

** Calculated from parameters in Table 7 using Eq. 27 for similar Ed.

The influent and effluent concentration history profiles were compared as concentration in μg/L versus the equivalent number of bed volumes fed for both pilot-scale adsorber and RSSCT. Chemicals monitored in the influent and effluent include cis-dichloroethene, trichloroethene, tetrachloroethene, vinyl chloride, 1,1,1 trichloroethene, toluene, ethyl benzene, m-xylene, and o- and p-xylenes. Toluene measurements from 5000-25000 bed volumes are considered inaccurate due to degradation of toluene in sample storage. The effect of this degradation on the accuracy of concentration measurement of other solutes is considered to be minimal. The o- and p- xylene concentrations are reported as a sum.

Influent concentrations decreased gradually during the course of the pilot study. Because it is necessary to have the same influent concentrations for breakthrough profiles between RSSCT and pilot-scale adsorber to be identical, the decrease in influent concentrations made interpretation of the results more difficult. This difficulty is resolved by plotting the data in terms of the mass of individual solute fed per mass of adsorbent versus the reduced concentration.

Pilot study operational parameters that are reported in Table 7 are averaged over this time period however, the pilot-scale columns were initially operating at a higher flowrate. The effect of increased hydraulic loading and shortened EBCT may have caused an earlier initial breakthrough of solutes in the early portion of the profiles for the pilot-scale adsorbers. This may account for the greater similarity observed for the more weakly adsorbing components for the shorter EBCT's.

Iron and manganese precipitates were observed at different locations in both the pilot-scale adsorbers and RSSCT's. Because these precipitates appeared abruptly towards the end of the RSSCT, they did not cause adsorption interferences during the test. However, the iron and manganese precipitates collecting in the fixed-bed cause excessive headloss and will bring a RSSCT to an early conclusion if precautions are not taken to prevent the introduction of air into the adsorber.

The apparent surface diffusivities were smaller at the smaller RSSCT carbon sizes. Because the RSSCT's were designed assuming constant surface diffusivities, large differences were observed between RSSCT and pilot-scale adsorber breakthrough profiles, especially for the more strongly adsorbing solutes. The scope of this study does not include quantitative conclusions about the dependency of surface diffusivity on the particle size. At the higher concentration of the laboratory study the assumption of constant D_s seemed sound and at the low concentrations of the field study the assumption that D_s is linearly dependent on the adsorbent particle size seems sound. More work needs to be done to relate the relationship of D_s and R with respect to the concentration. To better evaluate scaling procedures at the low concentrations of most applications in drinking water, groundwater, or waste water, pilot-scale and RSSCT studies need to be conducted at low concentrations under controlled conditions as a better test of these scaling relationships.

1. Discussion of RSSCT Results for Simulation of One Minute EBCT Adsorbers Assuming Constant Surface Diffusivity

Figures 34-42 display the breakthrough comparisons of 1 minute EBCT pilot-scale adsorber in Table 7(a) and the RSSCT in Table 8(a) using Calgon F-400 carbon. The RSSCT was designed for perfect similarity assuming constant diffusivity (Eqs. 22 and 25).

Similar breakthrough profiles were obtained between the RSSCT and the pilot-scale adsorber for cis-dichloroethene in Fig. 34, and trichloroethene in Fig. 35. The breakthrough profile comparisons for tetrachloroethene in

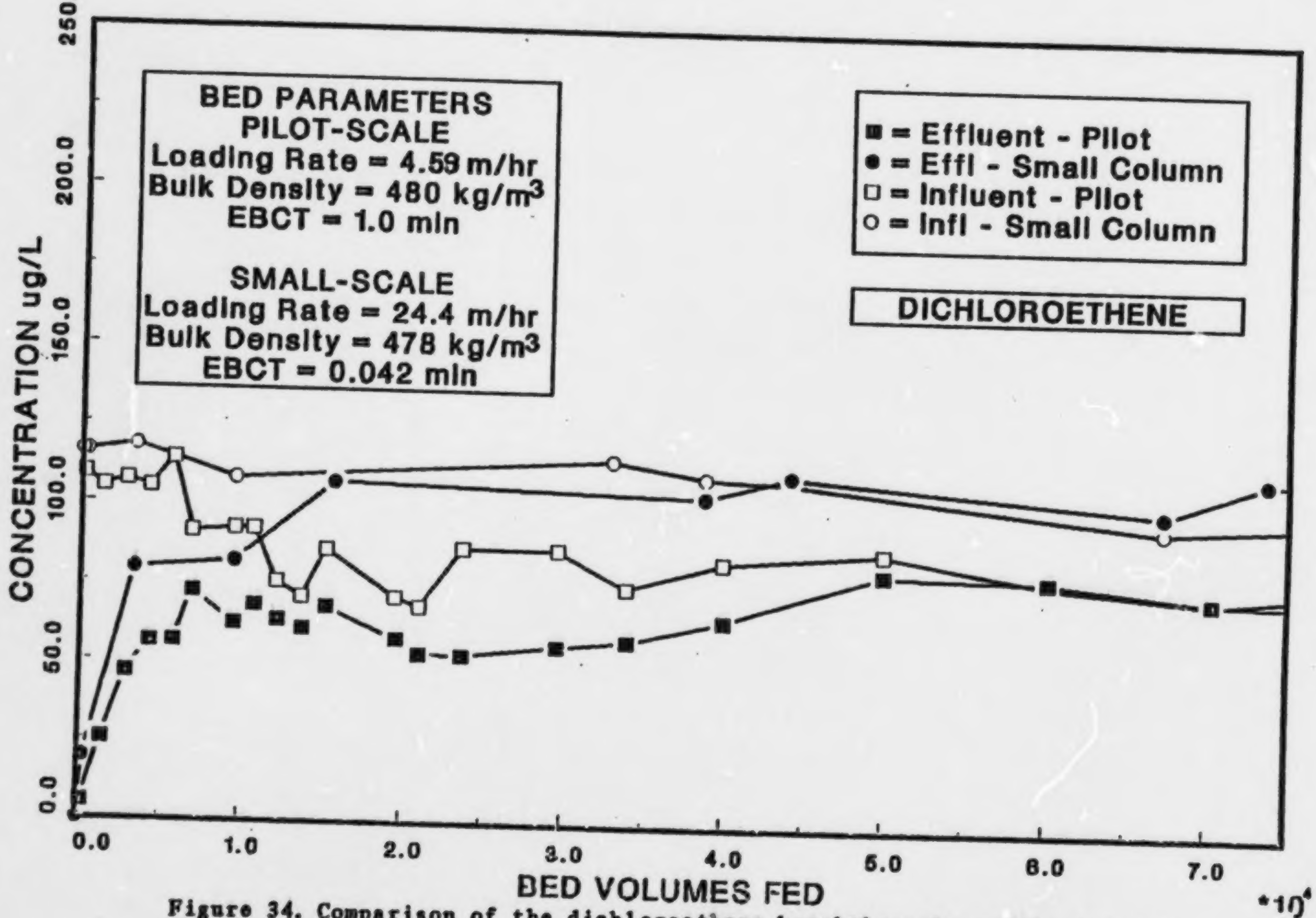

Figure 34. Comparison of the dichloroethene breakthrough profile for the small-column test to the pilot-scale column in the field study. Influent data are shown. Operating parameters are presented in Tables 7 and 8 (a).

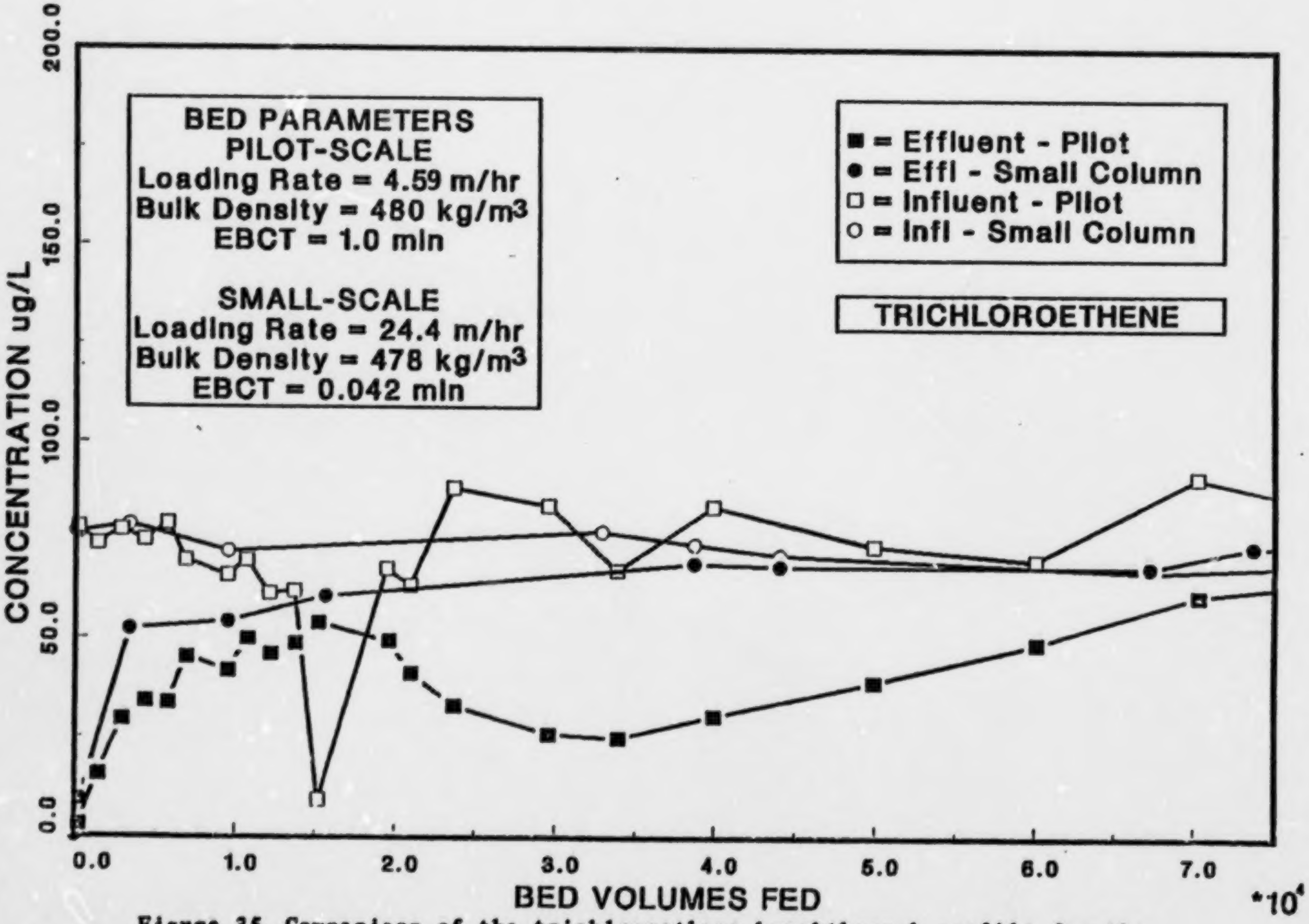

Figure 35. Comparison of the trichloroethene breakthrough profile for the small-column test to the pilot-scale column in the field study. Influent data are shown. Operating parameters are presented in Tables 7 and 8 (a).

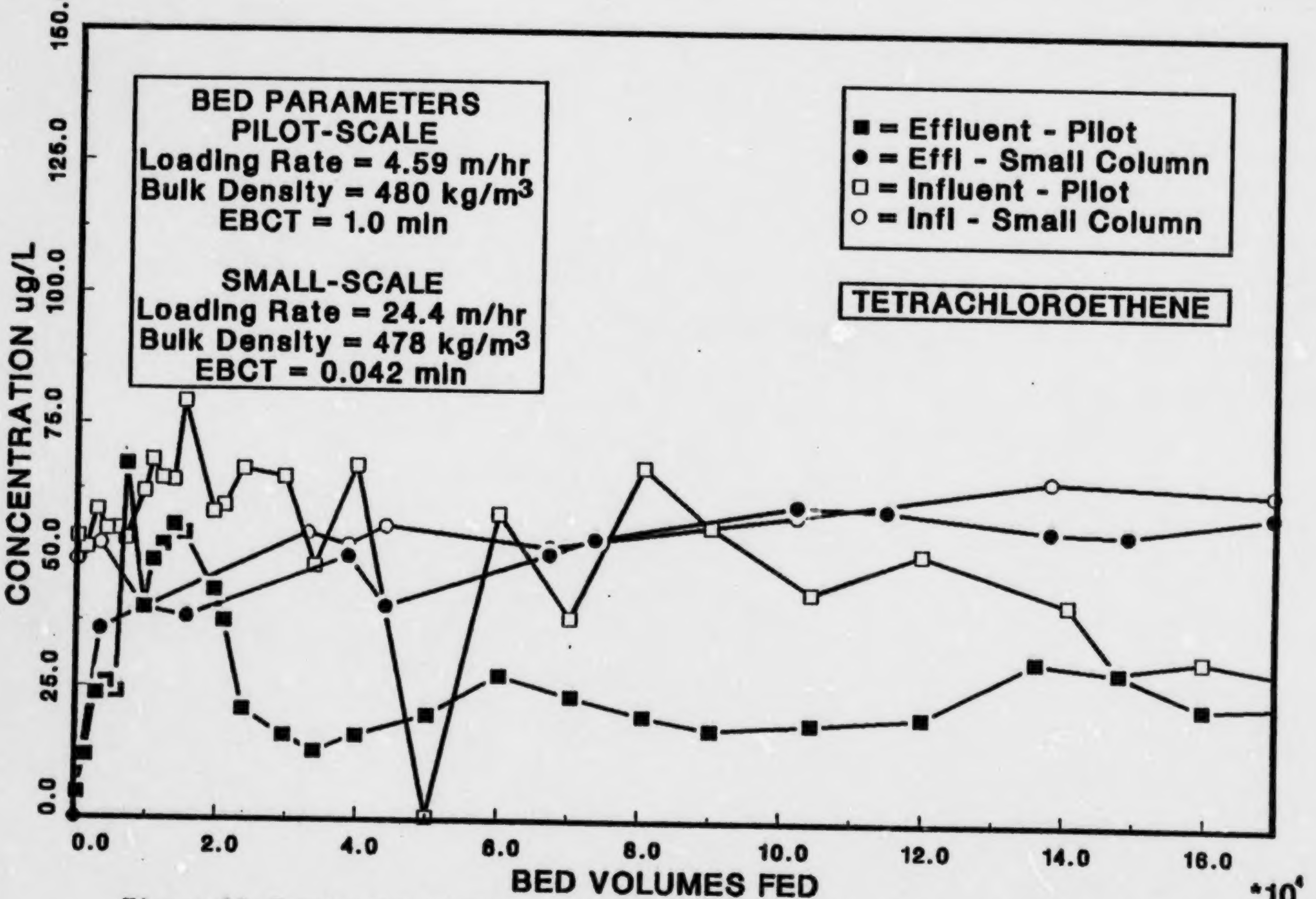

Figure 36. Comparison of the tetrachloroethene breakthrough profile for the small-column test to the pilot-scale column in the field study. Influent data are shown. Operating parameters are presented in Tables 7 and 8 (a).

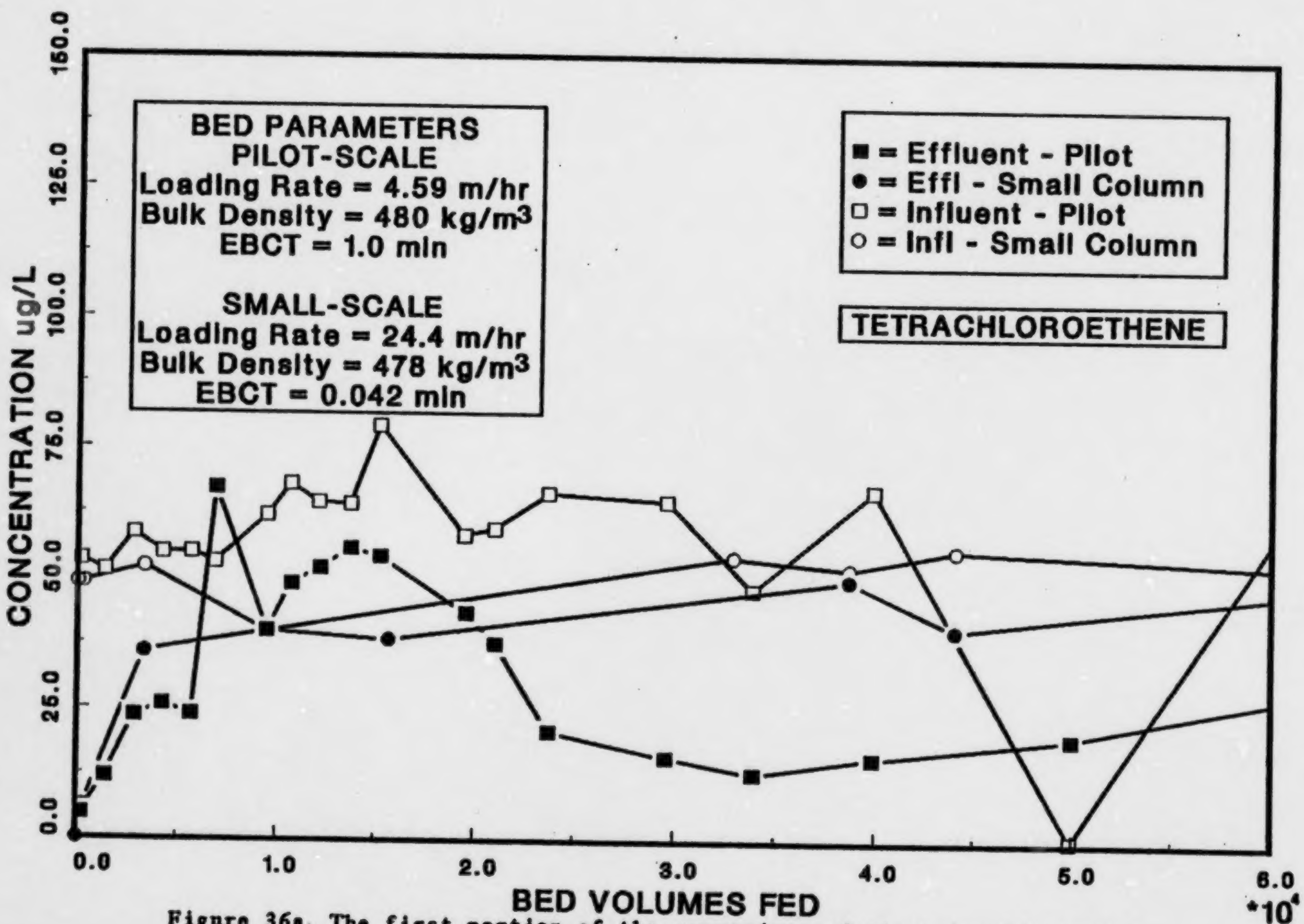

Figure 36a. The first portion of the comparison of the tetrachloroethene breakthrough profile for the small-column test to the pilot-scale column in the field study expanded along the bed volumes axis. Influent data are shown. Operating parameters are presented in Tables 7 and 8 (a).

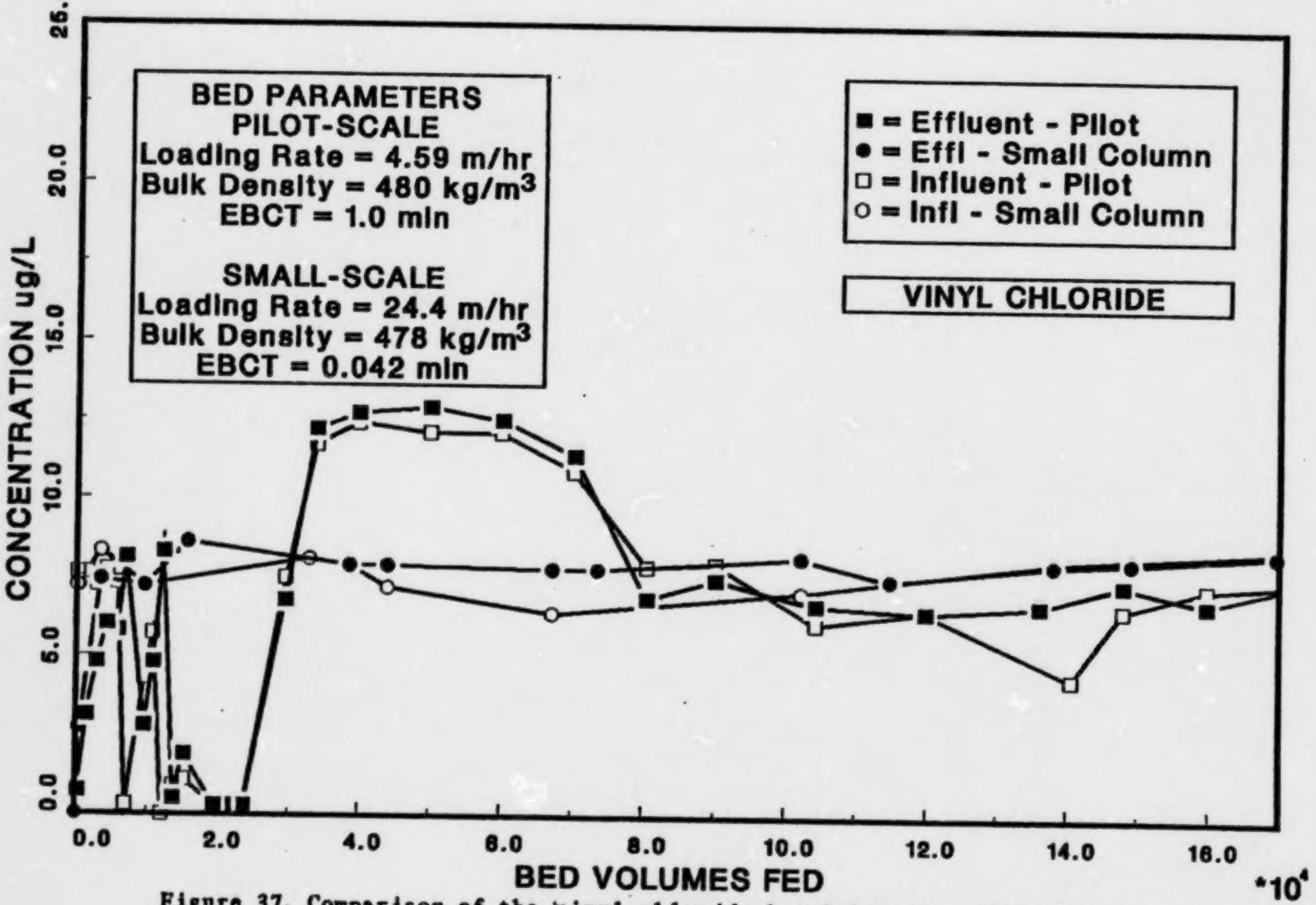

Figure 37. Comparison of the vinyl chloride breakthrough profile for the small-column test to the pilot-scale column in the field study. Influent data are shown. Operating parameters are presented in Tables 7 and 8 (a).

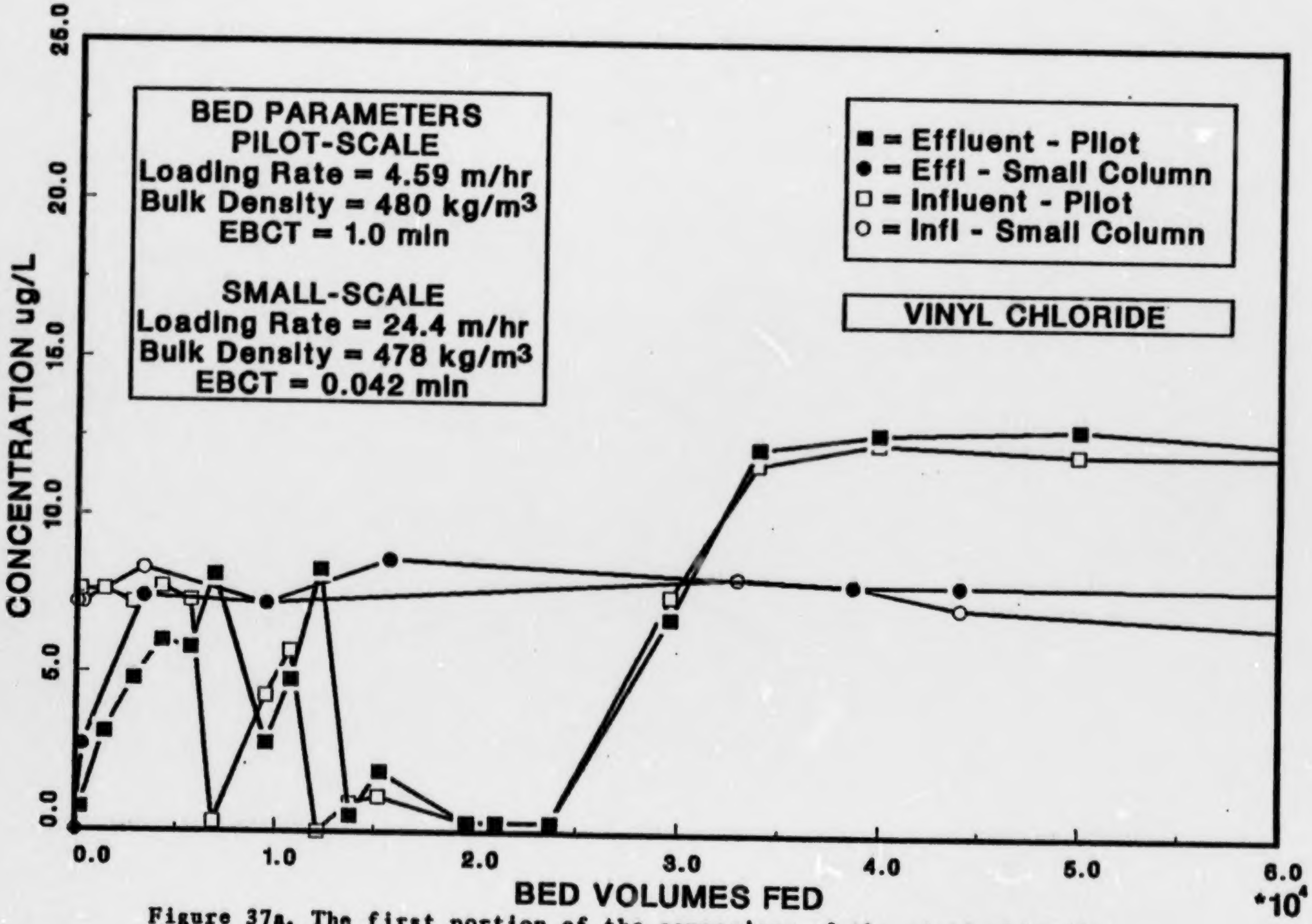

Figure 37a. The first portion of the comparison of the vinyl chloride breakthrough profile for the small-column test to the pilot-scale column in the field study expanded along the bed volumes axis. Influent data are shown. Operating parameters are presented in Tables 7 and 8 (a).

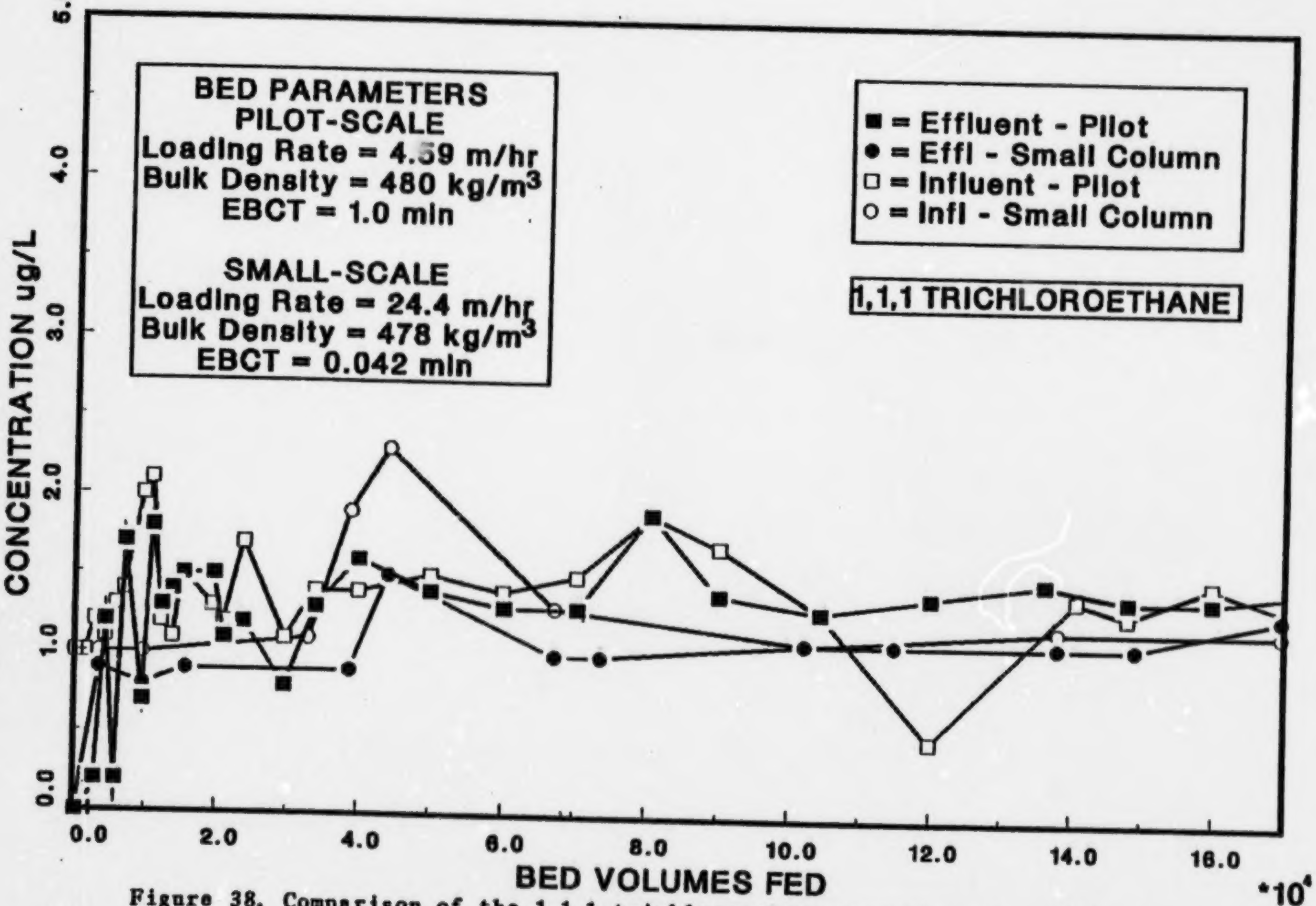

Figure 38. Comparison of the 1,1,1 trichloroethane breakthrough profile for the small-column test to the pilot-scale column in the field study. Influent data are shown. Operating parameters are presented in Tables 7 and 8 (a).

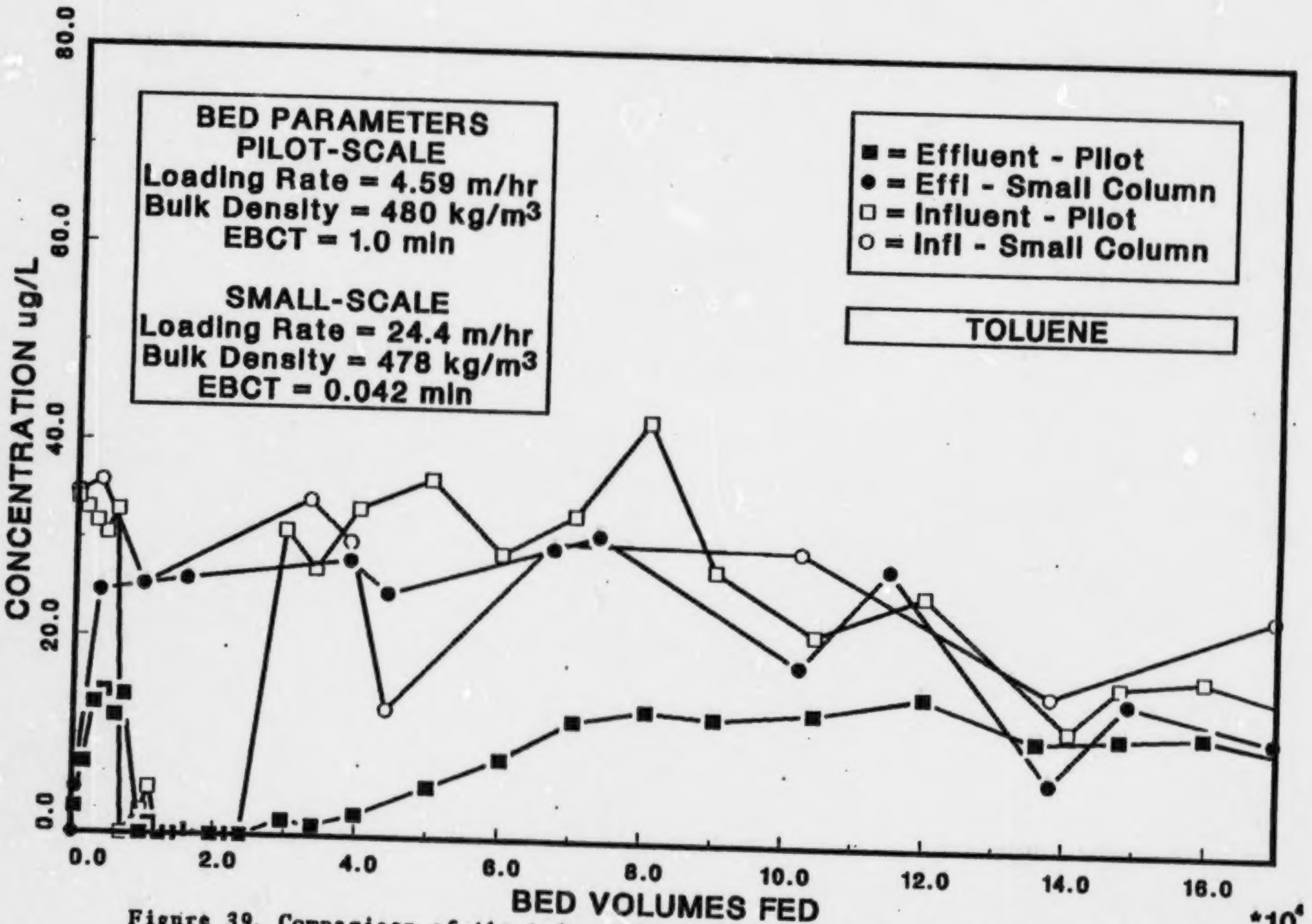

Figure 39. Comparison of the toluene breakthrough profile for the small-column test to the pilot-scale column in the field study. Influent data are shown. Operating parameters are presented in Tables 7 and 8 (a).

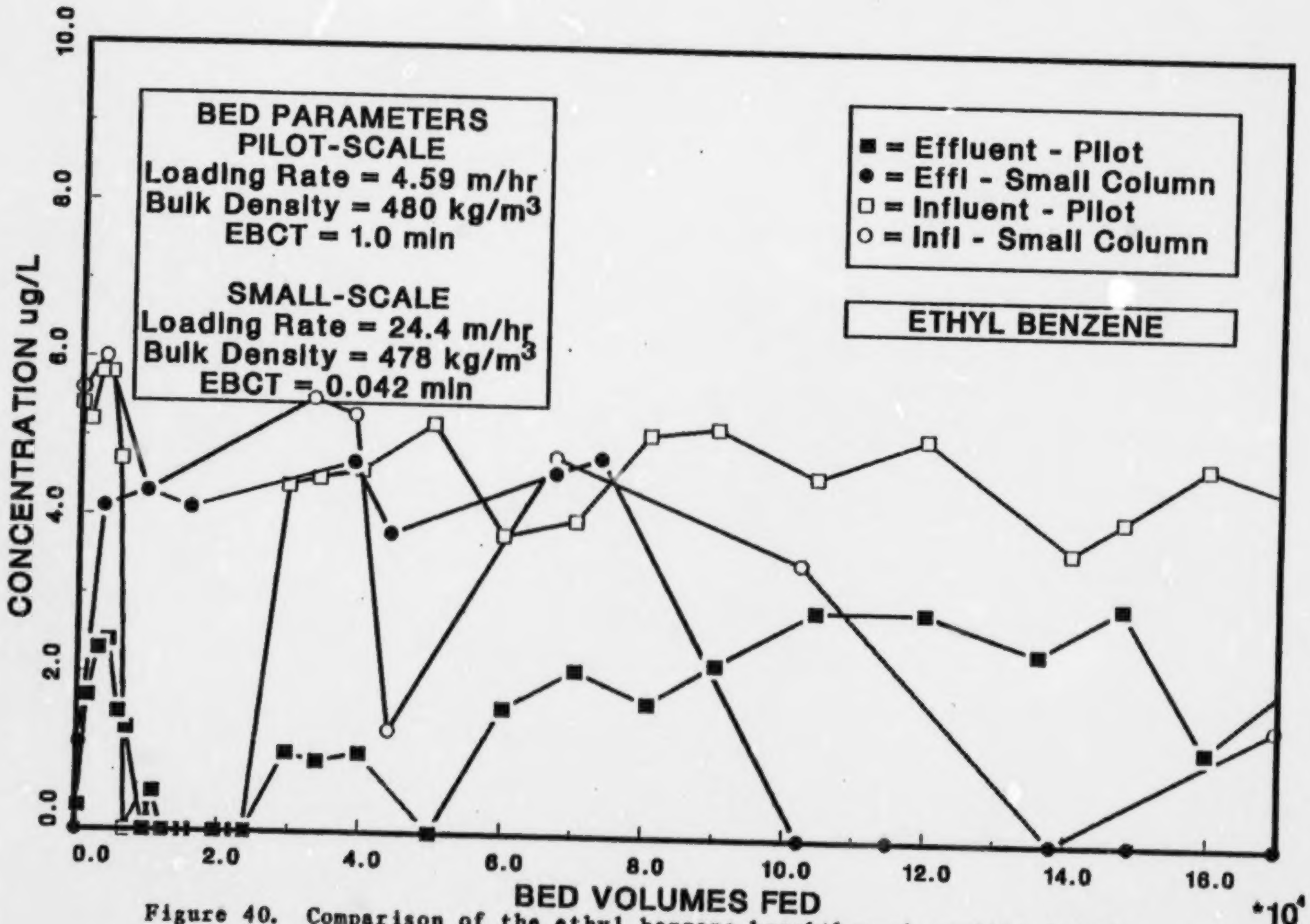

Figure 40. Comparison of the ethyl benzene breakthrough profile for the small-column test to the pilot-scale column in the field study. Influent data are shown. Operating parameters are presented in Tables 7 and 8 (a).

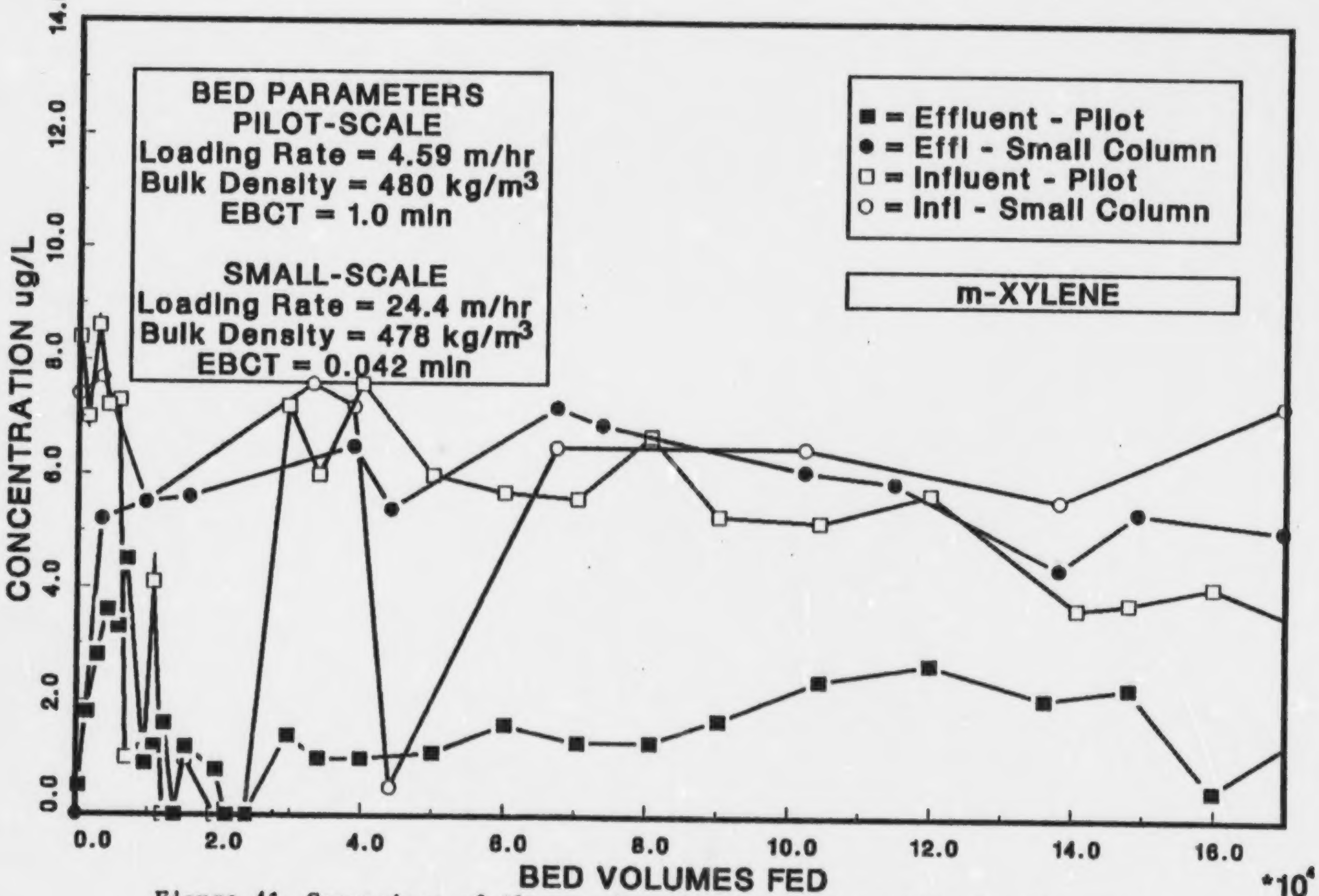

Figure 41. Comparison of the m-xylene breakthrough profile for the small-column test to the pilot-scale column in the field study. Influent data are shown. Operating parameters are presented in Tables 7 and 8 (a).

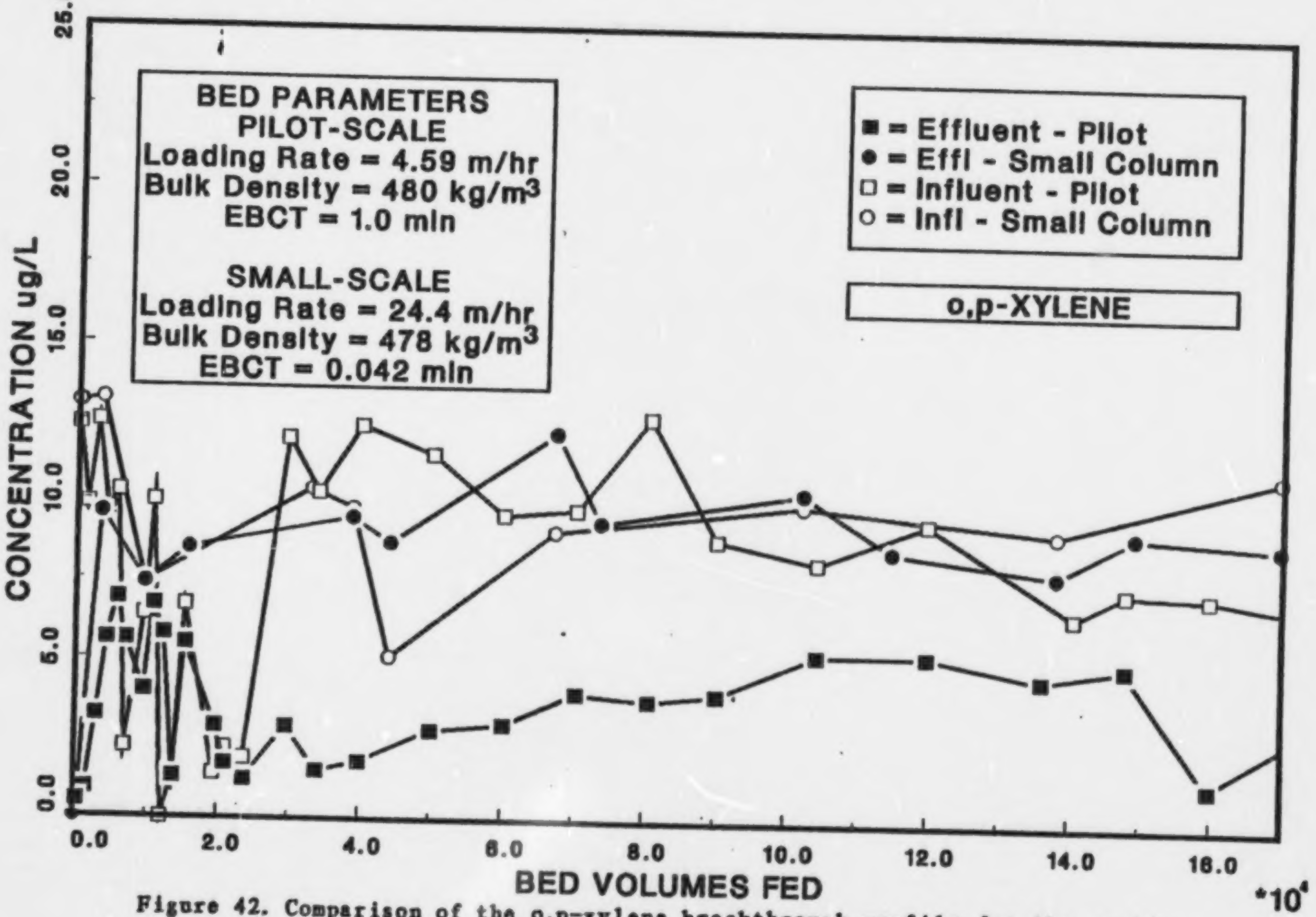

Figure 42. Comparison of the o,p-xylene breakthrough profile for the small-column test to the pilot-scale column in the field study. Influent data are shown. Operating parameters are presented in Tables 7 and 8 (#).

Fig. 36 are also similar. The similarity between the breakthrough profile comparisons is due to the higher initial flowrate in the pilot study. Figure 36a displays the first portion of the tetrachloroethene breakthrough profile expanded along the bed volumes axis to better show the comparison. The vinyl chloride breakthrough profile comparisons in Fig. 37 and expanded in Fig. 37(a) indicate that the compound is not well adsorbed by F-400 GAC. Because the influent concentration of 1,1,1 trichloroethane was very low, 1.3 μg/L, the breakthrough profile comparisons of this compound in Fig. 38 yield little information, but are included for completeness. The same is true of ethyl benzene in Fig. 40. However, the breakthrough profile comparisons for toluene in Fig. 39 show an earlier breakthrough for the RSSCT. An earlier RSSCT breakthrough is observed for m-xylene in Fig. 41, and for o- and p-xylenes as shown in Fig. 42. The more strongly adsorbing components break through much earlier for the RSSCT than would be expected by the the pilot-scale data.

Figures 43-50 display the breakthrough profile comparisons of the 1 minute EBCT pilot-scale adsorber and corresponding RSSCT using WV-G carbon in Tables 7(d) and 8(d) respectively. As with the comparison of pilot-scale and RSSCT in Tables 7(a) and 8(a), respectively, the results obtained for WV-G carbon show the same trends as the F-400 GAC. Similar breakthrough profiles were observed between the RSSCT and the pilot-scale adsorber for cis-dichloroethene in Fig. 43 and trichloroethene in Fig. 44. The breakthrough profile comparisons in Fig. 45 for tetrachloroethene are similar. The vinyl chloride breakthrough profile comparisons in Fig. 46 also indicate that the compound is not well adsorbed by WV-G GAC. The breakthrough profile comparisons for toluene in Fig. 47, show an earlier breakthrough for the RSSCT. An earlier RSSCT breakthrough is observed for ethyl benzene in Fig. 48, m-xylene in Fig. 49, and o- and p-xylenes as shown

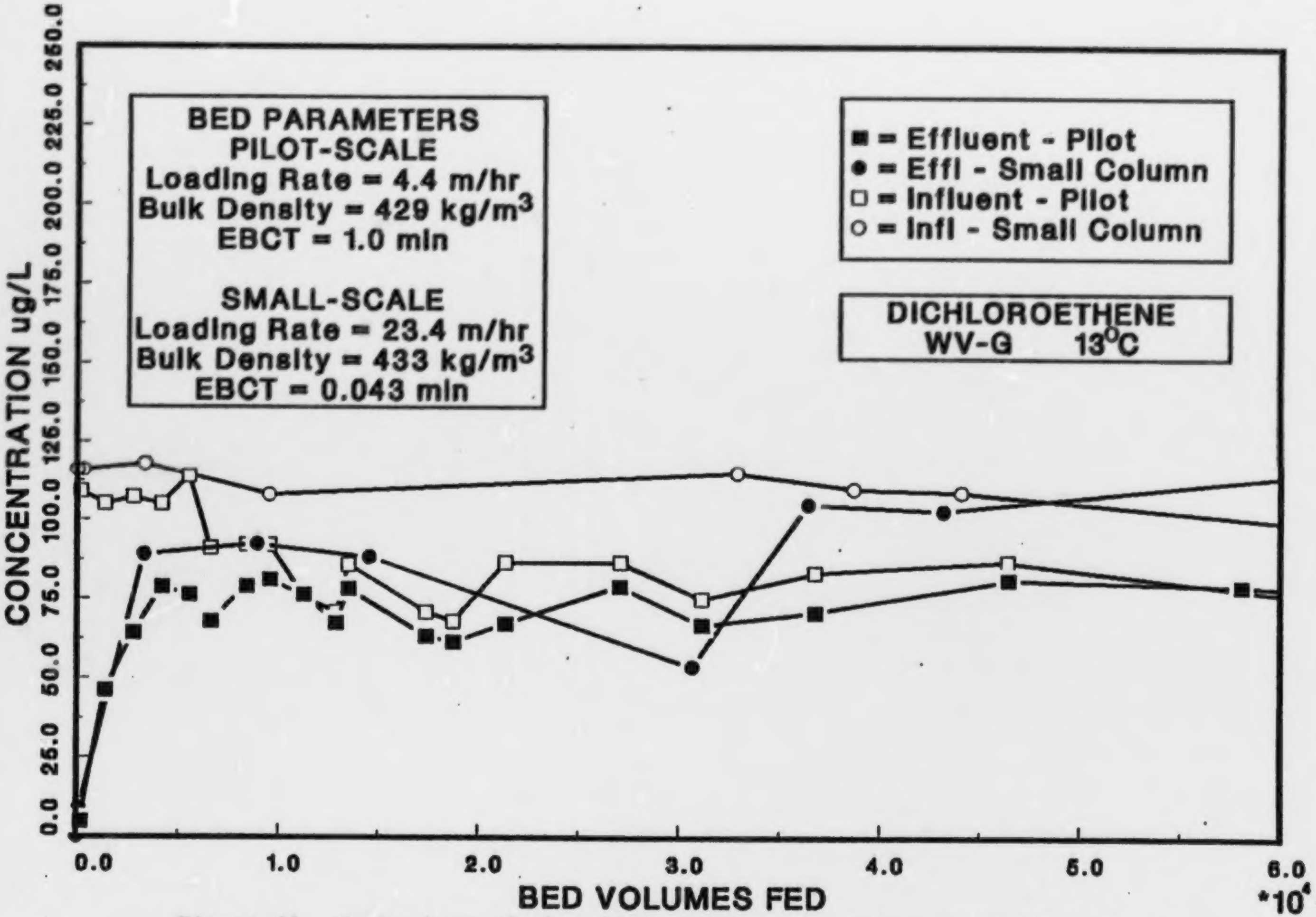

Figure 43. Comparison of the dichloroethene breakthrough profile for the small-column test to the pilot-scale column in the field study. Influent data are shown. Operating parameters are presented in Tables 7 and 8 (d).

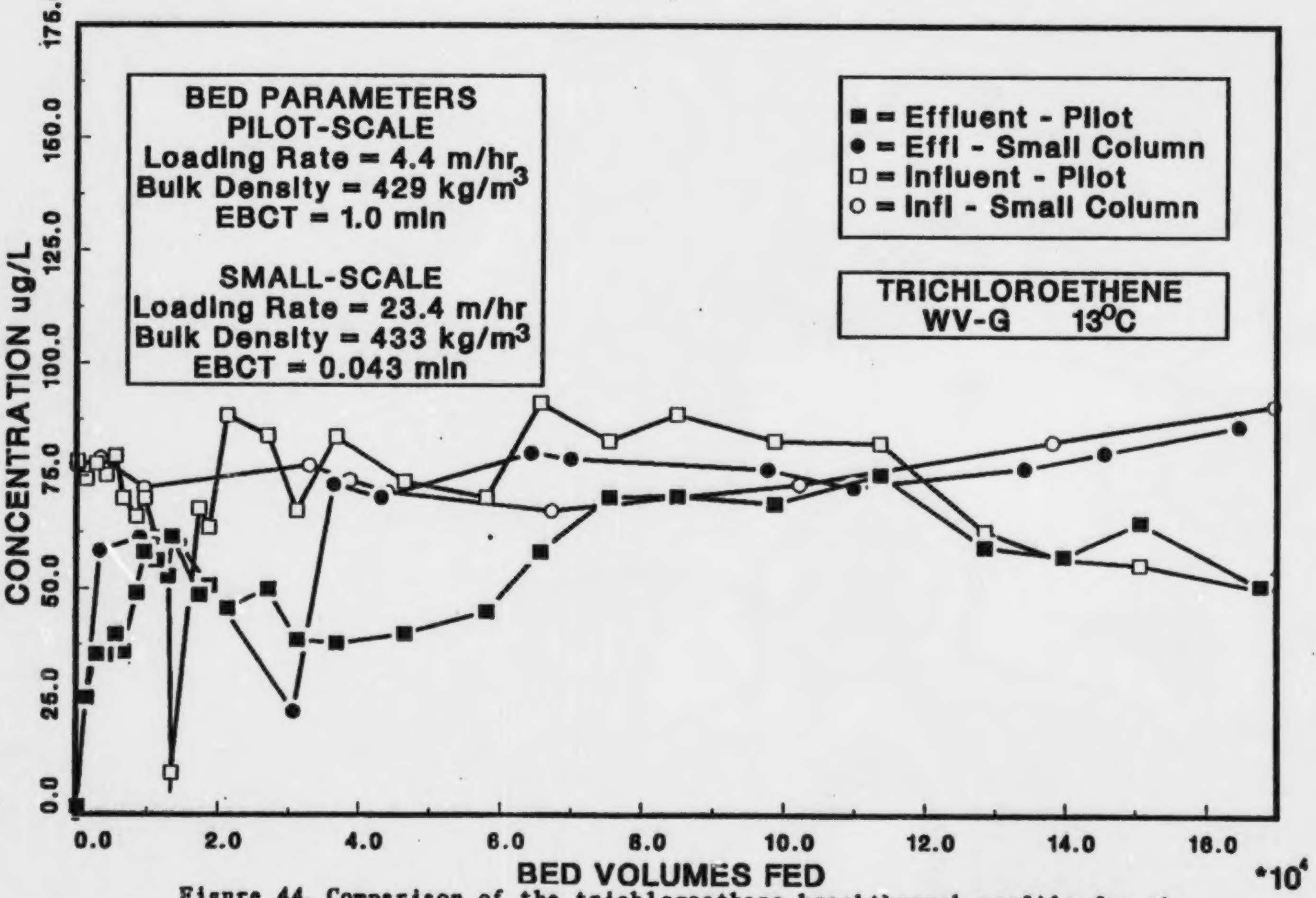

Figure 44. Comparison of the trichloroethene breakthrough profile for the small-column test to the pilot-scale column in the field study. Influent data are shown. Operating parameters are presented in Tables 7 and 8 (d).

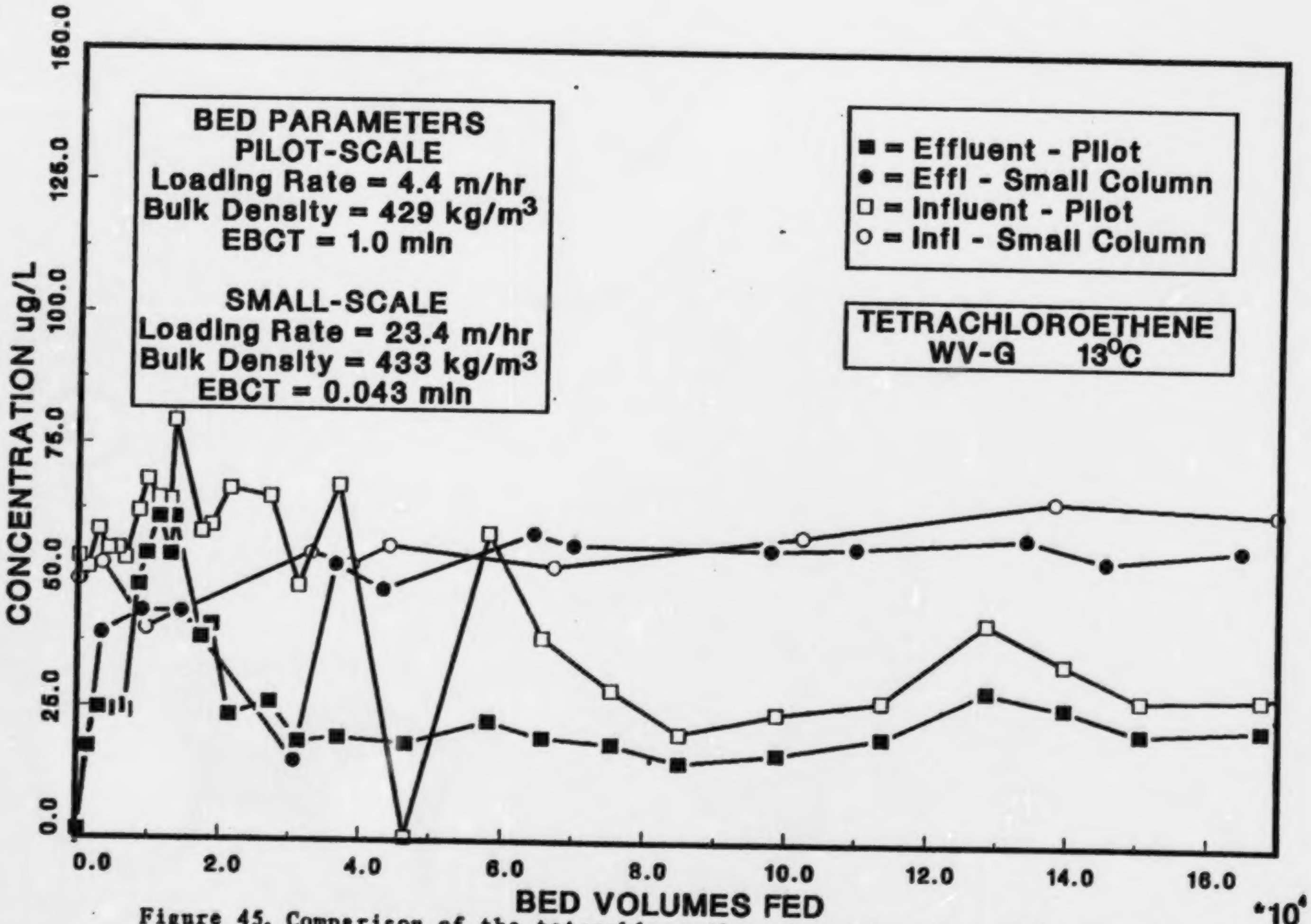

Figure 45. Comparison of the tetrachloroethene breakthrough profile for the small-column test to the pilot-scale column in the field study. Influent data are shown. Operating parameters are presented in Tables 7 and 8 (d).

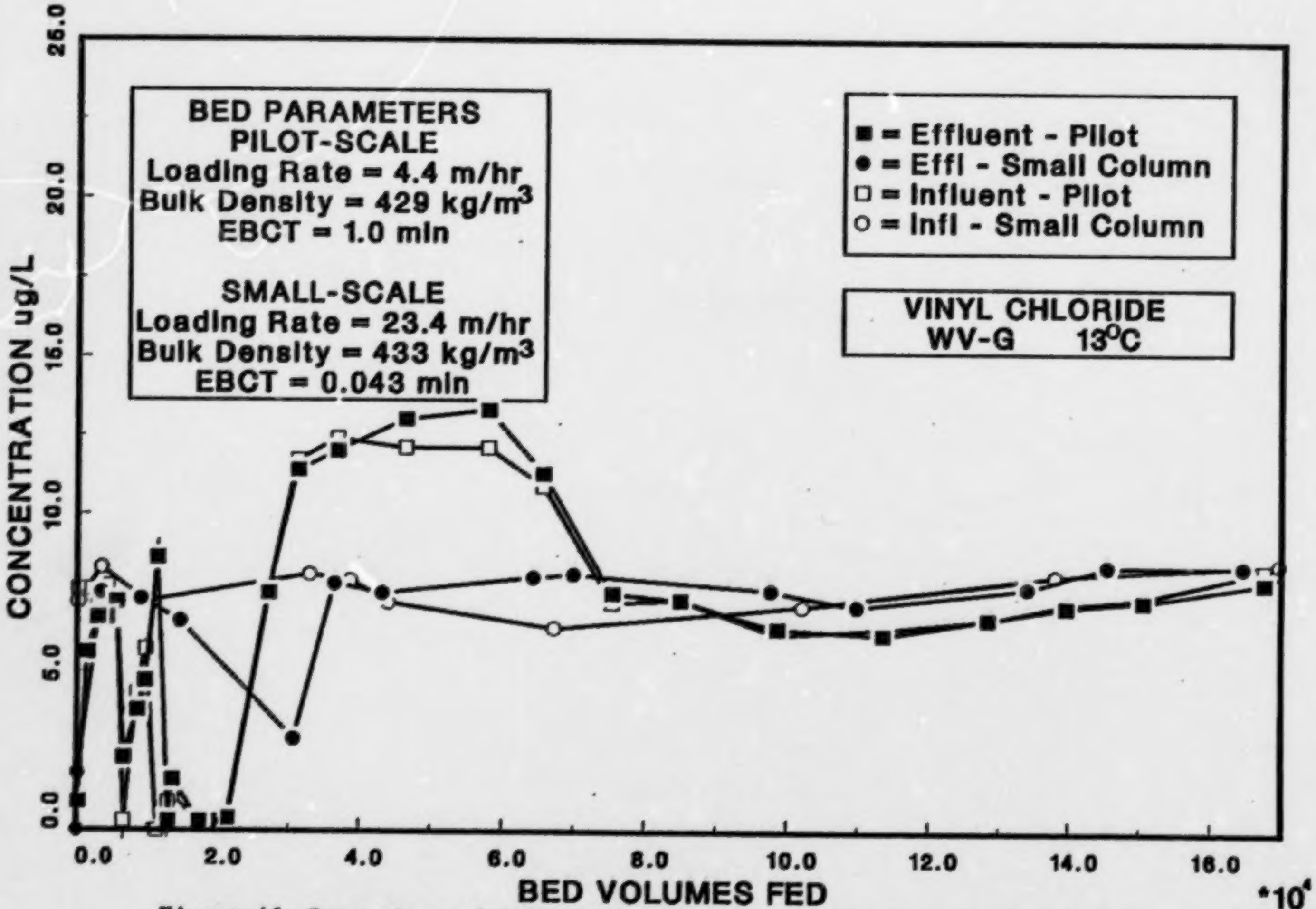

Figure 46. Comparison of the vinyl chloride breakthrough profile for the small-column test to the pilot-scale column in the field study. Influent data are shown. Operating parameters are presented in Tables 7 and 8 (d).

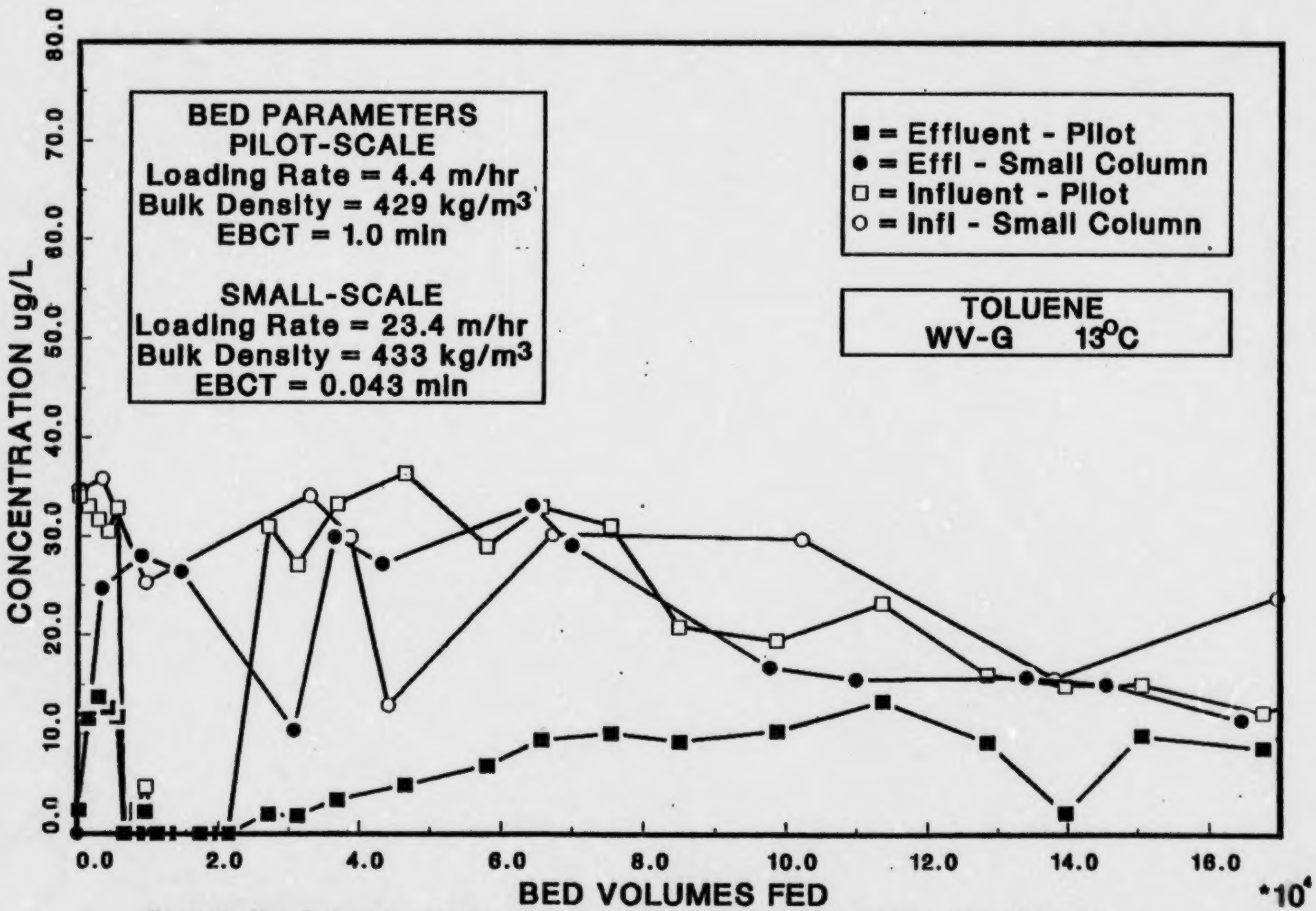

Figure 47. Comparison of the toluene breakthrough profile for the small-column test to the pilot-scale column in the field study. Influent data are shown. Operating parameters are presented in Tables 7 and 8 (d).

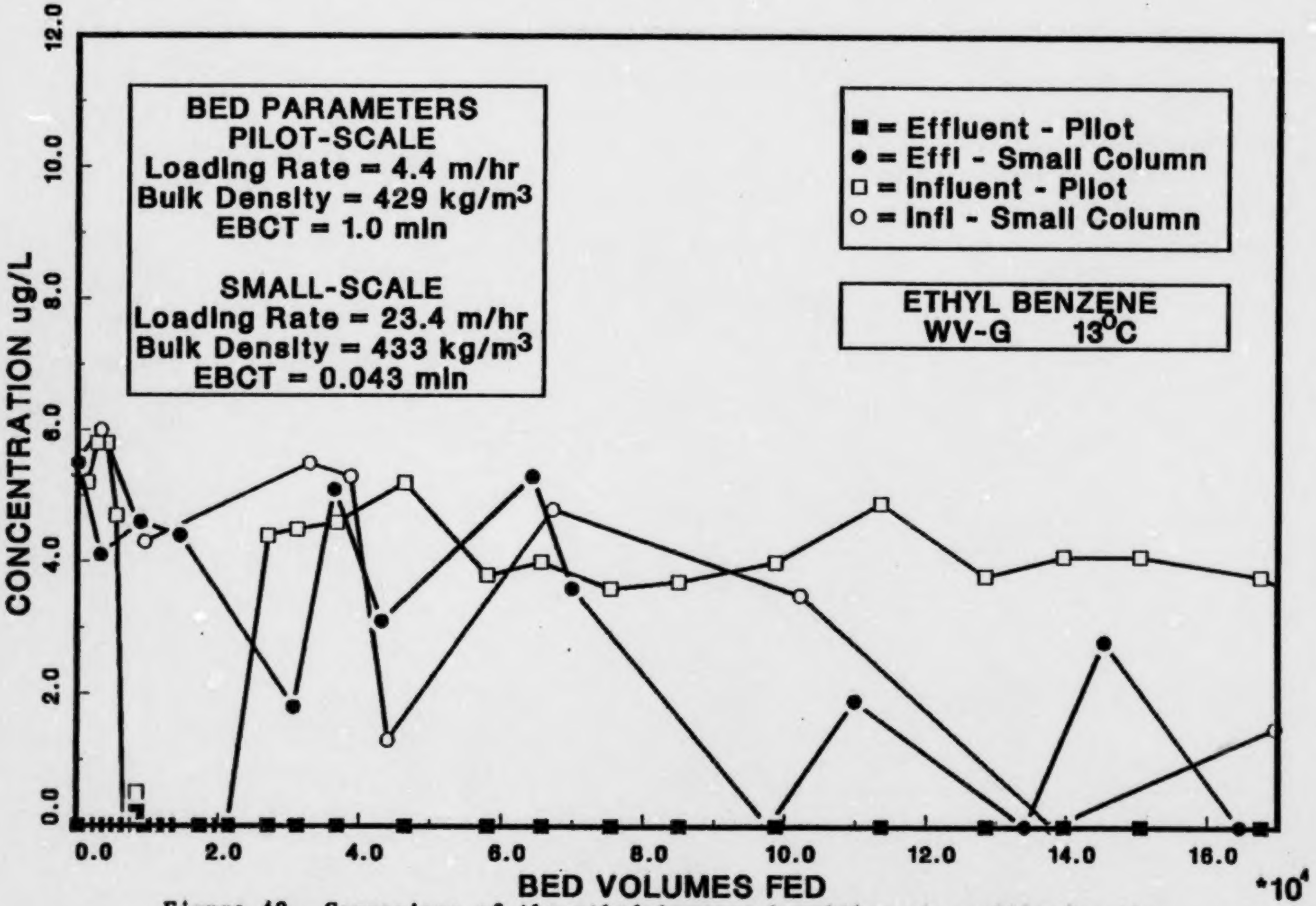

Figure 48. Comparison of the ethyl benzene breakthrough profile for the small-column test to the pilot-scale column in the field study. Influent data are shown. Operating parameters are presented in Tables 7 and 8 (d).

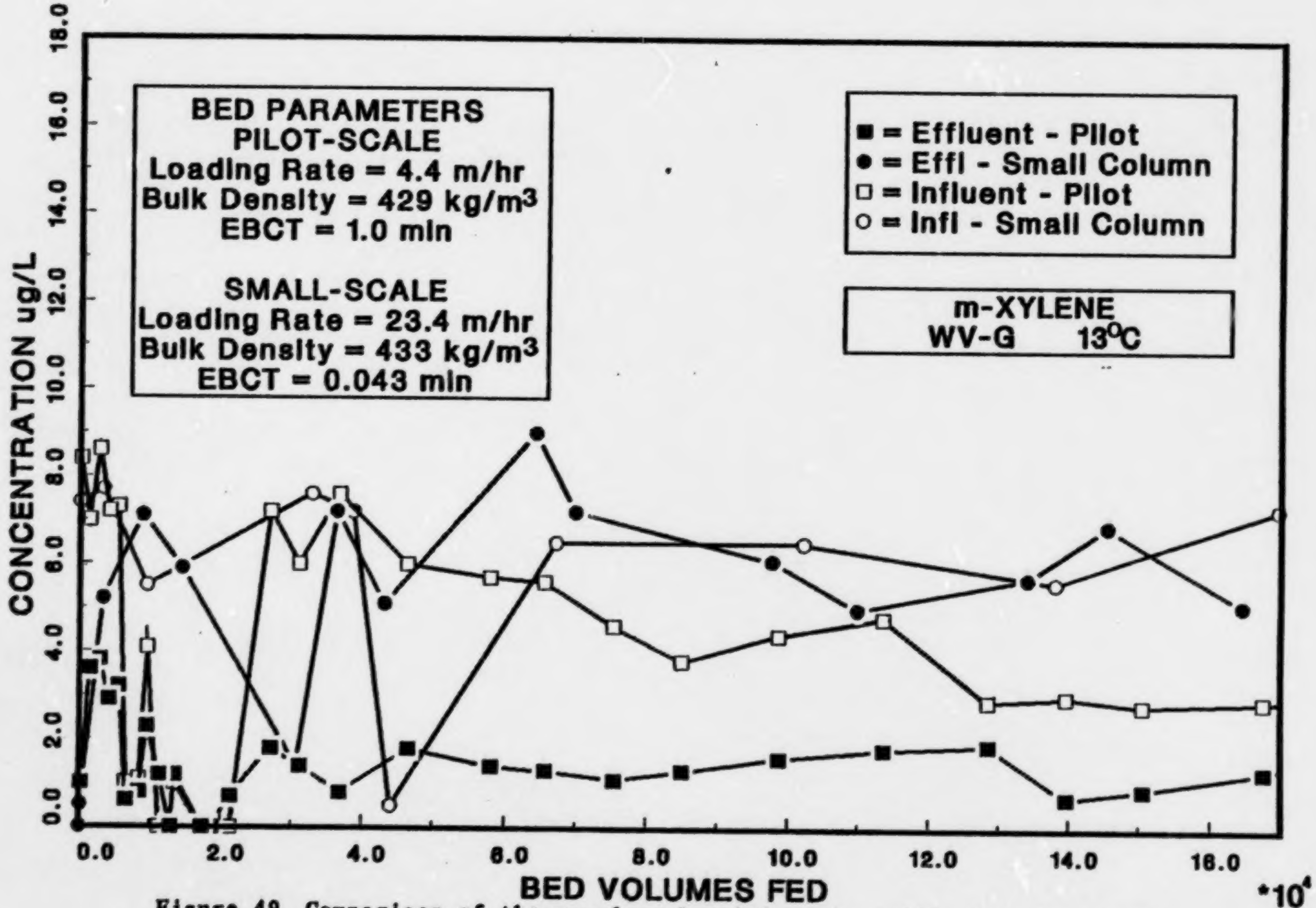

Figure 49. Comparison of the m-xylene breakthrough profile for the small-column test to the pilot-scale column in the field study. Influent data are shown. Operating parameters are presented in Tables 7 and 8 (d).

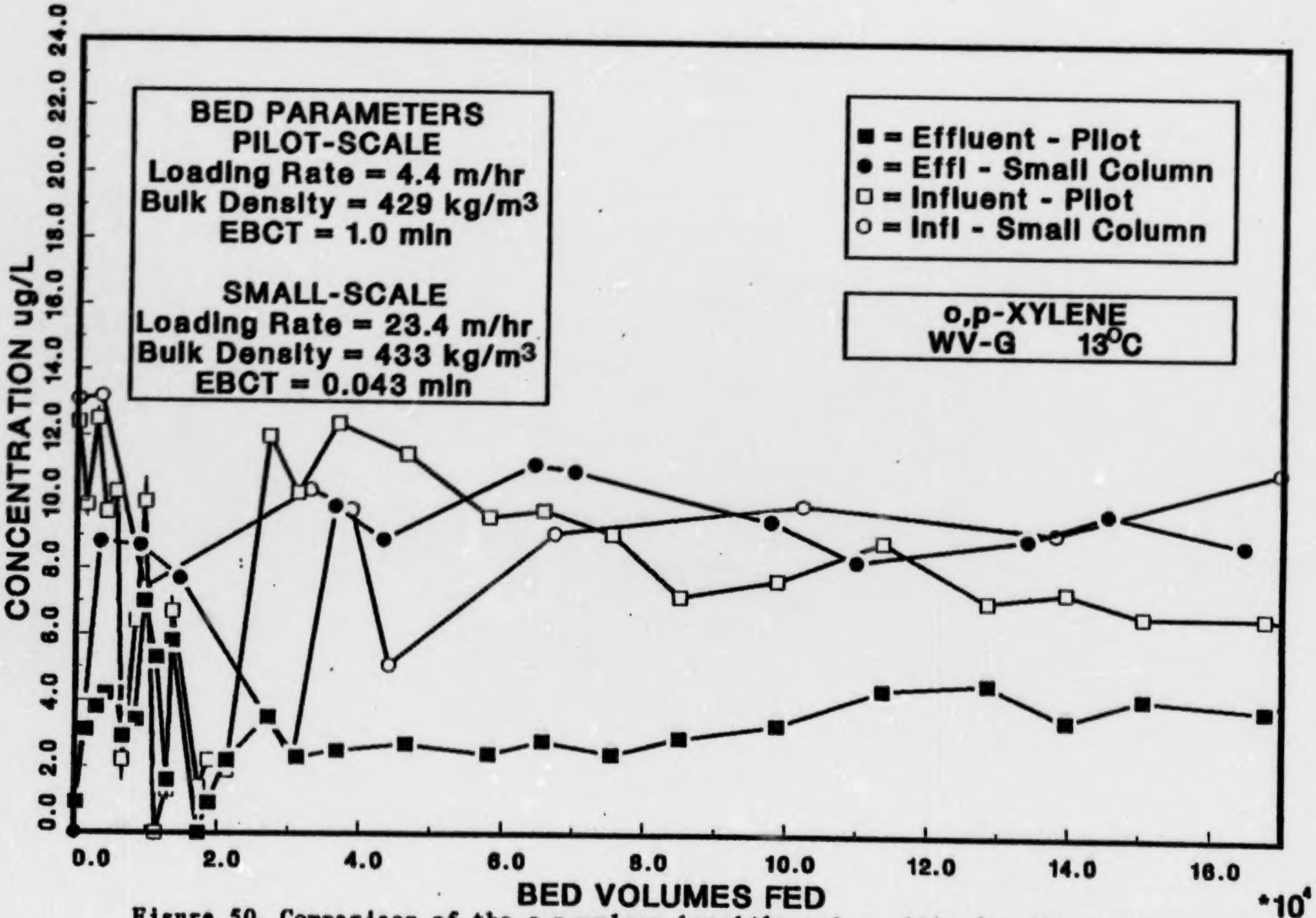

Figure 50. Comparison of the o,p-xylene breakthrough profile for the small-column test to the pilot-scale column in the field study. Influent data are shown. Operating parameters are presented in Tables 7 and 8 (d).

in Fig. 50. Both RSSCT's described in Tables 8(a) and 8(d) simulating 1 minute of EBCT showed iron precipitation on the last day of operation, after approximately 150000 bed volumes fed. The iron precipitate appeared immediately downstream of the carbon bed with very little or no precipitate in the actual bed of carbon. The appearance of the precipitate was believed to occur as the result of air drawn into the system.

The actual EBCT of the RSSCT in Table 8(a) was determined to be 2.51 seconds by dividing the total bed volumes fed during the run with the total elapsed time of the run which matches the desired EBCT of 2.51 seconds as determined by Eq. 22 from the pilot-scale parameters in Table 7(a). The actual hydraulic loading rate of 24.5 is close to the desired loading rate of 22.4 from Eq. 25. The bulk density of the F-400 carbon in the 1 minute pilot-scale adsorber, 480 kg/m^3, was very close to the bulk density of the F-400 carbon in the corresponding RSSCT, 478 kg/m^3. Because the particle void fraction, ε_p, was shown to have little impact on the breakthrough profile, differences in the particle void fraction cannot account for the dissimilarity between RSSCT and pilot-scale adsorber. Consequently the minor differences in the EBCT, hydraulic loading rate, particle density, particle void fraction or bed void fraction could not account for the dissimilarity in the breakthrough profile comparisons of toluene or the xylenes.

Since the loading rates, EBCT's, and bulk densities of the pilot-scale adsorber and RSSCT were very near to the requirements Eqs. 22 and 25, the slight differences in the effective Peclet and Stanton numbers are unimportant in accounting for the RSSCT dissimilarity with the 1 minute EBCT adsorber. Because the Reynolds numbers will be nearly equal, the Peclet numbers, Pe_L, will be nearly equal and the effects of dispersion, (whether negligible or not) are expected to occur similarly in both pilot-scale adsorber and RSSCT. The small variations the parameters of the Peclet number, D_e, v, and L, cannot account for the dissimilarity in the breakthrough profiles of toluene and the xylenes. In addition, the ratio of film transfer coefficients for solutes in the pilot-scale adsorber was near the requirement of Eq. 23 for perfect similarity. The requirements of Eqs. 22, 23, and 25 were met, therefore, the Stanton numbers of both systems are nearly equal. Because the values of the Stanton numbers were nearly the same for both pilot-scale adsorber and RSSCT the effects of film transfer were expected to have occurred similarly in both systems. The small deviations from the expected values of the parameters associated with the Stanton number, k_f, τ, ε, and R, could not account for the large dissimilarity of the breakthrough profile comparisons for toluene and xylenes and are unimportant.

The influent concentrations were similar during the initial portions of operation. The gradual decrease of the influent concentrations for the pilot-scale column caused the average values of the pilot-scale column to be lower. During the initial breakthrough, however, influent concentrations were fairly equal between the pilot-scale adsorber and RSSCT. From the sensitivity analysis a two to ten percent difference in the influent concentrations could not bring about a dissimilarity of the magnitude seen in the breakthrough profile comparisons of toluene in Figs. 39 and 47, or of the xylenes in Figs 41-42 and 49-50. Consequently, the difference in influent concentrations is unable to account for all the dissimilarity in the breakthrough profile comparisons of the 1 minute EBCT pilot-scale column and corresponding RSSCT.

Of the remaining parameters appearing in the DFPSDM, only D_s and D_p remain to account for the major portion of the dissimilarities in the toluene and xylene breakthrough profile comparisons of pilot-scale adsorber and RSSCT. While D_s has been reported to vary with adsorbent particle radius (Schneider, 1982), the pore diffusivity is believed to be merely the liquid diffusivity corrected for the tortuosity (Friedman, 1984). Only the surface diffusivity is reported to differ enough to account for the dissimilarity in the breakthrough profiles of toluene and the xylenes.

2. Discussion of RSSCT Results for Simulation of 3.2 Minute EBCT Adsorber Assuming Constant Surface Diffusivity

Figures 51-59 display the breakthrough comparisons of a 3.2 minute EBCT pilot-scale adsorber and corresponding RSSCT using F-400 carbon in Tables 7(b) and 8(b) respectively. Similar breakthrough profiles are observed between the RSSCT and the pilot-scale adsorber for cis-dichloroethene in Fig. 51. However, the breakthrough profile comparison of trichloroethene in Fig. 52 displays a similar breakthrough profile at markedly different influent concentrations The tetrachloroethene in Fig. 53 breakthrough profile comparison shows an earlier RSSCT breakthrough though the average RSSCT influent concentrations are lower than those of the 3.2 minute EBCT pilot-scale adsorber (Compare Tables 7(b) and 8(b)). A lower influent concentration should yield a later RSSCT breakthrough profile as shown in Figs. 23 and 24. The breakthrough comparisons are displayed for toluene in Fig. 56, ethyl benzene in Fig. 57, m-xylene in Fig. 58, and o- and p-xylenes as shown in Fig. 59. The RSSCT described in Table 8(b) simulating 3.2 minutes of EBCT was observed to have iron precipitation on the sixth day of operation, at approximately 47000 bed volumes fed. The appearance of precipitation was observed within the RSSCT carbon bed and in all lines downstream of the carbon bed. The iron was believed to precipitate as a result of air drawn into the system when a leaking valve was replaced.

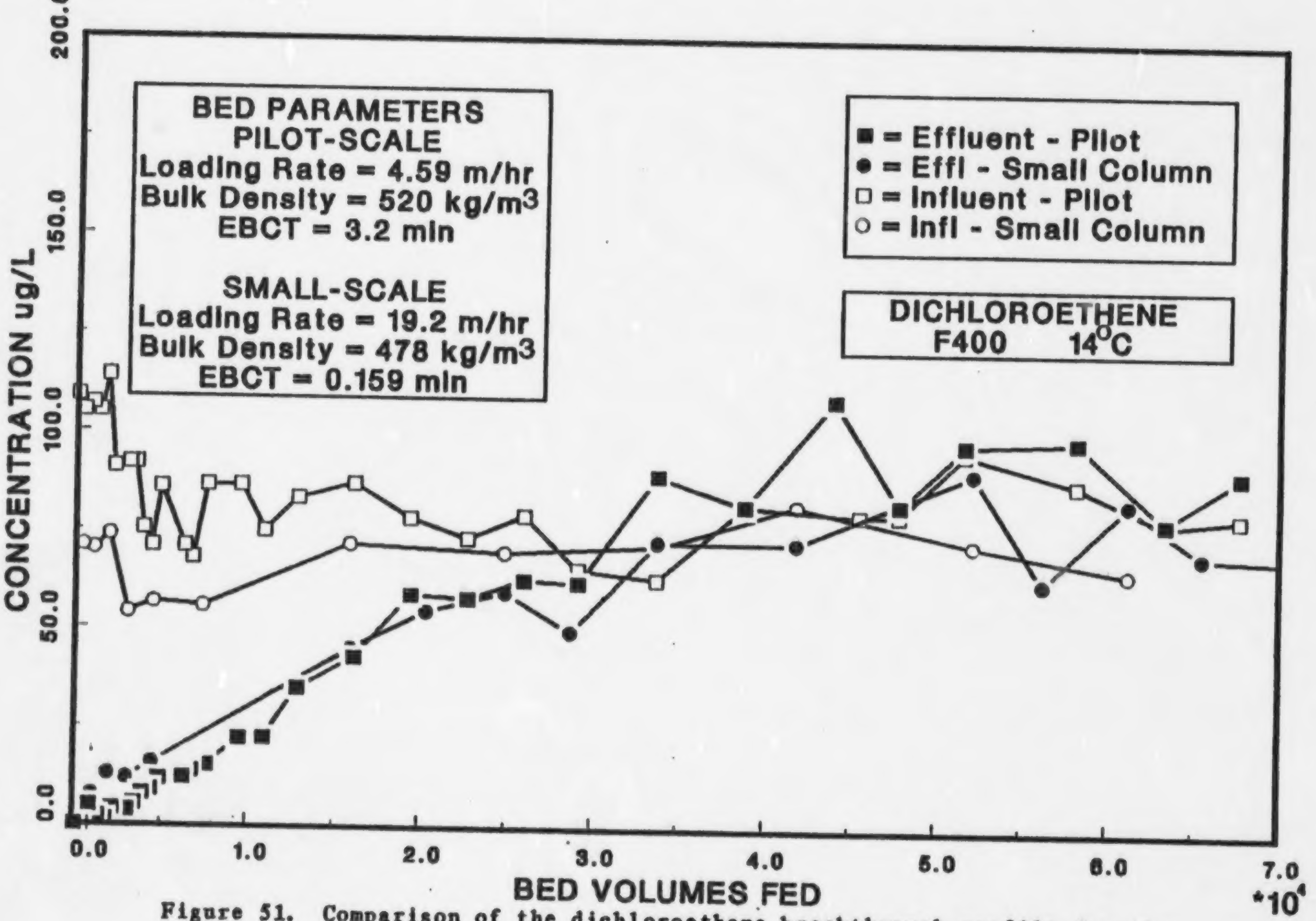

Figure 51. Comparison of the dichloroethene breakthrough profile for the small-column test to the pilot-scale column in the field study. Influent data are shown. Operating parameters are presented in Tables 7 and 8 (b).

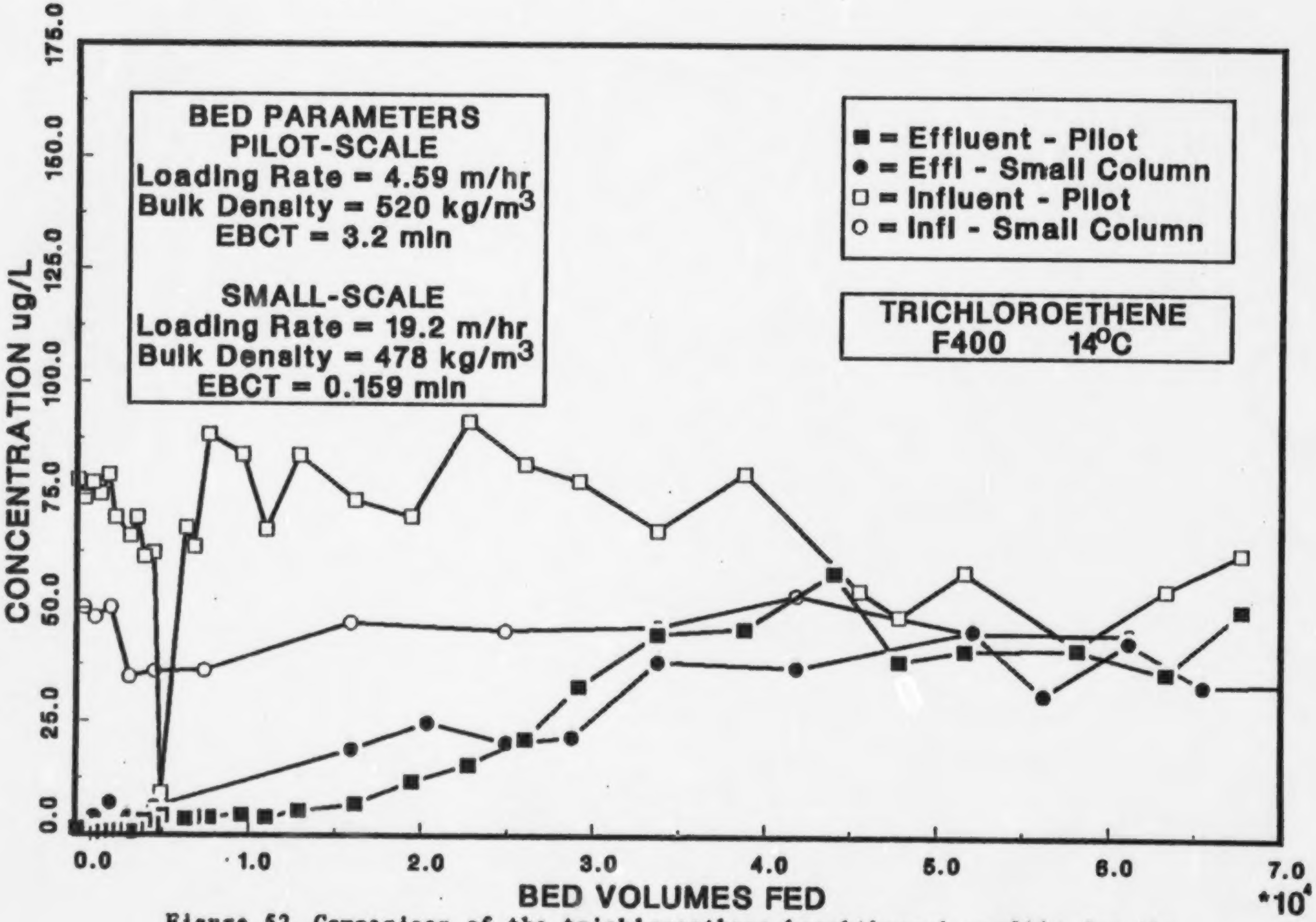

Figure 52. Comparison of the trichloroethene breakthrough profile for the small-column test to the pilot-scale column in the field study. Influent data are shown. Operating parameters are presented in Tables 7 and 8 (b).

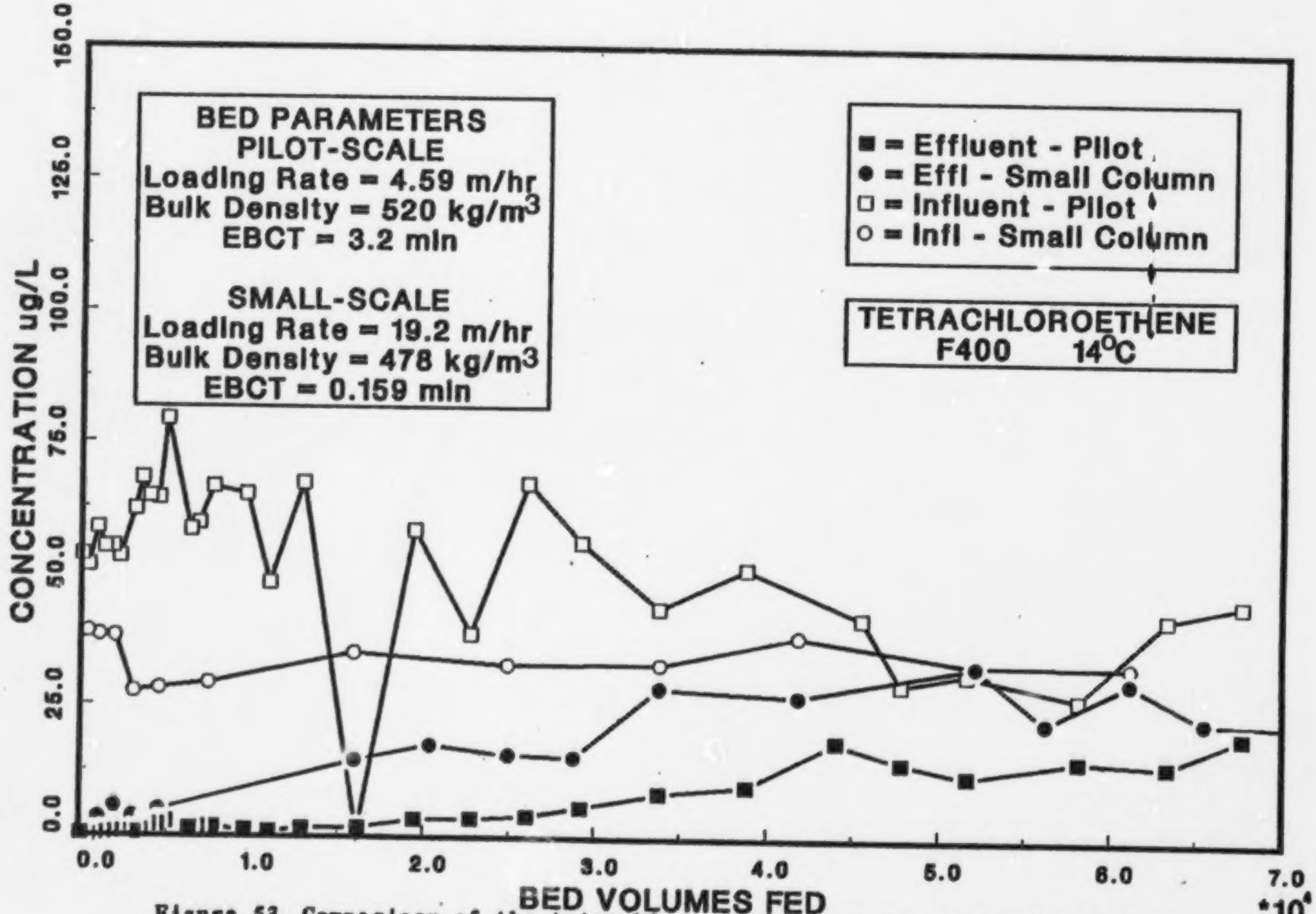

Figure 53. Comparison of the tetrachloroethene breakthrough profile for the small-column test to the pilot-scale column in the field study. Influent data are shown. Operating parameters are presented in Tables 7 and 8 (b).

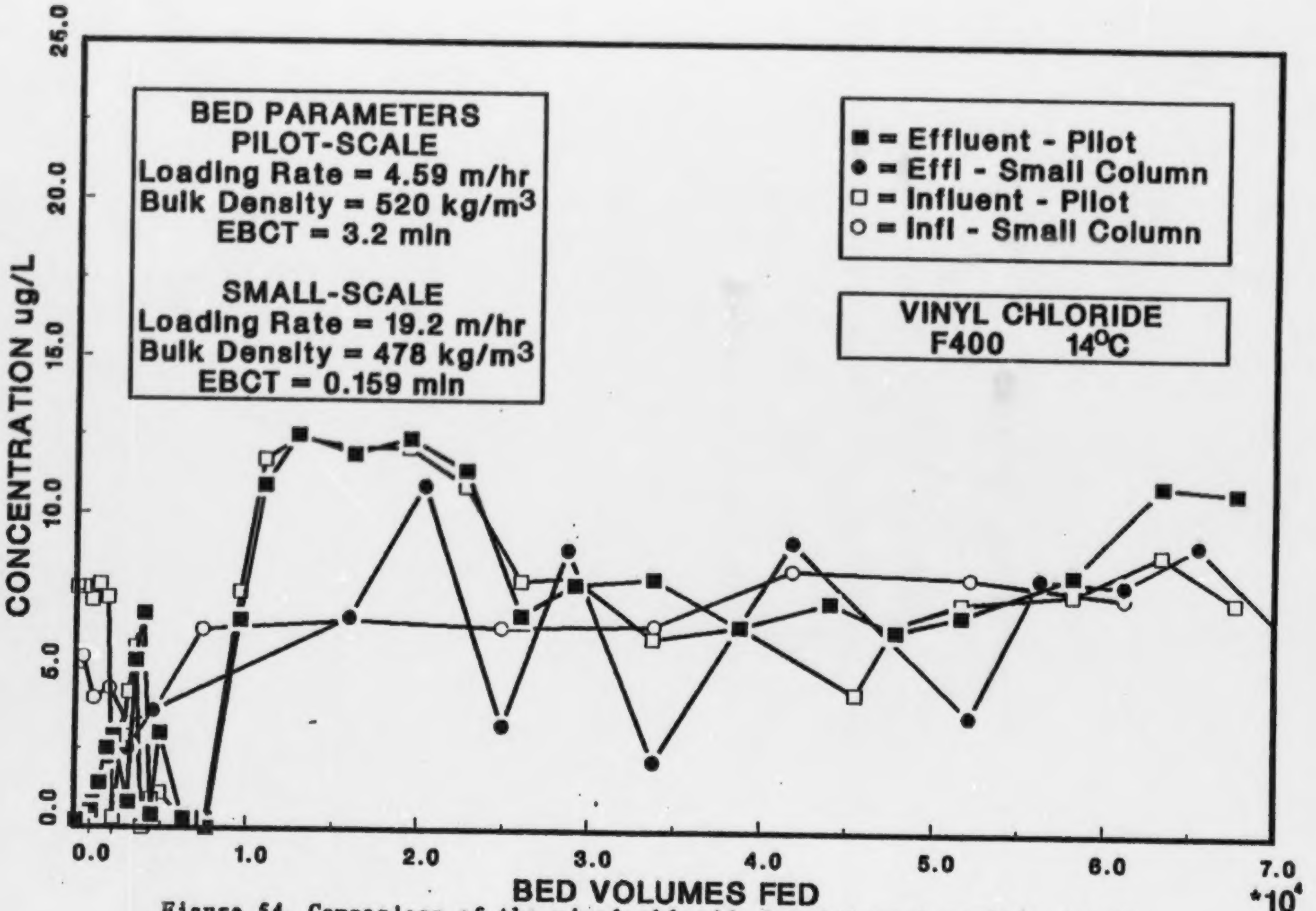

Figure 54. Comparison of the vinyl chloride breakthrough profile for the small-column test to the pilot-scale column in the field study. Influent data are shown. Operating parameters are presented in Tables 7 and 8 (b).

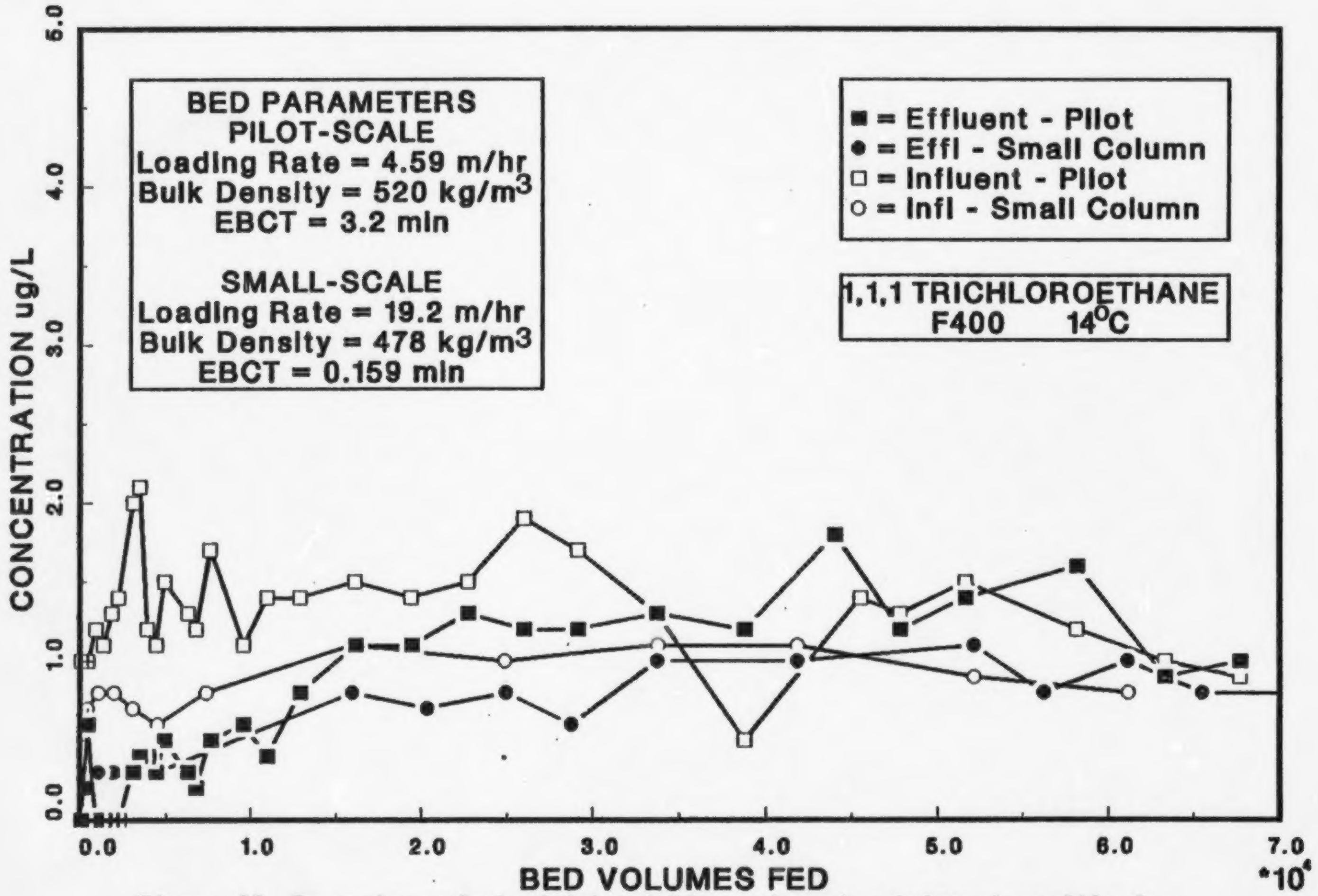

Figure 55. Comparison of the 1,1,1 trichloroethane breakthrough profile for the small-column test to the pilot-scale column in the field study. Influent data are shown. Operating parameters are presented in Tables 7 and 8 (b).

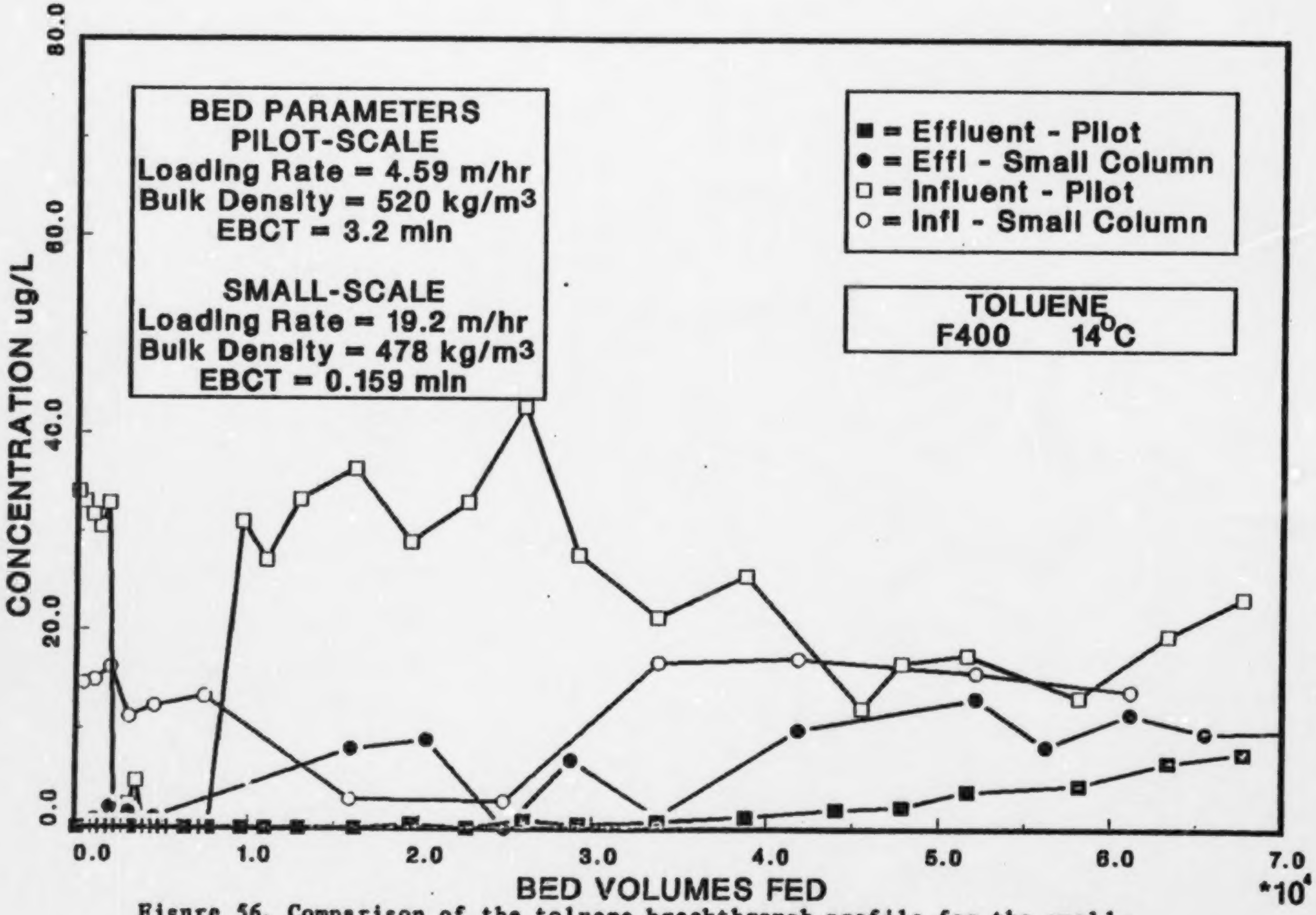

Figure 56. Comparison of the toluene breakthrough profile for the small-column test to the pilot-scale column in the field study. Influent data are shown. Operating parameters are presented in Tables 7 and 8 (b).

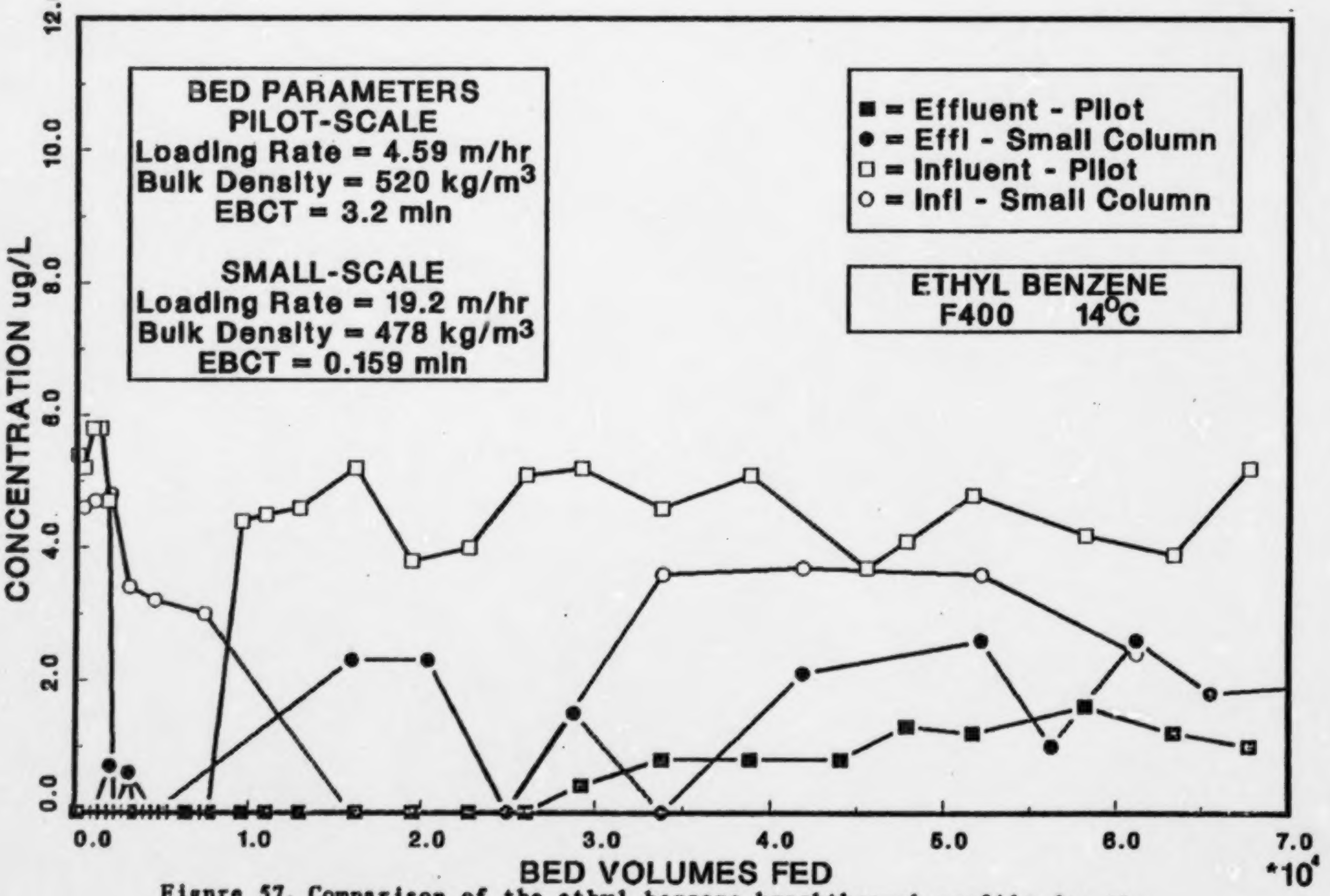

Figure 57. Comparison of the ethyl benzene breakthrough profile for the small-column test to the pilot-scale column in the field study. Influent data are shown. Operating parameters are presented in Tables 7 and 8 (b).

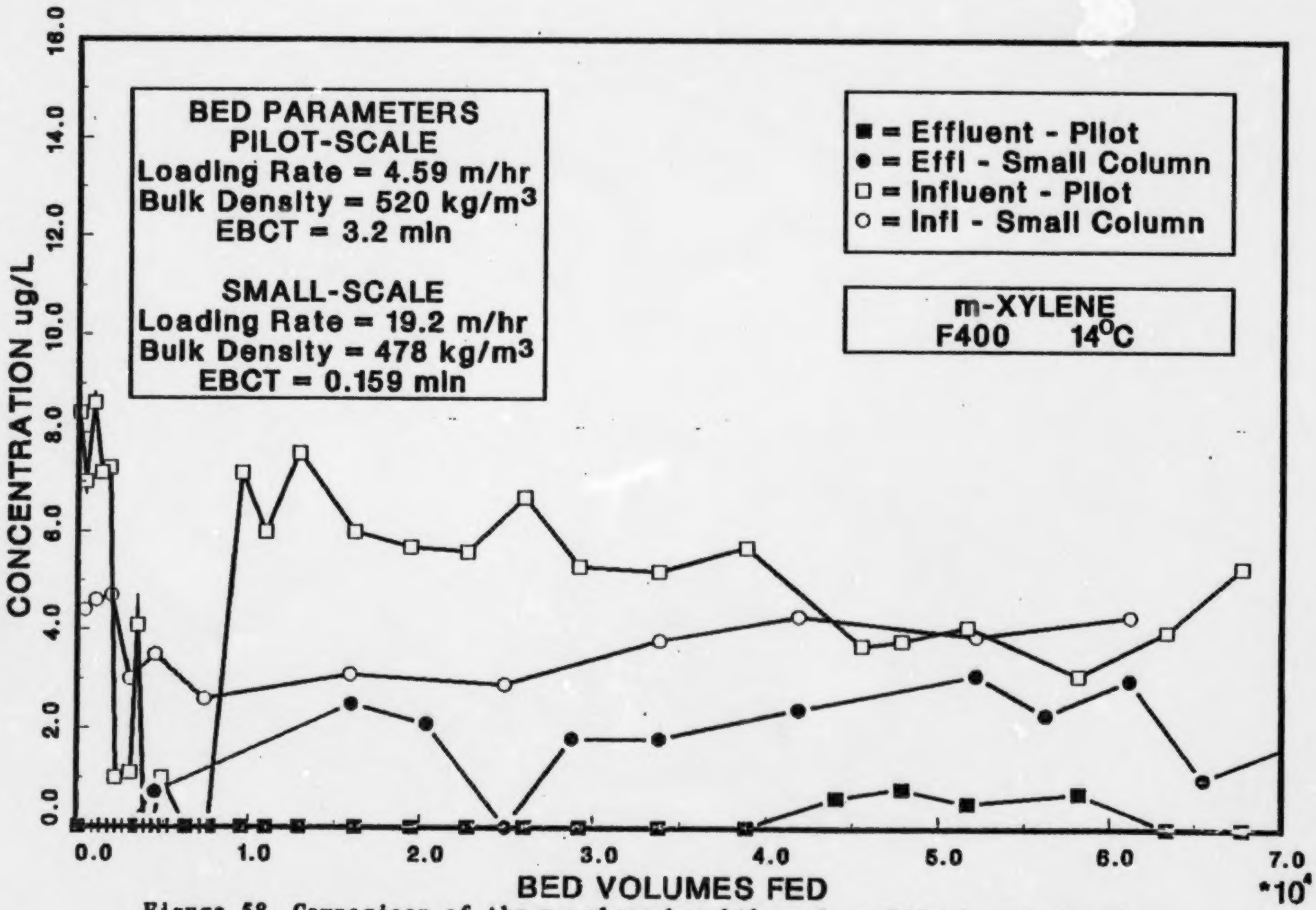

Figure 58. Comparison of the m-xylene breakthrough profile for the small-column test to the pilot-scale column in the field study. Influent data are shown. Operating parameters are presented in Tables 7 and 8 (b).

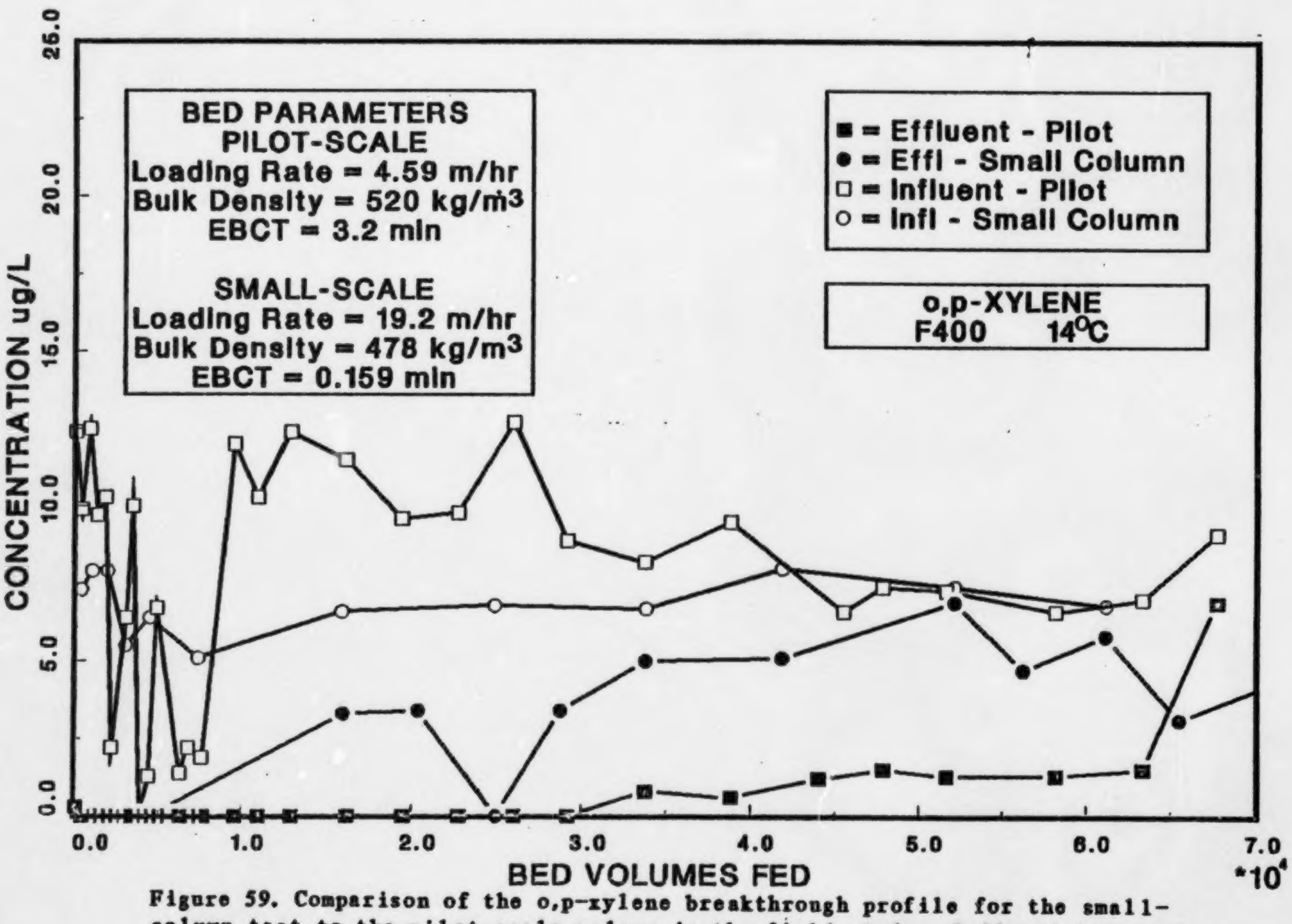

Figure 59. Comparison of the o,p-xylene breakthrough profile for the small-column test to the pilot-scale column in the field study. Influent data are shown. Operating parameters are presented in Tables 7 and 8 (b).

The pressure drop across the carbon bed increased with appearance of the iron precipitate. Consequently, the pumps were unable to deliver the desired flowrate. Averaged operating parameters, v_s, EBCT, and flowrate are reported over the first six days of operation. Other problems with RSSCT valves resulted EBCT's and loading rates differing from the desired values. The actual EBCT of 9.54 seconds is higher than the desired EBCT of 8.05 seconds (Table 8(b)) and the actual loading rate of 19.1 m/hr is much lower than the desired loading rate of 22.4 m/hr. The expected result of the difference in flowrate is a sharpening of the breakthrough profiles (Fig. 26). This effect is not seen in the RSSCT simulating the 3.2 minute EBCT pilot-scale adsorber. A difference in the surface diffusivities of the pilot-scale adsorber and RSSCT could explain the dissimilarity in the breakthrough profiles. For this study, however, the iron precipitation could possibly clog the pores of the carbon in the RSSCT and in this manner result in earlier RSSCT chemical breakthrough profiles.

3. Discussion of RSSCT Results for Simulation of 5.4 Minute EBCT Adsorber Assuming Constant Surface Diffusivity

Figures 60-68 display the breakthrough profile comparisons of a 5.4 minute EBCT pilot-scale adsorber and corresponding RSSCT using F-400 carbon in Tables 7(c) and 8(c) respectively for cis-dichloroethene in Fig. 60, trichloroethene in Fig. 61, tetrachloroethene in Fig. 62, vinyl chloride in Fig. 63, 1,1,1 trichloroethane in Fig. 64, toluene in Fig. 65, ethyl benzene in Fig. 66, m-xylene in Fig. 67, and o- and p-xylenes in Fig. 68. With the exception of vinyl chloride all the RSSCT chemical breakthrough profiles occur prior to the 5.4 minute EBCT pilot-scale adsorber. The experimental value of the hydraulic loading rate of 22.7 m/hr for the RSSCT (Table 8(c)) was near the value required by Eq. 25 of 22.4 m/hr. The experimental RSSCT empty bed contact time of 12.28 seconds was close to the value required by

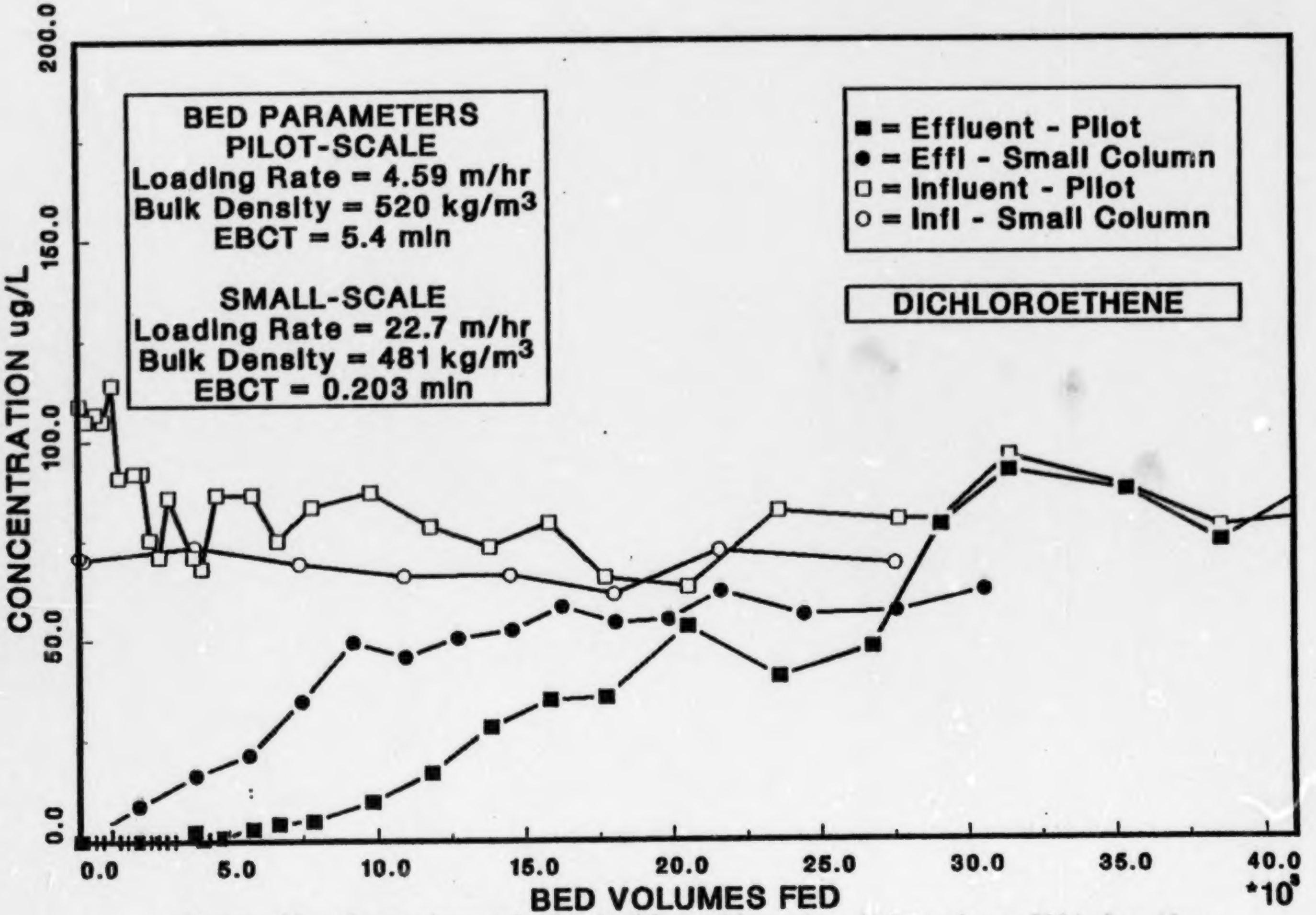

Figure 60. Comparison of the dichloroethene breakthrough profile for the small-column test to the pilot-scale column in the field study. Influent data are shown. Operating parameters are presented in Tables 7 and 8 (c).

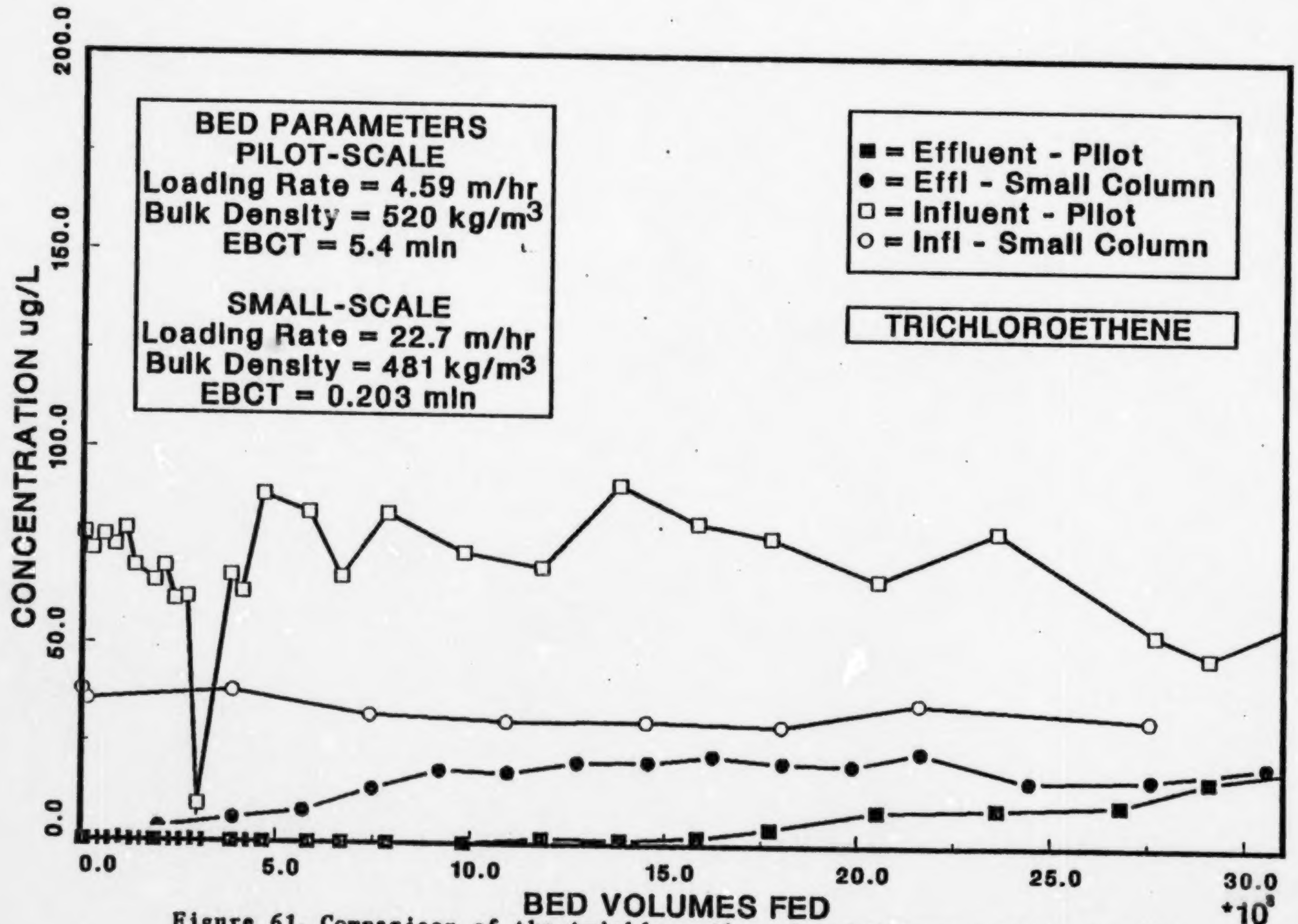

Figure 61. Comparison of the trichloroethene breakthrough profile for the small-column test to the pilot-scale column in the field study. Influent data are shown. Operating parameters are presented in Tables 7 and 8 (c).

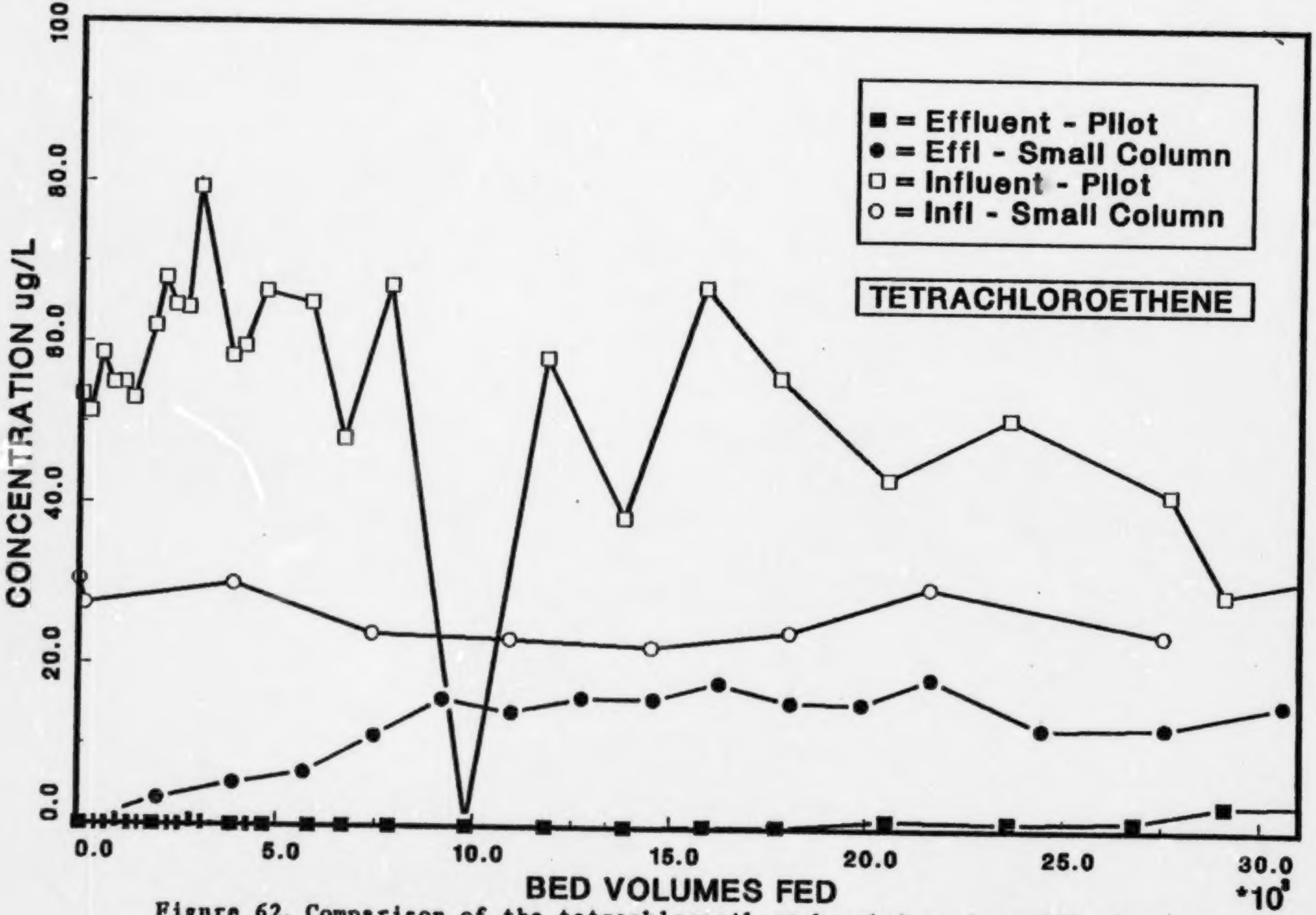

Figure 62. Comparison of the tetrachloroethene breakthrough profile for the small-column test to the pilot-scale column in the field study. Influent data are shown. Operating parameters are presented in Tables 7 and 8 (c).

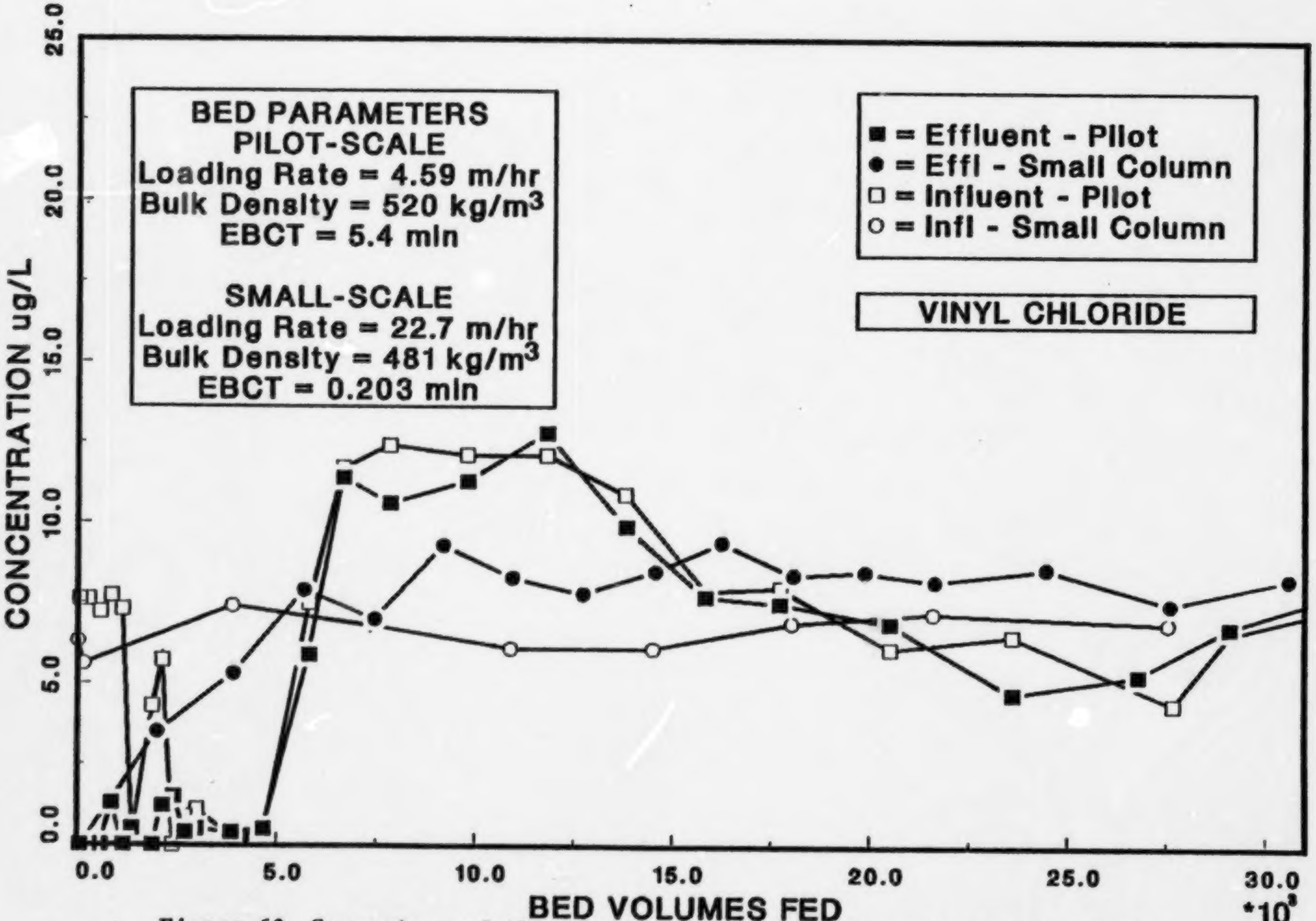

Figure 63. Comparison of the vinyl chloride breakthrough profile for the small-column test to the pilot-scale column in the field study. Influent data are shown. Operating parameters are presented in Tables 7 and 8 (c).

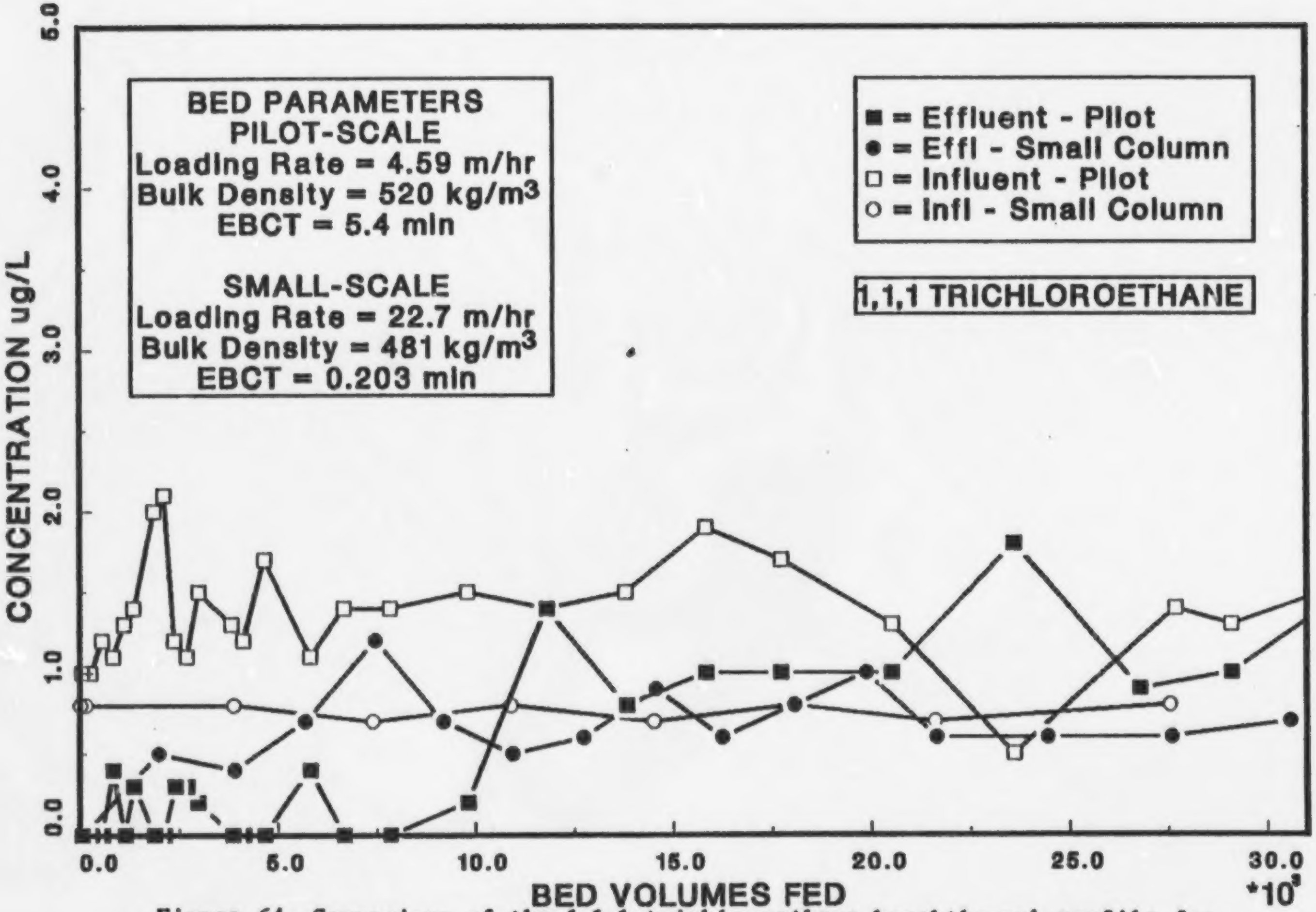

Figure 64. Comparison of the 1,1,1 trichloroethane breakthrough profile for the small-column test to the pilot-scale column in the field study. Influent data are shown. Operating parameters are presented in Tables 7 and 8 (c).

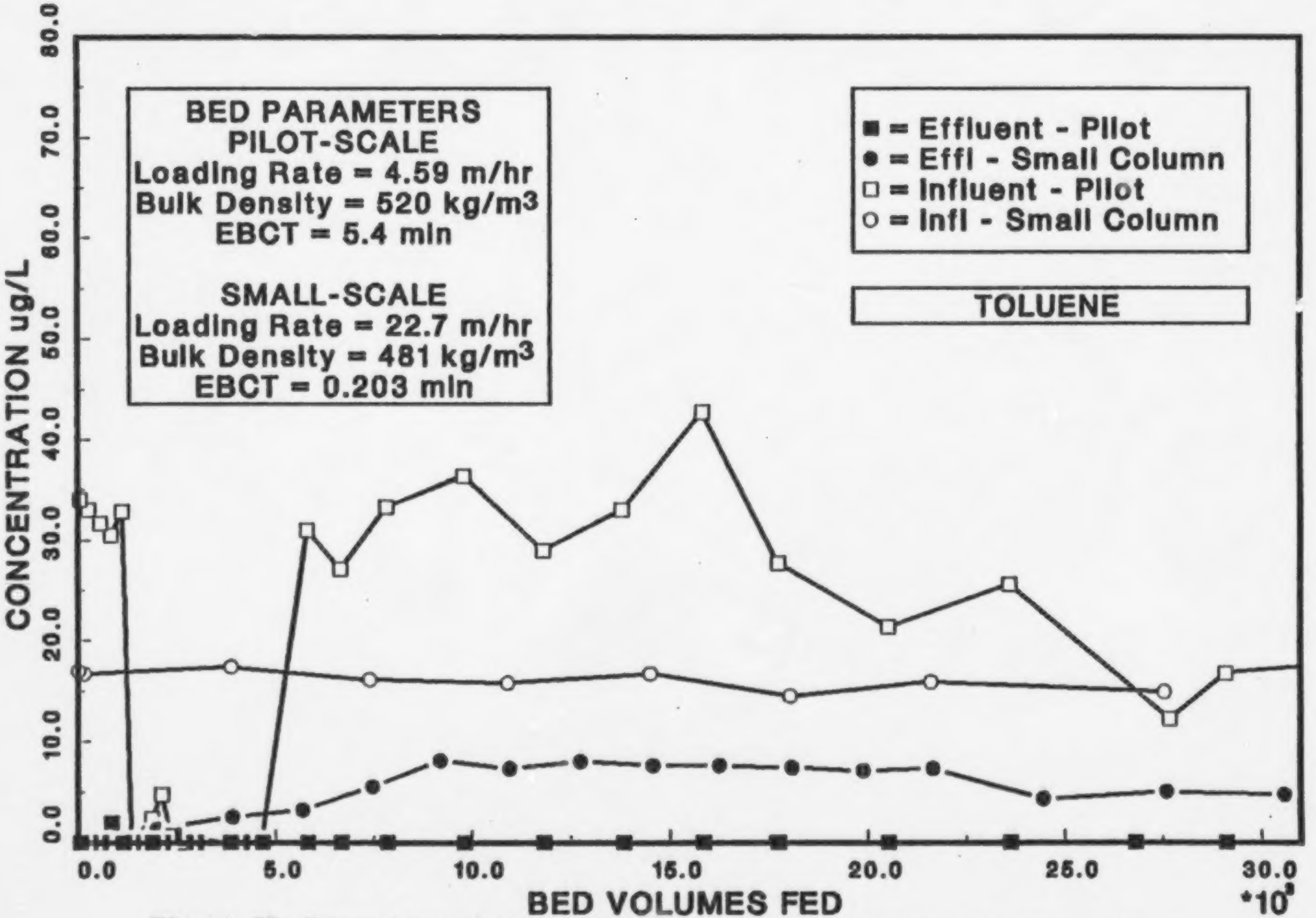

Figure 65. Comparison of the toluene breakthrough profile for the small-column test to the pilot-scale column in the field study. Influent data are shown. Operating parameters are presented in Tables 7 and 8 (c).

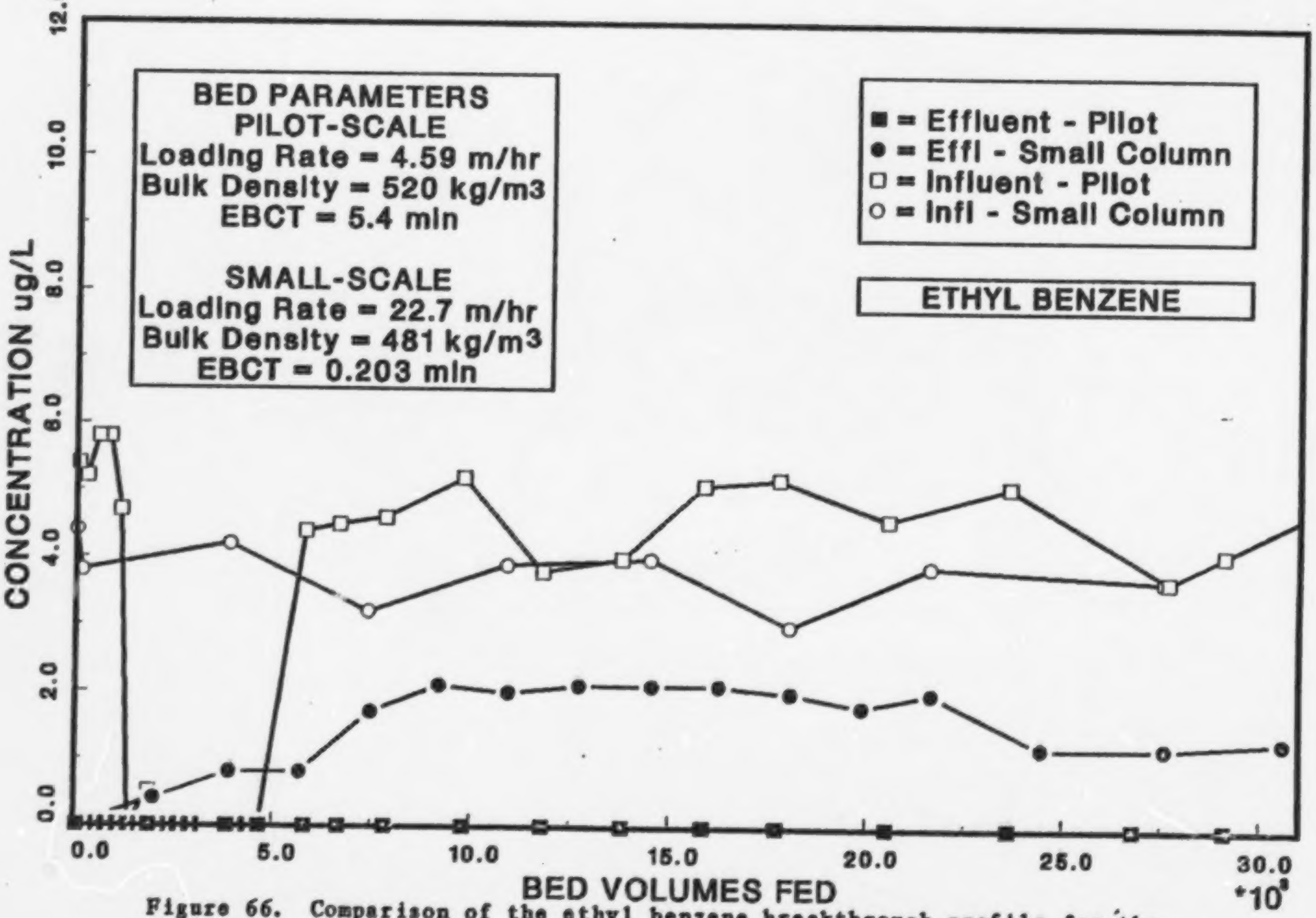

Figure 66. Comparison of the ethyl benzene breakthrough profile for the small-column test to the pilot-scale column in the field study. Influent data are shown. Operating parameters are presented in Tables 7 and 8 (c).

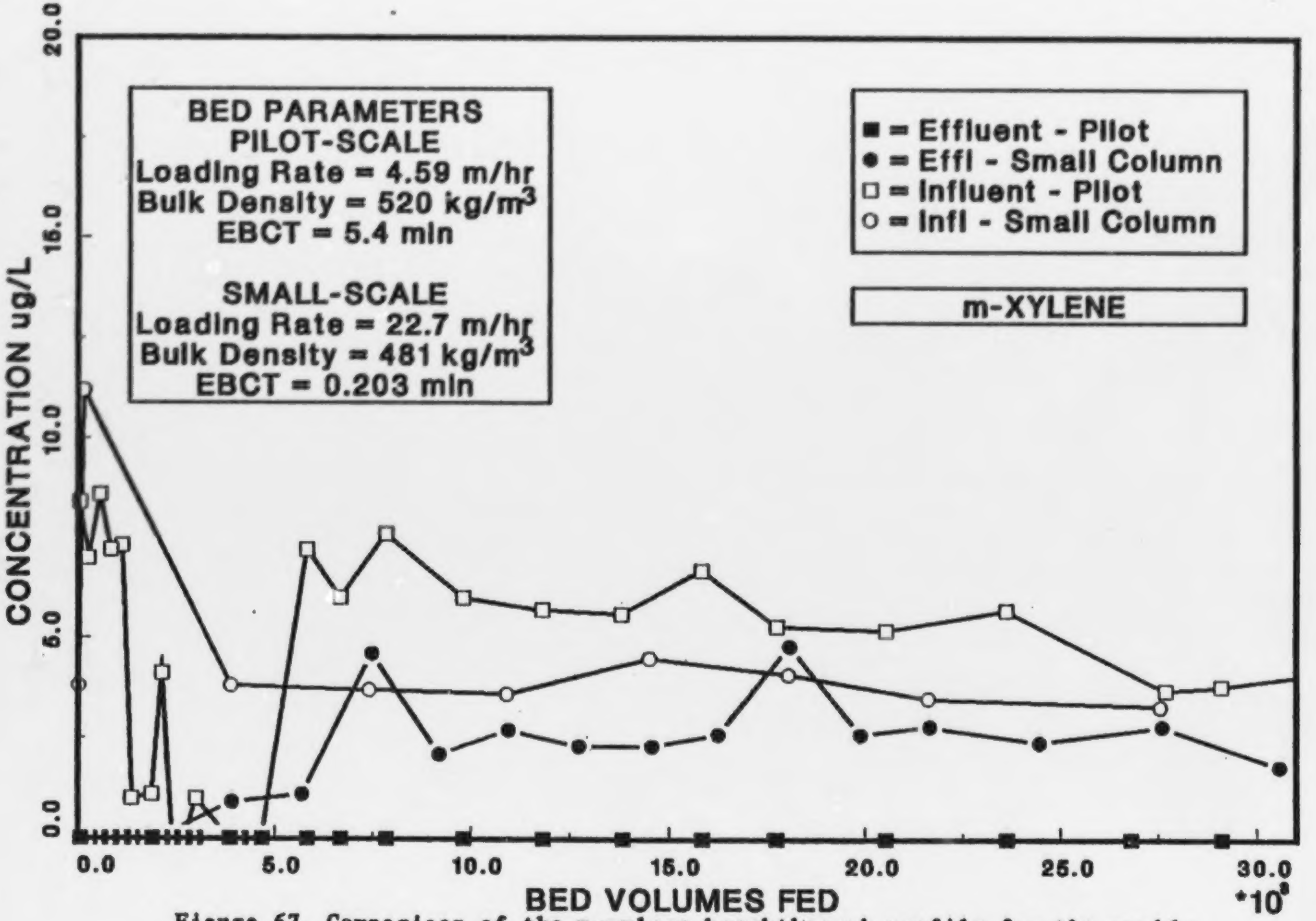

Figure 67. Comparison of the m-xylene breakthrough profile for the small-column test to the pilot-scale column in the field study. Influent data are shown. Operating parameters are presented in Tables 7 and 8 (c).

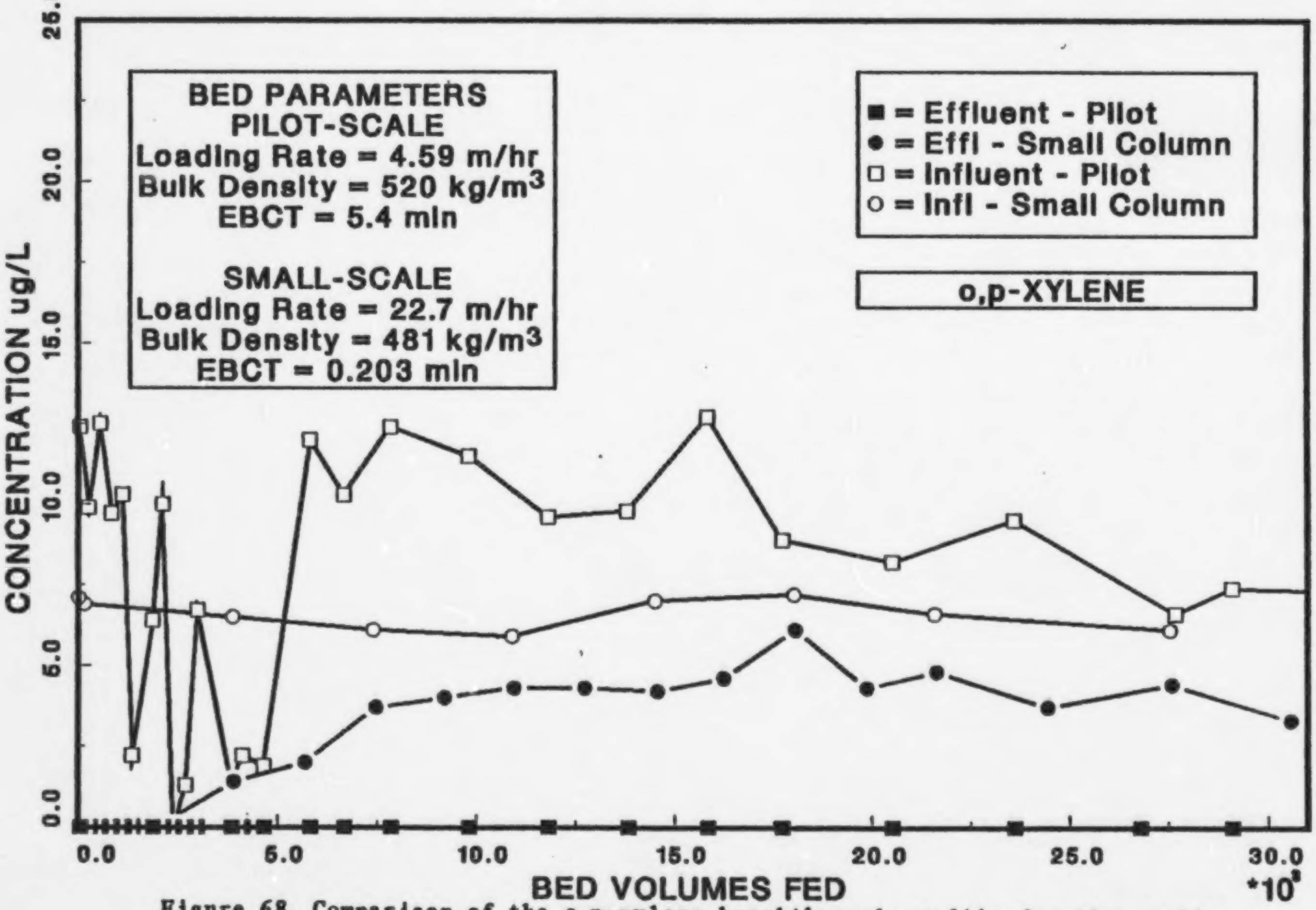

Figure 68. Comparison of the o,p-xylene breakthrough profile for the small-column test to the pilot-scale column in the field study. Influent data are shown. Operating parameters are presented in Tables 7 and 8 (c).

Eq. 22 of 13.57 seconds. Due to some settling, the bulk density of the 12x40 F-400 carbon, 520 kg/m³, was slightly greater than that of the RSSCT, 481 kg/m³, which yields a smaller pilot-scale bed void fraction. This settling was not observed for the smaller EBCT's. The effect of a smaller-than-expected void fraction is illustrated in Fig. 20 and may account for a slightly later pilot-scale breakthrough profile than expected. Without greater differences in the other operating parameters the difference in the bulk densities alone cannot account for the dissimilarities in the breakthrough profile comparisons of the 5.4 minute EBCT pilot-scale adsorber to the corresponding RSSCT.

4. Discussion of RSSCT Dissimilarity in the Field Study

Two effects that may account for the dissimilarity of the premature RSSCT breakthrough profiles with pilot-scale results include an iron precipitate formation possibly clogging adsorbent pores, or a difference in the surface diffusivities between RSSCT and pilot-scale systems. No iron precipitate was observed for the RSSCT until after at least the third day, approximately 17000 bed volumes fed. If scaling for perfect similarity assuming constant D_s was appropriate and the RSSCT influent concentrations (Table 8(c)) were lower than in the 5.4 minute EBCT pilot-scale adsorber (Table 7(c)), then the RSSCT breakthrough profiles would follow the pilot-scale breakthrough profile.

The deposition of iron precipitate on the GAC might explain the premature breakthrough of the RSSCT's if the accumulation of the iron precipitate had begun near the start of RSSCT operation. However, the precipitate appeared suddenly and in most cases near the end of the test. Most of the chemicals had broken through the RSSCT carbon beds before the appearance of the precipitate. In this study, it is unlikely that iron precipitation greatly influenced the breakthrough profiles of the RSSCT's.

The probable cause of the earlier RSSCT breakthrough is a difference in the surface diffusivities between the full-size carbon in the pilot-scale adsorbers and the smaller carbon in the RSSCT's. Schneider (1982) showed that the surface diffusivity could depend on particle size. Figure 11 displays the model simulations of a full-scale adsorber and an RSSCT designed for perfect similarity where the surface diffusivities change proportionally with the particle size. When compared to the results of the field studies, Fig. 11 shows that differing surface diffusivities alone may explain the dissimilarity between RSSCT and pilot-scale results.

The similarity of the RSSCT to pilot-scale adsorber in the laboratory study and the dissimilarity of the RSSCT to pilot-scale adsorber in the field studies may be explained by a difference of controlling intraparticle mass-transfer mechanisms between the laboratory study and the field studies. This difference may be explained in terms of the DFPSDM dimensionless groups.

Pore diffusion could be the predominant intraparticle mass-transport mechanism in the laboratory study. At higher influent concentrations the values of the surface solute distribution parameters (Eq. 10) will be less than it would be at lower concentrations, assuming that the Freundlich 1/n is less than one. The pore solute distribution parameter (Eq. 11), being a constant for a particular adsorbent, will remain the same. Consequently, the values of the surface diffusion moduli (Eq. 15) will decrease with influent concentration while the values of the pore diffusion moduli (Eq. 16) will remain constant. The ratio of the surface diffusion modulus to the pore diffusion modulus, being the ratio of the rates of surface diffusion to pore diffusion, will then increase as the influent concentrations are decreased. It may be possible then to have pore diffusion control at high concentrations and surface diffusion control at low concentrations. Pore diffusion coefficients, $D_{p,i}$, are not likely to depend on the particle radius., rather only the tortuosity and the porosity of the adsorbent. Thus, when pore diffusion controls then Eqs. 22 and 25 may be used in the design of an RSSCT to simulate full-scale adsorbers. When surface diffusion controls, then the design of an RSSCT assuming perfect similarity and constant intraparticle diffusivity may yield a RSSCT predicting earlier breakthrough profiles than would be observed in a pilot-scale or full-scale study if the surface diffusivity is proportional to the adsorbent particle radius. The effect of a surface diffusivity proportional to adsorbent particle radius is incorporated into Eq. 30 may be used in designing an RSSCT where surface diffusion is the controlling mass-transport mechanism.

5. Discussion of RSSCT Results for Simulation of 5.4 Minute EBCT Adsorber Assuming D_s Linearly Proportional to R

Because measured surface diffusivities for both full-size GAC and smaller RSSCT GAC were unavailable for any of the solutes at the groundwater conditions, the ratio of the surface diffusivities for full-size carbon in a pilot-scale adsorber to smaller RSSCT carbon was assumed to be proportional to the particle radius (Schneider *et al*.,1984). The RSSCT design assumed that the adsorption process was surface diffusion controlled. Conveniently, the RSSCT in Table 8(c) satisfied the necessary EBCT ratio required by Eq. 30. when compared to the 1 minute EBCT adsorber described in Table 7(a). In addition, the RSSCT in Table 8(c) satisfies the requirement for constant Reynolds number suggested by Eq. 25. Another RSSCT could be designed using the method of Eq. 31 to further reduce the loading rate requirements and the required influent volume. The RSSCT described in Table 8(c) may simulate the 1 minute EBCT pilot-scale adsorber described in Table 7(a) using F-400 carbon. Figures 69–72 display the breakthrough profile comparisons of the RSSCT in Table 8(c) and the pilot-scale column in Table 7(a) for cis-dichloroethene in Fig. 69, trichloroethene in Fig. 70, toluene in Fig. 71, and o- and p-xylenes in Fig. 72. The RSSCT breakthrough profiles appear later than the pilot-scale breakthrough profiles. The difference in concentration accounts for the the greater part of the dissimilarity between the breakthrough profiles of pilot-scale adsorber and RSSCT (Compare Tables 7(a) and 8(c)).

For the low concentrations and composition of the groundwater design of RSSCT's assuming surface diffusion control and a surface diffusivity proportional to the adsorbent particle radius (Eqs. 25 and 27) are more accurate at full-scale performance prediction than RSSCT's designed for perfect similarity assuming constant surface diffusivity (Eqs. 22 and 25). The wide varieties of influent compositions in various applications make the recommendation of any specific scaling equation impossible. However, measurement of surface diffusivities of a solute on the RSSCT smaller carbon, and the full-size carbon in pilot or full-scale adsorbers at the same temperature and influent characteristics as the full-scale system allow the use of Eqs 30 and 31 to design an RSSCT that will properly simulate surface diffusion controlled processes.

6. Discussion of Methods for RSSCT Interpretation where Influent Concentrations Change

The fluctuation and change in the solute concentrations can cause the results of the RSSCT studies to be difficult to interpret. Because the scaling method can show similar breakthrough profiles only when the influent concentrations are the same, and because the influent concentrations were not the same in all the field work, some deviations from similarity will be

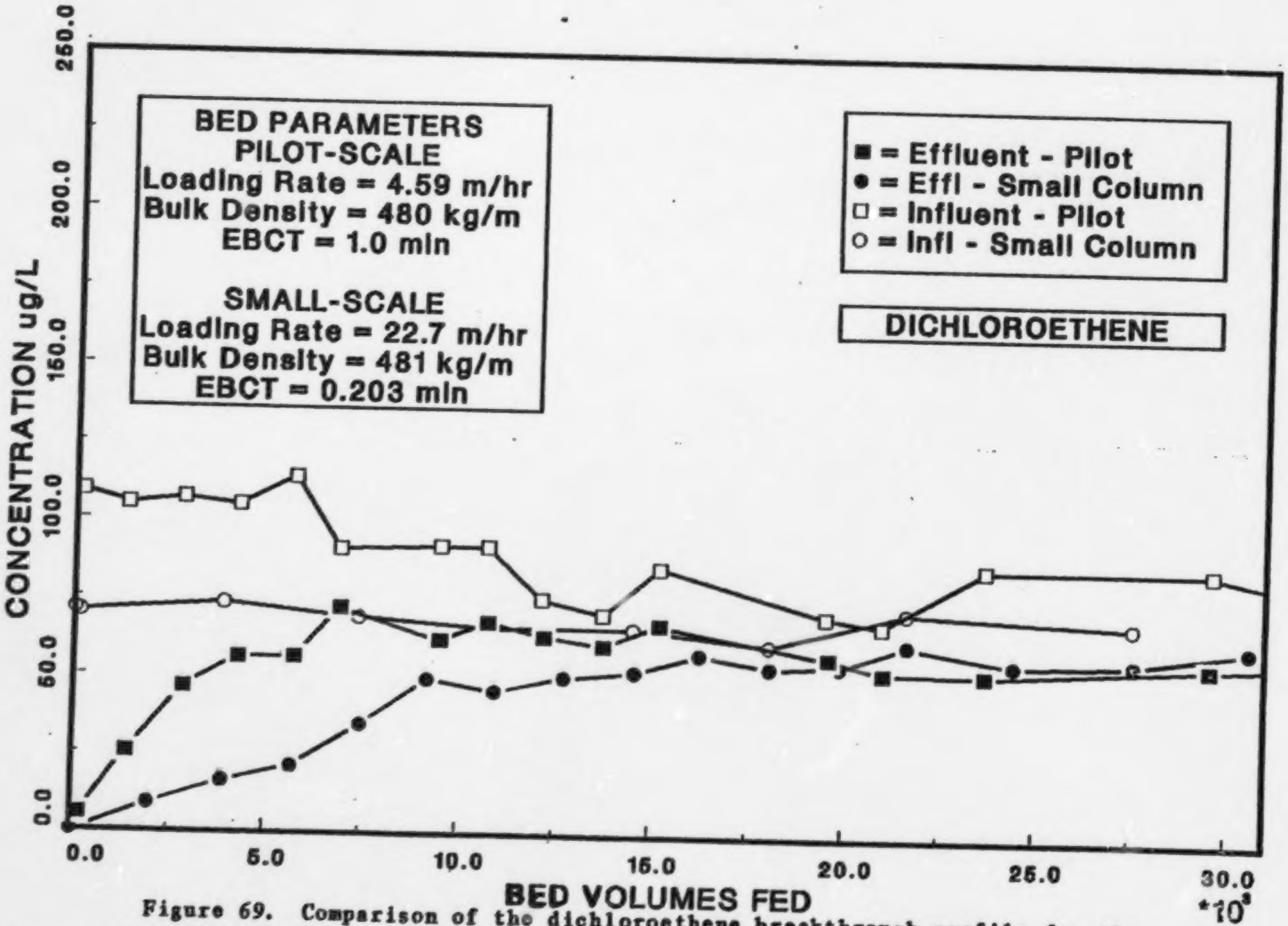

Figure 69. Comparison of the dichloroethene breakthrough profile for the small-column test to the pilot-scale column in the field study. Influent data are shown. Operating parameters are presented in Tables 7 (a) and 8 (c).

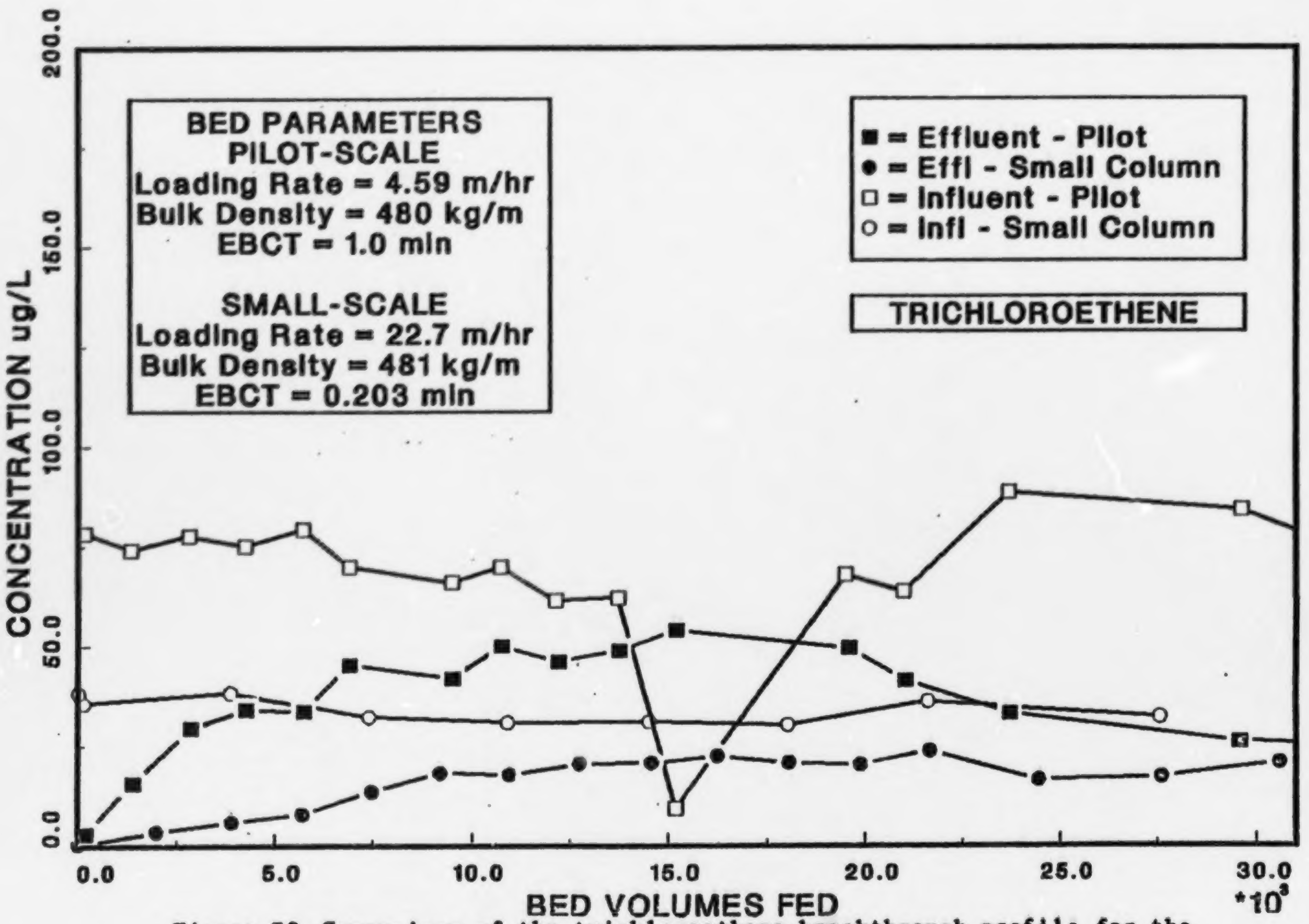

Figure 70. Comparison of the trichloroethene breakthrough profile for the small-column test to the pilot-scale column in the field study. Influent data are shown. Operating parameters are presented in Tables 7 (a) and 8 (c).

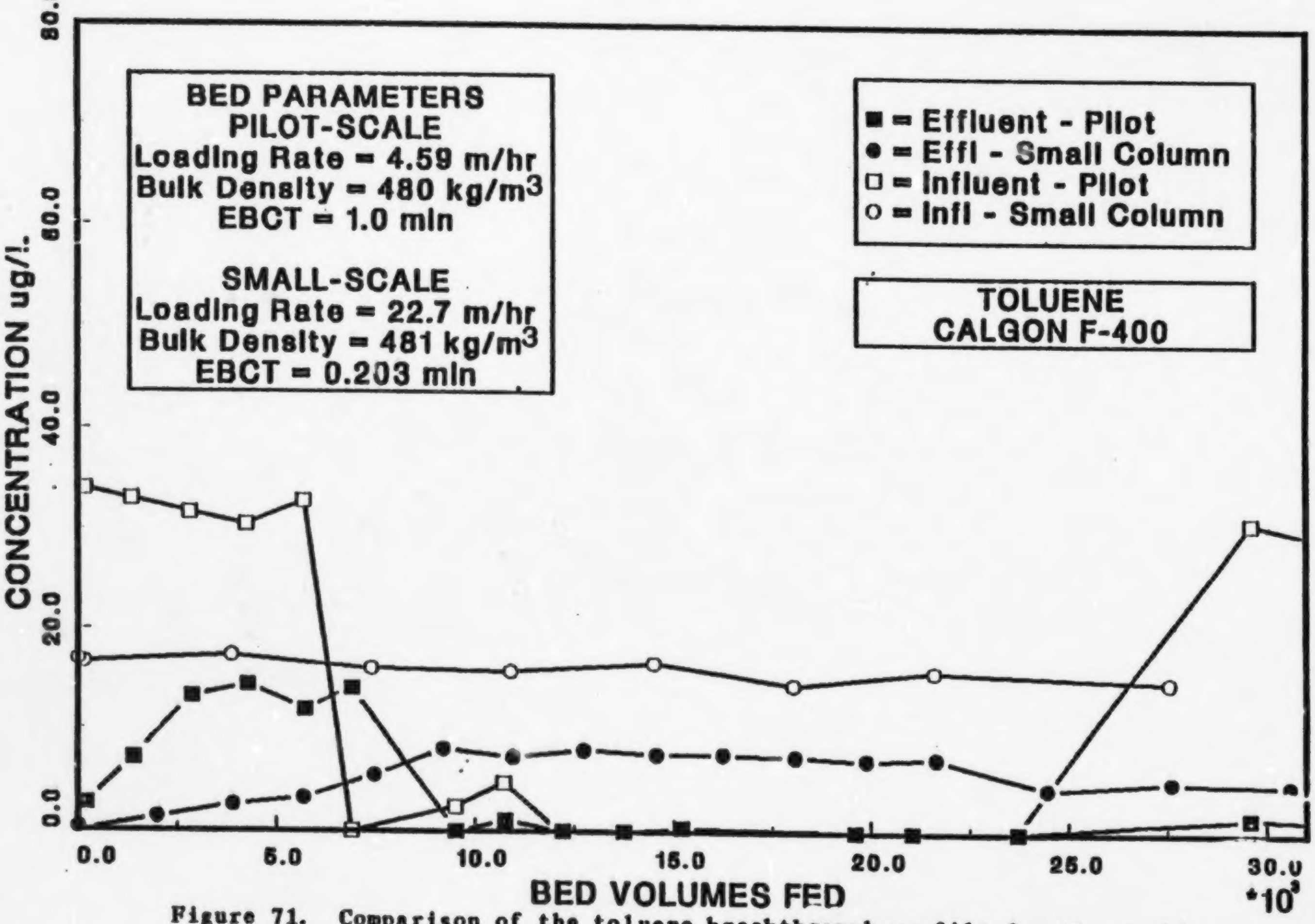

Figure 71. Comparison of the toluene breakthrough profile for the small-column test to the pilot-scale column in the field study. Influent data are shown. Operating parameters are presented in Tables 7 (a) and 8(c).

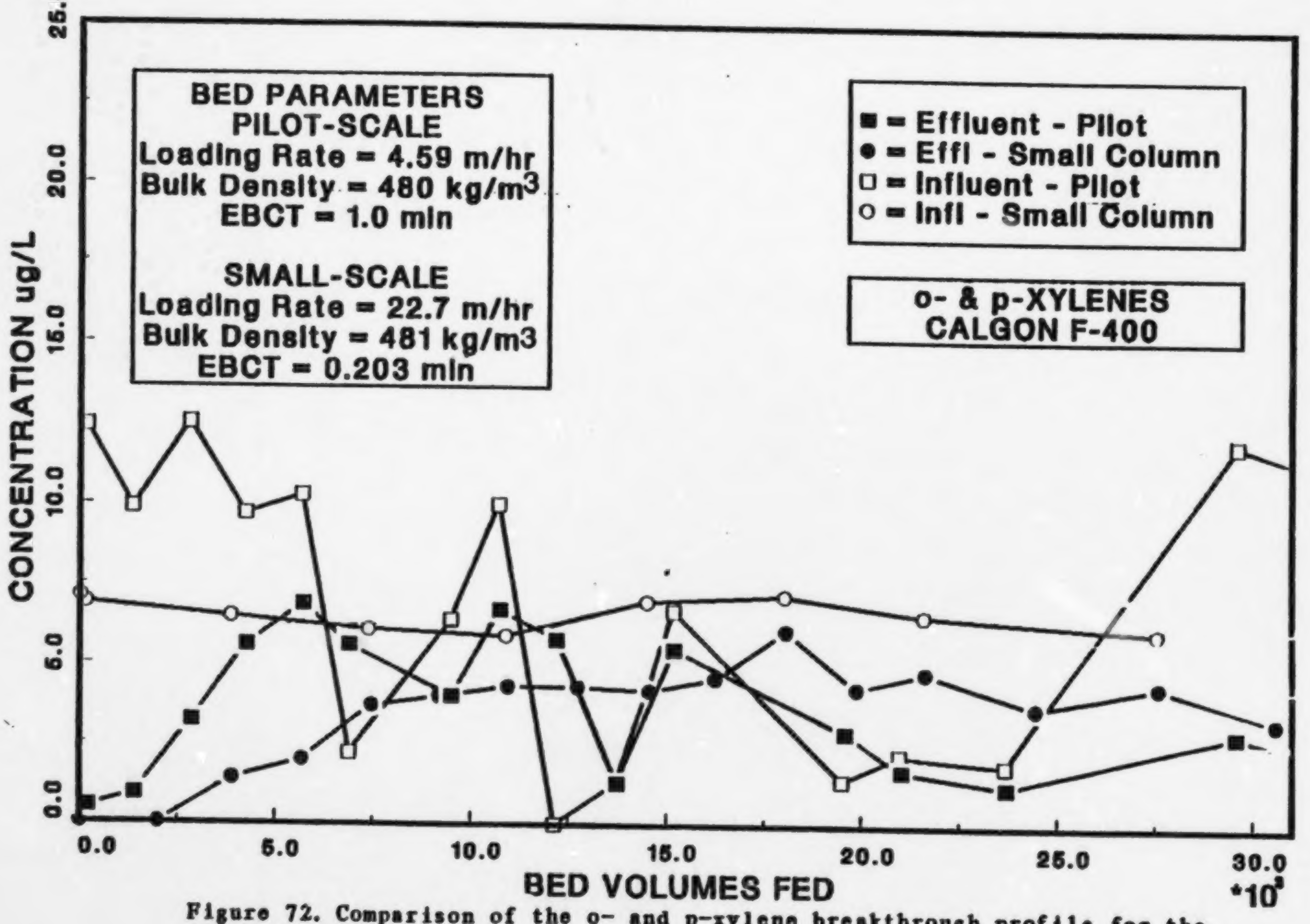

Figure 72. Comparison of the o- and p-xylene breakthrough profile for the small-column test to the pilot-scale column in the field study. Influent data are shown. Operating parameters are presented in Tables 7 (a) and 8 (c).

expected. The breakthrough profile concentrations can be aligned on the ordinate axis by converting the concentrations to dimensionless form dividing by the average influent concentration of the solute. Figures 73 - 76 display the breakthrough profile comparisons of cis-dichloroethene, trichloroethene, toluene, and o- and p-xylenes respectively for the RSSCT described in Table 7(c) and the pilot-scale adsorber described in Table 7(a). Concentration data were reduced by the average influent concentrations reported in Tables 7(a) and 8(c) with the exception of the pilot-scale toluene breakthrough profiles which were reduced by the average influent concentration of the first 5000 bed volumes because of solute decomposition. The advantage in reporting the results in this fashion is that expressing the breakthrough profiles in reduced concentration reduces the dissimilarity to a horizontal displacement of the breakthrough profile.

It may be possible to adjust the horizontal axis from bed volumes to some parameter that may take the accumulated mass of solute fed through the adsorber. Throughput accounts for accumulated solute mass fed, however to use throughput, it is necessary to calculate equilibrium solute distribution parameters of each solute. An alternative may be to use the mass of solute fed to the adsorber divided by the total mass of carbon in the bed. This parameter would then adjust the breakthrough profile horizontally to account for concentration differences with respect to time. Figures 77-80 display such breakthrough profile comparisons of the RSSCT described in Table 7(c) and the pilot-scale adsorber described in Table 7(a) for cis-dichloroethene and trichloroethene, tetrachloroethene, and toluene, respectively (Compare Figs. 69 and 77 for dichloroethene, Figs. 70 and 78 for trichloroethene, and Figs. 71 and 79 for toluene). The use of breakthrough profile data expressed in grams of solute fed per kilogram adsorbent versus the reduced concentration allow the RSSCT to be used in predicting full-scale

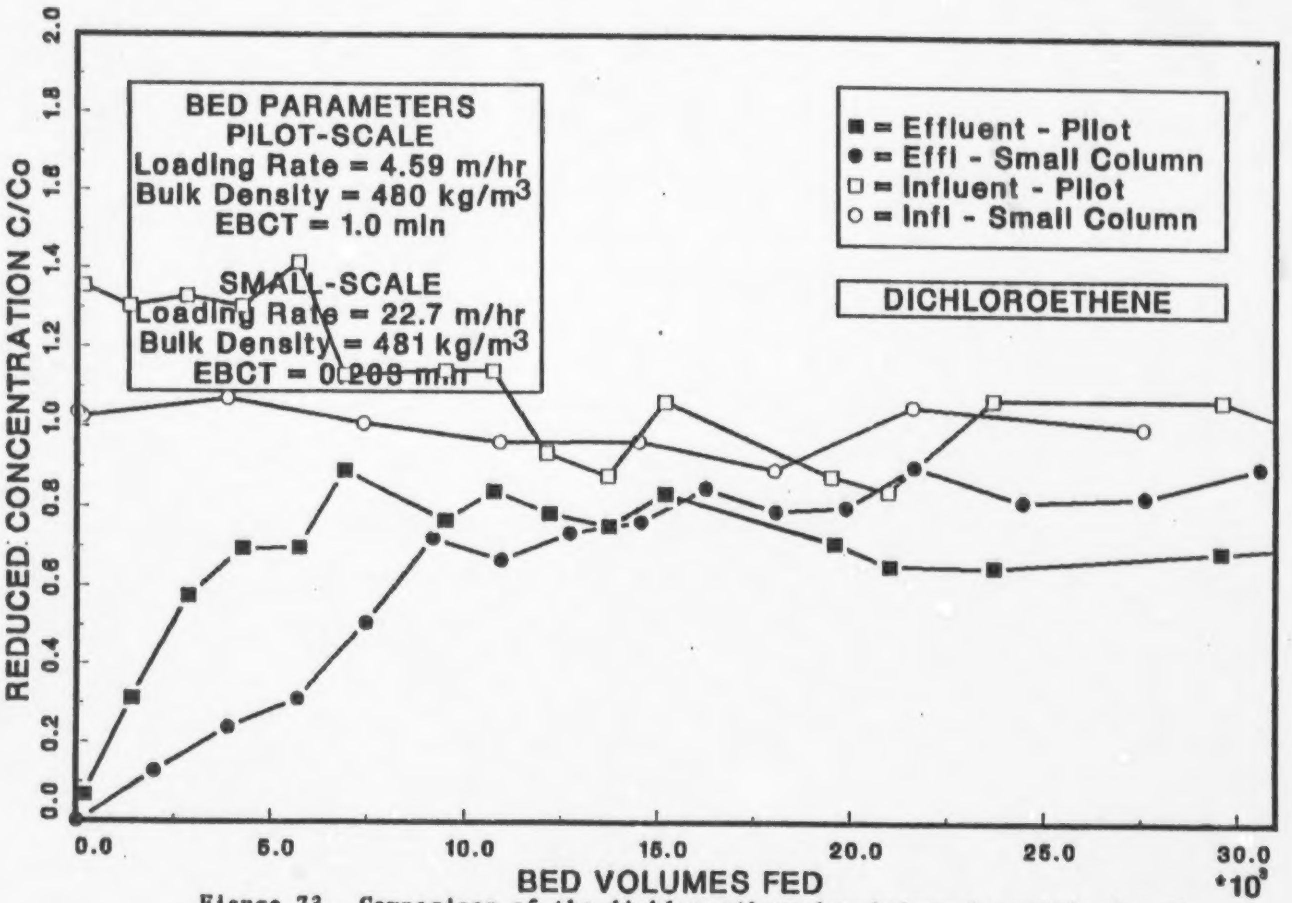

Figure 73. Comparison of the dichloroethene breakthrough profile for the small-column test to the pilot-scale column in the field study. Concentrations are normalized by the average influent concentration. Influent data are shown. Operating parameters are presented in Tables 7 (a) and 8 (c).

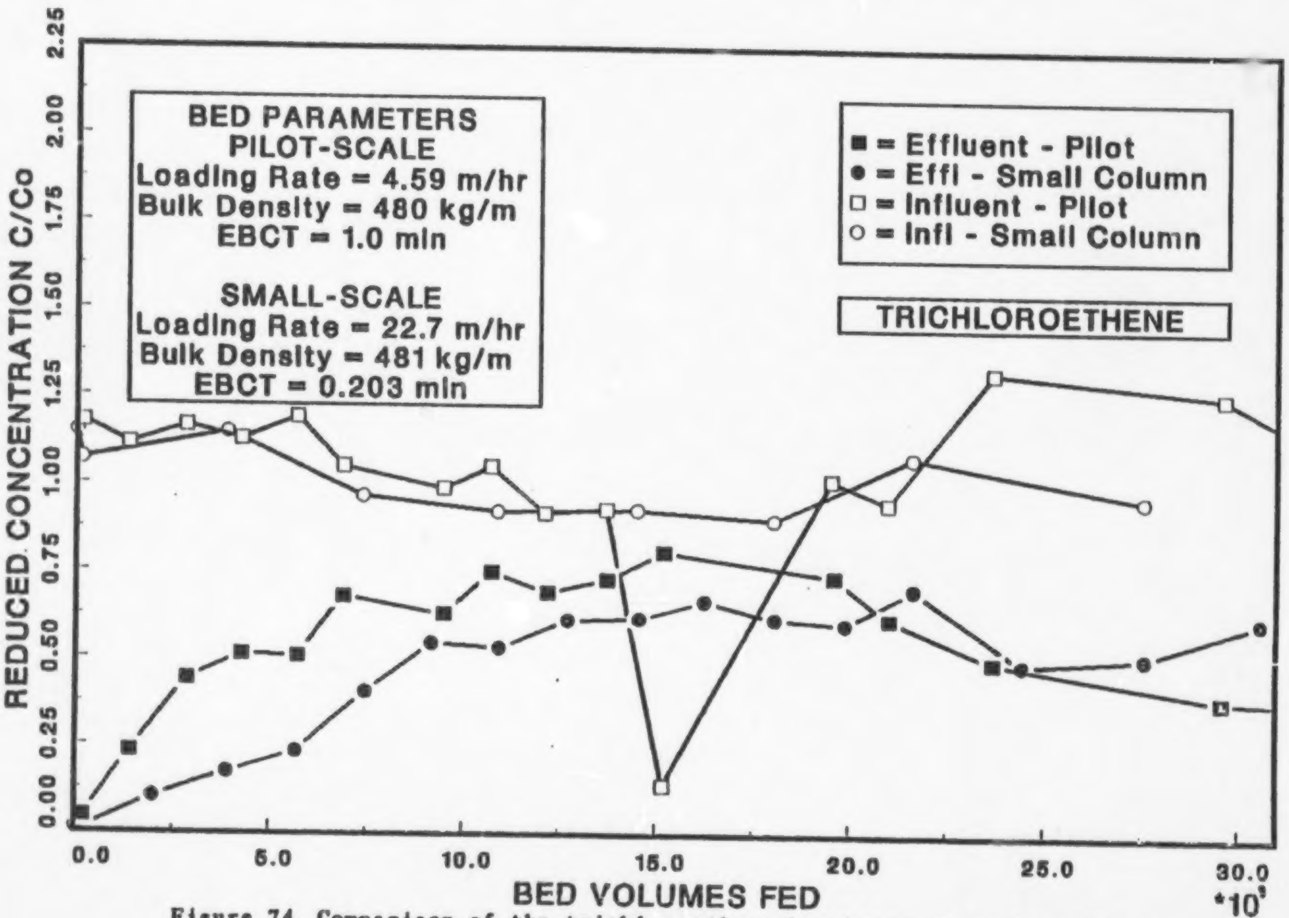

Figure 74. Comparison of the trichloroethene breakthrough profile for the small-column test to the pilot-scale column in the field study. Concentrations are normalized by the average influent concentration. Influent data are shown. Operating parameters are presented in Tables 7 (a) and 8 (c).

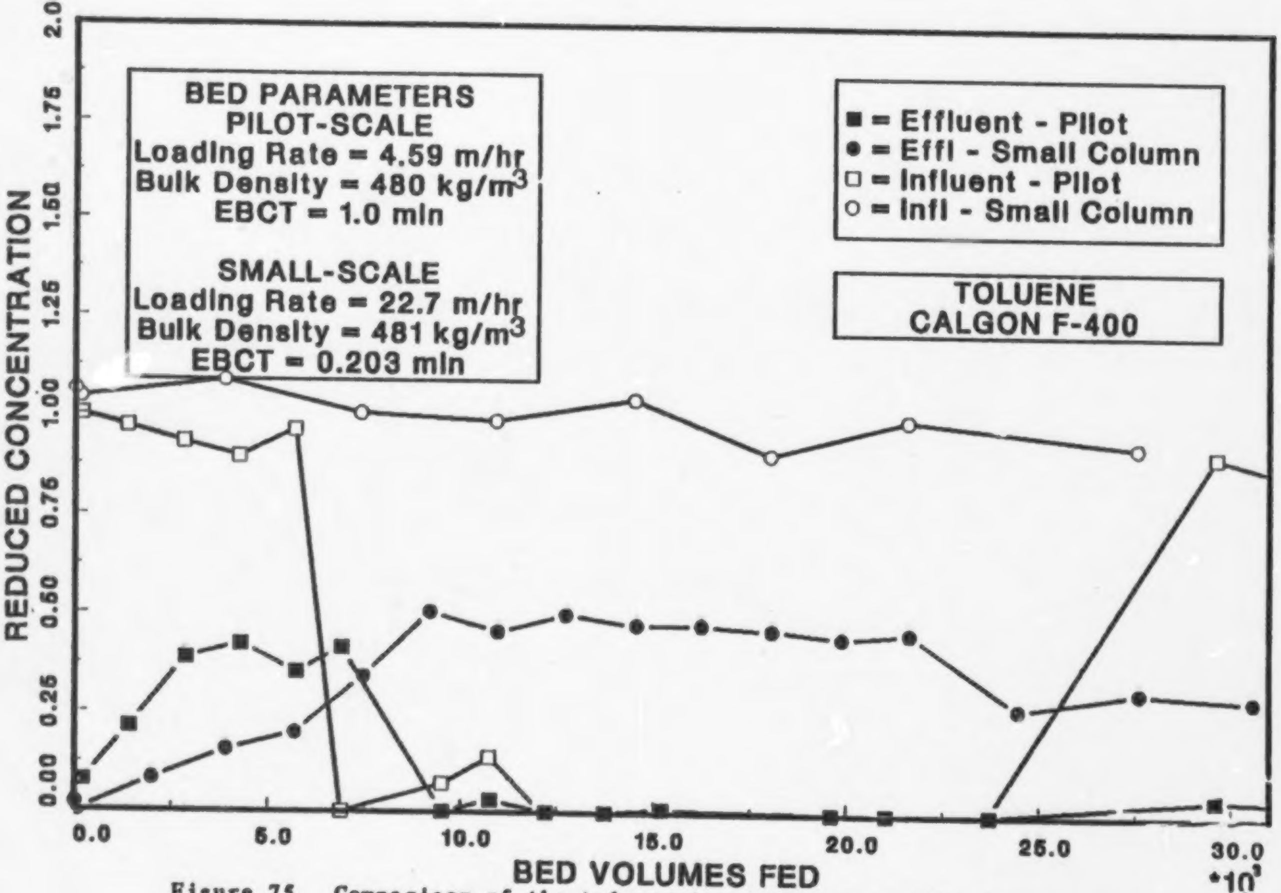

Figure 75. Comparison of the toluene breakthrough profile for the small-column test to the pilot-scale column in the field study. Concentrations are normalized by the average influent concentration. Influent data are shown. Operating parameters are presented in Tables 7 (a) and 8 (c).

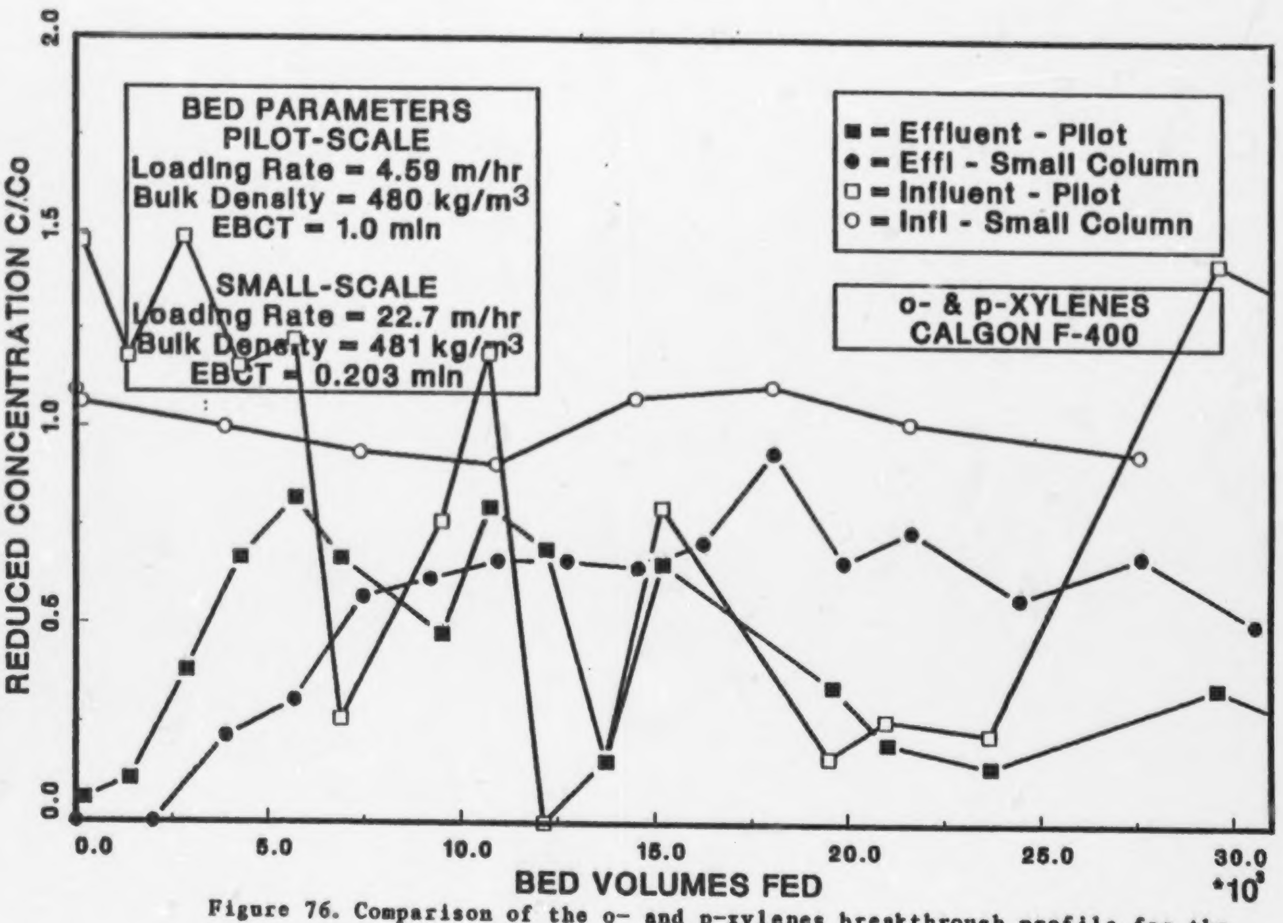

Figure 76. Comparison of the o- and p-xylenes breakthrough profile for the small-column test to the pilot-scale column in the field study. Concentrations are normalized by the average influent concentration. Influent data are shown. Operating parameters are presented in Tables 7 (a) and 8 (c).

]

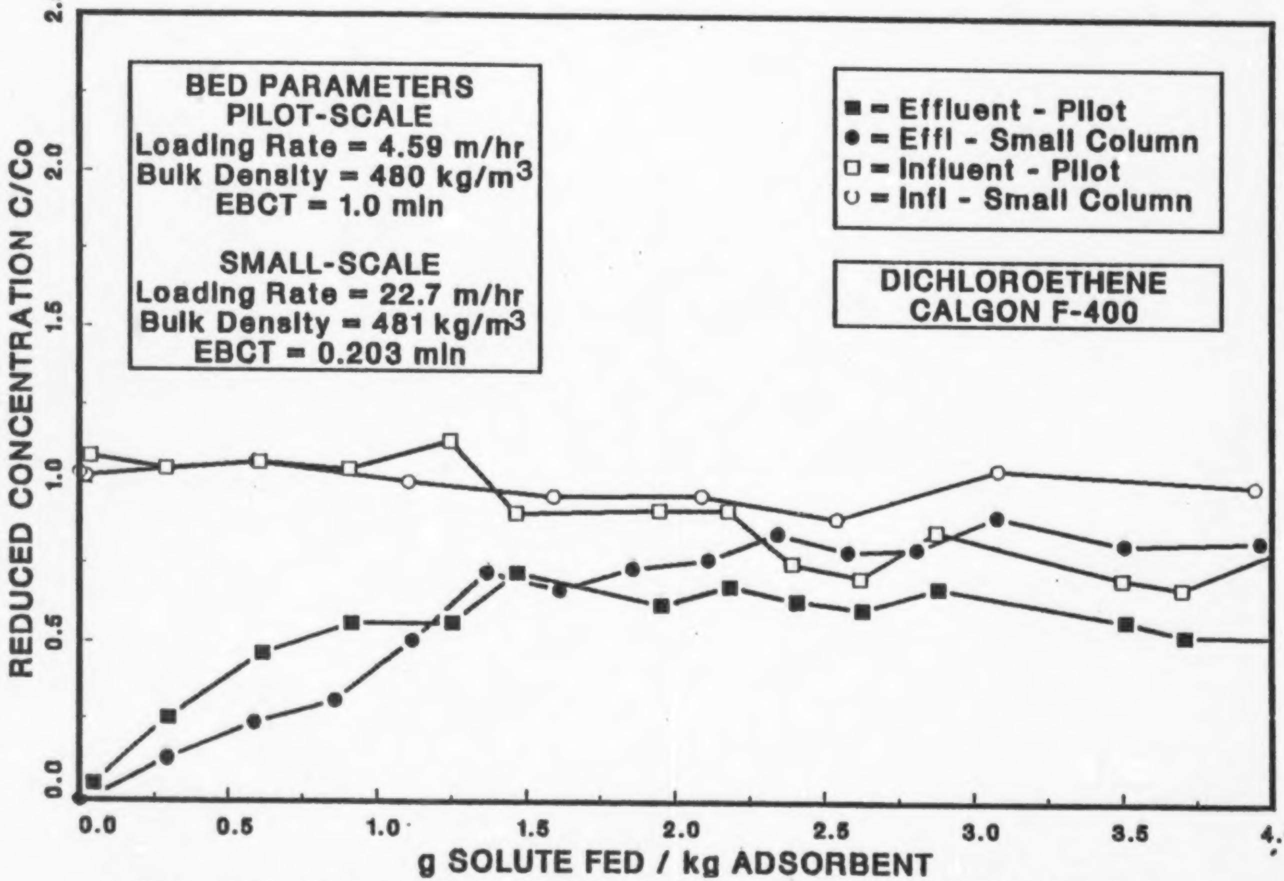

Figure 77. Comparison of the dichloroethene breakthrough profile for the small-column test to the pilot-scale column in the field study expressed as the grams of solute fed through the adsorber per kilogram carbon in the bed versus reduced concentration to normalize the effects of differing influent concentrations. Influent data are shown. Operating parameters are presented in Tables 7 (a) and 8 (c).

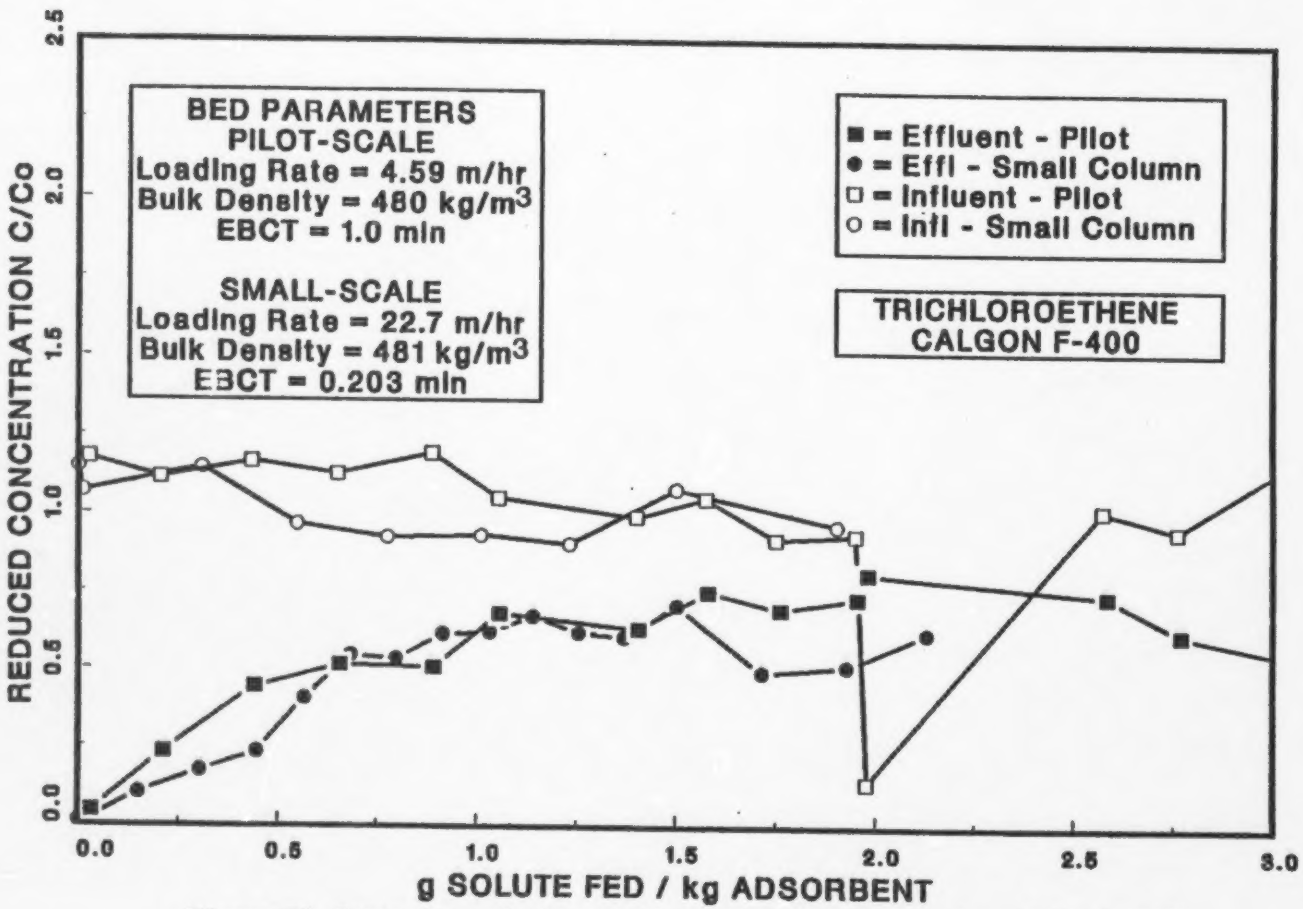

Figure 78. Comparison of the trichloroethene breakthrough profile for the small-column test to the pilot-scale column in the field study expressed as the grams of solute fed through the adsorber per kilogram carbon in the bed versus reduced concentration to normalize the effects of differing influent concentrations. Influent data are shown. Operating parameters are presented in Tables 7 (a) and 8 (c).

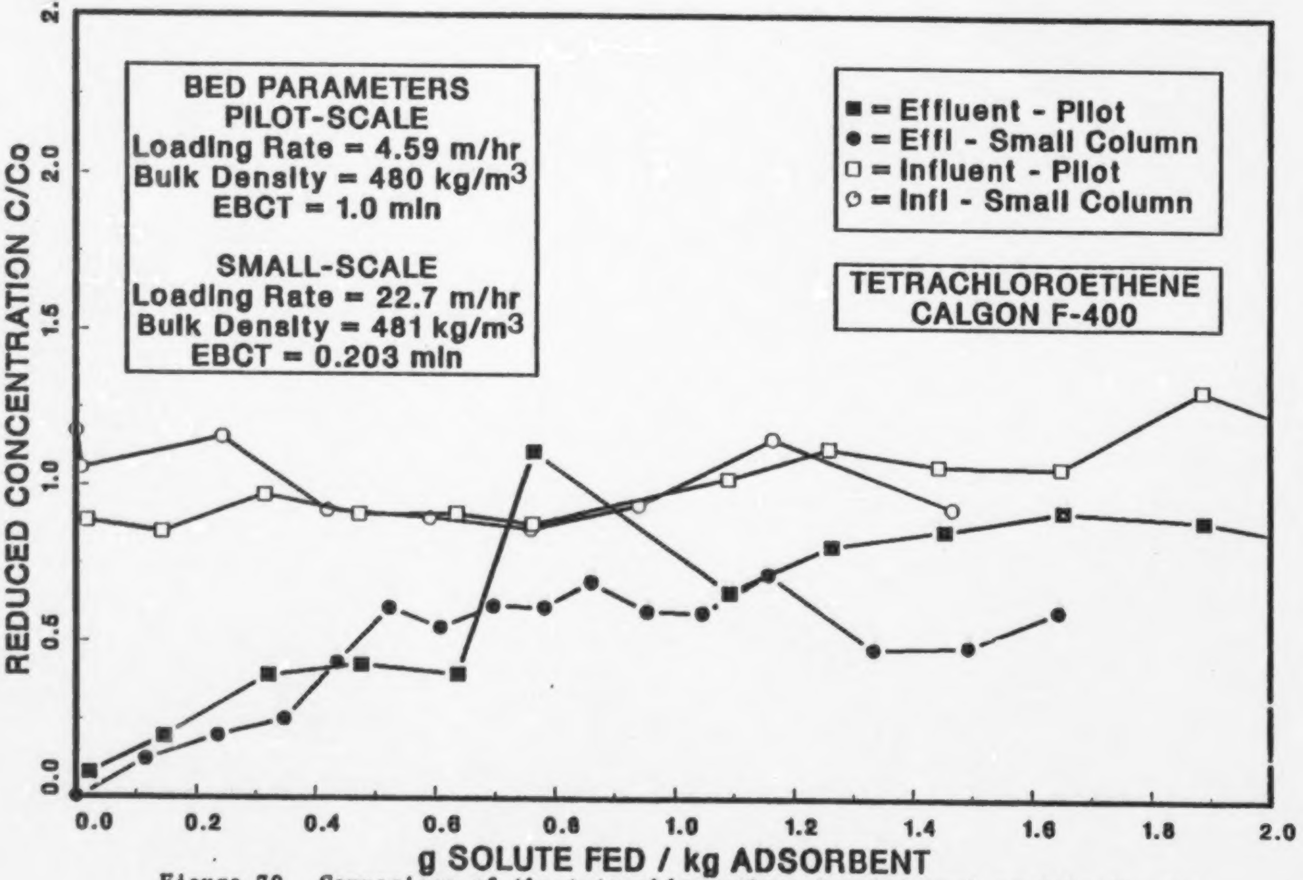

Figure 79. Comparison of the tetrachloroethene breakthrough profile for the small-column test to the pilot-scale column in the field study expressed as the grams of solute fed through the adsorber per kilogram carbon in the bed versus reduced concentration to normalize the effects of differing influent concentrations. Influent data are shown. Operating parameters are presented in Tables 7 (a) and 8 (c).

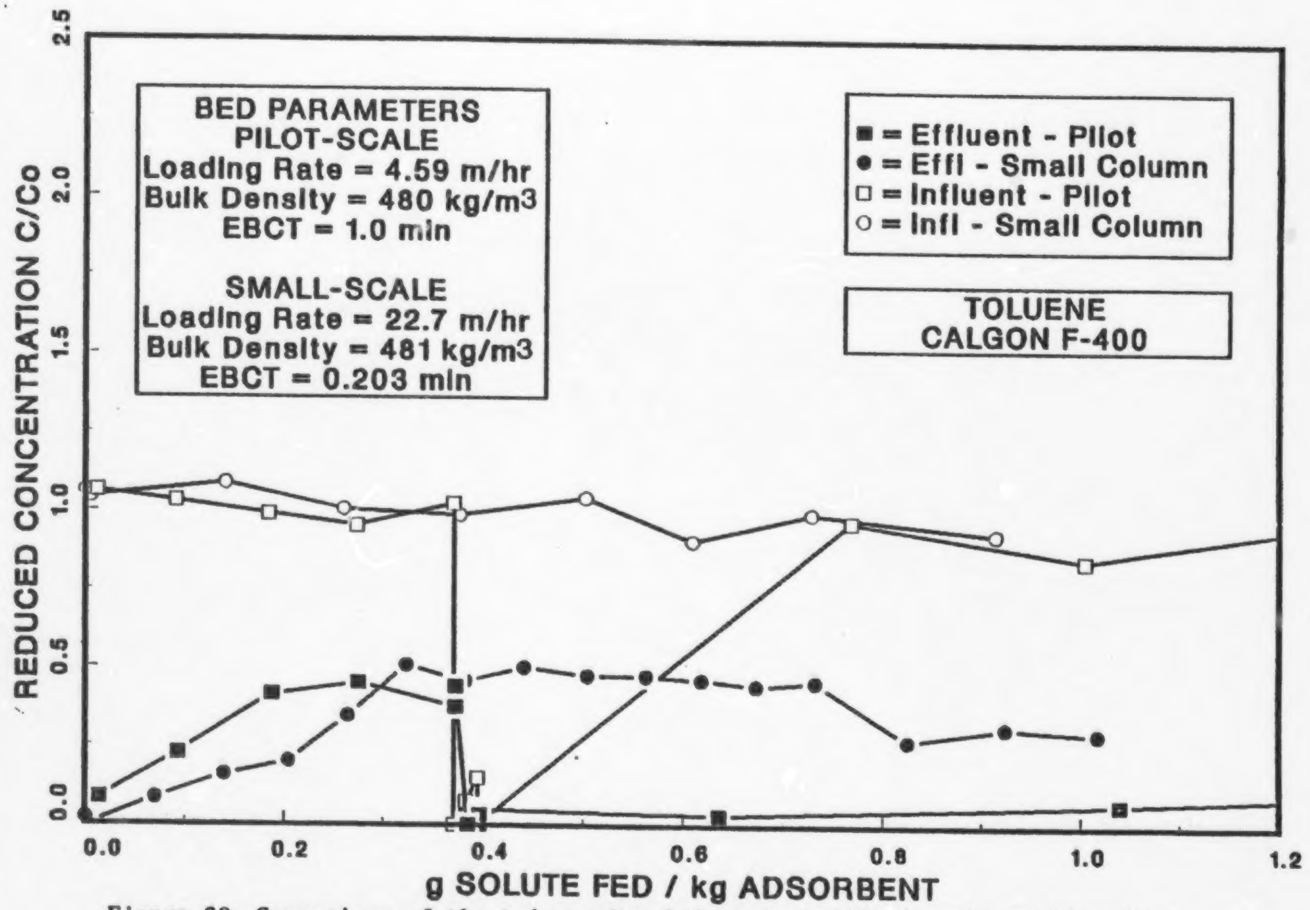

Figure 80. Comparison of the toluene breakthrough profile for the small-column test to the pilot-scale column in the field study expressed as the grams of solute fed through the adsorber per kilogram carbon in the bed versus reduced concentration to normalize the effects of differing influent concentrations. Influent data are shown. Operating parameters are presented in Tables 7 (a) and 8 (c).

performance when influent concentrations differ. Good agreement in the breakthrough profile comparison of Fig. 77 for dichloroethene, Fig. 78 for trichloroethene, and Fig. 79 for tetrachloroethene, show that the RSSCT in Table 8(c) could successfully simulates the pilot-scale adsorber in Table 7(a). The toluene breakthrough profile comparison was complicated by toluene degradation in the pilot-scale samples.

Figures 81-84 display the breakthrough profile comparisons of the RSSCT in Table 8(c) and the pilot-scale adsorber in Table 7(c) for dichloroethene, trichloroethene, tetrachloroethene, and toluene, respectively (Compare Fig. 60 and 81 for dichloroethene, Figs. 61 and 82 for trichloroethene, Figs. 62 and 83 for tetrachloroethene, and Figs. 65 and 84 for toluene). These figures display the breakthrough profile comparisons in terms of mass of solute fed per mass of adsorbent versus the reduced concentration, as in Figs. 77-80. However, the scaling method displayed in Figs. 81-84 assume that the surface diffusivity is constant. Figure 81 shows that dichloroethene breaks through the RSSCT much earlier than would be expected by the pilot-scale adsorber. The same trend is shown in Fig. 82 for trichloroethene and in Fig. 83 for tetrachloroethene. As seen in these figures, the breakthrough profiles do not compare well.

For the field study, assuming that the surface diffusivity is proportional to the particle size yields an RSSCT design that successfully simulated pilot-scale performance. To ensure a proper RSSCT design, however, the surface diffusivities of a solute in the influent mixture should be measured for the adsorbents that are to be used in the RSSCT and the full-scale adsorber.

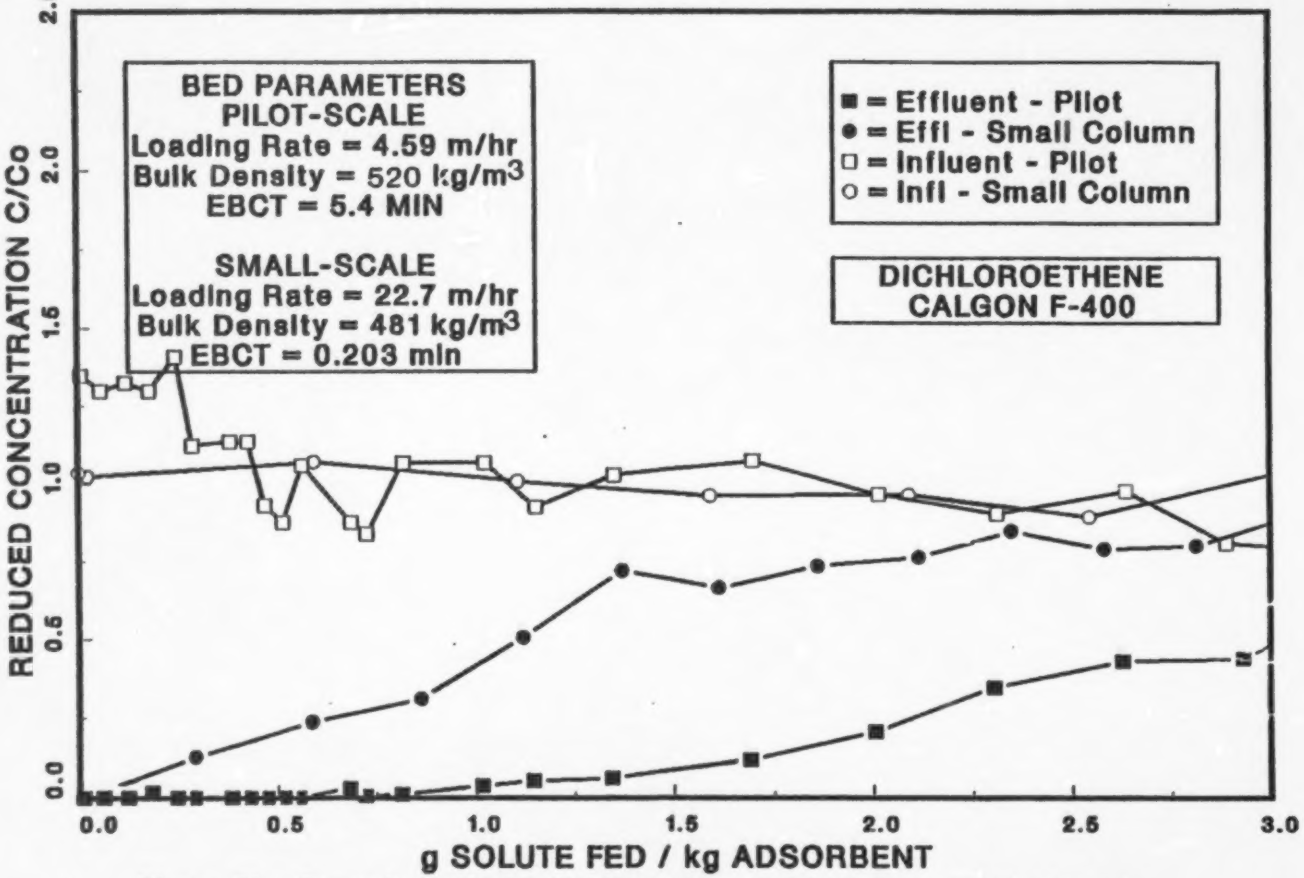

Figure 81. Comparison of the dichloroethene breakthrough profile for the small-column test to the pilot-scale column in the field study expressed as the grams of solute fed through the adsorber per kilogram carbon in the bed versus reduced concentration to normalize the effects of differing influent concentrations. Influent data are shown. Operating parameters are presented in Tables 7 (c) and 8 (c).

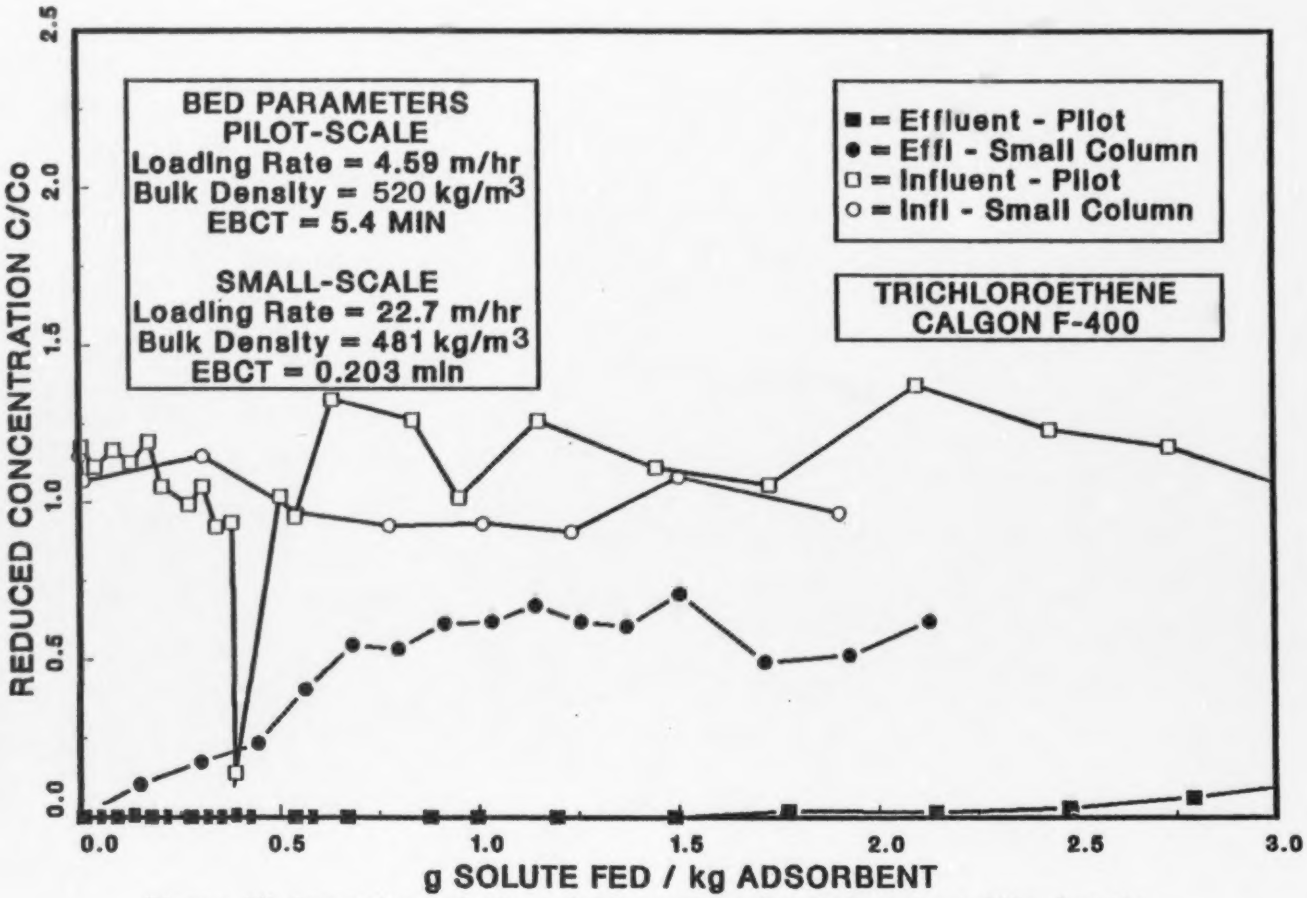

Figure 82. Comparison of the trichloroethene breakthrough profile for the small-column test to the pilot-scale column in the field study expressed as the grams of solute fed through the adsorber per kilogram carbon in the bed versus reduced concentration to normalize the effects of differing influent concentrations. Influent data are shown. Operating parameters are presented in Tables 7 (c) and 8 (c).

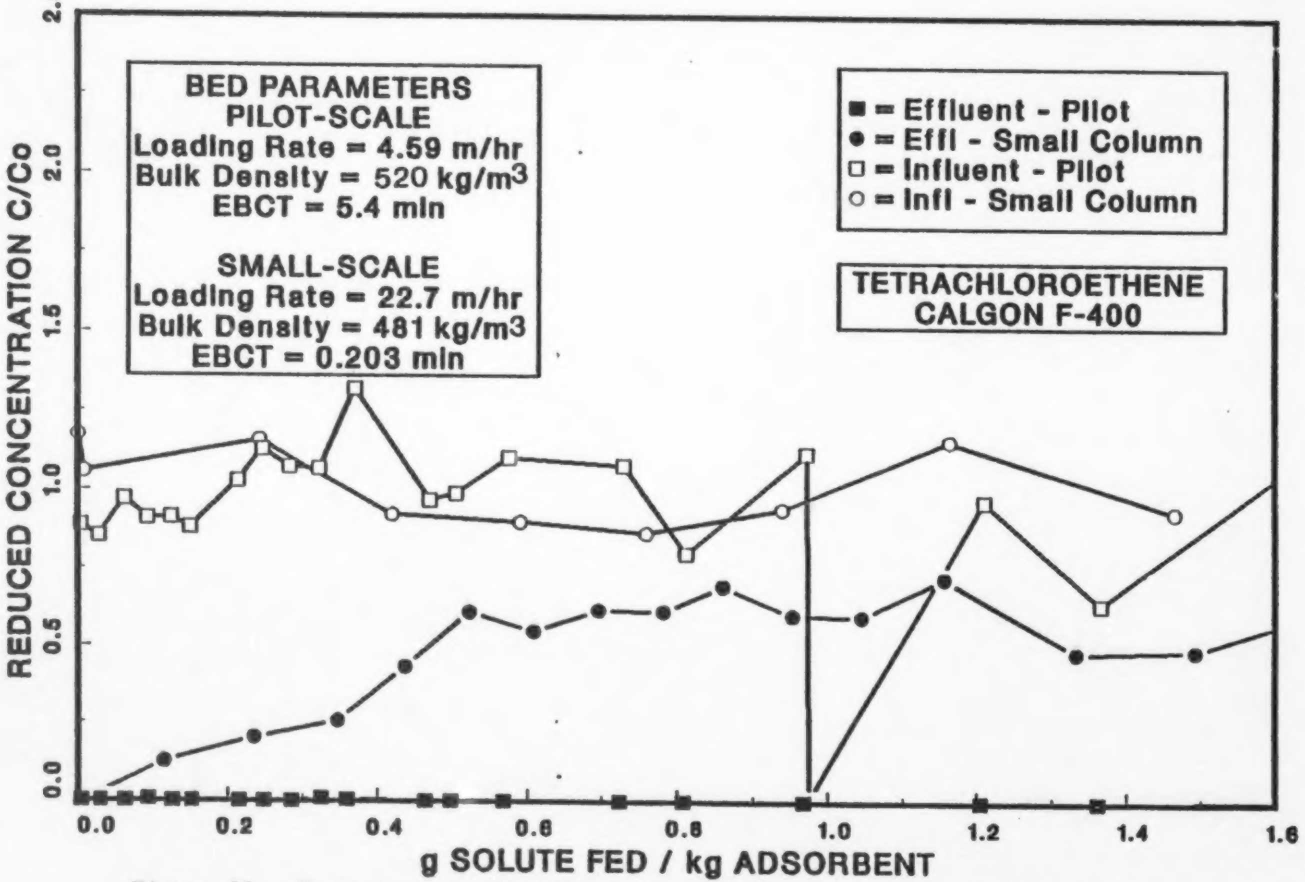

Figure 83. Comparison of the tetrachloroethene breakthrough profile for the small-column test to the pilot-scale column in the field study expressed as the grams of solute fed through the adsorber per kilogram carbon in the bed versus reduced concentration to normalize the effects of differing influent concentrations. Influent data are shown. Operating parameters are presented in Tables 7 (c) and 8 (c).

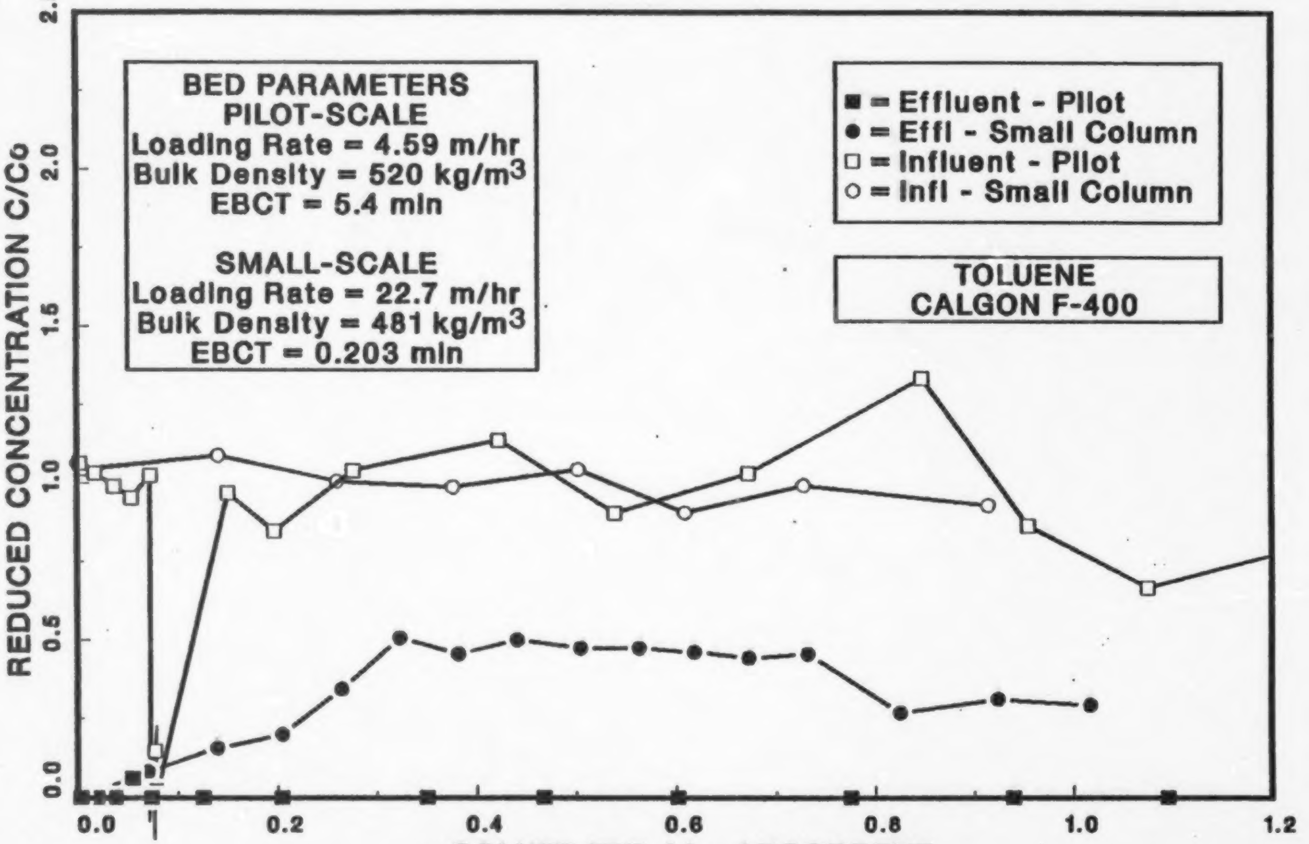

Figure 84. Comparison of the toluene breakthrough profile for the small-column test to the pilot-scale column in the field study expressed as the grams of solute fed through the adsorber per kilogram carbon in the bed versus reduced concentration to normalize the effects of differing influent concentrations. Influent data are shown. Operating parameters are presented in Tables 7 (c) and 8 (c).

VII. CONCLUSIONS

A. Rapid small-scale fixed bed adsorption tests (RSSCT) may predict full-scale adsorber performance in less time and at less expense than a pilot study by plotting the effluent concentration history in terms of the bed volumes fed. RSSCTs use a smaller size granular activated carbon (GAC) that is prepared from the full-scale GAC. Several RSSCTs may be used to rapidly evaluate several empty bed contact times of important process configurations such as beds-in-series or in-parallel. Like pilot studies, the RSSCT will match full-scale performance only if the granular activated carbon (GAC) used in the full-scale adsorber has the same equilibrium capacity, and bed void fraction as that used in the RSSCT. Also like pilot studies, the RSSCT can simulate the full-scale system only if the operating temperatures and the influent concentrations are the same.

B. Measurements made in this study demonstrated that the smaller GAC for RSSCTs can have the same equlibrium capacity, and bed void fraction as the original size carbon for pilot and full-scale adsorber.

C. Scaling equations were derived from dimensionless groups which appeared in the dispersed flow pore and surface diffusion model. The choice of a reduced size carbon determines the the proper hydraulic loading rate and empty bed contact time for the RSSCT. Perfect similarity between RSSCT and full-scale adsorber may be achieved if the ratio of the surface diffusivity for a representative influent solute on the RSSCT GAC is the same as that on the full-scale GAC. The following equations developed in Section II.D.1 as Eqs. 22 and 25 are all that is needed for the design of an RSSCT if surface diffusivities are the same:

$$\frac{EBCT_{LC}}{EBCT_{SC}} = \left[\frac{R_{LC}}{R_{SC}}\right] = \frac{t_{LC}}{t_{SC}} \qquad (22)$$

$$\frac{V_{SC}}{V_{LC}} = \frac{R_{LC}}{R_{SC}} \tag{25}$$

D. Measurement of the trichloroethene diffusivities of the carbon in the pilot-scale and RSSCT studies at concentrations of 1322 and 1329 µg/L indicated that it was possible to design an RSSCT to perfectly simulate the performance of a larger adsorber. Accordingly a laboratory verification of the RSSCT was conducted and agreement between the laboratory pilot-scale adsorbers and the RSSCT breakthrough profiles was good. The RSSCT which was conducted with 60X80 mesh GAC was conducted in 4.2% of the time that the pilot-scale column was conducted.

E. Based upon the success of the work done in the laboratory at higher concentrations, the same scaling approach was applied to design RSSCTs to simulate the performance of pilot-scale adsorbers that were treating contaminated groundwater in Wausau, Wisconsin. However, the field study results show that the RSSCTs which were designed under the assumptions of the laboratory study did not simulate the performance of pilot-scale adsorbers. The probable cause of the earlier RSSCT breakthrough was a difference in the surface diffusivities between the full-size carbon in the pilot-scale adsorbers and the smaller carbon in the RSSCTs. For the field study, the apparent surface diffusivity was much smaller for the smaller RSSCT carbon.

F. If the surface diffusivities of a solute on the RSSCT carbon cannot be expected to be the same, other scaling procedures cannot guarantee perfect similarity. These scaling procedures assume that surface diffusion is the controlling mechanism, because the effects of other mechanisms may be calculated without the need of experimental work.

One alternative approach to RSSCT design that is developed in Section II.D.2 assumes a surface diffusivity that is linearly proportional to the particle radius and is discussed in Section II.D.2. This scaling method was evaluated in the field study as an alternative and was found to be successful. However, to ensure that the proper scaling relationships are used in RSSCT design, the surface diffusivities of a representative solute in the influent mixture must be measured for both RSSCT and full-scale carbons.

G. The following general equations that were developed in this thesis as Eqs. 30 and 31 in Section II.D., are recommended to specify the operating characteristics of a small-column test to simulate a large-scale adsorber:

$$\frac{V_{SC}}{V_{LC}} = \frac{R_{LC}}{R_{SC}} \cdot \frac{Re_{SC,min}}{Re_{LC}} \qquad (30)$$

$$\frac{EBCT_{LC}}{EBCT_{SC}} = \left[\frac{R_{LC}}{R_{SC}}\right]^2 \cdot \frac{D_{s,SC}}{D_{s,LC}} = \frac{t_{LC}}{t_{SC}} \qquad (31)$$

These equations assume that only intraparticle processes determine the shape of the breakthrough profiles. To properly use Eq. 31, the surface diffusivities of a test compound must be measured or estimated to determine the proper ratio of surface diffusivities between the two sized carbons. Equation 30 can aid in determining the lowest required loading rate to minimize the headloss and is recommended for RSSCT design. Equation 30 will ensure that the dispersive effects in the RSSCT are caused by the same mechanical dispersion mechanism as in the full-scale system. To obtain the value of the minimum Reynolds number, the Schmidt number must be estimated using the known liquid diffusivity of a influent component, it may be estimated using parameter correlations that are described in Section IV.A., or it may be roughly estimated using typical liquid diffusivities from typical values.

H. To evaluate RSSCT data, it is sufficient to plot the effluent concentration versus the number of bed volumes fed, provided that the influent concentrations for the RSSCT are expected to be the same as those for the full-scale adsorber. Expressing the breakthrough profiles in terms of the mass of solute fed to the adsorber divided by the total mass of carbon in the bed versus the reduced concentration adjusts the breakthrough profile horizontally to account for influent concentration differences.

VIII. RECOMENDATIONS FOR FUTURE WORK

A. Further study of the effect of concentration on the relationship between the surface diffusivity and adsorbent particle radius is recommended so that determination of the proper scaling equations need not include rate studies to determine this relationship for every application.

B. Because the RSSCT data is quickly generated, use of RSSCT tests may be used in fine tuning mathematical models for performance predictions. This should be evaluated using the field study RSSCT data to predict pilot study performance.

C. Fluctuation and decline of the groundwater contaminant concentration made the field study difficult to interpret. A laboratory evaluation of the scaling equations should be conducted for low concentrations.

APPENDIX I. CITED REFERENCES

Beaudet B.A., *et al.* "Removal of Specific Organics from Wastewater by Activated Carbon Adsorption, Evaluation of a Rapid Method for Determining Carbon Usage Rates," Presented at the Industrial Waste Conference, Purdue University, 1980.

Beckner, H.A., *Dimensionless Parameters Theory and Methodology*, John Wiley & Sons, New York, 1976.

Bilello L.J., Beaudet B.A., "Evaluation of Activated Carbon by the Dynamic Minicolumn Adsorption Technique," *Treatment of Water by Activated Carbon*, Irwin R. Suffet, M.J. McGuire, American Chemical Society, 1983.

Crittenden, J.C., "Mathematical Modeling of Adsorber Dynamics - Single Components and Multicomponents," thesis presented in partial fulfillment of the requirements for the degree of Doctor of Philosophy, University of Michigan, Ann Arbor, (1976).

Crittenden, J.C. and W.J. Weber, Jr., "A Predicitve Model for Design of Fixed-Bed Adsorbers: Model Development and Parameter Estimation," *J. Env. Eng. Div.*, Proceedings of ASCE, *104* (EE2), 185 (1978).

Crittenden, J.C. and W.J. Weber, Jr., "A Predicitve Model for Design of Fixed-Bed Adsorbers: Multicomponent Model Verification " *J. Env. Eng. Div.*, Proceedings of ASCE, *104* (EE6), 1175 (1978).

Crittenden, J.C. and W.J. Weber, Jr., "A Predicitve Model for Design of Fixed-Bed Adsorbers: Single Component Model Verification " *J. Env. Eng. Div.*, Proceedings of ASCE, *104* (EE3), 433 (1978).

Crittenden, J.C., Bryant W.C. Wong, W. E. Thacker, V.L. Snoeyink and R.L. Hinrichs, "Mathematical Modeling of Sequential Loading of Two Solutes in Fixed-Bed Adsorbers," *J. Water Poll. Cont. Fed.* (11), 2780 (1980).

Crittenden, J.C. and D.W. Hand, "Design Considerations for the Removal of Synthetic Organic Chemicals and THM Precursors Using Granular Activated Carbon," Proceedings of Seminar Strategies for Controlling Trihalomethanes, American Water Works Association, 1983.

Crittenden, J.C., P.J. Luft, D.W. Hand, J. L. Oravitz, S.W. Loper, and M. Ari, "Prediction of Multicomponent Adsorption Equilibria Using Ideal Adsorbed Solution Theory," *Environmental Science and Technology*, In press, (1985).

Crittenden, J.C., N.J. Hutzler, J.L. Oravitz, and G. Friedman, "Transport of Organic Compounds with Saturated Groundwater Flow: Model Development and Parameter Sensitivity," *Water Resources Research*, in press, 1985.

Danckwerts, P.V., "Continuous Flow Systems," *Chemical Engineering Science*, 2:1-13, 1953.

Dobbs, R.A., and J.M. Cohen, "Carbon Adsorption Isotherms for Toxic Organics," EPA-600/880-023, U.S. Environmental Protection Agency, Office of Research and Development, MERL, Wastewater Treatment Division, Cincinnati, Ohio, Apr. 1980.

Dobrzelewski, M., and J.C. Crittenden, Personal Communication, Department of Civil Engineering, Michigan Technological University, Houghton, Michigan, 1984.

Ebach, E.A., and R.R. White, "Mixing of Fluids Flowing Through Beds of Packed Solids," AIChE Journal, 4(2):161-169, (1958).

Environmental Protection Agency, "The Analysis of Trihalomethanes in Finished Water by the Purge and Trap Method," US EPA, Environmental Monitoring and Support Laboratory, Cincinnati, Ohio, 1979.

Ergun, Chem. Eng. Progress, 48:89, 1952.

Fleck, R.D. Jr., D.J. Kirwan, and K.R. Hall, "Mixed-Resistance Diffusion Kinetics in Fixed-Beds Under Constant Pattern Conditions," Industrial and Engineering Chemistry Journal, Vol. 12, 1973.

Frick, B.R., "Theoretische Betrachtungen zu den Problemen des Scale-up von Aktivkohlefest belt adsorbern," Report, Univ. of Karlsruhe, Federal Republic of Germany, 1982.

Fried, J.J., Groundwater Pollution, Elsevier Scientific, Amsterdam, 1975.

Friedman, G., "Mathematical Modeling of Multicomponent Adsorption in Batch and Fixed-Bed Reactors," thesis presented in partial fulfillment of Master of Science degree in Chemical Engineering, Michigan Technological University, Houghton, Michigan, University Microfilms, Ann Arbor, 1984.

Gukhman, A.A., Introduction to the Theory of Similarity, Academic Press, New York, 1965.

Greenkorn, R.A., Flow Phenomena in Porous Media, Marcel Dekker, New York, 1983.

Hand, D.W., J.C. Crittenden, and W.E. Thacker, "Simplified Models for Design of Fixed-Bed Adsorbers," J. Env. Eng. Div., proceedings of ASCE, 110(EE2) 1984.

Hayduk, W. and H. Laudie, "Prediction of Diffusion Coefficients For Nonelectrolytes in Aqueous Solutions," AIChE J., 28, 611, (1974).

Kato, S., and J.C. Crittenden, Personal Communication, Department of Civil Engineering, Michigan Technological University, Houghton, Michigan, 1985.

Langhaar, H.L., "Dimensional Analysis and Theory of Models," Wiley, New York, 1951.

Lee, M.C., V.L. Snoeyink, and J.C. Crittenden, "Activated Carbon Adsorption of Humic Substances," J. AWWA, 73, 8:440 (1981)

Luft, P.J., "Modeling of Multicomponent Adsorption onto Granular Carbon in Mixtures of Known and Unknown Composition," Submitted in partial fulfillment of a Master of Science degree in Chemical Engineering, Michigan Technological University, Houghton, Michigan, University Microfilms, Ann Arbor, 1984.

Mieure, J.P., "A Rapid and Sensitive Method for Determining Volatile Organohalides in Drinking Water," *J. AWWA*, *69*(1):60-62 (1977).

Miyauchi, T., and T. Kikuchi, "Axial Dispersion in Packed Beds," *Chemical Engineering Science*, 30:343-348, 1975.

Ogata, A., "Theory of Dispersion in a Granular Medium," Geological Survey Professional Paper 411-I, U.S. Geological Survey, Washington, D.C., 1970.

Oravitz, J.L., "Transport of Trace Organics with One-Dimensional Saturated Flow: Mathematical Modeling and Parameter Sensitivity Analysis," thesis presented in partial fulfillment of the Master of Science degree in Civil Engineering, Michigan Technological University, Houghton, Michigan, University Microfilms, Ann Arbor, 1984.

Radke, C.J. and Prausnitz, "Thermodynamics of Multisolute Adsorption from Solute Liquid Solutions," *AIChE J.*, 18, 761 (1972).

Rosene, M.R., "Controlling Mechanisms for Granular Activated-Carbon Adsorption Columns in the Liquid Phase," *Treatment of Water by Activated Carbon*, Irwin R. Suffet, M.J. McGuire, American Chemical Society, 1983.

Rosene, M.R. *et al.*, "High Pressure Technique for Rapid Screening of Rapid Screening of Activated Carbons for use in Potable Water," *Activated Carbon Adsorption - Volume I*, Irwin R. Suffet, M.J. McGuire, American Chemical Society, 1983.

Schneider, R., "Bestimung der effektiven Korndiffusionskoeffizienten D_s nach dem Overflachendiffusionsmodell fur Korn-und Pulver kohlen unterschiedlicher Partikelgrobe," MS thesis, Univ. of Karlsruhe, Federal Republic of Germany, 1982.

Sherwood, T., R. Pigford, and C. Wilke, *Mass Transfer*, McGraw Hill Book Co. Inc., New York, (1975).

Taylor, E.S., *Dimensional Analysis for Engineers*, Oxford University Press, New York, 1974.

Thacker, W.E., V.L. Snoeyink and J.C. Crittenden, "Desorption of Compounds During Operation of GAC Adsorption Systems," *AWWA Journal*, *75* (3), 144 (1983).

Thacker, W.E., J.C. Crittenden and V.L. Snoeyink, "Modeling of Fixed-bed Adsorber Performance: Variable Influent Concentration and Comparison of Adsorbents," *J WPCF*, 56, 243 (1984).

Treybal, Mass Transfer Operations, McGraw-Hill, New York.

Williamson, J.E., K.E. Bazaire, and C.J. Geankoplis, "Liquid-Phase Mass Transfer at Low Reynolds Numbers," Ind. Chem. Fund., 2, 126 (1963).

Wilson, E.J. and C.J. Geankoplis, "Liquid Mass Transfer at Very Low Reynolds Numbers in Packed Beds," I & E C Fundamentals, 5(1):9-14, 1966.

APPENDIX II. NOMENCLATURE

Roman Letters

$Bi_{s,i}$	Biot number based on surface diffusivity (dimensionless); $Rk_{f,i}(1-\varepsilon)/(D_{s,i}\ Dg_{s,i}\ \varepsilon)$
BVF	bed volumes of feed (dimensionless)
BVF_{max}	maximum number of bed volumes that can be treated (dimensionless)
$\overline{C}_i(\overline{z},T)$	reduced adsorbate concentration in bulk phase as a function of dimensionless axial position and dimensionless time (dimensionless); $C_i(z,t)/C_{o,i}$
$C_{o,i}$	initial bulk phase concentration (M/L^3)
$\overline{C}_{p,i}(\overline{r},\overline{z},T)$	reduced adsorbate concentration in adsorbent pores as a function of dimensionless radial and axial position and dimensionless time (dimensionless); $C_{p,i}(r,z,t)/C_{o,i}$
CSA	cross sectional area of adsorber
De_i	axial dispersivity based on adsorber length and interstitial velocity (L^2/t)
Dg_i	combined solute distribution parameter (dimensionless); $(Dg_{s,i} + Dg_{p,i})$
$Dg_{p,i}$	pore solute distribution parameter (dimensionless); $\varepsilon_p(1-\varepsilon)/\varepsilon$
$Dg_{s,i}$	surface solute distribution parameter (dimensionless); $\rho_a q_{e,i}(1-\varepsilon)/\varepsilon C_{o,i}$
Dg_t	total solute distribution parameter (dimensionless); $(Dg_{p,i} + Dg_{s,i})$ over all all components
D_i	ratio of surface to pore diffusion transport (dimensionless); $(Ed_{s,i}Dg_{p,i})/(Ed_{p,i}Dg_{s,i})$
D_L	free liquid diffusivity (L^2/t)
$D_{p,i}$	pore diffusivity based on pore void fraction (L^2/t)
$D_{s,i}$	surface diffusivity (L^2/t)
Dia	column diameter (L)
EBCT	$\tau\varepsilon$, V_B/Q or L/V_s, fluid residence time in the bed which is devoid of the adsorbent or empty bed contact time (t)
$EBCT_{min}$	minimum empty bed contact time required for constant pattern (t)

$EBCT_{mtz}$	empty bed contact time of the mass transfer zone (t)
$Ed_{p,i}$	pore diffusion modulus (dimensionless); $D_{p,i}Dg_{p,i}\tau/R^3$
$Ed_{s,i}$	surface diffusion modulus (dimensionless); $D_{s,i}Dg_{s,i}\tau/R^3$
i	subscript denoting a solute i
K_i	Freundlich isotherm capacity constant (M/M)$(L^3/M)^{1/n}$
$k_{f,i}$	film transfer coefficient (L/t)
$1/n_i$	Freundlich isotherm intensity constant (dimensionless)
L	length of fixed-bed (L)
L_{min}	minimum adsorber length to establish a constant pattern (L)
L_{mtz}	length of the mass transfer zone (L)
LC	subscript denoting large scale adsorber
Pe_i	Peclet number based on interstitial velocity and adsorber length (dimensionless); Lv/De_i
$Pe_{i,D}$	$2vR/D_e$, Peclet number based on particle diameter (dimensionless)
$Pe_{i,mtz}$	$vL_{mtz}/D_e\mu$ Peclet number based on length of the mass transfer zone (dimensionless)
$q_{e,i}$	adsorbent phase concentration in equilibrium with initial bulk phase concentration (M/M); $K_iC_{o,i}^{1/n_i}$
$\overline{q_i}(\overline{r},\overline{z},T)$	reduced adsorbent phase concentration as a function of dimensionless radial and axial position and dimensionless time (dimensionless); $q_i(r,z,t)/q_{e,i}$
Q	fluid flow rate (L^3/t)
r	radial coordinate (L)
$\overline{r}$	reduced radial coordinate (dimensionless); r/R
R	adsorbent radius (L)
Re	Reynolds number (dimensionless)
Sc	Schmidt number (dimensionless)
SC	subscript denoting small adsorber
Sh_i	$k_{fi}2R/D_L$, Sherwood number, (dimensionless)

St_i	modified Stanton number (dimensionless); $k_{f,i}\tau(1-\varepsilon)/R\varepsilon$
$St_{i,min}$	minimum Stanton number required to establish constant pattern (dimensionless)
t	elapsed time (t)
$t_{i,min}$	elapsed time corresponding to the minimum EBCT required to establish constant pattern conditions (t)
$\bar{T}$	reduced time (mass Throughput) (dimensionless); $t/\tau(Dg_t + 1)$ (used in fixed-bed models)
v	interstitial velocity (L/t); v_s/ε
v_s	superficial velocity (L/t)
V_b	molal volume at the normal boiling point (L^3/M)
V_B	volume of the bed (L^3)
V_p	pore volume per mass of adsorbent (L^3/M)
$Y_{e,i}$	total adsorbent phase concentration in equilibrium with initial bulk phase concentration (M/M)
$Y_i(r,t)$	total adsorbent phase concentration as a function of radial position and time (M/M); $q_i(r,t) + [\varepsilon_p C_{p,i}(r,t)/\rho_a]$
$Y_i(r,z,t)$	total adsorbent phase concentration as a function of radial and axial position and time (M/M); $q_i(r,z,t) + [\varepsilon_p C_{p,i}(r,z,t)/\rho_a]$
$\bar{Y}_i(\bar{r},\bar{z},T)$	reduced total adsorbent phase concentration as a function of dimensionless radial and axial position and dimensionless time (dimensionless); $Y_i(r,z,t)/Y_{e,i}$
z	axial coordinate (L)
$\bar{z}$	reduced axial coordinate (dimensionless); z/L

Greek Letters

ε	fraction of volumetric space in reactor unoccupied by adsorbent, or void fraction (dimensionless)
ε_p	fraction of volumetric space in adsorbent phase unoccupied by adsorbent (dimensionless)
ρ_a	adsorbent density which includes pore volume (M/L^3)
ρ_b	adsorbent bulk density (M/L^3)

ρ_L	density of water (M/L³)
τ	fluid residence time in packed bed, or packed bed contact time (t)
τ_p	tortuosity of adsorbent (dimensionless)
μ	viscosity of water (M/Lt)

Acronyms

DCE	cis-dichloroethene
DFPSDM	dispersed-flow pore- surface- diffusion model
GAC	granular activated carbon
LC	large scale
PCE	tetrachloroethene
PFHSDM	plug flow homogeneous solid diffusion model
RSSCT	rapid small scale adsorber test
SC	small scale
TCE	trichloroethene

APPENDIX III. Development of Scaling Equations From the DFPSDM.

The PSDM equations in dimensionless form are used here in the development of scaling equations for the design of fixed-bed adsorption tests. The PSDM equations incorporate the following mechanisms: (a) advective flow, (b) axial dispersion and diffusion, (c) liquid-phase mass transfer resistance, (d) local adsorption equilibrium at the exterior surface of the adsorbent, (e) the surface diffusion flux represented by a surface diffusivity, (g) the pore diffusion flux represented by a pore diffusivity, and (h) competition of solutes upon the carbon surface.

To obtain a solution to the dispersed flow, Pore Surface Diffusion Model, the following set of equations are necessary:

The liquid phase mass balance:

$$- \frac{\partial \bar{C}_i(\bar{z},T)}{\partial z} + \frac{1}{Pe_i} \frac{\partial^2 \bar{C}_i(\bar{z},T)}{\partial z^2} = \frac{1}{Dg_t + 1} \frac{\partial \bar{C}_i(\bar{z},T)}{\partial T} \qquad (3\text{-}1)$$

$$+ \; 3 \, St_i \left[\bar{C}_i(\bar{z},T) - \bar{C}_{p,i}(\bar{r}=1,\bar{z},T) \right]$$

The liquid phase initial and boundary conditions:

$$\bar{C}_i \; (0 \leq \bar{z} \leq 1 \; , \; T = 0) \; = \; 0 \qquad (3\text{-}2)$$

$$\frac{\partial^2 \bar{C}_i(\bar{z}=1,T)}{\partial z \partial T} = 0 \quad \text{and} \quad \frac{\partial \bar{C}_i(\bar{z},T=0)}{\partial z} = 0 \qquad (3\text{-}3)$$

$$1 - \bar{C}_i(\bar{z}=1,T) = \frac{1}{(Dg_t + 1)} \frac{\partial}{\partial T}\left[\int_o^1 \left[\bar{C}_i(\bar{z},T) + 3\, Dg_i \int_o^1 \bar{Y}_i(\bar{r},\bar{z},T)\, \bar{r}^2 d\bar{r}\right] \partial\bar{z}\right] \qquad (3\text{-}4)$$

The intraparticle phase mass balance:

$$\frac{1}{\bar{r}^2} \frac{\partial}{\partial \bar{r}}\left[\bar{r}^2\left[(Ed_{s,i} + D_i\, Ed_{p,i}) \frac{\partial \bar{Y}_i(\bar{r},\bar{z},T)}{\partial \bar{r}} + (Ed_{p,i} - D_i\, Ed_{p,i}) \frac{\partial \bar{C}_{p,i}(\bar{r},\bar{z},T)}{\partial \bar{r}}\right]\right] = \frac{Dg_i}{Dg_t + 1} \frac{\partial \bar{Y}_i(\bar{r},\bar{z},T)}{\partial T} \qquad (3\text{-}5)$$

The intraparticle phase initial and boundary conditions:

$$\bar{Y}_i(0 \leq \bar{r} \leq 1\,, 0 \leq \bar{z} \leq 1\,,\ T = 0) = 0 \qquad (3\text{-}6)$$

$$\frac{\partial}{\partial \bar{r}} \bar{Y}_i(\bar{r} = 0, 0 \leq \bar{z} \leq 1\,,\ T \geq 0) = 0 \qquad (3\text{-}7)$$

$$\frac{Dg_i}{Dg_t + 1} \frac{\partial}{\partial t} \int_o^1 \bar{Y}_i(\bar{r},\bar{z},T)\, \bar{r}^2 d\bar{r} = St_i\left[\bar{C}_i(\bar{z},T) - \bar{C}_{p,i}(\bar{r}=1,\bar{z},T)\right] \qquad (3\text{-}8)$$

The nonlinear coupling equation:

$$\bar{C}_{p,i}(\bar{r},\bar{z},T) = \frac{\bar{Y}_i(\bar{r},\bar{z},T)Y_{e,i} - \frac{\varepsilon_p}{\rho_a}\bar{C}_{p,i}(\bar{r},\bar{z},T)C_{o,i}}{C_{o,i}\sum_{j=1}^{m}\left[\bar{Y}_j(\bar{r},\bar{z},T)Y_{e,j} - \frac{\varepsilon_p}{\rho_a}\bar{C}_{p,j}(\bar{r},\bar{z},T)C_{o,j}\right]} \cdot \left[\frac{\sum_{k=1}^{m}\left[n_k[\bar{Y}_k(\bar{r},\bar{z},T)Y_{e,k} - \frac{\varepsilon_p}{\rho_a}\bar{C}_{p,j}(\bar{r},\bar{z},T)C_{o,i}]\right]}{n_i K_i}\right]^{n_i} \tag{3-9}$$

The mass balances in dimensionless form are a function of a number of process parameters, such as the adsorbent radius, adsorbent density, etc. In dimensionless form, these parameters become combined to form a set dimensionless groups. The solutions to the equations are now characterized by fewer variables.

The following groups appear in Eqs. 1-9:

$$Dg_{s,i} = \frac{\rho_a q_{e,i}(1-\varepsilon)}{\varepsilon C_{o,i}} \tag{3-10}$$

$$Dg_{p,i} = \frac{\varepsilon_p(1-\varepsilon)}{\varepsilon} \tag{3-11}$$

$$Dg_i = Dg_{s,i} + Dg_{p,i} \tag{3-12}$$

$$Dg_t = \sum_i (Dg_{s,i} + Dg_{p,i}) \qquad (i = 1, \text{no. components}) \tag{3-13}$$

$$D_i = \frac{D_{s,i}}{D_{p,i}} \tag{3-14}$$

$$St_i = \frac{k_{f,i}L(1-\varepsilon)}{vR\varepsilon} = \frac{k_{f,i}\tau(1-\varepsilon)}{R\varepsilon} \qquad (3\text{-}15)$$

$$Ed_{s,i} = \frac{LD_{s,i}Dg_{s,i}}{vR^2} = \frac{\tau D_{s,i}Dg_{s,i}}{R^2} \qquad (3\text{-}16)$$

$$Ed_{p,i} = \frac{LD_{p,i}Dg_{p,i}}{vR^2} = \frac{\tau D_{p,i}Dg_{p,i}}{R^2} \qquad (3\text{-}17)$$

$$Pe_i = \frac{Lv}{D_{e,i}} \qquad (3\text{-}18)$$

The dimensionless quantities above characterize a solution to the fixed-bed PSDM. A small-column test would yield the same solution as a full-scale system if the values of dimensionless groups associated with the small-column test equal the values of the corresponding dimensionless groups for a full-scale adsorber. In this manner, we can simulate the performance of a full-scale adsorber with a small-column test if the small-column design and operating parameters can be chosen so that the corresponding dimensionless groups of both adsorbers are equal. By setting the mathematical expressions for the characteristic dimensionless groups of a large column adsorber (LC) equal to the mathematical expressions for the corresponding dimensionless groups of a small-column test (SC), we may identify necessary relationships among process variables in scaling to a small-scale study. The result here is expressed as ratios of measurable and controllable design parameters.

Six of the nine dimensionless quantities (Eqs. 10 - 18) may be considered to be independent quantities. Dg_i, Dg_t, and D_i are combinations of the pore and surface solute distribution parameters, $Dg_{p,i}$ and $Dg_{s,i}$. The independent dimensionless groups treated are as follows:

$Dg_{s,i}$ $\qquad$ $Dg_{p,i}$

$Ed_{s,i}$ $\qquad$ $Ed_{p,i}$

St_i $\qquad$ Pe_i

These six dimensionless parameters are treated individually in the following discussion to develop the scaling equations and to address the assumptions and simplifications of the method.

Surface Solute Distribution Parameter ($Dg_{s,i}$) - The surface solute distribution parameter based on single solute capacity is the ratio of the mass of adsorbate i in the solid phase to the mass of i in the liquid phase under equilibrium conditions. As $Dg_{s,i}$ increases, the adsorbate's affinity for the adsorbent phase increases. Conversely, as $Dg_{s,i}$ decreases, the adsorbate's affinity increases for the liquid phase. For a perfect experimental simulation, $Dg_{s,i}$ for the large column must be equal to $Dg_{s,i}$ for the small column:

$$Dg_{s,i,LC} = Dg_{s,i,SC} \tag{3-19}$$

Where LC denotes the larger adsorption column and SC denotes the small-column test. Substituting the mathematical expression for $Dg_{s,i}$ Eq. 19 becomes:

$$\frac{\rho_{a,LC}\, q_{e,i,LC}(1-\varepsilon_{LC})}{\varepsilon_{LC}\, C_{o,i,LC}} = \frac{\rho_{a,SC}\, q_{e,i,SC}(1-\varepsilon_{SC})}{\varepsilon_{SC}\, C_{o,i,SC}} \tag{3-20}$$

Here it is assumed that the carbon in the small-column test exhibits some of the same properties as the carbon in the large-scale adsorber. If the carbon particles used in both columns are of similar shape and density so that:

$$\varepsilon_{LC} = \varepsilon_{SC} \tag{3-21}$$

and

$$\rho_{a,LC} = \rho_{a,SC} \tag{3-22}$$

Then Eqs. 21 and 22 may be substituted into Eq. 20. The result becomes:

$$\frac{q_{e,i,LC}}{C_{o,i,LC}} = \frac{q_{e,i,SC}}{C_{o,i,SC}} \qquad (3\text{-}23)$$

Normally, the adsorbent-phase concentration is expressed as a function of the liquid-phase concentration. To satisfy Equation 23 the same influent concentrations anticipated or observed in a full-scale system must be used in the small-column test and that the carbon in both adsorbers must have the same equilibrium capacity. It may be assumed that careful preparation of the carbon sample in the small-column test.

Pore Solute Distribution Parameter ($Dg_{p,i}$) - The pore solute distribution parameter is the mass of adsorbate i in the adsorbent pores divided by the mass of adsorbate i in the liquid phase under equilibrium conditions. $Dg_{p,i}$ will be the same for all solutes in any given system since it is only a function of the bed void fraction and the adsorbent void fraction. In the same manner, $Dg_{p,i}$ of the large-column adsorber may be equated to $Dg_{p,i}$ of the small-column test:

$$Dg_{p,i,LC} = Dg_{p,i,SC} \qquad (3\text{-}24)$$

Substituting the mathematical expression of $Dg_{p,i}$ into Eq. 24:

$$\frac{\varepsilon_{p,LC}(1-\varepsilon_{LC})}{\varepsilon_{LC}} = \frac{\varepsilon_{p,SC}(1-\varepsilon_{SC})}{\varepsilon_{SC}} \qquad (3\text{-}25)$$

Equation 25 may be simplified assuming the void fraction of the large-column is the same as that of the small-column (Eq. 21):

$$\varepsilon_{p,LC} = \varepsilon_{p,SC} \qquad (3\text{-}26)$$

Equation 26 states that perfect similarity will not be achieved unless the void fraction of the adsorbent particle, ε_p in the small-column test is the same as that of the large-column.

Surface Diffusion Modulus ($Ed_{s,i}$) - $Ed_{s,i}$ is the ratio of mass transport rates of intraparticle surface diffusion to the rate of mass transport by advection. Equating the mathematical expressions of $Ed_{s,i}$ for large and small columns:

$$\frac{\tau_{LC} D_{s,i,LC} Dg_{s,i,LC}}{R_{LC}^2} = \frac{\tau_{SC} D_{s,i,SC} Dg_{s,i,SC}}{R_{SC}^2} \qquad (3\text{-}27)$$

Using the assumptions corresponding to Eq. 19 we may eliminate $Dg_{s,i}$ from Eq. 27:

$$\frac{\tau_{LC} D_{s,i,LC}}{R_{LC}^2} = \frac{\tau_{SC} D_{s,i,SC}}{R_{SC}^2} \qquad (3\text{-}28)$$

The surface diffusion coefficient, $D_{s,i}$, is a physical/chemical parameter characteristic of the adsorbent. Because the relationship of D_s with other physical parameters is not fully understood, we assume $D_{s,i}$ can be measured, calculated, or estimated for a compound in the water matrix for large- and small-scale adsorber. Equation 28 becomes:

$$\frac{\tau_{LC}}{\tau_{SC}} = \left[\frac{R_{LC}}{R_{SC}}\right]^2 \cdot \left[\frac{D_{s,LC}}{D_{s,SC}}\right] \qquad (3\text{-}29)$$

Noting that τ = EBCTs we may rewrite Eq. 29 as follows:

$$\frac{EBCT_{LC}}{EBCT_{SC}} = \left[\frac{R_{LC}}{R_{SC}}\right]^2 \cdot \left[\frac{D_{s,LC}}{D_{s,SC}}\right] \qquad (3\text{-}30)$$

Equation 30 is the first scaling equation because the remaining variables in this development are deliberately chosen operating parameters. By satisfying Eq. 30 and the assumptions already stated, $Ed_{s,i}$ will remain constant in scaling down to a small-column test. In other words, the ratio of the rates of mass transfer due to advection and intraparticle diffusion will remain constant in reducing the size of a desired fixed-bed adsorption system to a small-column test. To arrive at Equation 30 it must be assumed that the physical/chemical properties of the adsorbents in both columns are the same. Thus, the particle size of the adsorbent is the only property of the adsorbent that may change when scaling down to a small column test and maintain a proper experimental simulation. The packed bed contact time of the small-scale test is reduced according to the reduction in the size of the adsorbent.

Pore Diffusion Modulus ($Ed_{p,i}$) – The pore diffusion modulus has the same significance as the surface diffusion modulus, $Ed_{s,i}$, except that it compares the transport rate by pore diffusion to the advective rate. Analogous to $Ed_{s,i}$, as $Ed_{p,i}$ increases, advective transport becomes controlling. Equating the mathematical expressions of $Ed_{p,i}$ for large and small columns:

$$\frac{\tau_{LC} D_{p,i,LC} Dg_{p,i,LC}}{R_{LC}^2} = \frac{\tau_{SC} D_{p,i,SC} Dg_{p,i,SC}}{R_{SC}^2} \qquad (3\text{-}31)$$

Similarly, the pore diffusion coefficient, $D_{p,i}$, is assumed to be the same for the adsorbents in both adsorbers. With the additional assumptions in equating $Dg_{p,i}$, Eq. 31 becomes:

$$\frac{EBCT_{LC}}{EBCT_{SC}} = \left[\frac{R_{LC}}{R_{SC}} \right]^2 \qquad (3\text{-}32)$$

The result is the same as that of Eq. 30 if D_s is constant.

Stanton Number (St_i) – St_i is the ratio of the rate of mass transfer by film transfer to the rate by advection. As St_i increases, the rate of transport by advection becomes controlling. As St_i decreases, film transfer controls. Equating the mathematical expressions of St_i for large and small columns:

$$\frac{k_{f,i,LC}\tau_{LC}(1-\varepsilon_{LC})}{R_{LC}\varepsilon_{LC}} = \frac{k_{f,i,SC}\tau_{SC}(1-\varepsilon_{SC})}{R_{SC}\varepsilon_{SC}} \qquad (3\text{-}33)$$

Noting that ε_{LC} has been assumed to be equal to ε_{SC}, Eq. 33 becomes:

$$\frac{k_{f,i,LC}\tau_{LC}}{R_{LC}} = \frac{k_{f,i,SC}\tau_{SC}}{R_{SC}} \qquad (3\text{-}34)$$

Substituting Eq. 29 for τ_{LC}, Eq. 33 becomes:

$$\frac{k_{f,i,LC}}{k_{f,i,SC}} = \frac{R_{SC}}{R_{LC}} \left[\frac{D_{s,LC}}{D_{s,SC}} \right] \qquad (3\text{-}35)$$

For low Reynolds numbers, as is common in fixed-bed adsorption, the correlations of Wilson (1966) and Williamson (1963) are quite accurate in predicting film transfer coefficients. They are, respectively:

$$k_{f,i} = \frac{2.4v_s}{Sc_i^{0.58}Re^{0.66}} \qquad (3\text{-}36)$$

$$k_{f,i} = \frac{1.09v_s}{\varepsilon(ReSc_i)^{2/3}} \qquad (3\text{-}37)$$

The Schmidt number, expressed mathematically by $\mu/\rho D_L$, will remain a constant if the density, viscosity, and liquid diffusivity remain constant. These parameters remain constant for the conditions of constant temperature and dilute solution. Assuming that the temperature remains constant and the solute concentration remains dilute, the Schmidt number will remain constant. Reynolds number is expressed by $2Rv_s\rho/\mu$. The liquid density, ρ, and the viscosity, μ, are assumed constant.

Substituting Eqs. 36 or 37 into Eq. 35 yields:

$$\frac{v_{s,LC}}{v_{s,SC}} = \frac{R_{SC}}{R_{LC}} \left[\frac{D_{s,LC}}{D_{s,SC}} \right]^3 \qquad (3\text{-}38)$$

Using Equation 38 the Stanton number will remain constant in scaling to a small column test. In keeping the Stanton number constant, the ratio of the mass transfer rates of advection and film transfer remains a constant. To arrive at Eq. 38 the bed void fraction is assumed to be constant. The correlations of Wilson or Williamson are assumed to accurately predict film transfer coefficients. The liquid density, viscosity, and liquid diffusivity are also assumed to be constant.

Because the value of the Reynolds number affects the values of both the Stanton and Peclet numbers, an additional restriction equating the Reynolds numbers of large and small columns may be applied to produce the following equation:

$$\frac{v_{s,LC}}{v_{s,SC}} = \frac{R_{SC}}{R_{LC}} \qquad (3\text{-}39)$$

Equations 38 and 39 may both be satisfied only when the surface diffusivity is not dependent upon the particle radius. It will be shown that equal Reynolds numbers will ensure equal Peclet numbers for fixed-bed adsorbers.

Peclet Number (Pe_i) - The Peclet number based on column length and interstitial velocity is a measure of the amount of dispersion in the bed. Dispersion is due to a number of phenomena including molecular diffusion, eddy diffusion, and hydrodynamic dispersion. These mechanisms are discussed by Ogata (1970), Fried (1975), and Greenkorn (1983).

Equating the mathematical expressions of Pe_i for large and small columns:

$$\frac{L_{LC}v_{LC}}{D_{e,i,LC}} = \frac{L_{SC}v_{SC}}{D_{e,i,SC}} \qquad (3\text{-}40)$$

Substituting $v_s\varepsilon$ for v, and v_sEBCT for L:

$$\frac{EBCT_{LC}v_{s,LC}^2}{D_{e,i,LC}\varepsilon_{LC}} = \frac{EBCT_{SC}v_{s,SC}^2}{D_{e,i,SC}\varepsilon_{SC}} \qquad (3\text{-}41)$$

Substituting Eq. 30 for $EBCT_{LC}$ and assuming ε to be a constant yields:

$$\frac{D_{e,i,SC}v_{s,LC}^2}{D_{e,i,LC}v_{s,SC}^2} = \frac{R_{SC}^2}{R_{LC}^2} \qquad (3\text{-}42)$$

Many of the literature correlations for the dispersion coefficient, $D_{e,i}$, (Ebach and White, 1958; Harleman, 1963; Ogata, 1970; Bear, 1972; Fried, 1975) describe the dispersion coefficient as a function of the liquid diffusivity, liquid density, viscosity, and product of the interstitial velocity and particle radius:

$$D_e = f(D_L, \mu, \rho, vR) \qquad (3\text{-}43)$$

The liquid diffusivity, density, and viscosity have previously been assumed to be constant. The interstitial velocity may be expressed as $v_s\varepsilon$. The product of the interstitial velocity and the particle radius may be assumed constant by Eq. 39. Because the bed void fraction is also assumed constant vR would then be constant and it may be assumed that $D_{e,i}$ is constant. Equation 42 then becomes:

$$\frac{v_{s,LC}^2}{v_{s,SC}^2} = \frac{R_{SC}^2}{R_{LC}^2} \qquad (3\text{-}44)$$

Taking the square root of both sides gives:

$$\frac{v_{s,LC}}{v_{s,SC}} = \frac{R_{SC}}{R_{LC}} \qquad (3\text{-}45)$$

Equation 45 is the same as Eq. 39. To arrive at Eq. 45, the correlations of the form of Ebach and White, Harleman, Ogata, Bear, or Fried are assumed to accurately predict film transfer coefficients. The liquid density, viscosity, liquid diffusivity, and bed void fraction are also assumed to be constant.

If the surface diffusivity is independent of the particle radius, then Eqs. 30 and 45 are all that is necessary to determine the parameters to simulate desired full-scale conditions with a small-column test. If D_s varies with R, Eq. 30 may be used to determine the proper EBCT's. The determination of the proper hydraulic loading rates is complicated by the contradicting Eqs. 38 and 45. Here it is necessary to use a small column loading rate that is small enough to reduce the treatment mixture volume as much as possible by minimizing the required hydraulic loading rate for the small column, and yet use a loading rate great enough to maintain similar dispersive mechanisms (Fried, 1975).

Appendix IV. Trichloroethene Isotherm Data for 60x80 F400 GAC at 13°C

Initial Concentration: 24.12 µmol/L
pH: 7.5
Bottle Volume: 160 mL
Date Isotherm Started: 3/25/85
Equilibration Time: 14 Days

Carbon Dosage mg	Equilibrium Liquid-Phase Conc. µmol/L	Solid-Phase Conc. µmol/g
1.28	1.933	274.658
1.61	4.612	361.682
3.25	9.917	477.780
4.24	10.610	510.165
4.28	10.389	513.125
8.63	21.250	699.176

Least Squares Analysis Results

```
SUM OF SQUARES FOR Ce=     .71032
SUM OF SQUARES FOR qe=     .13321
SUM OF qeCe          =     .29687

Ce BAR =     .84896
qe BAR =    2.62771

COVARIANCE                 =     .04241
CORRELATION COEFFICIENT =     .96510
STANDARD DEVIATION         =     .04274

CONFIDENCE LEVEL,ALPHA  = .025

LOWER CONFIDENCE LIMIT OF 1/n =     .28754
                          1/n =     .41793
UPPER CONFIDENCE LIMIT OF 1/n =     .54833

LOWER CONFIDENCE LIMIT OF K   = .1427792+003
                          K   = .1874559+003
UPPER CONFIDENCE LIMIT OF K   = .2461122+003
```

Appendix V. Laboratory Study Pilot-Scale Data

GAC Packing Characteristics

ρ_b	g/cm^3	0.478
ρ_a	g/cm^3	0.8034
ε		0.40
R	cm	0.0513

Flow Specifications

Column Diameter	cm	5.0
Column Length	cm	8.33
EBCT	s	60
CSA	cm^2	19.63
V_s	m/hr	5

Bed Volume	cm^3	163.6
Flow rate	cm^3/min	163.6

Influent Temperature	°C	11±1
pH		6.5±1.0

Appendix V. Laboratory Study Pilot-Scale Data (Continued)

Influent Data

Concentrations in µg/L

	1	2	3	4	5	6
Average	2609	3397	5367	5730	4366	2281

Time (hrs)	BVF	1	2	3	4	5	6
1.0	60	2209	2452	4139	4413	3261	1134
2.7	160	2449	2703	4703	5016	3490	1223
5.5	330	2477	2781	4897	5378	3873	1269
5.5	330	2721	3124	5381	5908	4060	1486
11.5	550	2323	2878	4648	5089	3639	1289
11.5	550	2525	3094	4937	5433	3654	1362
13.5	660	2061	2677	4108	4636	3242	1258
15.5	772	2398	3153	4867	5425	3911	1559
17.5	882	2607	3282	5030	5479	3882	1603
19.5	998	2537	3392	5316	5812	4242	1767
21.5	1122	2314	2987	4625	5147	3745	1554
23.7	1242	3645	4378	6602	7139	4914	2493
25.5	1344	3274	3960	5897	6275	4502	2383
27.5	1459	3171	3917	5785	6294	4319	2409
33.5	1812	2809	3632	5378	5950	4411	2068
35.5	1919	2733	3670	5552	6074	4573	2202
37.5	2027	2705	3617	5431	5948	4964	2114
39.5	2134	2884	3836	5900	6299	4625	2329
41.5	2239	2820	3773	5770	6295	4721	2406
43.5	2342	3500	4184	6641	7229	5286	2779
44.5	2392	3153	4156	6099	6653	4840	2610
45.5	2446	2874	3927	5994	6534	4973	2557
47.5	2499	2738	3508	5904	6090	4994	2734
48.8	2563	2549	3336	5693	5767	4794	2597
53.5	2632	2899	3734	6040	6532	4963	2762
57.5	2672	2662	3667	5518	5966	4563	2574
59.5	2872	3088	4220	6251	6725	4858	2761
63.5	3098	2519	3577	5255	5728	4451	2574
65.5	3213	2675	3766	5498	5889	4192	2601
67.5	3314	2288	2988	5133	5207	4228	2485
69.5	3445	2407	3203	5464	5600	4641	2737
71.8	3562	2445	3241	5445	5501	4770	2749
74.5	4080	2457	3260	5508	5548	4752	2731
80.0	4406	2399	3135	5357	5449	4440	2585
81.5	4495	2399	3162	5367	5398	4506	2695
85.3	4715	2384	3123	5326	5432	4400	2576
87.3	4825	2534	3647	5454	6244	4474	2740
91.0	5042	2613	3732	5293	6152	4466	2733

Where:

1 = Chloroform
2 = Trichloroethene
3 = Chlorodibromoethane
4 = 1,2 Dibromoethane
5 = Bromoform
6 = Tetrachloroethene

Appendix V. Laboratory Study Pilot-Scale Data (Continued)

Effluent Data

		Concentrations in µg/L					
Time (hrs)	BVF	1	2	3	4	5	6
1.0	60	0	0	0	0	0	0
2.5	150	0	0	39	18	22	0
11.5	550	409	0	141	119	52	49
13.5	660	531	0	168	139	173	37
15.5	772	598	0	177	141	181	25
17.5	882	804	3	248	206	183	41
19.5	998	910	6	297	251	215	31
21.5	1122	1072	18	346	295	177	17
23.7	1242	1662	578	784	753	248	357
25.5	1344	1794	548	805	400	246	345
27.5	1459	1546	100	578	511	282	36
30.0	1603	1772	67	588	524	211	22
33.5	1812	1975	138	803	707	261	25
35.5	1919	1879	111	774	671	343	36
37.5	2027	2283	150	921	840	342	24
39.5	2134	2284	151	973	867	293	17
41.5	2239	2096	138	946	840	359	18
43.5	2342	2677	192	1167	1068	405	22
44.5	2392	2960	171	1123	1018	674	132
45.5	2446	2530	172	1149	1026	347	18
47.5	2499	2449	189	1488	1100	240	31
48.7	2563	2307	176	1455	1101	335	26
53.5	2632	2801	263	1569	1424	564	20
57.5	2672	2984	366	1544	1756	692	27
59.5	2872	2732	296	2198	1741	433	28
63.5	3098	3190	495	2392	2258	810	37
65.5	3213	3166	488	2460	2313	875	30
67.5	3314	2802	422	2804	2342	767	28
69.5	3445	2737	445	2837	2418	691	32
71.8	3562	2739	469	2946	2469	909	37
74.5	4080	2786	485	3069	2593	879	34
80.0	4406	2768	594	3355	2955	1014	37
81.5	4495	2680	596	3366	2964	1398	43
83.5	4610	2747	644	3483	3095	1164	39
87.3	4825	3070	795	3379	3505	1232	42
89.0	4929	3098	889	3564	3759	1236	42
91.0	5042	3127	900	3706	3928	1369	44

Where:

1 = Chloroform
2 = Trichloroethene
3 = Chlorodibromoethane
4 = 1,2 Dibromoethane
5 = Bromoform
6 = Tetrachloroethene

Appendix VI. Laboratory Study Small-Column Data

GAC Packing Characteristics

ρ_b	g/cm^3	0.482
ρ_a	g/cm^3	0.8034
ε		0.40
R	cm	0.0105

Flow Specifications

Column Diameter	cm	1.10
Column Length	cm	1.71
EBCT	s	2.51
CSA	cm^2	0.950
V_s	m/hr	24.4

Bed Volume	cm^3	1.621
Flow rate	cm^3/min	38.7

Influent Temperature	°C	11 ± 1
pH		6.5 ± 1.0

Appendix VI. Laboratory Study Small-Column Data (Continued)

Influent Data

		Concentrations in µg/L					
		1	2	3	4	5	6
	Average	2670	3763	5293	5845	4731	3017

Time (hrs)	BVF	1	2	3	4	5	6
0.0	0	2741	3828	5322	5916	4761	2913
0.1	119	2792	3895	5426	6014	4877	3000
0.5	745	2736	3823	5330	5936	4807	2949
1.0	1542	2743	3810	5361	5925	4806	2916
1.5	2329	2700	3791	5306	5892	4790	2949
2.0	3100	2714	3677	5308	5857	4750	2846
2.5	3687	2739	3801	5350	5926	4780	2920
3.0	4669	2749	3853	5409	5994	4876	3002
4.0	6264	2722	3814	5348	5927	4824	2992
5.0	7793	2657	3759	5261	5866	4757	3017
6.0	9483	2671	3747	5277	5941	4761	2997
7.0	10883	2737	3861	5393	5990	4881	3075
8.0	12349	2722	3824	5642	5974	4876	3080
9.0	13968	2686	3767	5271	5866	4727	3017
10.0	15441	2681	3781	5276	5857	4767	3042
11.0	16883	2606	3697	5196	5794	4707	3028
12.0	18653	2637	3793	5245	5900	4742	3089
13.0	20193	2719	3822	5316	5945	4805	3118
14.0	21784	2701	3810	5319	5945	4810	3118
15.0	23334	2740	3861	5390	6009	4855	3110
16.0	24830	2808	3907	5510	6072	4871	3093
17.0	26539	2698	3791	5335	5913	4829	3103
18.0	27932	2665	3752	5241	5804	4716	3009
19.0	29871	2613	3686	5120	5670	4589	2980
20.0	31525	2565	3646	5005	5548	4441	2917
21.0	33784	2503	3600	4932	5510	4437	2915
22.0	35092	2525	3596	5767	5538	4491	2933
23.0	36389	2552	3636	5079	5641	4599	3010
24.0	37625	2614	3682	5105	5690	4576	3024

Where:

1 = Chloroform
2 = Trichloroethene
3 = Chlorodibromoethane
4 = 1,2 Dibromoethane
5 = Bromoform
6 = Tetrachloroethene

Appendix VI. Laboratory Study Small-Column Data (Continued)

Effluent Data

		Concentrations in µg/L					
Time (min)	BVF	1	2	3	4	5	6
0.2	237	227	0	119	74	56	0
0.3	473	500	69	272	215	151	0
0.5	745	835	124	423	344	234	14
0.7	1005	1030	167	537	436	297	17
0.8	1275	1309	204	689	565	368	32
1.0	1542	1463	213	730	596	381	34
1.2	1796	1653	235	840	685	425	38
1.3	2074	1892	318	1090	915	549	52
1.5	2329	2036	295	1083	894	521	51
1.7	2582	2389	506	1568	1366	795	140
1.8	2846	2539	506	1679	1448	812	106
2.0	3099	2484	520	1717	1558	851	85
2.3	3479	2711	601	1998	1840	967	90
2.5	3866	2795	658	2175	1997	1041	91
2.8	4276	2918	857	2652	2522	1304	114
3.0	4669	3062	900	2829	2719	1358	111
3.3	5219	3137	1014	3147	3058	1507	124
3.7	5709	3173	1215	3580	3560	1752	137
4.0	6264	3126	1490	4077	4152	2073	176
4.3	6770	3078	1643	4378	4491	2286	191
4.7	7286	3053	1750	4535	4722	2366	185
5.0	7793	3024	1833	4748	4979	2464	176
5.5	8608	3019	2090	5172	5524	2779	187
6.0	9483	3148	2421	5688	6108	3174	204
6.5	10138	2970	2581	5666	6166	3325	224
7.0	10883	2919	2840	5926	6478	3685	267
7.5	11617	2893	3034	5967	6571	3868	275
8.0	12349	2797	3150	5900	6503	3990	299
8.5	13212	2789	3338	6000	6720	4277	340
9.0	13968	2745	3488	5886	6614	4417	411
9.5	14648	2740	3555	5804	6559	4486	382
10.0	15441	3592	3684	5956	6721	4708	414
10.5	16289	2635	3679	5671	6351	4624	484
11.0	16883	2667	3807	5770	6487	4799	450
11.5	17967	2659	3814	5621	6290	4741	439
12.0	18653	2603	3721	5539	6233	4663	389
12.5	19408	2679	3892	5583	6315	4858	472
13.0	20193	2708	3908	5575	6285	4885	531
13.5	20978	2713	4004	5722	6444	5178	542
14.0	21764	2740	4030	5647	6324	5070	537
14.5	22579	2774	4059	5703	6392	5095	537
15.0	23334	2791	4160	5799	6507	5309	625
15.5	24119	2741	4073	5626	6285	5215	666
16.0	24830	2824	4189	5849	6515	5444	727
16.5	25815	2756	4153	5706	6371	5303	822
17.0	26539	2725	4154	5743	6410	5376	708
17.5	27371	2711	4131	5605	6306	5285	854
18.0	27932	2644	4077	5508	6120	5219	839

Appendix VI. Laboratory Study Small-Column Data (Continued)

Effluent Data (Continued)

Time (min)	BVF	Concentrations in µg/L 1	2	3	4	5	6
18.5	28992	2659	4106	5573	6275	5326	837
19.0	29781	2635	4101	5477	6099	5205	1023
19.5	30300	2586	4015	5378	6035	5179	1085
20.0	31525	2560	4029	5287	5939	5064	1006
21.0	33284	2552	4002	5224	5857	5008	1062
22.0	35092	2502	3920	5118	5713	4996	1019
23.0	36389	2600	3944	5224	5813	5028	1118
24.0	37625	2621	3933	5306	5918	5059	1382

Where:

1 = Chloroform
2 = Trichloroethene
3 = Chlorodibromoethane
4 = 1,2 Dibromoethane
5 = Bromoform
6 = Tetrachloroethene

Appendix VII. Field Study Pilot-Column Data

Pilot-Scale Column (a) Operating parameters found in Table 7a.

Data Collected from 8/26/84 to 1/24/84 Run Time : 151 days

Carbon:	F-400	Loading Rate :	4.59 m/hr
Size :	12x40 mesh	EBCT :	60 sec
	0.0513 cm particle radius	Influent Temp:	12 °C

Influent Data Concentrations in µg/L

	1	2	3	4	5	6	7	8	9	10
Average	80.9	66.6	45.2	7.5	1.3	22.0	0.1	4.1	4.7	8.4

Time (days)	BVF	1	2	3	4	5	6	7	8	9	10
0.12	166.0	109.0	78.3	53.4	7.6	1.0	34.0	5.4	0.0	8.4	12.4
0.98	1355.6	105.0	74.2	51.3	7.6	1.0	33.0	5.2	0.0	7.0	9.9
2.01	2818.5	107.0	77.7	58.5	7.2	1.2	31.7	5.8	0.0	8.6	12.5
3.00	4247.5	105.0	75.1	54.8	7.7	1.1	30.5	5.8	1.9	7.2	9.7
4.00	5709.4	114.0	79.4	54.9	7.3	1.3	32.8	4.7	0.0	7.3	10.3
4.93	6900.0	91.0	70.0	53.0	0.3	1.4	0.0	0.0	0.0	1.0	2.2
8.05	9503.7	92.0	66.0	62.0	4.3	2.0	2.4	0.5	0.3	1.1	6.4
9.01	10726.1	92.0	70.0	68.0	5.7	2.1	4.7	0.0	0.0	4.1	10.0
9.95	12132.9	75.4	61.4	64.6	0.0	1.2	0.0	0.0	0.0	0.0	0.0
11.00	13717.8	70.9	62.2	64.3	0.9	1.1	0.0	0.0	0.0	0.0	1.3
12.00	15193.8	85.9	9.3	79.3	1.1	1.5	0.3	0.0	0.0	1.0	6.7
14.97	19508.4	70.9	67.8	58.3	0.3	1.3	0.0	0.0	0.0	0.0	1.4
16.01	20983.6	68.0	63.5	59.6	0.3	1.2	0.0	0.0	0.0	0.0	2.2
17.97	23666.2	86.5	88.4	66.4	0.3	1.7	0.0	0.0	0.0	0.0	1.9
22.04	29602.7	86.5	84.0	65.0	7.5	1.1	31.0	4.4	0.0	7.2	12.0
25.00	33902.2	75.0	67.5	48.2	11.7	1.4	27.1	4.5	0.0	6.0	10.3
29.04	39883.2	83.3	83.8	67.3	12.4	1.4	33.3	4.6	0.0	7.6	12.4
36.02	49918.3	87.0	73.9	0.5	12.1	1.5	36.4	5.2	0.4	6.0	11.5
42.94	60065.5	78.3	70.3	58.3	12.1	1.4	29.0	3.8	0.0	5.7	9.6
49.90	70246.8	73.3	91.3	38.5	10.9	1.5	33.0	4.0	0.0	5.6	9.8
56.93	80524.3	79.2	81.9	67.3	7.9	1.9	42.7	5.1	0.0	6.7	12.7
63.93	90176.0	65.6	78.3	56.1	8.0	1.7	27.7	5.2	0.0	5.3	8.9
73.94	104298.5	63.2	67.5	43.6	6.1	1.3	21.4	4.6	0.0	5.2	8.2
84.93	119985.1	82.0	80.2	51.2	6.5	0.5	25.6	5.1	0.0	5.7	9.5
102.03	140737.1	79.8	54.4	41.8	4.4	1.4	12.2	3.7	0.0	3.7	6.6
106.94	147943.7	79.9	48.6	29.4	6.6	1.3	16.8	4.1	0.0	3.8	7.4
114.94	159760.7	95.7	58.5	31.5	7.3	1.5	17.6	4.8	0.0	4.1	7.3
128.93	179861.6	88.1	42.1	26.9	7.6	1.2	13.3	4.2	0.0	3.1	6.6
140.93	195871.2	78.0	54.8	42.3	8.9	1.0	19.6	3.9	0.0	4.0	7.0
150.93	209209.9	80.1	62.8	45.1	7.4	0.9	23.4	5.2	0.0	5.3	9.1

Where:
1 = cis-Dichloroethene
2 = Trichloroethene
3 = Tetrachloroethene
4 = Vinyl Chloride
5 = 1,1,1 Trichloroethane
6 = Toluene
7 = Benzene
8 = Ethyl Benzene
9 = m-Xylene
10 = o,p-Xylene

Appendix VII. (continued)

Pilot-Scale Data (a) Operating parameters found in Table 7a.

Effluent Data Concentrations in µg/L

Time (days)	BVF	1	2	3	4	5	6	7	8	9	10
0.14	194.5	5.2	3.0	4.7	0.7	0.0	2.6	0.0	0.3	0.5	0.5
1.01	1387.6	25.2	15.5	11.9	3.1	0.0	7.2	0.0	1.7	1.8	0.9
2.04	2861.0	46.4	29.4	23.6	4.8	0.2	13.2	0.0	2.3	2.8	3.2
3.01	4273.7	56.1	34.1	25.7	6.0	1.2	14.4	0.0	2.4	3.6	5.6
4.02	5729.5	56.3	33.7	23.9	5.8	0.2	12.0	0.0	1.5	3.3	6.9
4.95	6912.5	72.0	45.3	67.2	8.1	1.7	14.1	0.0	1.3	4.5	5.6
8.07	9518.5	62.0	42.0	40.0	2.8	0.7	0.0	0.0	0.0	0.9	4.0
9.03	10756.0	68.0	50.0	49.0	4.8	1.8	1.0	0.0	0.5	1.2	6.7
10.00	12217.0	63.5	46.2	52.0	8.3	1.3	0.0	0.0	0.0	1.6	5.8
11.01	13739.7	60.9	48.8	55.7	0.5	1.4	0.0	0.0	0.0	0.0	1.3
12.01	15210.9	67.6	53.9	54.1	1.9	1.5	0.3	0.0	0.0	1.2	5.5
15.02	19581.4	57.6	49.4	43.4	0.3	1.5	0.0	0.0	0.0	0.8	2.9
16.04	21025.0	53.0	41.3	37.6	0.3	1.1	0.0	0.0	0.0	0.0	1.7
17.99	23694.9	52.7	33.1	20.8	0.3	1.2	0.0	0.0	0.0	0.0	1.2
22.02	29566.1	56.0	26.0	16.0	6.8	0.8	1.5	0.0	1.0	1.4	2.9
25.02	33927.2	58.2	25.0	12.9	12.2	1.3	1.0	0.0	0.9	1.0	1.5
29.05	39905.5	65.1	30.5	16.0	12.7	1.6	2.2	0.0	1.0	1.0	1.8
36.03	49939.3	80.5	39.2	19.9	12.9	1.4	5.1	0.0	0.0	1.1	2.8
42.95	60088.5	79.4	49.0	27.5	12.5	1.3	8.1	0.0	1.6	1.6	3.0
49.93	70288.1	73.9	61.3	23.5	11.4	1.3	12.1	0.0	2.1	1.3	4.0
56.93	80520.3	73.1	66.1	19.9	6.9	1.9	13.3	0.0	1.7	1.3	3.8
63.92	90173.0	66.7	72.5	17.4	7.5	1.4	12.7	0.0	2.2	1.7	4.0
73.93	104287.1	77.7	72.7	18.6	6.7	1.3	13.4	0.0	2.9	2.4	5.3
84.92	119974.1	82.9	72.4	20.0	6.5	1.4	15.3	0.0	2.9	2.7	5.3
98.93	136137.0	90.8	60.5	30.9	6.7	1.5	11.1	0.0	2.4	2.1	4.6
106.94	147938.6	92.1	54.6	29.0	7.4	1.4	11.5	0.0	3.0	2.3	5.0
114.94	159755.8	97.6	55.1	22.4	6.8	1.4	11.9	0.0	1.2	0.5	1.3
128.93	179857.9	94.3	51.1	23.5	7.9	1.5	8.9	0.0	2.7	2.1	4.0
140.93	195867.5	67.9	44.7	24.2	9.0	0.8	11.8	0.0	2.2	1.8	4.2
150.93	209206.2	74.5	57.1	30.7	9.5	0.9	14.2	0.0	3.0	2.7	5.6

Where: 1 = cis-Dichloroethene
2 = Trichloroethene
3 = Tetrachloroethene
4 = Vinyl Chloride
5 = 1,1,1 Trichloroethane
6 = Toluene
7 = Benzene
8 = Ethyl Benzene
9 = m-Xylene
10 = o,p-Xylene

Appendix VII. Field Study Pilot-Column Data (continued)

Pilot-Scale Column (b) Operating parameters found in Table 7b.

Data Collected from 8/26/84 to 1/24/84 Run Time : 151 days

Carbon: F-400 Loading Rate : 4.59 m/hr
Size : 12x40 mesh EBCT : 192 sec
0.0513 cm particle radius Influent Temp: 12 °C

Influent Data Concentrations in µg/L

	1	2	3	4	5	6	7	8	9	10
Average	80.9	66.6	45.2	7.5	1.3	22.0	0.1	4.1	4.7	8.4

Time (days)	BVF	1	2	3	4	5	6	7	8	9	10
0.12	53.6	109.0	78.3	53.4	7.6	1.0	34.0	5.4	0.0	8.4	12.4
0.98	438.2	105.0	74.2	51.3	7.6	1.0	33.0	5.2	0.0	7.0	9.9
2.01	911.0	107.0	77.7	58.5	7.2	1.2	31.7	5.8	0.0	8.6	12.5
3.00	1372.7	105.0	75.1	54.8	7.7	1.1	30.5	5.8	1.9	7.2	9.7
4.00	1845.2	114.0	79.4	54.9	7.3	1.3	32.8	4.7	0.0	7.3	10.3
4.93	2230.1	91.0	70.0	53.0	0.3	1.4	0.0	0.0	0.0	1.0	2.2
8.05	3072.0	92.0	66.0	62.0	4.3	2.0	2.4	0.5	0.3	1.1	6.4
9.01	3467.0	92.0	70.0	68.0	5.7	2.1	4.7	0.0	0.0	4.1	10.0
9.95	3921.8	75.4	61.4	64.6	0.0	1.2	0.0	0.0	0.0	0.0	0.0
11.00	4434.3	70.9	62.2	64.3	0.9	1.1	0.0	0.0	0.0	0.0	1.3
12.00	4911.5	85.9	9.3	79.3	1.1	1.5	0.3	0.0	0.0	1.0	6.7
14.97	6307.0	70.9	67.8	58.3	0.3	1.3	0.0	0.0	0.0	0.0	1.4
16.01	6783.8	68.0	63.5	59.6	0.3	1.2	0.0	0.0	0.0	0.0	2.2
17.97	7651.4	86.5	88.4	66.4	0.3	1.7	0.0	0.0	0.0	0.0	1.9
22.04	9571.5	86.5	84.0	65.0	7.5	1.1	31.0	4.4	0.0	7.2	12.0
25.00	10962.1	75.0	67.5	48.2	11.7	1.4	27.1	4.5	0.0	6.0	10.3
29.04	12896.8	83.3	83.8	67.3	12.4	1.4	33.3	4.6	0.0	7.6	12.4
36.02	16142.9	87.0	73.9	0.5	12.1	1.5	36.4	5.2	0.4	6.0	11.5
42.94	19425.2	78.3	70.3	58.3	12.1	1.4	29.0	3.8	0.0	5.7	9.6
49.90	22718.6	73.3	91.3	38.5	10.9	1.5	33.0	4.0	0.0	5.6	9.8
56.93	26043.0	79.2	81.9	67.3	7.9	1.9	42.7	5.1	0.0	6.7	12.7
63.93	29164.8	65.6	78.3	56.1	8.0	1.7	27.7	5.2	0.0	5.3	8.9
73.94	33733.2	63.2	67.5	43.6	6.1	1.3	21.4	4.6	0.0	5.2	8.2
84.93	38807.9	82.0	80.2	51.2	6.5	0.5	25.6	5.1	0.0	5.7	9.5
102.03	45521.8	79.8	54.4	41.8	4.4	1.4	12.2	3.7	0.0	3.7	6.6
106.94	47853.3	79.9	48.6	29.4	6.6	1.3	16.8	4.1	0.0	3.8	7.4
114.94	51676.5	95.7	58.5	31.5	7.3	1.5	17.6	4.8	0.0	4.1	7.3
128.93	58179.7	88.1	42.1	26.9	7.6	1.2	13.3	4.2	0.0	3.1	6.6
140.93	63359.3	78.0	54.8	42.3	8.9	1.0	19.6	3.9	0.0	4.0	7.0
150.93	67674.7	80.1	62.8	45.1	7.4	0.9	23.4	5.2	0.0	5.3	9.1

Where: 1 = cis-Dichloroethene
2 = Trichloroethene
3 = Tetrachloroethene
4 = Vinyl Chloride
5 = 1,1,1 Trichloroethane
6 = Toluene
7 = Benzene
8 = Ethyl Benzene
9 = m-Xylene
10 = o,p-Xylene

Appendix VII. (continued)

Pilot-Scale Data (b)   Operating parameters found in Table 7b.

Effluent Data   Concentrations in µg/L

Time (days)	BVF	1	2	3	4	5	6	7	8	9	10
0.14	61.3	0.0	1.2	0.3	0.2	0.0	0.0	0.0	0.0	0.0	0.3
1.00	446.9	0.0	0.0	0.0	0.0	0.6	0.0	0.3	0.0	0.0	0.0
2.04	922.8	4.9	0.3	0.3	0.5	0.0	0.0	0.0	0.0	0.0	0.0
3.01	1380.2	2.2	0.6	0.4	1.4	0.0	0.0	0.0	0.0	0.0	0.0
4.01	1850.7	1.2	0.8	0.6	2.5	0.0	0.0	0.0	0.0	0.0	0.0
4.95	2233.9	4.1	0.9	0.7	2.9	0.0	0.0	0.0	0.0	0.0	0.0
8.07	3077.2	3.8	0.6	0.5	0.8	0.3	0.0	0.0	0.0	0.0	0.0
9.02	3475.3	5.5	1.0	0.9	5.3	0.4	0.0	0.0	0.0	0.0	0.0
10.00	3948.0	8.0	3.2	2.0	6.8	0.4	0.0	0.0	0.0	0.0	0.0
11.01	4440.7	9.0	2.3	2.0	0.4	0.3	0.0	0.0	0.0	0.0	0.0
12.00	4916.1	11.8	4.2	2.7	3.0	0.5	0.0	0.0	0.0	0.0	0.0
15.01	6328.7	12.3	3.5	1.5	0.3	0.3	0.0	0.0	0.0	0.0	0.0
16.02	6789.7	13.8	3.8	1.7	0.3	0.2	0.0	0.0	0.0	0.0	0.0
17.98	7659.4	15.3	3.9	1.7	0.0	0.5	0.0	0.0	0.0	0.0	0.0
22.01	9558.3	22.0	4.5	1.2	6.6	0.6	0.0	0.0	0.0	0.0	0.0
25.01	10968.6	22.4	3.8	0.9	10.9	0.4	0.0	0.0	0.0	0.0	0.0
29.05	12902.9	34.9	5.3	1.6	12.5	0.8	0.0	0.0	0.0	0.0	0.0
36.03	16148.7	42.8	6.8	1.7	11.9	1.1	0.0	0.0	0.0	0.0	0.0
42.95	19431.4	58.7	11.7	3.3	12.4	1.1	0.4	0.5	0.0	0.0	0.0
49.92	22730.6	58.0	15.5	3.5	11.4	1.3	0.0	0.0	0.0	0.0	0.0
56.93	26040.4	62.8	21.1	4.0	6.8	1.2	0.8	0.0	0.0	0.0	0.0
63.92	29162.4	62.1	32.7	5.7	7.8	1.2	0.4	0.0	0.4	0.0	0.0
73.93	33728.6	89.5	44.4	8.5	8.0	1.3	0.7	0.0	0.8	0.0	0.8
84.92	38803.4	82.0	45.7	9.9	6.5	1.2	1.2	0.0	0.8	0.0	0.6
98.93	44032.1	109.0	58.2	18.4	7.3	1.8	1.9	0.0	0.8	0.6	1.2
106.94	47850.0	82.6	38.6	14.6	6.4	1.2	2.2	0.0	1.3	0.8	1.5
114.93	51673.3	97.8	41.1	12.1	6.9	1.4	3.8	0.0	1.2	0.5	1.3
128.93	58177.3	99.0	41.4	15.2	8.2	1.6	4.4	0.0	1.6	0.7	1.3
140.93	63356.9	78.8	36.2	14.3	11.1	0.9	6.7	0.0	1.2	0.0	1.5
150.93	67672.3	90.8	50.3	20.0	10.9	1.0	7.7	0.0	1.0	0.0	6.9

Where: 1 = cis-Dichloroethene
2 = Trichloroethene
3 = Tetrachloroethene
4 = Vinyl Chloride
5 = 1,1,1 Trichloroethane
6 = Toluene
7 = Benzene
8 = Ethyl Benzene
9 = m-Xylene
10 = o,p-Xylene

Appendix VII. Field Study Pilot-Column Data (continued)

Pilot-Scale Column (c) Operating parameters found in Table 7c.

Data Collected from 8/26/84 to 1/24/84 Run Time : 151 days

Carbon: F-400 Loading Rate : 4.59 m/hr
Size : 12x40 mesh EBCT : 324 sec
0.0513 cm particle radius Influent Temp: 12 °C

Influent Data Concentrations in µg/L

	1	2	3	4	5	6	7	8	9	10
Average	80.9	66.6	45.2	7.5	1.3	22.0	0.1	4.1	4.7	8.4

Time (days)	BVF	1	2	3	4	5	6	7	8	9	10
0.12	32.6	109.0	78.3	53.4	7.6	1.0	34.0	5.4	0.0	8.4	12.4
0.98	266.2	105.0	74.2	51.3	7.6	1.0	33.0	5.2	0.0	7.0	9.9
2.01	553.5	107.0	77.7	58.5	7.2	1.2	31.7	5.8	0.0	8.6	12.5
3.00	833.9	105.0	75.1	54.8	7.7	1.1	30.5	5.8	1.9	7.2	9.7
4.00	1121.1	114.0	79.4	54.9	7.3	1.3	32.8	4.7	0.0	7.3	10.3
4.93	1355.1	91.0	70.0	53.0	0.3	1.4	0.0	0.0	0.0	1.0	2.2
8.05	1866.9	92.0	66.0	62.0	4.3	2.0	2.4	0.5	0.3	1.1	6.4
9.01	2106.9	92.0	70.0	68.0	5.7	2.1	4.7	0.0	0.0	4.1	10.0
9.95	2383.5	75.4	61.4	64.6	0.0	1.2	0.0	0.0	0.0	0.0	0.0
11.00	2695.1	70.9	62.2	64.3	0.9	1.1	0.0	0.0	0.0	0.0	1.3
12.00	2985.2	85.9	9.3	79.3	1.1	1.5	0.3	0.0	0.0	1.0	6.7
14.97	3833.9	70.9	67.8	58.3	0.3	1.3	0.0	0.0	0.0	0.0	1.4
16.01	4123.6	68.0	63.5	59.6	0.3	1.2	0.0	0.0	0.0	0.0	2.2
17.97	4651.2	86.5	88.4	66.4	0.3	1.7	0.0	0.0	0.0	0.0	1.9
22.04	5819.1	86.5	84.0	65.0	7.5	1.1	31.0	4.4	0.0	7.2	12.0
25.00	6664.7	75.0	67.5	48.2	11.7	1.4	27.1	4.5	0.0	6.0	10.3
29.04	7841.4	83.3	83.8	67.3	12.4	1.4	33.3	4.6	0.0	7.6	12.4
36.02	9815.8	87.0	73.9	0.5	12.1	1.5	36.4	5.2	0.4	6.0	11.5
42.94	11812.3	78.3	70.3	58.3	12.1	1.4	29.0	3.8	0.0	5.7	9.6
49.90	13815.4	73.3	91.3	38.5	10.9	1.5	33.0	4.0	0.0	5.6	9.8
56.93	15837.3	79.2	81.9	67.3	7.9	1.9	42.7	5.1	0.0	6.7	12.7
63.93	17736.0	65.6	78.3	56.1	8.0	1.7	27.7	5.2	0.0	5.3	8.9
73.94	20514.8	63.2	67.5	43.6	6.1	1.3	21.4	4.6	0.0	5.2	8.2
84.93	23601.8	82.0	80.2	51.2	6.5	0.5	25.6	5.1	0.0	5.7	9.5
102.03	27686.2	79.8	54.4	41.8	4.4	1.4	12.2	3.7	0.0	3.7	6.6
106.94	29104.6	79.9	48.6	29.4	6.6	1.3	16.8	4.1	0.0	3.8	7.4
114.94	31430.4	95.7	58.5	31.5	7.3	1.5	17.6	4.8	0.0	4.1	7.3
128.93	35386.6	88.1	42.1	26.9	7.6	1.2	13.3	4.2	0.0	3.1	6.6
140.93	38537.6	78.0	54.8	42.3	8.9	1.0	19.6	3.9	0.0	4.0	7.0
150.93	41162.9	80.1	62.8	45.1	7.4	0.9	23.4	5.2	0.0	5.3	9.1

Where: 1 = cis-Dichloroethene
2 = Trichloroethene
3 = Tetrachloroethene
4 = Vinyl Chloride
5 = 1,1,1 Trichloroethane
6 = Toluene
7 = Benzene
8 = Ethyl Benzene
9 = m-Xylene
10 = o,p-Xylene

Appendix VII. (continued)

Pilot-Scale Data (c) Operating parameters found in Table 7c.

Effluent Data Concentrations in µg/L

Time (days)	BVF	1	2	3	4	5	6	7	8	9	10
0.13	36.3	0.0	0.0	0.0	0.0	0.0	0.0	0.0	0.0	0.0	0.0
1.00	270.4	0.0	0.0	0.0	0.0	0.0	0.0	0.0	0.0	0.0	0.0
2.03	559.4	0.0	0.0	0.0	0.0	0.0	0.0	0.0	0.0	0.0	0.0
3.01	837.3	1.2	0.4	0.3	1.3	0.4	1.9	0.0	0.0	0.0	0.0
4.01	1123.6	0.0	0.0	0.0	0.0	0.0	0.0	0.0	0.0	0.0	0.0
4.94	1357.1	0.0	0.0	0.0	0.5	0.3	0.0	0.0	0.0	0.0	0.0
8.06	1869.0	0.0	0.0	0.0	0.0	0.0	0.0	0.0	0.0	0.0	0.0
9.02	2110.8	0.0	0.0	0.0	1.2	0.0	0.0	0.0	0.0	0.0	0.0
10.00	2399.0	0.0	0.0	0.0	1.5	0.3	0.7	0.0	0.0	0.0	0.0
11.01	2698.3	0.0	0.3	0.4	0.4	0.3	0.0	0.0	0.0	0.0	0.0
11.92	2963.6	0.0	0.0	0.2	0.5	0.2	0.0	0.8	0.0	0.0	0.0
15.01	3846.1	2.4	0.0	0.0	0.4	0.0	0.0	0.0	0.0	0.0	0.0
16.03	4130.0	0.5	0.0	0.0	0.3	0.0	0.0	0.0	0.0	0.0	0.0
17.98	4655.3	0.8	0.0	0.0	0.5	0.0	0.0	0.0	0.0	0.0	0.0
22.01	5808.3	3.0	0.0	0.0	5.9	0.4	0.0	0.0	0.0	0.0	0.0
25.01	6667.9	4.3	0.0	0.0	11.4	0.0	0.0	0.0	0.0	0.0	0.0
29.05	7844.5	4.9	0.0	0.0	10.6	0.0	0.0	0.0	0.0	0.0	0.0
36.03	9818.6	9.6	0.0	0.0	11.3	0.2	0.0	0.0	0.0	0.0	0.0
42.95	11815.2	16.8	1.3	0.0	12.8	1.4	0.0	0.0	0.0	0.0	0.0
49.92	13822.0	28.2	1.1	0.0	9.9	0.8	0.0	0.0	0.0	0.0	0.0
56.93	15835.2	34.9	1.9	0.2	7.7	1.0	0.0	0.0	0.0	0.0	0.0
63.92	17734.0	35.6	4.1	0.2	7.5	1.0	0.0	0.0	0.0	0.0	0.0
73.92	20511.3	53.3	8.6	1.1	6.9	1.0	0.0	0.0	0.0	0.0	0.0
84.92	23597.7	40.6	9.5	0.9	4.7	1.8	0.0	0.0	0.0	0.0	0.0
98.92	26779.1	48.0	10.5	1.1	5.3	0.9	0.0	0.0	0.0	0.0	0.0
106.93	29101.6	78.6	16.8	3.1	6.8	1.0	0.0	0.0	0.0	0.0	0.0
114.93	31427.5	92.0	20.0	3.2	7.7	1.4	0.0	0.0	0.0	0.0	0.0
128.92	35384.4	87.2	19.4	4.3	6.7	1.4	0.0	0.0	0.0	0.0	0.0
140.92	38535.4	74.4	19.1	4.9	11.0	0.8	0.0	0.0	0.0	0.0	0.0
150.92	41160.7	85.7	27.5	7.1	8.1	0.8	0.3	0.0	0.0	0.0	0.0

Where: 1 = cis-Dichloroethene
2 = Trichloroethene
3 = Tetrachloroethene
4 = Vinyl Chloride
5 = 1,1,1 Trichloroethane
6 = Toluene
7 = Benzene
8 = Ethyl Benzene
9 = m-Xylene
10 = o,p-Xylene

Appendix VII. Field Study Pilot-Column Data (continued)

Pilot-Scale Column (d) Operating parameters found in Table 7d.

Data Collected from 8/26/84 to 1/24/84 Run Time : 151 days

Carbon: WV-G Loading Rate : 4.40 m/hr
Size : 12x40 mesh EBCT : 60 sec
0.0513 cm particle radius Influent Temp: 12 °C

Influent Data Concentrations in µg/L

	1	2	3	4	5	6	7	8	9	10
Average	81.9	69.7	36.7	7.7	1.4	20.4	0.1	3.7	4.0	8.0

Time (days)	BVF	1	2	3	4	5	6	7	8	9	10
0.12	170.8	109.0	78.3	53.4	7.6	1.0	34.0	5.4	0.0	8.4	12.4
0.98	1367.5	105.0	74.2	51.3	7.6	1.0	33.0	5.2	0.0	7.0	9.9
2.01	2790.2	107.0	77.7	58.5	7.2	1.2	31.7	5.8	0.0	8.6	12.5
3.00	4165.9	105.0	75.1	54.8	7.7	1.1	30.5	5.8	1.9	7.2	9.7
4.00	5560.5	114.0	79.4	54.9	7.3	1.3	32.8	4.7	0.0	7.3	10.3
4.93	6611.6	91.0	70.0	53.0	0.3	1.4	0.0	0.0	0.0	1.0	2.2
8.05	8385.0	92.0	66.0	62.0	4.3	2.0	2.4	0.5	0.3	1.1	6.4
9.01	9558.6	92.0	70.0	68.0	5.7	2.1	4.7	0.0	0.0	4.1	10.0
9.95	11283.7	75.4	61.4	64.6	0.0	1.2	0.0	0.0	0.0	0.0	0.0
11.00	12887.4	70.9	62.2	64.3	0.9	1.1	0.0	0.0	0.0	0.0	1.3
12.00	13500.3	85.9	9.3	79.3	1.1	1.5	0.3	0.0	0.0	1.0	6.7
14.97	17383.7	70.9	67.8	58.3	0.3	1.3	0.0	0.0	0.0	0.0	1.4
16.01	18757.3	68.0	63.5	59.6	0.3	1.2	0.0	0.0	0.0	0.0	2.2
17.97	21339.5	86.5	88.4	66.4	0.3	1.7	0.0	0.0	0.0	0.0	1.9
22.04	27114.0	86.5	84.0	65.0	7.5	1.1	31.0	4.4	0.0	7.2	12.0
25.00	31158.9	75.0	67.5	48.2	11.7	1.4	27.1	4.5	0.0	6.0	10.3
29.04	36790.7	83.3	83.8	67.3	12.4	1.4	33.3	4.6	0.0	7.6	12.4
36.02	46388.3	87.0	73.9	0.5	12.1	1.5	36.4	5.2	0.4	6.0	11.5
42.94	58074.0	78.3	70.3	58.3	12.1	1.4	29.0	3.8	0.0	5.7	9.6
49.90	65704.7	73.3	91.3	38.5	10.9	1.5	33.0	4.0	0.0	5.6	9.8
56.92	75352.9	73.4	82.9	28.7	7.2	1.6	31.1	3.6	0.0	4.6	9.1
63.90	85020.1	64.7	88.7	20.6	7.3	1.4	20.9	3.7	0.0	3.8	7.2
73.91	98764.2	75.7	82.9	24.4	6.2	1.4	19.5	4.0	0.0	4.4	7.7
84.91	113662.2	84.2	82.4	27.0	6.4	1.5	23.3	4.9	0.0	4.8	8.9
98.91	128546.0	85.4	62.9	42.0	6.7	1.7	16.1	3.8	0.0	2.9	7.1
106.92	139660.8	86.4	56.6	34.4	7.2	1.3	15.0	4.1	0.0	3.0	7.4
114.92	150589.9	96.6	55.5	27.6	7.4	1.5	15.1	4.1	0.0	2.8	6.7
128.91	167576.7	91.6	50.2	28.3	8.3	1.5	12.3	3.8	0.0	2.9	6.7
140.91	183107.1	69.4	50.8	32.0	6.7	0.9	15.7	3.0	0.0	3.1	6.3
150.91	195798.9	79.0	62.3	36.6	10.9	0.9	20.5	4.7	0.0	3.8	7.9

Where: 1 = cis-Dichloroethene
2 = Trichloroethene
3 = Tetrachloroethene
4 = Vinyl Chloride
5 = 1,1,1 Trichloroethane
6 = Toluene
7 = Benzene
8 = Ethyl Benzene
9 = m-Xylene
10 = o,p-Xylene

Appendix VII. (continued)

Pilot-Scale Data (d)   Operating parameters found in Table 7d.

Effluent Data   Concentrations in µg/L

Time (days)	BVF	1	2	3	4	5	6	7	8	9	10
0.12	165.9	4.8	1.7	1.4	0.9	0.0	2.4	0.1	0.0	1.0	0.9
0.98	1360.9	46.0	25.7	17.2	5.6	0.5	11.5	2.1	0.0	3.6	3.1
2.01	2785.3	64.3	35.4	24.7	6.7	0.7	13.7	2.3	0.0	3.8	3.8
2.99	4162.0	78.6	35.1	24.2	6.7	0.9	12.6	2.2	0.0	2.9	4.2
4.00	5557.7	76.3	39.7	24.8	7.2	0.7	11.7	1.8	0.0	3.2	4.2
4.93	6610.0	68.0	36.0	24.0	2.3	0.9	0.0	0.0	0.0	0.6	2.9
8.05	8383.6	79.0	49.0	48.0	3.8	1.7	0.0	0.3	0.2	0.8	3.4
9.00	9554.4	81.0	58.0	54.0	4.7	1.4	2.2	0.0	0.0	2.3	7.0
9.94	11270.7	76.2	56.2	61.0	8.6	1.0	0.0	0.0	0.0	1.2	5.3
11.00	12886.7	67.5	52.7	53.8	0.3	1.2	0.0	0.0	0.0	0.0	1.6
11.98	13483.3	78.1	61.6	60.9	1.6	1.3	0.4	0.0	0.0	1.2	5.8
14.96	17378.1	63.2	48.6	38.2	0.3	1.2	0.0	0.0	0.0	0.0	0.0
16.00	18750.2	61.4	50.6	40.5	0.3	1.2	0.0	0.0	0.0	0.0	0.9
17.96	21335.6	67.1	45.6	23.5	0.4	1.3	0.0	0.0	0.0	0.7	2.2
21.99	27048.5	79.0	50.0	26.0	7.5	1.2	1.9	0.3	0.0	1.8	3.5
24.99	31155.2	66.8	38.6	18.6	11.4	1.3	1.8	1.2	0.0	1.4	2.3
29.03	36786.5	70.9	37.9	19.4	12.0	1.1	3.4	1.0	0.0	0.8	2.5
36.03	46407.9	81.2	40.0	18.3	13.0	1.2	4.9	1.6	0.0	1.8	2.7
42.93	58073.1	79.6	44.9	22.6	13.3	1.3	6.8	1.1	0.0	1.4	2.4
49.90	65701.8	76.5	58.2	19.6	11.3	1.3	9.4	4.0	0.0	1.3	2.8
56.91	75350.1	81.3	70.4	18.4	7.5	1.7	10.1	1.4	0.0	1.1	2.4
63.91	85036.6	69.6	70.6	15.0	7.3	1.4	9.3	1.6	0.0	1.3	2.9
73.91	98770.6	76.5	68.9	16.7	6.4	1.5	10.4	2.3	0.0	1.6	3.3
84.91	113659.3	85.2	75.4	20.0	6.2	1.5	13.4	2.5	0.0	1.8	4.4
98.91	128542.2	86.0	59.4	29.0	6.7	1.6	9.3	2.4	0.0	1.9	4.6
106.92	139656.0	88.8	57.2	26.0	7.1	1.3	2.1	2.6	0.0	0.7	3.5
114.91	150586.0	106.0	64.8	21.3	7.3	1.5	9.9	2.8	0.0	0.9	4.2
128.91	167572.0	92.2	50.8	22.4	7.9	1.4	8.7	2.5	0.0	1.3	3.9
140.91	183103.5	103.0	76.6	39.4	11.7	1.3	16.9	3.2	0.0	1.9	5.3
150.91	195795.3	79.3	63.1	29.7	9.5	0.9	15.1	3.0	0.0	2.2	5.2

Where: 1 = cis-Dichloroethene
2 = Trichloroethene
3 = Tetrachloroethene
4 = Vinyl Chloride
5 = 1,1,1 Trichloroethane
6 = Toluene
7 = Benzene
8 = Ethyl Benzene
9 = m-Xylene
10 = o,p-Xylene

Appendix VIII. Field Study Small-Column Data

RSSCT (a) Operating parameters found in Table 8a.

Conducted from 8/26/84 to 8/31/84		Run Time	: 5 days
Carbon:	F-400	Loading Rate	: 22.4 m/hr
Size :	60x80 mesh	EBCT	: 2.51 sec
	0.0105 cm particle radius	Influent Temp:	13 °C

Influent Data Concentrations in µg/L

	1	2	3	4	5	6	7	8	9	10
Average	108.9	76.1	56.4	7.5	1.3	25.3	0.4	3.1	6.0	9.3

Time (hrs)	BVF	1	2	3	4	5	6	7	8	9	10
0.00	0	116.0	77.1	49.0	7.2	1.0	34.7	0.0	5.6	7.4	13.1
0.20	295	116.0	77.1	49.0	7.2	1.0	34.7	0.0	5.6	7.4	13.1
2.25	3348	118.0	79.0	52.1	8.3	1.0	35.8	0.0	6.0	7.7	13.2
6.33	9531	108.0	72.3	39.8	7.2	1.0	25.3	0.0	4.3	5.5	7.4
21.83	32929	115.0	77.4	54.4	8.1	1.1	34.1	0.0	5.5	7.6	10.4
26.08	38706	110.0	74.2	52.2	7.9	1.9	29.9	0.0	5.3	7.2	9.8
30.73	44044	109.0	71.5	55.8	7.2	2.3	12.9	1.7	1.3	0.5	5.1
45.95	67260	95.8	67.4	52.0	6.4	1.3	30.2	0.0	4.8	6.5	9.1
69.83	102230	106.0	73.2	58.2	7.1	1.1	29.8	0.0	3.5	6.5	10.0
95.93	138103	114.0	82.7	65.3	8.1	1.2	15.7	0.0	0.0	5.6	9.2
118.17	169552	120.0	90.7	63.4	8.5	1.2	23.9	2.7	1.5	7.3	11.1

Effluent Data Concentrations in µg/L

Time (hrs)	BVF	1	2	3	4	5	6	7	8	9	10
0.00	0	0.0	0.0	0.0	0.0	0.0	0.0	0.0	0.0	0.0	0.0
0.20	295	19.4	9.2	6.1	2.7	0.0	4.6	0.0	1.1	0.4	0.4
2.25	3348	79.2	52.3	35.8	7.4	0.9	24.6	0.0	4.1	5.2	9.6
6.33	9531	81.8	54.2	39.8	7.2	0.8	25.3	0.0	4.3	5.5	7.4
10.35	15685	107.0	60.7	38.3	8.6	0.9	25.9	0.0	4.1	5.6	8.5
26.08	38706	104.0	69.3	50.0	7.9	0.9	28.0	0.0	4.7	6.5	9.5
30.73	44044	111.0	68.6	40.5	7.9	1.5	24.7	0.0	3.8	5.4	8.7
45.95	67260	101.0	68.5	50.6	7.8	1.0	29.6	0.0	4.6	7.2	12.2
50.23	73680	112.0	73.8	53.6	7.8	1.0	31.0	0.0	4.8	6.9	9.4
69.83	102230	110.0	76.1	60.2	8.2	1.1	18.2	0.0	0.0	6.1	10.4
78.85	114880	110.0	76.5	59.5	7.5	1.1	28.2	0.0	0.0	5.9	8.6
95.93	138103	106.0	76.1	55.8	8.0	1.1	6.9	0.0	0.0	4.4	7.9
104.03	149079	118.0	81.5	55.3	8.1	1.1	15.1	0.0	0.0	5.4	9.2
118.17	169552	115.0	84.1	59.2	8.4	1.3	11.5	0.0	0.0	5.1	8.9

Where:

1 = cis-Dichloroethene
2 = Trichloroethene
3 = Tetrachloroethene
4 = Vinyl Chloride
5 = 1,1,1 Trichloroethane
6 = Toluene
7 = Benzene
8 = Ethyl Benzene
9 = m-Xylene
10 = o,p-Xylene

Appendix VIII. Field Study Small-Column Data (continued)

RSSCT (b) Operating parameters found in Table 8b.

Conducted from 1/ 9/85 to 1/18/85		Run Time :	9 days
Carbon:	F-400	Loading Rate :	19.1 m/hr
Size :	60x80 mesh	EBCT :	9.54 sec
	0.0105 cm particle radius	Influent Temp:	14 °C

Influent Data Concentrations in µg/L

	1	2	3	4	5	6	7	8	9	10
Average	69.8	45.1	33.3	6.8	1.0	11.7	0.0	2.4	3.6	6.8

Time (hrs)	BVF	1	2	3	4	5	6	7	8	9	10
0.8	421	70.9	50.1	38.8	5.4	0.7	14.6	0.0	4.6	4.4	7.3
2.0	1057	70.1	47.9	38.1	4.1	0.8	14.9	0.0	4.7	4.6	7.9
4.1	1974	73.7	50.1	37.9	4.4	0.8	16.2	0.0	4.8	4.7	7.9
8.2	3050	54.0	34.8	27.4	3.3	0.7	11.2	0.0	3.4	3.0	5.5
14.0	4500	56.6	36.0	28.0	3.6	0.6	12.3	0.0	3.2	3.5	6.4
20.0	7395	55.7	36.2	29.1	6.3	0.8	13.3	0.0	3.0	2.6	5.1
44.0	15900	71.6	46.8	34.9	6.6	1.1	2.9	0.0	0.0	3.1	6.6
68.0	24900	69.7	45.1	32.7	6.4	1.0	2.7	0.0	0.0	2.9	6.8
92.0	33800	71.6	46.1	32.9	6.5	1.1	16.8	0.0	3.6	3.8	6.7
116.0	41850	82.2	53.2	38.3	8.3	1.1	17.2	0.0	3.7	4.3	8.0
134.0	52150	72.5	45.1	33.2	8.1	0.9	15.8	0.0	3.6	3.9	7.4
152.1	61200	65.6	44.8	33.1	7.5	0.8	13.9	0.0	2.4	4.3	6.8

Where:

1 = cis-Dichloroethene
2 = Trichloroethene
3 = Tetrachloroethene
4 = Vinyl Chloride
5 = 1,1,1 Trichloroethane
6 = Toluene
7 = Benzene
8 = Ethyl Benzene
9 = m-Xylene
10 = o,p-Xylene

Appendix VIII. (continued)

RSSCT (b) Operating parameters found in Table 8b.

Effluent Data   Concentrations in µg/L

Time (hrs)	BVF	1	2	3	4	5	6	7	8	9	10
0.9	421	1.1	0.3	0.3	0.0	0.2	0.0	0.0	0.0	0.0	0.0
2.2	1057	7.6	3.9	3.4	1.0	0.3	0.8	0.0	0.0	0.0	0.0
4.1	1974	12.9	7.0	5.5	2.2	0.3	2.0	0.0	0.7	0.0	0.0
8.2	3047	11.9	3.7	3.6	2.5	0.3	1.5	0.0	0.6	0.0	0.0
14.5	4523	15.8	6.1	4.9	3.7	0.3	1 8	0.0	0.7	0.0	0.0
44.2	15974	45.0	18.8	14.5	6.7	0.8	8.0	0.0	2.3	2.5	3.3
56.2	20352	54.6	24.7	17.4	10.9	0.7	8.9	0.0	2.3	2.1	3.4
68.1	24952	59.6	20.4	15.6	3.3	0.8	0.0	0.0	0.0	0.0	0.0
80.1	28762	49.7	21.6	15.2	8.9	0.6	6.9	0.0	1.5	1.8	3.4
92.1	33782	72.6	38.3	28.4	2.2	1.0	1.2	0.0	0.0	1.8	5.0
116.0	41852	72.5	37.1	26.9	9.2	1.0	10.0	0.0	2.1	2.4	5.1
139.9	52148	90.6	45.5	33.0	3.7	1.1	13.2	0.0	2.6	3.1	6.9
152.2	56245	62.9	31.3	22.3	8.1	0.8	8.3	0.0	1.0	2.3	4.7
163.8	61189	83.4	43.1	30.1	7.9	1.0	11.6	0.0	2.6	3.0	5.8
176.2	65504	70.1	33.5	22.8	9.2	0.8	9.7	0.0	1.8	1.0	3.1
188.0	70466	69.2	33.9	22.3	6.5	0.8	9.9	0.0	1.9	1.7	4.2
200.2	75354	56.9	30.1	21.2	4.5	0.7	8.0	0.0	1.4	2.0	4.3
206.0	77393	71.2	37.4	26.2	6.5	0.9	9.9	0.0	2.1	2.3	5.0

Where:

1 = cis-Dichloroethene
2 = Trichloroethene
3 = Tetrachloroethene
4 = Vinyl Chloride
5 = 1,1,1 Trichloroethane
6 = Toluene
7 = Benzene
8 = Ethyl Benzene
9 = m-Xylene
10 = o,p-Xylene

Appendix VIII. Field Study Small-Column Data (continued)

RSSCT (c) Operating parameters found in Table 8c.

Conducted from 3/ 1/85 to 3/ 6/85

Run Time : 5 days

Carbon: F-400
Size : 60x80 mesh
0.0105 cm particle radius

Loading Rate : 22.7 m/hr
EBCT : 12.2 sec
Influent Temp: 14 °C

Influent Data Concentrations in µg/L

	1	2	3	4	5	6	7	8	9	10
Average	68.5	33.4	25.9	6.7	0.8	16.0	0.0	3.7	4.3	6.5

Time (hrs)	BVF	1	2	3	4	5	6	7	8	9	10
0.0	0	70.9	38.3	30.4	6.3	0.8	17.0	0.0	4.4	3.8	7.1
25.2	149	70.2	35.7	27.4	5.6	0.8	16.7	0.0	3.8	11.2	6.9
786.0	3877	73.4	38.3	30.0	7.4	0.8	17.4	0.0	4.2	3.8	6.5
1506.0	7413	69.1	32.3	23.9	6.8	0.7	16.1	0.0	3.2	3.7	6.1
2220.0	10920	66.0	30.9	23.3	6.1	0.8	15.8	0.0	3.9	3.6	5.9
2946.0	14518	66.2	31.1	22.4	6.1	0.7	16.7	0.0	4.0	4.5	7.0
3666.0	18034	61.4	30.2	24.4	6.9	0.8	14.5	0.0	3.0	4.1	7.2
4386.0	21597	72.3	36.1	30.0	7.2	0.7	15.9	0.0	3.9	3.5	6.6
5838.0	27555	68.8	32.2	24.2	6.9	0.8	14.9	0.0	3.7	3.3	6.1

Effluent Data Concentrations in µg/L

Time (hrs)	BVF	1	2	3	4	5	6	7	8	9	10
0.0	0.0	0.0	0.4	0.0	0.0	0.0	0.3	0.0	0.0	0.0	0.0
0.2	84.2	0.0	0.2	0.0	0.0	0.0	0.0	0.0	0.0	0.0	0.0
6.6	1988.3	8.7	3.4	3.2	3.5	0.5	1.3	0.0	0.4	0.0	0.0
13.1	3909.0	16.3	5.8	5.2	5.3	0.4	2.5	0.0	0.8	0.9	1.4
19.2	5690.6	21.3	7.8	6.6	7.9	0.7	3.2	0.0	0.8	1.1	2.0
25.2	7472.2	34.7	13.5	11.2	7.0	1.2	5.5	0.0	1.7	4.6	3.7
31.1	9205.3	49.4	18.2	15.8	9.3	0.7	8.1	0.0	2.1	2.1	4.0
37.1	10958.8	45.7	17.8	14.2	8.3	0.5	7.3	0.0	2.0	2.7	4.3
43.2	12751.2	50.4	20.5	16.0	7.8	0.6	8.0	0.0	2.1	2.3	4.3
49.2	14578.6	52.4	20.7	15.9	8.5	0.9	7.6	0.0	2.1	2.3	4.2
55.2	16258.1	58.2	22.4	18.0	9.4	0.6	7.6	0.0	2.1	2.6	4.6
61.2	18070.9	54.3	20.7	15.6	8.4	0.8	7.4	0.0	2.0	4.8	6.1
67.3	19875.7	55.0	20.2	15.5	8.5	1.0	7.1	0.0	1.8	2.6	4.3
73.2	21640.1	62.0	23.6	18.7	8.2	0.6	7.3	0.0	2.0	2.8	4.8
85.3	24448.7	56.1	16.4	12.5	8.6	0.6	4.3	0.0	1.2	2.4	3.7
97.4	27598.8	56.9	17.1	12.7	7.5	0.6	5.0	0.0	1.2	2.8	4.4
109.3	30577.4	62.1	20.7	15.7	8.3	0.7	4.7	0.0	1.3	1.8	3.3

Where:
1 = cis-Dichloroethene
2 = Trichloroethene
3 = Tetrachloroethene
4 = Vinyl Chloride
5 = 1,1,1 Trichloroethane
6 = Toluene
7 = Benzene
8 = Ethyl Benzene
9 = m-Xylene
10 = o,p-Xylene

Appendix VIII. Field Study Small-Column Data

RSSCT (d) Operating parameters found in Table 8d.

Conducted from 8/26/84 to 8/31/84 Run Time : 5 days

Carbon: WV-G Loading Rate : 23.4 m/hr
Size . : 60x80 mesh EBCT : 2.29 sec
0.0105 cm particle radius Influent Temp: 13 °C

Influent Data Concentrations in μg/L

	1	2	3	4	5	6	7	8	9	10
Average	108.9	76.1	56.4	7.5	1.3	25.3	0.4	3.1	6.0	9.3

Time (hrs)	BVF	1	2	3	4	5	6	7	8	9	10
0.0	0	116.0	77.1	49.0	7.2	1.0	34.7	0.0	5.6	7.4	13.1
0.2	295	116.0	77.1	49.0	7.2	1.0	34.7	0.0	5.6	7.4	13.1
2.3	3348	118.0	79.0	52.1	8.3	1.0	35.8	0.0	6.0	7.7	13.2
6.3	9531	108.0	72.3	39.8	7.2	1.0	25.3	0.0	4.3	5.5	7.4
22.8	32929	115.0	77.4	54.4	8.1	1.1	34.1	0.0	5.5	7.6	10.4
26.1	38706	110.0	74.2	52.2	7.9	1.9	29.9	0.0	5.3	7.2	9.8
30.7	44044	109.0	71.5	55.8	7.2	2.3	12.9	1.7	1.3	0.5	5.1
46.0	67260	95.8	67.4	52.0	6.4	1.3	30.2	0.0	4.8	6.5	9.1
69.8	102230	106.0	73.2	58.2	7.1	1.1	29.8	0.0	3.5	6.5	10.0
95.9	138103	114.0	82.7	65.3	8.1	1.2	15.7	0.0	0.0	5.6	9.2
118.2	169552	120.0	90.7	63.4	8.5	1.2	23.9	2.7	1.5	7.3	11.1

Effluent Data Concentrations in μg/L

Time (hrs)	BVF	1	2	3	4	5	6	7	8	9	10
0.00	0	0.0	0.0	0.0	0.0	0.0	0.0	0.0	0.0	0.0	0.0
0.07	92	9.0	2.9	0.0	1.8	0.3	2.3	0.0	5.5	0.5	0.8
2.38	3304	89.0	58.3	38.8	7.5	0.9	24.7	0.0	4.1	5.2	8.8
6.43	8932	92.3	61.2	43.1	7.3	0.9	28.0	0.0	4.6	7.1	8.7
10.45	14537	88.2	60.1	43.0	6.6	0.8	26.4	0.0	4.4	5.9	7.7
21.95	30684	53.6	22.8	14.9	2.9	0.0	10.4	0.0	1.8	1.4	2.2
26.05	36438	105.0	73.2	52.2	7.8	1.0	29.9	0.0	5.1	7.2	9.9
30.86	43167	103.0	70.3	47.5	7.5	0.9	27.2	0.0	3.1	5.1	8.9
46.05	64365	117.0	80.2	58.3	8.0	1.3	33.1	0.0	5.3	9.0	11.2
50.05	69948	116.0	78.9	56.1	8.1	1.0	29.1	0.0	3.6	7.2	11.0
69.96	97770	111.0	76.5	55.6	7.6	1.0	16.8	0.0	0.0	6.1	9.5
78.65	109886	103.0	72.5	56.1	7.1	1.0	15.6	0.0	1.9	5.0	8.3
96.02	134113	105.0	76.8	58.2	7.7	1.2	15.8	0.0	0.0	5.7	9.0
104.13	145454	116.0	80.3	54.0	8.4	1.7	15.1	0.0	2.8	6.9	9.8
117.78	164556	126.0	86.2	56.5	8.4	1.3	11.5	0.0	0.0	5.1	8.9

Where:

1 = cis-Dichloroethene
2 = Trichloroethene
3 = Tetrachloroethene
4 = Vinyl Chloride
5 = 1,1,1 Trichloroethane
6 = Toluene
7 = Benzene
8 = Ethyl Benzene
9 = m-Xylene
10 = o,p-Xylene